The Dissertation Committee for Robert Jun Ono Certifies that this is the approved version of the following dissertation:

Synthesis of Conjugated Polymers and Block Copolymers Via Catalyst Transfer Polycondensation

Committee:

Christopher W. Bielawski, Supervisor

Jonathan L. Sessler, Co-Supervisor

Arumugam Manthiram

David A. Vanden Bout

C. Grant Willson

Synthesis of Conjugated Polymers and Block Copolymers Via Catalyst Transfer Polycondensation

by

Robert Jun Ono, B.A.

Dissertation

Presented to the Faculty of the Graduate School of

The University of Texas at Austin

in Partial Fulfillment

of the Requirements

for the Degree of

Doctor of Philosophy

The University of Texas at Austin

August 2013

Dedication

To my family.

Acknowledgements

To my advisor Prof. Chris Bielawski, who welcomed me into his research group, who listened to my research interests, and gave me the freedom to pursue those interests. I am extremely grateful for his guidance, motivation, and dedication, as well as for his hard work, which afforded me the luxury of working in a world-class research facility during my time at UT-Austin.

To all past and present members of the Bielawski group, who have collectively been sources of guidance, encouragement, inspiration and entertainment over the years. You are all brilliant scientists in your own right, but more importantly you are all good peoples. Special shout outs to: Kyle Williams, Brent Norris, Andy Tennyson, and Todd Hudnall who listened to and answered this first-year's incessant questions, and didn't even act annoyed; Evie Rosen and Daphne Sung, who were like big sisters; Kelly Wiggins and Beth Neilson, who were there with me through the whole ride, from start to finish; and Daniel Varnado and Jonathan Moerdyk, excellent officemates. "Thanks guys."

To my co-advisor Prof. Jonathan Sessler and his research group, who were like a second support system.

To all of my collaborators and co-authors, who were absolutely instrumental in my successes in graduate school. Amazing what you can accomplish when you surround yourself with smart people. In particular, I am extremely grateful to Prof. David Vanden Bout, Takuji Adachi, Johanna Brazard, Zhongjian Hu, Songsu Kang, Zong-Quan Wu, and Reeja Jayan, for being really, really smart people.

To Prof. Grant Willson, an invaluable mentor, an excellent teacher and all-around nice guy.

To colleagues and co-workers within the UT-Austin Department of Chemistry, who keep the place running smoothly 24/7. Special thanks to Steve Sorey in the NMR facilities, and to Brooke Graham, Betsy Hamblen, and Penny Kile, who cut through administrative red tape and made it look easy.

To friends that I've made along the way, who've helped to maintain balance and sanity. If I had to write an experimental procedure for obtaining a chemistry PhD, the essential reagents would be coffee and beer (not sure which one's the limiting reagent, though…), and so I am grateful to everyone who has accompanied me on countless coffee runs and trips to the Crown & Anchor. Special thanks to my roommates Yasuo Suzuki, Johanna Brazard, and especially Eric Silver, who always knew how to balance "extremely intelligent scientist" with "laid back roommate". To my darts team buddies and my food soulmate.

To my family, for their unwavering support and encouragement.

Synthesis of Conjugated Polymers and Block Copolymers Via Catalyst Transfer Polycondensation

Robert Jun Ono, Ph. D.

The University of Texas at Austin, 2013

Supervisor: Christopher W. Bielawski

Co-Supervisor: Jonathan L. Sessler

Conjugated polymers hold tremendous potential as low-cost, solution processable materials for electronic applications, such as organic light-emitting diodes and photovoltaics. While the concerted efforts of many research groups have improved the performance of organic electronic devices to near-relevant levels for commercial exploitation over the last decade, the overall performance of organic light-emitting diode and organic photovoltaic devices still lags behind that of their traditional, inorganic counterparts. Realizing the full potential of organic electronics will require a comprehensive, molecular-level understanding of conjugated polymer photophysics. Studying pure, well-defined, and reproducible conjugated polymer materials should enable these efforts; unfortunately, conjugated polymers are typically synthesized by metal-catalyzed step-growth polycondensation reactions that do not allow for rigorous control over polymer molecular weight or molecular weight distribution (i.e., dispersity). Chain-growth syntheses of conjugated polymers would not only allow for precise control over the aforementioned polymer metrics such as molecular weight and dispersity, but could also potentially create new applications by enabling the preparation of more advanced macromolecular structures such as block copolymers and surface grafted

polymers. Our efforts toward realizing these goals as well as toward exploiting chain-growth methodologies to better understand fundamental conjugated polymer photophysics and self-assembly will be presented.

Table of Contents

List of Tables

List of Figures

List of Schemes

Chapter 1: Catalyst Transfer Polycondensation for the Controlled Synthesis of Conjugated Polymers

1.1 Introduction

The synthesis of novel conjugated polymers (CPs) has spearheaded the rapidly developing field of organic electronics in the last two decades. Although organic electronic devices derived from CPs generally lag behind their traditional, inorganic semiconductor-based counterparts in terms of raw performance, their amenity to solution processing for printing onto flexible substrates makes them tremendously desirable for a number of technologies, including organic photovoltaics, organic light emitting diodes, chemosensors, and organic thin film transistors. Furthermore, the ability to process CPs from solution allows them to be integrated into existing processing technologies, such as roll-to-roll or inkjet printing for large scale production, thereby providing an economic impetus for their development.

The abovementioned applications have experienced a tremendous amount of growth in recent years, resulting in ever-increasing device performances and lifetimes through improved device engineering and fabrication methods. However, the development and synthesis of new CPs has also played a critical role in driving these fields of research. This chapter will focus on the basic principles governing the design and synthesis of solution processable CPs, as well as highlight recent advances in conjugated polymer synthesis, with an emphasis on the development of controlled chain-growth syntheses of CPs via catalyst transfer polycondensation. Finally, the opportunities and challenges surrounding the field will be discussed.

1.2 Conjugated Polymer Design and Synthesis

The desirable properties of CPs, such as strong light absorption ability and high conductivity, are an inherent consequence of their molecular structure, namely polymer backbones comprised of contiguous sp^2–sp^2 (and sometimes sp–sp^2) carbon linkages. It follows, then, that polymerization methods used to prepare the vast majority of CPs are based upon chemical transformations that are suitable for the formation of Csp^2–Csp^2 or Csp–Csp^2 bonds. Such transformations can be achieved via chemical or electrochemical oxidations of aromatic compounds, Wittig–Horner[1] or Knoevenagel-type[2] condensations (when vinyl linkages are desired), and transition metal-mediated C–C bond forming reactions. Transformations of the latter variety include Rh-catalyzed acetylene polymerizations,[3] W-catalyzed acyclic diyne metathesis reactions,[4] and Ni-mediated Yamamoto dehalogenative coupling reactions;[5] however, the most widely used and versatile method for the construction of CPs is the use of transition metal catalyzed cross-coupling reactions.

The catalytic cycle for a typical cross-coupling reaction is shown in Figure 1.1. The cycle consists of oxidative addition of a transition metal across the C–X bond of an electrophile, transmetalation with a main group organometallic nucleophile, and finally reductive elimination of the metal to form the new C–C bond, with simultaneous regeneration of the catalytic species. Common catalysts used include relatively inexpensive complexes of nickel or palladium. The biggest advantage of the cross-coupling reaction, however, is that many types of organometallic reagents can be used as the coupling partners, including magnesium- (i.e., Grignard), zinc-, copper-, tin-, and boron-based reagents; coupling reactions involving each of these organometallics are commonly referred to by their named reactions, after their founder(s) (Kumada–Corriu, Negishi, Sonogashira, Stille, and Suzuki–Miyaura couplings, respectively). Within the

context of CP synthesis, the availability of a large variety of organometallic coupling partners is especially beneficial, as suitable conditions can be chosen in order to tolerate any other functional groups that may decorate the monomers. Furthermore, empirically-derived guidelines have been established for determining which types of cross-coupling reactions are most effective for generating various types of CPs.[6] For example, Stille couplings are highly effective for synthesizing thiophene-containing polymers where the stannyl groups are located on the thiophene-based monomers. On the other hand, the same coupling reaction is not suitable for stannylated benzene-based monomers under similar conditions. For benzene-based CPs, the Suzuki coupling is most widely used, with the boron groups located on the benzene ring of the monomers.

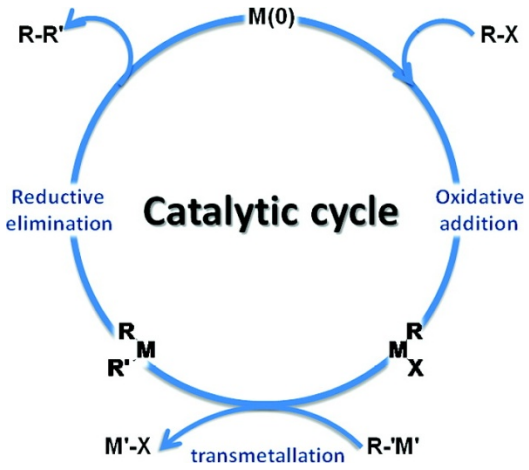

Figure 1.1: Catalytic cycle of a typical transition metal-catalyzed cross-coupling reaction. Reprinted with permission from "Synthesis of Conjugated Polymers for Organic Solar Cell Applications", Yen-Ju Cheng, Sheng-Hsiung Yang, and Chain-Shu Hsu. *Chem. Rev.* **2009**, *109*, 5868-5923. Copyright 2009 American Chemical Society.

CPs are typically synthesized using cross-coupling reactions via A–A + B–B type step-growth polymerizations of a dihalogenated monomer and a difunctionalized

organometallic monomer. Because cross-couplings are generally very high yielding reactions, their use in a step-growth polymerization scheme allows for high molecular weight materials to be achieved. This strategy also enables rapid development of libraries of novel polymers and copolymers, as a virtually infinite combination of distinct comonomers can be chosen as the coupling partners.

In terms of polymer metrics, such as molecular weight and dispersity (i.e., molecular weight distribution, defined as the ratio of the weight-averaged molecular weight to the number-average molecular weight, M_w/M_n), CPs synthesized in the aforementioned manner exhibit characteristics that are typical of step-growth polymerizations, namely molecular weights that can be difficult to control and broad dispersities approaching (and often exceeding) 2. This represents a severe limitation to current methods for synthesizing CPs, as a lack of molecular weight or dispersity control can lead to ill-defined materials and problems with reproducibility. Additionally, polymers synthesized via step-growth polymerizations are difficult to elaborate into more complex macromolecular structures, such as block copolymers and surface-grafted polymers, due to an inability to control the end-groups when semi- or heterotelechelic polymers (telechelic polymer = end-functionalized polymer) are desired.

1.3 Catalyst Transfer Polycondensation

To address the limitations associated with step-growth polymerizations for the synthesis of CPs, recent research has focused on converting the aforementioned step-growth polycondensations into chain-growth polycondensations. Metal-catalyzed polycondensation reactions can be endowed with chain-growth polymerization behavior by a process called catalyst transfer, in which the catalyst activates the end-group of the polymer, reacts with the monomer, and transfers in an intrachain fashion to the end of the

propagating polymer. Catalyst transfer polycondensation (CTP) (the term Grignard metathesis (GRIM) polymerization is also used when Kumada-type cross-couplings are employed), was simultaneously pioneered by McCullough[7,8] and Yokozawa,[9,10] who observed chain-growth behavior in the Ni-catalyzed polymerization of a Grignard-based thiophene monomer to afford poly(3-hexylthiophene) (P3HT) of controllable molecular weight and narrow dispersity.

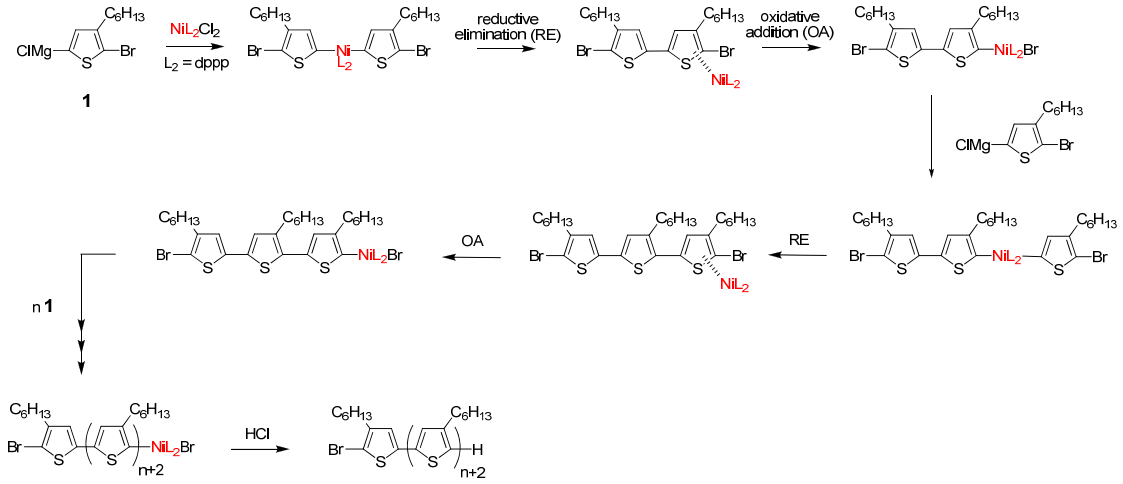

Scheme 1.1: Mechanism of Kumada catalyst transfer polycondensation leading to well-defined poly(3-hexylthiophene).

Yokozawa specified four experimental observations from the Ni-catalyzed polymerization of 5-chloromagnesio-2-bromo-3-hexylthiophene (**1**) that led to the proposal of a CTP mechanism: (1) the polymerization is initiated by the in situ formation of a dimer of **1**; (2) the number of polymer chains formed is equal to the number of molecules of Ni catalyst; (3) the propagating polymer end-group is a polymer–Ni–Br complex; and (4) when the polymerization is quenched with hydrochloric acid, all of the polymer chains have the same end-groups, wherein one end of the polymer is terminated with Br and the other with H.[11] The mechanism of the Kumada CTP of **1** is outlined in

Scheme 1.1. **1** is generated in situ by a Grignard metathesis reaction of 2,5-dibromo-3-hexylthiophene or 2-bromo-5-iodo-3-hexylthiophene with isopropylmagnesium chloride. The polymerization is initiated by generating the active zero-valent form of the catalyst via the dimerization of **1** using dichloro(1,3-bis(diphenylphosphino)propane)nickel ($Ni(dppp)Cl_2$). Subsequent intramolecular oxidative addition of the newly 'liberated' Ni(dppp) across the thiophene–Br bond forms a thiophene–Ni(dppp)–Br complex. Propagation of the growing polymer chain therefore occurs through successive reactions of monomer **1** to the aforementioned thiophene–Ni(dppp)–Br end-group, resulting in chain-growth polymerization behavior. Finally, quenching the polymerization with protic acid results in removal of the Ni-complex from the chain end, which is consistent with the previously described experimental observation of Br/H-terminated polymers.

Notably, the CTP method affords a regioregular P3HT, in which all of the 3-hexylthiophene repeating units are coupled together in a head-to-tail (HT) fashion (defining the 2-position as the 'head' and the 5-position as the 'tail'), with the exception of the initial tail-to-tail dimerization. Regioregularity, or the %HT couplings, is an extremely important parameter for poly(3-alkylthiophene)s, as a low %HT content (and consequently an increasing percentage of HH and TT couplings) causes twisting of the polymer backbone in response to the increased steric interactions of the side-chains (Figure 1.2).[12] In turn, this twisting of the backbone leads to attenuation of the conjugation length of the polymer, destroying its electrical conductivity and other desirable electronic properties. CTP is therefore not only a useful method for controlling molecular weight and dispersity of CPs, but is also a powerful method for controlling their regiochemistry, and hence their physical properties.

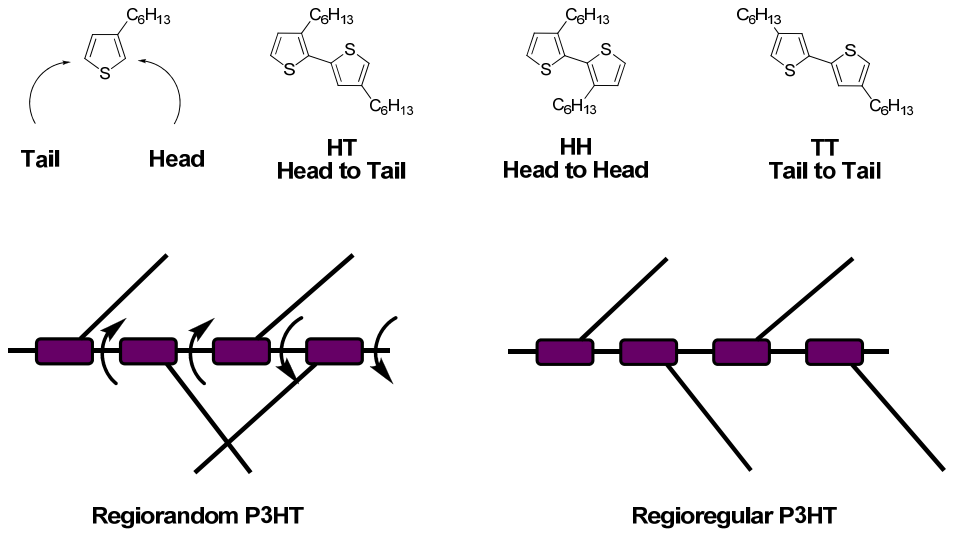

Figure 1.2: Regioisomeric outcomes from coupling of 3-hexylthiophenes (top) can lead to regiorandom and/or regioregular P3HT (bottom).[12]

The chemical processes involved in catalyst transfer polycondensations, e.g., the reaction described in Scheme 1.1, are no different from those involved in typical metal-catalyzed cross coupling reactions (cf. Figure 1.1), in that they involve a series of transmetalations, oxidative additions, and reductive eliminations to form new C–C bonds. In the context of CP synthesis, however, several factors can favor a chain-growth catalyst transfer process over a conventional step-growth polycondensation involving cross-coupling (e.g., an A–A + B–B type polymerization). First, an A–B type monomer must be used, in which both the aryl halide electrophile and organometallic nucleophile are present on the same molecule. Second, catalysts bound to bidentate ligands such as dppp or 1,2-bis(diphenylphosphino)ethane (dppe) are almost exclusively used, especially in Kumada CTPs, in order to force the two coupling partners into a cis configuration around the metal center so as to facilitate reductive elimination. Finally, and most importantly, the intramolecular "ring walking" of the catalyst to the end of the polymer chain, and subsequent oxidative addition, is necessary to impart the desired chain-growth behavior

on the polymerization. To date, no direct experimental evidence for this crucial 'ring-walking' step has been observed in CTP reactions; rather, evidence for the process has been inferred through the observation of narrowly disperse (i.e., low M_w/M_n) polymers prepared by CTP, along with Yokozawa's observations described above. However, analogous intramolecular catalyst transfer processes have been directly observed for related small molecule systems.[13-16] For example, Nakamura showed through theoretical calculations and kinetic isotope experiments that π-complexation of the catalyst to the haloarene substrate is the first irreversible step in Ni-catalyzed cross-coupling reactions.[14] Similarly, van der Boom demonstrated that a Ni complex will preferentially activate the aryl–Br bond of a halogenated stilbazole via a 'ring-walking' process starting with η^2-coordination of the Ni to the vinyl group, followed by intramolecular oxidative addition across the C–Br bond.[16] Remarkably, this catalyst transfer process occurrs quantitatively even in the presence of a highly reactive aryl iodide. This observation is consistent with intramolecular catalyst transfer taking place with kinetic preference over the competing thermodynamically favored activation of the aryl–I (Scheme 1.2).

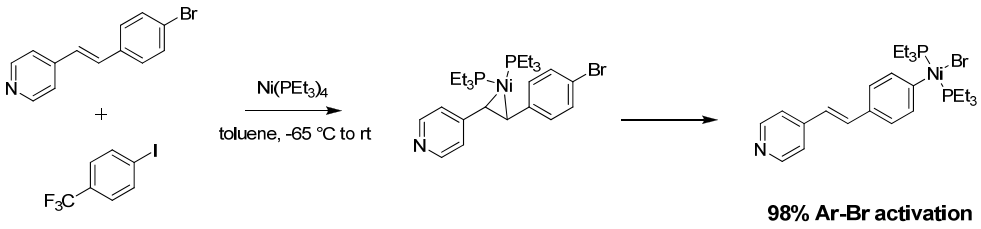

Scheme 1.2: Intramolecular Ar–Br bond activation via 'ring-walking'.[16]

Following McCullough and Yokozawa's initial discovery of the Kumada CTP of **1** to form well-defined, regioregular P3HT, the method was quickly extended to effect the controlled chain-growth polymerization of many other aromatic and heteroaromatic

monomers, including fluorenes,[17] phenylenes,[18] pyrroles,[19] and selenophenes.[20] A corresponding CTP process based on the Suzuki cross-coupling reaction, which utilizes a Pd catalyst and a boronic acid-based monomer (Scheme 1.3), was also developed.[21] This new modification has greatly expanded the scope of polymerizable monomers, as well as increased functional group tolerance.

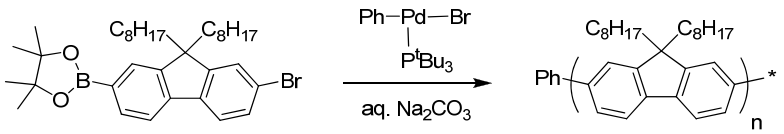

Scheme 1.3: Pd-catalyzed Suzuki catalyst transfer polycondensation.[21]

1.4 CONTROLLING END-GROUPS IN CATALYST TRANSFER POLYMERIZATION

The greatest merit of CTP stems from its chain-growth nature; that is, it can facilitate the preparation of highly complex macromolecular structures such as block copolymers, surface-grafted brush polymers, star polymers, and more. The basis of this lies in the ability to control and manipulate polymer end-groups. In a seminal example, McCullough recognized that mono- and di-end-functionalized P3HT species could be accessed by quenching Kumada CTPs of monomer **1** with an excess of an appropriate monotopic Grignard reagent.[22] As shown in Scheme 1.4, the propagating polymer–Ni–Br endgroup can preferentially undergo a transmetalation reaction with the added Grignard capping agent when it is present in high concentrations relative to other reactive species in the reaction mixture. Upon reductive elimination, the resulting product affords the mono end-functionalized P3HT. Using this method, useful functionalities, such as vinyl, allyl, and ethynyl end-groups, may be incorporated into the polymers, as well as hydroxyl, formyl, and amino groups when suitable protecting groups were used. This end-capping method has been widely used in the synthesis of CP-containing rod–coil

block copolymers, wherein the aforementioned functionalities are elaborated into macroinitiators for various controlled polymerization reactions, such as ATRP, RAFT, nitroxide-mediated polymerization (NMP), as well as ring-opening polymerization (ROP).[23] Thus, innumerable combinations of CPs and coil-type polymers can be designed and accessed via this convenient end-group functionalization approach.

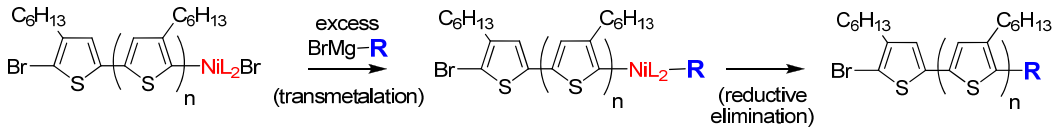

Scheme 1.4: In situ end-capping of P3HT by quenching a Kumada CTP with a Grignard reagent.[22]

Alternatively, desired end-group functionalities can be introduced into CPs at the beginning of the polymerization. This is accomplished by initiating the CTP using suitable Ni(II) or Pd(II) catalysts with the following structure: Ar–M–Br. Luscombe showed by ^{1}H NMR spectroscopy and MALDI mass spectrometry that an o-tol–Ni(dppp)–Br (o-tol = ortho-tolyl) complex is capable of efficiently initiating the polymerization of **1** while simultaneously installing a tolyl end-group into every P3HT chain (Scheme 1.5).[24] Note also that Suzuki CTPs may be performed via a similar ex situ initiation approach (cf. Scheme 1.3). When the metal complex is bound to a surface, this approach provides a powerful method for the preparation of surface-grafted CPs. This is illustrated by the elegant work of Kiriy, who showed that P3HT could be grown from poly(4-bromostyrene) films[25] as well as from functionalized silica surfaces.[26,27]

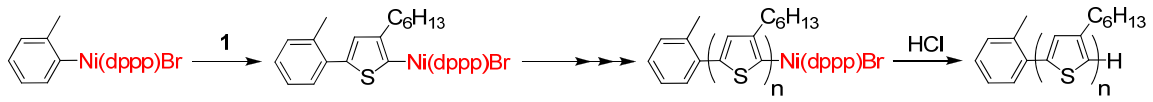

Scheme 1.5: Ex situ initiated CTP of **1** using a o-tol–Ni(dppp)–Br catalyst leads quantitatively to mono aryl-functionalized P3HT.[24]

1.5 Conclusion and Outlook

In order to keep pace with the rapidly growing field of organic electronics, the continued development of novel, high performance conjugated polymers using new and clever synthetic methodologies will be necessary. As a nascent technique, catalyst transfer polycondensations have already contributed greatly to the field. They have, for instance, facilitated the development well-defined CPs, as well as previously inaccessible CP-containing architectures. In view of CP synthesis as a whole, however, CTP still currently only pertains to a small subset of polymerizable monomers. This represents a limitation to its utility. Thus, the continued growth of CTP as a polymerization methodology will surely hinge upon expanding its scope toward other coupling chemistries beyond the Kumada and Suzuki couplings. For example, the development of a Heck-type CTP is envisioned to give rise to well-defined poly(arylenevinylene)s, a very prominent class of polymers that are useful for several emerging technologies, in particular organic light emitting diodes (OLEDs).

Another challenge involves pushing the limits of the CTP approach, especially with regard to the critical intramolecular catalyst transfer step. Specifically, while the putative 'ring-walking' step wherein the zerovalent catalyst associates with the π system of the propagating polymer is well-established for short distances (e.g., the length of one aromatic ring), the question remains whether this catalyst transfer process can take place across longer distances spanning multiple arene rings. In 2008, Kiriy observed that catalyst 'ring-walking' could take place across monomers comprising two or even three

thiophene rings, thus maintaining chain-growth polymerization polymerization behavior.[28] Ensuing reports have established that the aforementioned catalyst transfer step is a robust process that is capable of traveling over distances of several tens of nanometers[29] and even across nonconjugated (i.e., saturated) C–C bonds[30] without detriment to the chain-growth nature of the polymerization. These finding are important because the ability of the catalyst to traverse long distances in the catalyst transfer step will be necessary for the preparation of increasingly structurally-complex CPs via CTP, including copolymers containing alternating monomer structures. Many new high performance CPs exhibit such an alternating arrangement of repeat units, and have been shown to outperform their homopolymer counterparts (e.g., P3HT) in a variety of applications. These types of conjugated copolymers are often called "donor–acceptor" polymers, because their photophysical properties may be tuned by mixing-and-matching electron-donating and -withdrawing monomer units, effectively forming an alternating repeating structure in the polymer main chain.[6] While donor–acceptor polymers are conveniently synthesized using step-growth polycondensation methods, recent reports[31-34] indicate that CTP can indeed provide a chain-growth route for the preparation of these polymers in a well-controlled manner.

It is expected that the synthesis of novel CPs will continue to drive technological advances in the area of organic electronics. As a polymerization methodology, catalyst transfer polycondensation has experienced a considerable amount of growth in the last decade, and has cemented its place as an invaluable tool for the synthesis of CPs. Through further development in the aforementioned areas, CTP has the potential to enable the preparation of previously inaccessible classes of CPs, as well as various advanced polymer architectures. This is expected to advance the field of organic electronics by providing new materials with a range of desired properties.

1.6 ACKNOWLEDGEMENTS

Portions of this dissertation have been reprinted, with permission, from published works. Although this dissertation represents the author's thesis research, numerous individuals have contributed to the work described herein in one way or another. To the best of the author's knowledge, none of the work described herein has appeared in another dissertation, treatise, or thesis. The purpose of this section is to acknowledge, on a chapter by chapter basis, each individual's contribution to the work described and, if applicable, the original publication(s) used to write the chapter. Note also that a similar acknowledgements section has been placed at the end of each chapter.

Chapter 1. Chapter 1 was written by Robert J. Ono and has not appeared in any other publication, partially nor in its entirety, prior to publication of this dissertation.

Chapter 2. Portions of Chapter 2 were reprinted with permission from Ono, R. J.; Kang, S.; Bielawski, C. W. *Macromolecules* **2012**, *45*, 2321-2326. Copyright 2012 American Chemical Society. Robert J. Ono performed the polymerizations and characterization, and wrote the original manuscript. Songsu Kang assisted with the monomer synthesis. Prof. Christopher W. Bielawski helped to write the original manuscript.

Chapter 3. Portions of Chapter 3 were reprinted with permission from Kang, S.; Ono, R. J.; Bielawski, C. W. *J. Am. Chem. Soc.* **2013**, *135*, 4984-4987. Copyright 2012 American Chemical Society. Songsu Kang performed the monomer and polymer syntheses and characterizations. Robert J. Ono performed the surface initiated polymerizations and characterization, and wrote the original manuscript. Prof. Christopher W. Bielawski helped to write the original manuscript.

Chapter 4. Portions of Chapter 4 were reprinted with permission from Li, Z.; Ono, R. J.; Wu, Z.-Q.; Bielawski, C. W. *Chem. Commun.* **2011**, *47*, 197-199. Copyright

2011 The Royal Society of Chemistry. Zicheng Li performed the monomer and polymer syntheses and characterizations. Robert J. Ono assisted with the polymer synthesis, performed the TEM characterization, and wrote the original manuscript. Zong-Quan Wu assisted with the polymer synthesis. Prof. Christopher W. Bielawski helped to write the original manuscript.

Chapter 5. Portions of Chapter 5 were reprinted with permission from Brazard, J.; Ono, R. J.; Bielawski, C. W.; Barbara, P. F.; Vanden Bout, D. A. *J. Phys. Chem. B,* **2013**, *117*, 4170-4176. Copyright 2013 American Chemical Society. Johanna Brazard performed the photophysical experiments and wrote the original manuscript. Robert J. Ono performed the polymer synthesis and characterization, and helped to write the original manuscript. Prof. David A. Vanden Bout and Prof. Christopher W. Bielawski also helped to write the original manuscript. (Prof. Paul F. Barbara deceased).

Chapter 6. Portions of Chapter 6 were reprinted with permission from Wu, Z.-Q.; Ono, R. J.; Chen, Z.; Bielawski, C. W. *J. Am. Chem. Soc.* **2010**, *132*, 14000-14001, Copyright 2010 American Chemical Society, and Wu, Z.-Q.; Radcliffe, J. R.; Ono, R. J.; Chen, Z.; Li, Z.; Bielawski, C. W. *Polym. Chem.* **2012**, *3*, 874-881, Copyright 2012 The Royal Society of Chemistry. Zong-Quan Wu performed the monomer and polymer syntheses and characterizations. Robert J. Ono assisted with the polymer synthesis, performed the AFM characterization, wrote the original *J. Am. Chem. Soc.* manuscript, and helped to write the original *Polym. Chem.* manuscript. Jonathan D. Radcliffe assisted with the monomer and polymer syntheses and characterizations, and wrote the original *Polym. Chem.* manuscript. Zheng Chen performed the DSC measurements. Zicheng Li performed the TEM characterization. Prof. Christopher W. Bielawski helped to write both original manuscripts.

Chapter 7. Portions of Chapter 7 were reprinted with permission from Ono, R. J.; Todd, A. D.; Hu. Z.; Vanden Bout, D. A.; Bielawski, C. W. *Macromol. Rapid Commun.* **2013**, *Vol. 34*, In Press (DOI: 10.1002/marc.201300440). Copyright 2013 John Wiley and Sons. Robert J. Ono performed the monomer and polymer syntheses and characterizations, assisted with the photophysical measurements, and wrote the original manuscript. Alex D. Todd performed the XRD experiments. Zhongjian Hu performed the photophysical experiments. Prof. Christopher W. Bielawski and Prof. David A. Vanden Bout helped to write the original manuscript.

1.7 REFERENCES

(1) Liao, L.; Pang, Y.; Ding, L.; Karasz, F. E. *Macromolecules* **2001**, *34*, 6756-6760.

(2) Moratti, S. C.; Cervini, R.; Holmes, A. B.; Baigent, D. R.; Friend, R. H.; Greenham, N. C.; Grüner, J.; Hamer, P. J. *Synth. Met.* **1995**, *71*, 2117-2120.

(3) Liu, J.; Lam, J. W. Y.; Tang, B. Z. *Chem. Rev.* **2009**, *109*, 5799-5867.

(4) Bunz, U. H. F. *Acc. Chem. Res.* **2001**, *34*, 998-1010.

(5) Yamamoto, T.; Morita, A.; Miyazaki, Y.; Maruyama, T.; Wakayama, H.; Zhou, Z. H.; Nakamura, Y.; Kanbara, T.; Sasaki, S.; Kubota, K. *Macromolecules* **1992**, *25*, 1214-1223.

(6) Cheng, Y.-J.; Yang, S.-H.; Hsu, C.-S. *Chem. Rev.* **2009**, *109*, 5868-5923.

(7) Loewe, R. S.; Khersonsky, S. M.; McCullough, R. D. *Adv. Mater.* **1999**, *11*, 250-253.

(8) Sheina, E. E.; Liu, J.; Iovu, M. C.; Laird, D. W.; McCullough, R. D. *Macromolecules* **2004**, *37*, 3526-3528.

(9) Yokoyama, A.; Miyakoshi, R.; Yokozawa, T. *Macromolecules* **2004**, *37*, 1169-1171.

(10) Miyakoshi, R.; Yokoyama, A.; Yokozawa, T. *J. Am. Chem. Soc.* **2005**, *127*, 17542-17547.

(11) Yokozawa, T.; Yokoyama, A. *Chem. Rev.* **2009**, *109*, 5595-5619.

(12) Osaka, I.; McCullough, R. D. *Acc. Chem. Res.* **2008**, *41*, 1202-1214.

(13) Dong, C.-G.; Hu, Q.-S. *J. Am. Chem. Soc.* **2005**, *127*, 10006-10007.

(14) Yoshikai, N.; Matsuda, H.; Nakamura, E. *J. Am. Chem. Soc.* **2008**, *130*, 15258-15259.

(15) Weber, S. K.; Galbrecht, F.; Scherf, U. *Org. Lett.* **2006**, *8*, 4039-4041.

(16) Zenkina, O. V.; Karton, A.; Freeman, D.; Shimon, L. J. W.; Martin, J. M. L.; van der Boom, M. E. *Inorg. Chem.* **2008**, *47*, 5114-5121.

(17) Huang, L.; Wu, S.; Qu, Y.; Geng, Y.; Wang, F. *Macromolecules* **2008**, *41*, 8944-8947.

(18) Miyakoshi, R.; Shimono, K.; Yokoyama, A.; Yokozawa, T. *J. Am. Chem. Soc.* **2006**, *128*, 16012-16013.

(19) Yokoyama, A.; Kato, A.; Miyakoshi, R.; Yokozawa, T. *Macromolecules* **2008**, *41*, 7271-7273.

(20) Hollinger, J.; Jahnke, A. A.; Coombs, N.; Seferos, D. S. *J. Am. Chem. Soc.* **2010**, *132*, 8546-8547.

(21) Yokoyama, A.; Suzuki, H.; Kubota, Y.; Ohuchi, K.; Higashimura, H.; Yokozawa, T. *J. Am. Chem. Soc.* **2007**, *129*, 7236-7237.

(22) Jeffries-El, M.; Sauve, G.; McCullough, R. D. *Macromolecules* **2005**, *38*, 10346-10352.

(23) Stefan, M. C.; Bhatt, M. P.; Sista, P.; Magurudeniya, H. D. *Polym. Chem.* **2012**, *3*, 1693-1701.

(24) Bronstein, H. A.; Luscombe, C. K. *J. Am. Chem. Soc.* **2009**, *131*, 12894-12895.

(25) Beryozkina, T.; Boyko, K.; Khanduyeva, N.; Senkovskyy, V.; Horecha, M.; Oertel, U.; Simon, F.; Stamm, M.; Kiriy, A. *Angew. Chem. Int. Ed.* **2009**, *48*, 2695-2698.

(26) Senkovskyy, V.; Khanduyeva, N.; Komber, H.; Oertel, U.; Stamm, M.; Kuckling, D.; Kiriy, A. *J. Am. Chem. Soc.* **2007**, *129*, 6626-6632.

(27) Senkovskyy, V.; Tkachov, R.; Beryozkina, T.; Komber, H.; Oertel, U.; Horecha, M.; Bocharova, V.; Stamm, M.; Gevorgyan, S. A.; Krebs, F. C.; Kiriy, A. *J. Am. Chem. Soc.* **2009**, *131*, 16445-16453.

(28) Beryozkina, T.; Senkovskyy, V.; Kaul, E.; Kiriy, A. *Macromolecules* **2008**, *41*, 7817-7823.

(29) Tkachov, R.; Senkovskyy, V.; Komber, H.; Sommer, J.-U.; Kiriy, A. *J. Am. Chem. Soc.* **2010**, *132*, 7803-7810.

(30) Wu, S.; Sun, Y.; Huang, L.; Wang, J.; Zhou, Y.; Geng, Y.; Wang, F. *Macromolecules* **2010**, *43*, 4438-4440.

(31) Elmalem, E.; Kiriy, A.; Huck, W. T. S. *Macromolecules* **2011**, *44*, 9057-9061.

(32) Ono, R. J.; Kang, S.; Bielawski, C. W. *Macromolecules* **2012**, *45*, 2321-2326.

(33) Senkovskyy, V.; Tkachov, R.; Komber, H.; Sommer, M.; Heuken, M.; Voit, B.; Huck, W. T. S.; Kataev, V.; Petr, A.; Kiriy, A. *J. Am. Chem. Soc.* **2011**, *133*, 19966-19970.

(34) Yokozawa, T.; Nanashima, Y.; Ohta, Y. *ACS Macro Lett.* **2012**, *1*, 862-866.

Chapter 2: Controlled Chain-Growth Kumada Catalyst Transfer Polycondensation of a Conjugated Alternating Copolymer

2.1 INTRODUCTION

McCullough's[1] and Yokozawa's[2] seminal reports on the chain-growth polymerization of 3-hexylthiophene have enabled the corresponding polymer, P3HT, to become one of the most prevalent conjugated polymers (CPs) in the literature. Despite the synthetic versatility and impressive electronic properties of P3HT, significant research efforts are now being directed toward the synthesis of new CPs that feature properties tailored toward specific applications. For example, in the field of organic photovoltaics, a growing number of CPs have been shown to outperform P3HT when incorporated into solar cells.[3,4] These improvements are ascribed to a broader absorption overlap with the solar spectrum and better energy matching with commonly used electron acceptors (e.g., phenyl-C61-butyric acid methyl ester; PCBM). Many of these new, high performance CPs are effectively "donor–acceptor" (D–A) polymers, designed to feature reduced optical bandgaps (and hence broader absorption bands that extend into the red) by virtue of incorporating electron-donating and -withdrawing components into the polymer main chain.[5] Structurally, nearly all of these types of CPs take the form of an alternating copolymer comprised of donor and acceptor groups (e.g., -[D-A]-$_n$) and are generally synthesized by metal-catalyzed step-growth polycondensations. Typically, the methods used to create these polymers do not permit rigorous control over polymer molecular weight or dispersity (M_w/M_n), and oftentimes afford ill-defined materials. A controlled, chain-growth synthesis of donor–acceptor CPs would not only allow for precise control over the aforementioned polymerization metrics, but could also enable the preparation of more advanced macromolecular structures, such as block copolymers and surface-grafted polymers. Moreover, the successful preparation of such well-defined

structures could potentially facilitate greater control over the polymer morphology, which is another important parameter that governs the performance of organic electronic devices.[6,7]

We reasoned that such controlled polymerizations could be achieved by applying the Ni-catalyzed Kumada catalyst transfer polycondensation (CTP) to monomers that feature "built in" alternating repeat units. Recently, during the course of our investigations, Huck and coworkers reported a synthesis of the alternating copolymer poly(9,9'-dioctylfluorene-*alt*-benzothiadiazole) (PF8BT) using Pd-catalyzed Suzuki CTP.[8] While the chain-growth nature of the aforementioned polymerization was elegantly demonstrated, only polymers having moderate molecular weights (up to ca. 10 kDa or 19 repeat units) were isolated and efforts toward controlling the polymerization (e.g., establishing a linear relationship between polymer molecular weight and monomer conversion) appeared to be underway. We chose to continue our pursuit of Ni-catalyzed Kumada CTPs because they offer, as a complementary methodology, several potential advantages over analogous Suzuki-type polycondensations. For instance, Kumada CTPs do not require the use of specially synthesized catalysts or *ex-situ* initiation. Furthermore, despite the evidence that a chain-growth mechanism is operative in the Kumada CTP of monomers containing multiple arene rings (e.g., fluorenes, carbazoles, oligothiophenes, etc.), control over such polymerizations largely remains an unsolved problem. Presumably, this reflects inefficient catalyst transfer across the length of the monomer.[9-15] Herein, we describe the controlled, chain-growth synthesis of a π-conjugated alternating copolymer, poly(thiophene-*alt*-*p*-phenylene) (PTPP), via the Kumada catalyst transfer polycondensation of a novel bicyclic monomer.

2.2 RESULTS AND DISCUSSION

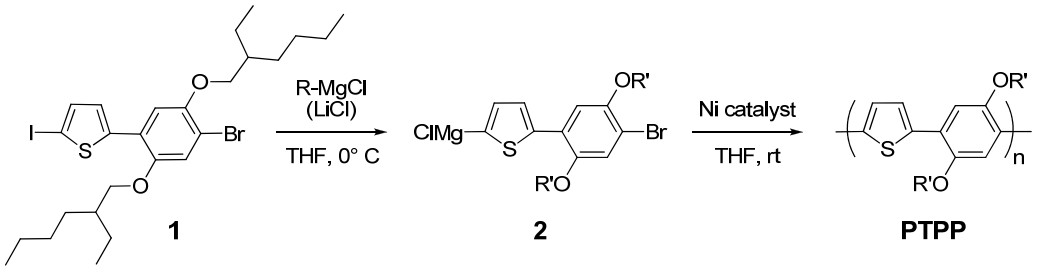

Scheme 2.1: Synthesis of PTPP. R = *t*-butyl or *i*-propyl. R' = 2-ethylhexyl.

We elected to incorporate thiophene and dialkoxybenzene into a single monomer unit because the Kumada catalyst transfer polymerizations of both thiophenes[1,2] and dialkoxybenzenes[16] have already been independently established. Pre-monomer **1** was prepared in two steps by the Suzuki coupling of 2-thiopheneboronic acid and 1,4-dibromo-2,5-di(2-ethylhexyloxy)benzene followed by iodination with N-iodosuccinimide in 57% overall yield (see the experimental section for additional details). As summarized in Scheme 2.1, treatment of **1** with 1.0 equiv of ^{i}PrMgCl at 0 °C in THF resulted in the fast, quantitative conversion to **2**, as deduced by ^{1}H NMR spectroscopic analysis of the reaction mixture after quenching with HCl (aq.). The reaction was complete within 20 min, and metalation occurred selectively at the α-position of the thiophene, leaving the aryl bromide intact. Support for this conclusion came from ^{1}H NMR spectroscopic analysis of the corresponding quenched product, which revealed signals that were identical to that of 2-(4-bromo-2,5-bis(2-ethylhexyloxy)phenyl)thiophene (i.e., the precursor to **1**).

With respect to the monomer design, our decision to use a monomer that metalates at the thiophene as opposed to the phenyl moiety was based on the work of Yokozawa and coworkers, who demonstrated that the order of polymerization was critical to successfully forming block copolymers containing P3HT and poly(p-

phenylene) (PPP) segments. Specifically, successive polymerization of the phenylene monomer followed by the thiophene monomer yielded a well-defined block copolymer with narrow molecular weight distribution. Conversely, reversing the order of monomer addition resulted in polymers with broad molecular weight distributions.[17] In other words, we anticipated that if metalation occurred at the thiophene unit, the propagating end of the resulting polymer (i.e., polymer–NiLBr) would feature a terminus where Ni is connected to a phenyl group, reminiscent of a Ni-terminated PPP. Ultimately, this should result in a controlled polymerization process. In contrast, metalation at the phenyl unit would lead to polymers with termini that are reminiscent of Ni-terminated P3HT, resulting in ill-defined polymers.

Polymerization was carried out at 23 °C by the addition of a Ni catalyst (3 mol%) to a THF solution of **2**, and monitored by gel permeation chromatography (GPC) over time until the respective polymer molecular weight ceased to increase. Two Ni catalysts, Ni(dppp)Cl_2 and Ni(dppe)Cl_2 (dppp = 1,3-bis(diphenylphosphino)propane; dppe = 1,2-bis(diphenylphosphino)ethane), were investigated for the polymerization of **2**, as they have been shown to be suitable catalysts for the homopolymerization of 2,5-dibromo-3-alkylthiophenes as well as 2,5-dibromo-1,4-dialkoxybenzenes.[2,16,18] As summarized in Table 2.1, both of these catalysts afforded polymeric products. When Ni(dppe)Cl_2 was used at the catalyst, a relatively high number average molecular weight (M_n) polymer was obtained; however, the resulting polymer also exhibited a broad dispersity ($Đ$; M_w/M_n) (Table 2.1, entry 1). In contrast, when Ni(dppp)Cl_2 was used, the dispersity of the resultant polymer was much narrower, but only materials with relatively low M_ns were obtained (entry 2).

Entry	Catalyst	Equiv of LiCl	Grignard Reagent	M_n [b]	M_w/M_n [b]
1	Ni(dppe)Cl_2	0	^{i}PrMgCl	12000	2.03
2	Ni(dppp)Cl_2	0	^{i}PrMgCl	3700	1.32
3	Ni(dppe)Cl_2	1.0	^{i}PrMgCl	12000	1.74
4[c]	Ni(dppp)Cl_2	1.0	^{i}PrMgCl	14500	1.33
5	Ni(dppe)Cl_2	1.0	^{t}BuMgCl	15200	2.03
6	Ni(dppp)Cl_2	1.0	^{t}BuMgCl	10500	1.53

Table 2.1: Polycondensation of **2** with various Ni catalysts. Polymerizations were carried out by treating **1** with 1.0 equiv of Grignard reagent in THF ($[\mathbf{1}]_0$ = 0.1 M) for 20 min at 0 °C, followed by warming to 23 °C and addition of the Ni catalyst ($[\mathbf{1}]_0/[Ni]_0$ = 33). In all cases, the expected M_n was based on a degree of polymerization of 33 and calculated to be 13700 Da. [b] Determined by GPC based on polystyrene standards (eluent: THF). [c] Conversion of **2** to polymer: 87%; isolated yield: 71%.

It has been shown that the addition of LiCl to Kumada CTP reactions can have beneficial effects on the chain-growth polymerization characteristics of aryl-Grignard monomers. For example, Yokozawa and coworkers reported that the addition of LiCl conferred controlled, chain-growth characteristics to the polymerization of 1-bromo-4-chloromagnesio-2,5-dihexyloxybenzene to afford poly(*p*-phenylene)s with high molecular weights and narrow *Đ*s (e.g., 1.18).[16] We thus performed the polymerization of **2** with the aforementioned Ni catalysts in the presence of 1.0 equiv of LiCl. As shown in Table 2.1, the addition of LiCl had little effect on the polymerization when Ni(dppe)Cl_2 was used as the catalyst, as the molecular weight of PTPP remained unchanged from that which was obtained from the corresponding reaction without LiCl, although a slight

decrease in dispersity was observed (entry 3). When Ni(dppp)Cl_2 was used, however, the M_n of the resulting polymer increased significantly compared to that obtained from the analogous polymerization without LiCl, while the dispersity of the polymer remained relatively low (entry 4). After quenching the polymerization with HCl (aq.), the pure homopolymer, poly(thiophene-*alt*-*p*-phenylene) (PTPP), was isolated in 71% yield by means of precipitation from methanol, followed by collection with the aid of vacuum filtration. When the polymerization was repeated in the presence of an internal standard (1,4-dihexyloxybenzene) and monitored over time by ^{1}H NMR spectroscopy, we found that the polymerization proceeded rapidly at 23 °C, consuming 87% of **2** within 15 min (Figure 2.1). Substituting ^{t}BuMgCl for ^{i}PrMgCl to facilitate the Grignard metathesis reaction did not lead to any significant molecular weight increase or narrowing of the dispersity of the respective polymers (entries 5 and 6).

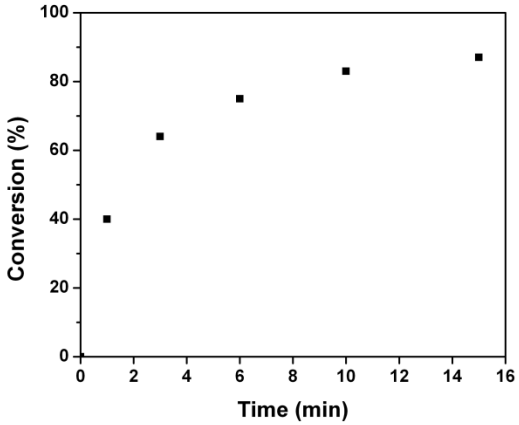

Figure 2.1: Monomer conversion as a function of polymerization time. Conversion was determined by ^{1}H NMR spectroscopy ($CDCl_3$) using 1,4-dihexyloxybenzene as an internal standard.

Elegant mechanistic studies by McNeil and co-workers revealed that the role of LiCl in the controlled formation of poly(*p*-phenylene) and P3HT depends on the catalyst

used. In Ni(dppe)Cl_2-catalyzed polymerizations, LiCl was found to have no effect on the polymerization rate, whereas in the Ni(dppp)Cl_2-catalyzed polymerizations a rate dependence on LiCl was observed.[18,19] Our results are thus consistent with these observations: The addition of LiCl had a significant effect on the polymerization of **2** when Ni(dppp)Cl_2 was used as the catalyst, affording PTPP with a high molecular weight and low dispersity. Conversely, LiCl had little effect on the polymerization when Ni(dppe)Cl_2 was used. We therefore presume that the polymerization of **2**, as catalyzed by Ni(dppp)Cl_2, exhibits a rate dependence on [LiCl]. To the extent this is true, it may serve to explain the rapid kinetics of polymerization observed in the presence of LiCl.

The M_n of the PTPP obtained using Ni(dppp)Cl_2 as the catalyst in the presence of 1.0 equiv LiCl (M_n = 14500 Da, M_w/M_n = 1.33) was close to the theoretically expected value of 13700 Da, assuming both quantitative initiation and conversion of monomer to polymer. These results suggested to us that the polymerization was proceeding via a chain-growth mechanism. To probe whether the polymerization was controlled, the molecular weight of the polymer formed in the reaction was monitored as a function of monomer conversion. Briefly, a polymerization reaction was set up under the aforementioned conditions (i.e., catalyst = Ni(dppp)Cl_2, 1.0 equiv LiCl, 23 °C in THF) at an initial monomer to catalyst ratio of 56 in the presence of an internal standard (1,4-dihexyloxybenzene); aliquots were then removed at regular intervals, quenched with aq. HCl, and poured into excess methanol. After collection of the precipitated solids via filtration, the isolated polymers and filtrates were analyzed by GPC and ^{1}H NMR spectroscopy, respectively.

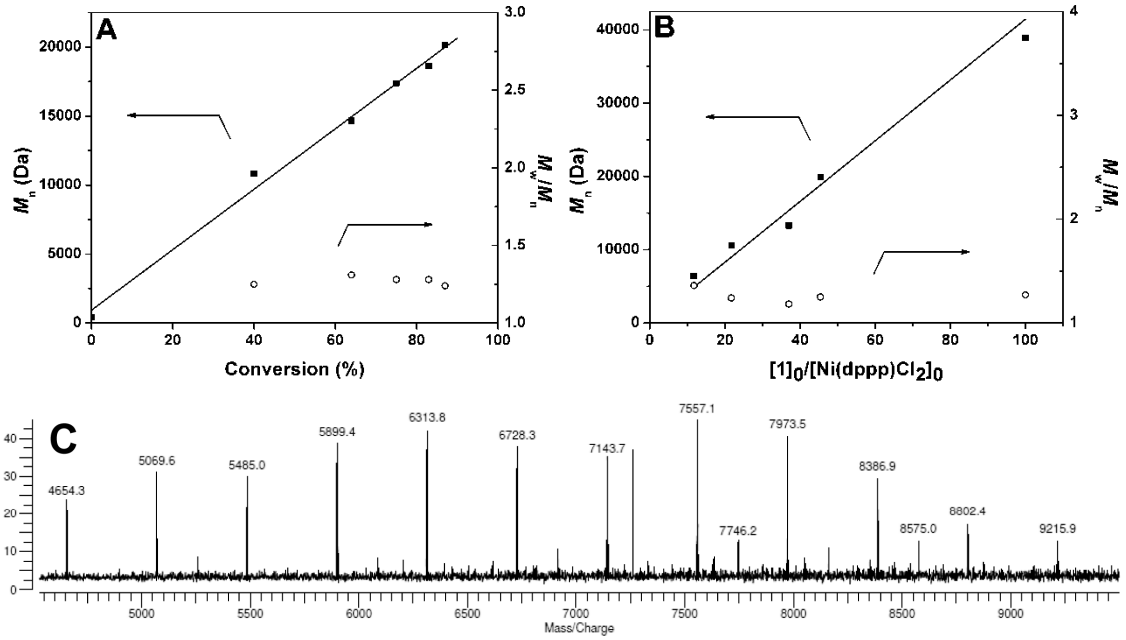

Figure 2.2: (A) M_n and M_w/M_n of PTPP plotted as a function of monomer conversion ([**1**]$_0$/[Ni(dppp)Cl$_2$]$_0$ = 56); see text for further details. (B) M_n and M_w/M_n of PTPP plotted as a function of Ni(dppp)Cl$_2$ loading (conversion of **2** to polymer: 78–85%). Solid line indicates the theoretically expected M_n at a given Ni(dppp)Cl$_2$ loading. (C) MALDI mass spectrum of PTPP (M_n = 10800 Da, M_w/M_n = 1.25, as determined by GPC). The peak at m/z ~ 7257 reflects electronic noise. For all polymerizations, [**1**]$_0$ = 0.10 M.

As shown in Figure 2.2A, a linear dependence of the M_n versus the percent conversion of monomer over the course of the polymerization was observed. Moreover, the *Đ*s of the isolated polymers remained at or below 1.3 over the course of the polymerization reaction. When the polymerization of **2** was performed using varying initial catalyst loadings, the M_n increased proportionally with the initial monomer to catalyst ratio ([**1**]$_0$/[Ni(dppp)Cl$_2$]$_0$) while *Đ*s remained relatively low (Figure 2.2B), indicating that the molecular weight of PTPP was successfully controlled over a wide M_n range (i.e., 6.4 to 39 kDa). Furthermore, the experimentally determined M_n values were in good agreement with the theoretically expected values at all of the initial catalyst loadings explored.

Taken together, these results suggested to us that the polymerization followed a controlled chain-growth mechanism. It is also worth noting that PTPP, even at high molecular weights, maintained excellent solubility in THF (ca. 80 mg mL^{-1}), presumably due to the presence of the branched alkoxy side-chains in every repeat unit.

Endgroup analysis using matrix-assisted laser desorption ionization (MALDI) mass spectrometry has been shown to provide important insight into polymerization mechanisms.[2,8,20] We therefore obtained MALDI mass spectra of a sample of PTPP (isolated after quenching the polymerization with HCl). As shown in Figure 2.2C, we observed a major population of signals that corresponded to H_2O adducts of H/Br end-capped PTPP, as calculated by the formula: 414.3*n* (mass of *n* repeat units) + 1 (H) + 79.9 (Br) + 18 (H_2O).[21] The presence of H/Br end-capped polymers, along with a negligible population of polymers bearing Br/Br or H/H endgroups, is a hallmark of efficient catalyst transfer in self-initiated catalyst transfer polycondensation reactions.[2,20] Collectively, these results suggested to us that nearly every polymer grew via catalyst transfer to the end of the polymer chain, as opposed to the catalyst freely diffusing through the reaction mixture to initiate a new polymerization or transferring to another chain. Therefore, we concluded that the polymerization proceeded through a chain-growth mechanism with minimal chain termination (Scheme 2.2).

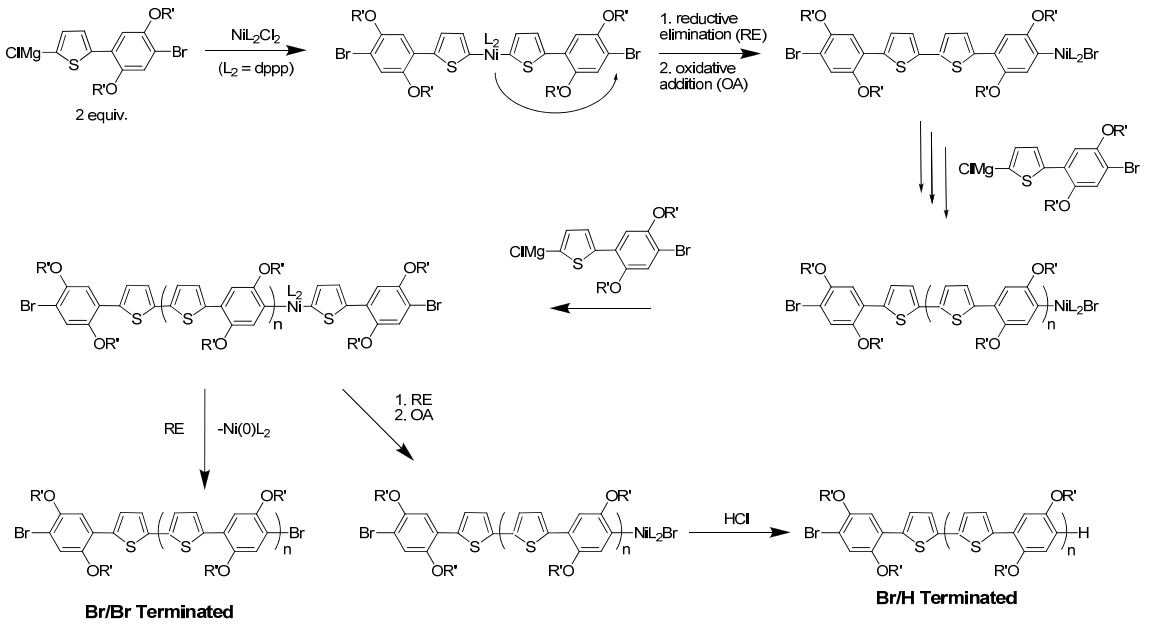

Scheme 2.2: Proposed mechanistic pathways leading to the formation of H/Br end-capped PTPP.

To further demonstrate the controlled, chain-growth nature of the aforementioned Kumada CTPs, a series of chain extension and block copolymerization experiments were performed. First, a monomer addition experiment was conducted, wherein a fresh feed of monomer **2** was added to an unquenched, stirring solution of PTPP (PTPP-1) (initial conditions: $[\mathbf{1}]_0/[\text{Ni(dppp)Cl}_2]_0 = 20$; conversion of **2** to PTPP-1: 80%; PTPP-1 M_n = 8700 Da, $M_w/M_n = 1.25$). As shown in Figure 2.3A, the GPC trace of the polymer formed at the conclusion of this reaction (PTPP-1') was clearly shifted toward higher molecular weight ([remaining and added $\mathbf{1}]_0/[\text{Ni(dppp)Cl}_2]_0 = 31$; PTPP-1': conversion of **2** = 72%, M_n = 17000 Da, $M_w/M_n = 1.29$) with respect to PTPP-1. No discernible signal attributable to the presence of unreacted PTPP-1 was observed, suggesting to us that the added feed of **2** was successfully polymerized via chain extension from the terminus of PTPP-1.

We subsequently shifted our attention to the formation of diblock copolymers, choosing to incorporate P3HT as the second block because of its well-behaved

polymerization behavior via Kumada CTP (Scheme 2.3).[9] As shown in Figure 2.3B, addition of 2-bromo-5-chloromagnesio-3-hexylthiophene[20] (**3**) to an unquenched solution of PTPP (M_n = 11600 Da, M_w/M_n = 1.29) afforded a polymer with a monomodal GPC profile that was of higher molecular weight (M_n = 21900 Da) than that obtained for its parent PTPP homopolymer. Furthermore, the dispersity of the product remained low ($Đ$ = 1.33). This is consistent with the notion that the unquenched PTPP in solution was active and effectively initiated the polymerization of **3**, which proceeded in a chain-growth manner. The formation of a diblock copolymer, consistent with the expected structure (i.e., PTPP-*b*-P3HT), was further confirmed by ^{1}H NMR spectroscopy, which revealed signals attributable to both PTPP and P3HT (Figure A1).

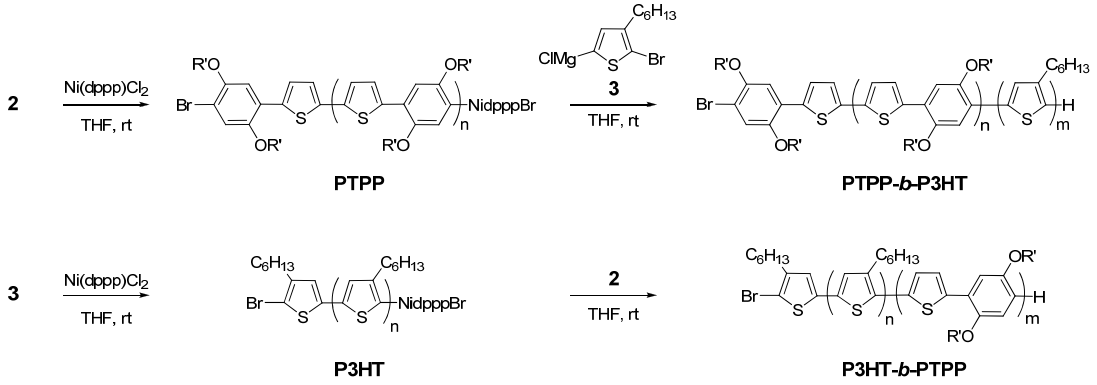

Scheme 2.3: Synthesis of diblock copolymers PTPP-*b*-P3HT and P3HT-*b*-PTPP. R' = 2-ethylhexyl.

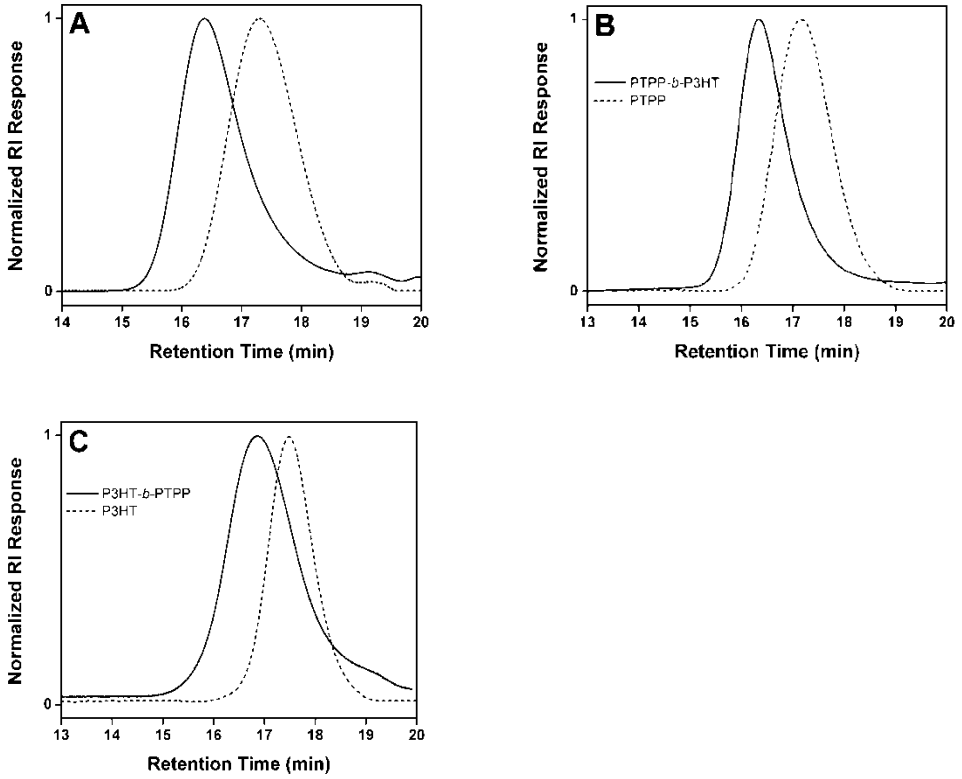

Figure 2.3: GPC traces of polymers obtained from chain extension polymerization experiments. (A) A monomer addition experiment: PTPP-1 (dashed line) ([**1**]$_0$/[Ni(dppp)Cl$_2$]$_0$ = 20, conversion of **2** to polymer: 80%; PTPP-1: M_n = 8700 Da, M_w/M_n = 1.25); PTPP-1' (solid line) ([remaining and added **1**]$_0$/[Ni(dppp)Cl$_2$]$_0$ = 31; conversion of **2** to polymer: 72%; PTPP-1': M_n = 17000 Da, M_w/M_n = 1.29). (B) A block copolymerization experiment (polymerization order: PTPP followed by P3HT). PTPP (dashed line): [**1**]$_0$/[Ni(dppp)Cl$_2$]$_0$ = 18, conversion of **2** to polymer: 86%; polymer: M_n = 11600 Da, M_w/M_n = 1.29. PTPP-*b*-P3HT (solid line): [**3**]$_0$/[Ni(dppp)Cl$_2$]$_0$ = 51, conversion of **3** to polymer: 96%; polymer: M_n = 21900 Da, M_w/M_n = 1.33. (C) A block copolymerization experiment (polymerization order: P3HT followed by PTPP). P3HT (dashed line): [**3**]$_0$/[Ni(dppp)Cl$_2$]$_0$ = 60; conversion of **3** to polymer: 84%; polymer: M_n = 7500 Da, M_w/M_n = 1.22. P3HT-*b*-PTPP (solid line): [**1**]$_0$/[Ni(dppp)Cl$_2$]$_0$ = 24, conversion of **2** to polymer: 67%; polymer: M_n = 9200 Da, M_w/M_n = 1.70.

Considering recent reports that have shown that the order of polymerization can affect the outcome of block copolymerizations involving Kumada CTPs,[13,17,22] we next attempted to synthesize the aforementioned diblock copolymer P3HT-*b*-PTPP by reversing the order of monomer addition. Thus, a THF solution of **2** ($[\mathbf{1}]_0/[Ni(dppp)Cl_2]_0$ = 24) was added to a stirring solution of unquenched P3HT (M_n = 7500 Da, M_w/M_n = 1.22). In this case, the resulting copolymer (M_n = 9200 Da, M_w/M_n = 1.70) displayed a broader molecular weight distribution than the parent P3HT homopolymer, and the conversion of **2** remained relatively low (conversion of **2** to polymer: 67%), even after prolonged reaction periods (Figure 2.3C). This result suggested to us that P3HT was not an efficient macroinitiator for the polymerization of PTPP, possibly due to the strong association of the Ni catalyst with P3HT.[17,23] Nevertheless, successful chain extension polymerizations of PTPP were achieved, which provided additional support that chain-growth polymerization of **2** proceeded in a controlled fashion.

The absorption and fluorescence spectra of the PTPP synthesized using the aforementioned procedures were acquired in dilute $CHCl_3$ solution and in the solid state (as thin films) (Figure 2.4). A slight bathochromic shift was observed in the respective absorption spectra upon concentration (λ_{max} = 467 nm $\rightarrow$ 477 nm), with a small shoulder appearing at 500 nm for the thin film. The emission spectra of PTPP in solution and as a thin film exhibited maxima at 523 nm and 629 nm, respectively. These results were consistent with those obtained for similar copolymers (e.g., poly(alkoxyphenylene-thienylene)s) previously reported in the literature.[15,24-27] The absorption spectra of the diblock copolymer PTPP-*b*-P3HT were also recorded in dilute $CHCl_3$ solution as well as in the solid state as a thermally annealed thin film (Figure 2.4). In this case, a large red shift of absorption was observed upon concentration (λ_{max} = 464 $\rightarrow$ 505 nm), likely a consequence of the π–π stacking and subsequent planarization of the P3HT chains.[28,29]

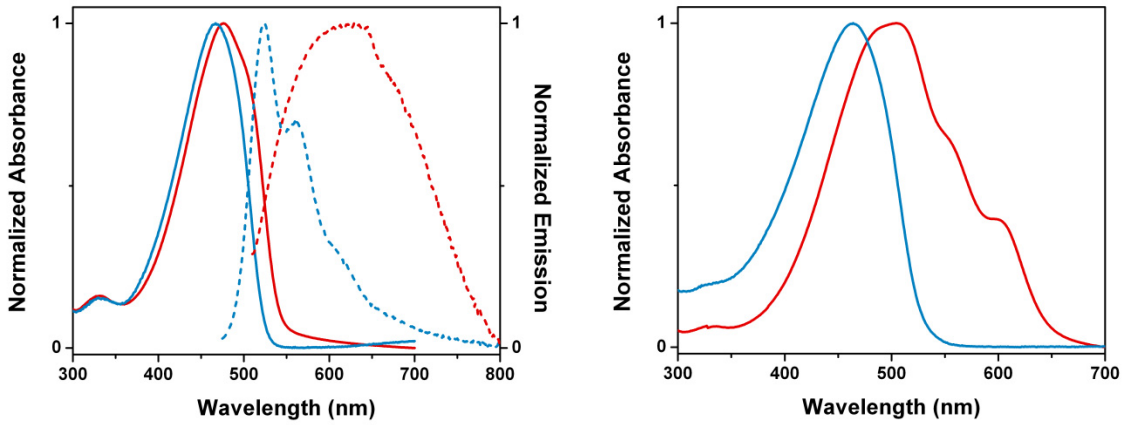

Figure 2.4: (left) Absorption (solid lines) and fluorescence (dashed lines) spectra of PTPP in chloroform (blue) and as thin films (spin-coated from chloroform) (red). (right) Absorption spectra of block copolymer PTPP-*b*-P3HT in chloroform (blue) and as thin films (spin-coated from chloroform) (red).

Moreover, vibronic structures reminiscent of P3HT homopolymer thin films were clearly visible at 560 and 605 nm. Compared to the solid state absorption of a P3HT homopolymer, however, the corresponding spectrum of PTPP-*b*-P3HT exhibited an absorption maximum at higher energies (λ_{max} = 560[30] and 505 nm for P3HT homopolymer and PTPP-*b*-P3HT, respectively). We believe that the solid state spectrum of PTPP-*b*-P3HT reflects the summed profiles of PTPP and P3HT homopolymers; thus, the blue-shifted λ_{max} of PTPP-*b*-P3HT compared to that of P3HT is a consequence of the overwhelming contribution of PTPP to the absorption profile of the copolymer, rather than a morphological and/or energy transfer effect. Regardless, the absorption characteristics of PTPP-*b*-P3HT should be amenable to further fine-tuning by controlling the relative block lengths of the respective polymers, an otherwise laborious synthetic task that is effectively streamlined by the methodologies presented here. This thus highlights the potential utility of Kumada CTPs for producing conjugated alternating copolymers with tunable optical properties.

2.3 CONCLUSION

In conclusion, we have demonstrated that Kumada catalyst transfer polycondensation is a viable method for synthesizing well-defined conjugated *alt*-copolymers. We found that controlled chain-growth characteristics were conferred to the polymerization when Ni(dppp)Cl_2 was used as the catalyst in the presence of LiCl. This result is consistent with efficient intramolecular catalyst transfer within the growing polymer backbone, despite the relatively large length of the repeat unit. As a benefit of this chain-growth mechanism, excellent control over copolymer molecular weight, dispersity, and endgroup composition was obtained, all of which facilitated the successful preparation of a new, well-defined block copolymer, PTPP-*b*-P3HT. These results show, for the first time, that conjugated polymers with alternating repeating units can be synthesized in a controlled, chain-growth manner. Many low-bandgap and D–A conjugated polymers exhibit complex, alternating structures, but are currently synthesized by means that do not permit the aforementioned degree of control over the polymerization. It is expected that the method presented herein will be amenable to attaining control over the synthesis of such D–A and other conjugated polymers, and enable access to more complex macromolecular structures thereof.

2.4 EXPERIMENTAL

2.4.1 General Considerations

All solvents were purchased from Fisher Scientific and used without additional further purification unless otherwise noted. All other chemicals were purchased from Aldrich, Alfa Aesar, or Fisher, and were used as received. 1,4-Dibromo-2,5-di(2-ethylhexyloxy)benzene[31] and 2-bromo-5-chloromagnesio-3-hexylthiophene[20] were prepared according to literature procedures. THF was distilled over Na/benzophenone

ketyl prior to use. Proton and $^{13}C[^{1}H]$ NMR spectra were recorded using a Varian 400 MHz spectrometer. Chemical shifts are reported in delta (δ) units and expressed in parts per million (ppm) downfield from tetramethylsilane using the residual solvent as an internal standard. For ^{1}H NMR: $CDCl_3$, 7.24 ppm. For ^{13}C NMR: $CDCl_3$, 77.0 ppm. Coupling constants (J) are expressed in Hertz. Gel permeation chromatography (GPC) was performed using THF as the eluent on a Viscotek GPCmax Solvent/Sample Module, two fluorinated polystyrene columns (IMBHW-3078 and I-MBLMW-3078) thermostatted at 24 °C arranged in series, and a Viscotek VE 3580 Refractive Index Detector or a Viscotek 2600 Photodiode Array Detector (tuned at 460 nm). Molecular weight and dispersity data are reported relative to polystyrene standards in THF. UV/vis spectra were recorded using a Perkin Elmer Instruments Lambda 35 spectrometer. Emission spectra were recorded using a Horiba Jobin Yvon Fluorolog3 fluorimeter. Microanalyses were performed by Midwest Microlabs, LLC (Indianapolis, IN). High resolution mass spectra (HRMS) were obtained with a VG analytical ZAB2-E instrument (ESI or CI). MALDI mass spectra were obtained on a 12T Varian ProMALDI FT-ICR system equipped with a Nd:YAG laser (355 nm) using 2,5-dihydroxybenzoic acid (DHB) as the matrix.

2.4.2 Syntheses

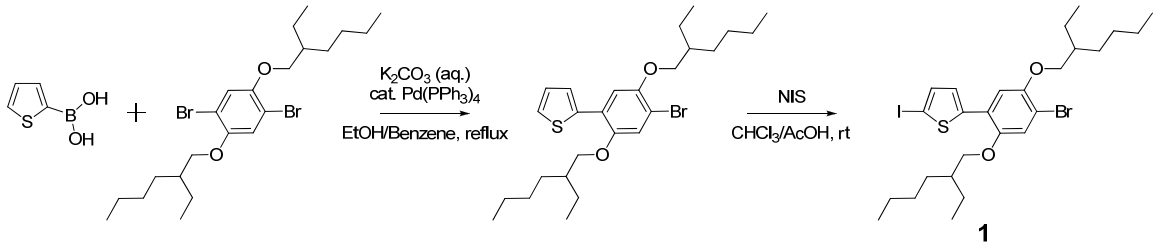

Scheme 2.4: Synthesis of **1**.

Synthesis of 2-(4-bromo-2,5-bis(2-ethylhexyloxy)phenyl)thiophene. An oven-dried, 100 mL two neck flask was charged with a stirbar, 2-thiopheneboronic acid (0.387 g, 3.0 mmol), 1,4-dibromo-2,5-di(2-ethylhexyloxy)benzene (2.23 g, 4.53 mmol), benzene (25 mL), and ethanol (25 mL). Upon dissolution of the solids, 2 M K_2CO_3 (aq.) (7.5 mL) and $Pd(PPh_3)_4$ (0.173 g, 0.15 mmol) were added. The flask was fitted with a water-jacketed condenser and a rubber septum, and the reaction mixture was subjected to three consecutive freeze-pump-thaw cycles. The mixture was then heated to reflux and stirred for 18 h under an atmosphere of N_2. After concentrating the reaction mixture under reduced pressure to remove the residual benzene and ethanol, the crude material was taken up in hexanes (100 mL), washed with water (2×100 mL) and brine (75 mL), dried over Na_2SO_4, and concentrated to an oil. The crude product was purified by column chromatography (silica gel; eluent: hexanes for first band, followed by 99:1 v/v hexanes:dichlormethane) to afford the desired product as a pale yellow oil (yield: 0.997 g, 67%). ^{1}H NMR ($CDCl_3$, 400 MHz): δ 0.90 (m, 12H), 1.25–1.60 (m, 16H), 1.76 (m, 2H), 3.88 (m, 4H), 7.06 (dd, *J* = 4 Hz, 1H), 7.13 (s, 1H), 7.15 (s, 1H), 7.32 (d, *J* = 4 Hz, 1H), 7.45 (d, J = 2.4 Hz, 1H). ^{13}C NMR ($CDCl_3$, 100 MHz): δ 11.10, 11.19, 14.07, 14.09, 22.99, 23.04, 23.88, 23.93, 29.02, 29.07, 30.48, 30.51, 39.48, 71.90, 72.45, 111.28, 113.59, 117.55, 123.05, 125.38, 125.71, 126.62, 138.82, 149.65, 149.72. HRMS m/z calcd for $C_{26}H_{39}BrO_2S$ $[M+H]^+$: 494.1854; Found: 494.1851. Anal. calcd for $C_{26}H_{39}BrO_2S$: C, 63.02; H, 7.93. Found: C, 63.17; H, 8.04.

Synthesis of 2-(4-bromo-2,5-bis(2-ethylhexyloxy)phenyl)-5-iodothiophene (1). A 50 mL round bottom flask was charged with a stir bar, 2-(4-bromo-2,5-bis(2-ethylhexyloxy)phenyl)thiophene (0.997 g, 2 mmol), chloroform (20 mL), and acetic acid (10 mL). N-iodosuccinimide (0.453 g, 2 mmol) was then added to this mixture over a period of 5 min. The resulting reaction mixture was stirred at room temperature for 3 h.

The mixture was then transferred to a separatory funnel, diluted with dichloromethane (50 mL), washed with water (3×75 mL) and brine (50 mL), dried over Na_2SO_4, and concentrated to an oil. The crude product was purified by column chromatography (silica gel; eluent: hexanes) to afford the desired product as a pale yellow oil (yield: 1.08 g, 86%). ^{1}H NMR ($CDCl_3$, 400 MHz): δ 0.87–0.96 (m, 12H), 1.25–1.60 (m, 16H), 1.70–1.85 (m, 2H), 3.86 (d, J = 5.6 Hz, 4H), 7.08 (s, 1H), 7.10 (d, J = 4 Hz, 1H), 7.12 (s, 1H), 7.19 (d, J = 4 Hz, 1H). ^{13}C NMR ($CDCl_3$, 100 MHz): δ 11.11, 11.19, 14.09, 14.12, 23.02, 23.87, 23.91, 29.034, 29.07, 30.45, 30.57, 39.41, 39.47, 72.17, 72.42, 74.66, 111.84, 112.44, 117.48, 122.16, 126.08, 136.25, 144.66, 149.39, 149.76. HRMS m/z calcd for $C_{26}H_{38}BrIO_2S$ $[M+H]^+$: 620.0821; Found: 620.0817. Anal. calcd for $C_{26}H_{38}BrIO_2S$: C, 50.25; H, 6.16. Found: C, 50.39; H, 6.26.

General Polymerization Procedure. To an oven dried 25 mL Schlenk flask was added **1** (446 mg, 0.708 mmol), LiCl (0.5 M in THF; 1.42 mL), THF (6 mL), and 1,4-dihexyloxybenzene (25 mg) as an internal standard. After cooling to 0 °C, ^{i}PrMgCl (2.0 M in THF; 0.35 mL) was added, and the reaction mixture stirred for 20 min. An aliquot of the mixture (0.2 mL) was removed for analysis, and the reaction mixture was warmed to room temperature. Ni(dppp)Cl_2 (11.5 mg, 0.0212 mmol) was then added in one portion to initiate the polymerization. Aliquots were removed periodically to monitor the progress of the polymerization. When it was determined that the reaction was complete (~20–30 min), 6 M HCl (2 mL) was added to the mixture to quench the polymerization, and excess methanol was added which caused a precipitate to form. The polymer product was collected by vacuum filtration, washed with methanol, and obtained as an orange powder (yield: 209 mg, 71%). GPC: M_n = 14900 Da, M_w/M_n = 1.23. ^{1}H NMR ($CDCl_3$, 400 MHz): δ 0.89 (s, 6H), 0.97 (s, 6H), 1.34–1.65 (m, 20H), 1.88 (br, 2H), 4.03 (br s, 4H), 7.31 (s, 2H), 7.60 (s, 2H).

Block Copolymerization Procedure. To an oven dried 25 mL Schlenk flask was added **1** (190 mg, 0.306 mmol), LiCl (0.5M in THF; 0.61 mL), THF (3 mL), and 1,4-dihexyloxybenzene (15 mg) as an internal standard. After cooling to 0 °C, ^{i}PrMgCl (2.0 M in THF; 0.15 mL) was added, and the reaction mixture stirred for 20 min. An aliquot of the mixture (0.2 mL) was removed for analysis, and the reaction mixture was warmed to room temperature. Ni(dppp)Cl_2 (9.2 mg, 0.018 mmol) was then added in one portion to initiate the polymerization. After 30 min of stirring at room temperature, GPC and ^{1}H NMR analysis of an aliquot removed from the reaction mixture showed that the polymer prepared *in situ* exhibited the following characteristics: M_n = 11600 Da, M_w/M_n = 1.29, conversion of **2** = 86%. Using a nitrogen flushed syringe, a solution of 1:1 2-bromo-5-chloromagnesio-3-hexylthiophene:LiCl in THF (0.2M; 4.3 mL) was then added to the polymerization reaction. The resulting mixture was stirred for a further 1 h at room temperature, then 6 M HCl (2 mL) was added to the mixture to quench the polymerization, and excess methanol was added which caused a precipitate to form. The polymer product was collected by vacuum filtration, washed with methanol and obtained as a dark purple solid (yield: 168 mg, 62%). GPC: M_n = 21900 Da, M_w/M_n = 1.33. ^{1}H NMR ($CDCl_3$, 400 MHz): δ 0.89–0.92 (br, Ph CH_3), 0.96–0.99 (t, thiophene CH_3), 1.32–1.70 (m, thiophene and Ph CH_2), 1.80–1.90 (m, Ph C*H*), 2.79 (t, thiophene CH_2), 4.04 (d, Ph OCH_2), 6.97 (s, thiophene Ar*H*), 7.32 (s, Ph Ar*H*), 7.60 (s, Ph Ar*H*).

2.5 ACKNOWLEDGMENTS

Portions of this chapter were reprinted with permission from Ono, R. J.; Kang, S.; Bielawski, C. W. *Macromolecules* **2012**, *45*, 2321-2326. Copyright 2012 American Chemical Society. Songsu Kang is gratefully acknowledged for assistance with the

monomer synthesis. Prof. Christopher W. Bielawski is also gratefully acknowledged for helping to write the original manuscript.

2.6 REFERENCES

(1) Sheina, E. E.; Liu, J.; Iovu, M. C.; Laird, D. W.; McCullough, R. D. *Macromolecules* **2004**, *37*, 3526-3528.

(2) Miyakoshi, R.; Yokoyama, A.; Yokozawa, T. *J. Am. Chem. Soc.* **2005**, *127*, 17542-17547.

(3) Liang, Y.; Feng, D.; Wu, Y.; Tsai, S.-T.; Li, G.; Ray, C.; Yu, L. *J. Am. Chem. Soc.* **2009**, *131*, 7792-7799.

(4) Peet, J.; Kim, J. Y.; Coates, N. E.; Ma, W. L.; Moses, D.; Heeger, A. J.; Bazan, G. C. *Nat. Mater.* **2007**, *6*, 497-500.

(5) Cheng, Y.-J.; Yang, S.-H.; Hsu, C.-S. *Chem. Rev.* **2009**, *109*, 5868-5923.

(6) Adachi, T.; Brazard, J.; Ono, R. J.; Hanson, B.; Traub, M. C.; Wu, Z.-Q.; Li, Z.; Bolinger, J. C.; Ganesan, V.; Bielawski, C. W.; Vanden Bout, D. A.; Barbara, P. F. *J. Phys. Chem. Lett.* **2011**, *2*, 1400-1404.

(7) Segalman, R. A.; McCulloch, B.; Kirmayer, S.; Urban, J. J. *Macromolecules* **2009**, *42*, 9205-9216.

(8) Elmalem, E.; Kiriy, A.; Huck, W. T. S. *Macromolecules* **2011**, *44*, 9057-9061.

(9) Proper spacial arrangement of neighboring aromatic rings has been shown to promote the controlled chain-growth Kumada CTP of a nonconjugated monomer, 3-(5-bromo-2-thienyl)-3-(5-iodo-2-thienyl)nonane. See: Wu, S.; Sun, Y.; Huang, L.; Wang, J.; Zhou, Y.; Geng, Y.; Wang, F. *Macromolecules* **2010**, *43*, 4438-4440.

(10) Beryozkina, T.; Senkovskyy, V.; Kaul, E.; Kiriy, A. *Macromolecules* **2008**, *41*, 7817-7823.

(11) Huang, L.; Wu, S.; Qu, Y.; Geng, Y.; Wang, F. *Macromolecules* **2008**, *41*, 8944-8947.

(12) Javier, A. E.; Varshney, S. R.; McCullough, R. D. *Macromolecules* **2010**, *43*, 3233-3237.

(13) Wu, S.; Bu, L.; Huang, L.; Yu, X.; Han, Y.; Geng, Y.; Wang, F. *Polymer* **2009**, *50*, 6245-6251.

(14) Stefan, M. C.; Javier, A. E.; Osaka, I.; McCullough, R. D. *Macromolecules* **2008**, *42*, 30-32.

(15) Wang, F.; Wilson, M. S.; Rauh, R. D.; Schottland, P.; Thompson, B. C.; Reynolds, J. R. *Macromolecules* **2000**, *33*, 2083-2091.

(16) Miyakoshi, R.; Shimono, K.; Yokoyama, A.; Yokozawa, T. *J. Am. Chem. Soc.* **2006**, *128*, 16012-16013.

(17) Miyakoshi, R.; Yokoyama, A.; Yokozawa, T. *Chem. Lett.* **2008**, *37*, 1022-1023.

(18) Lanni, E. L.; McNeil, A. J. *Macromolecules* **2010**, *43*, 8039-8044.

(19) Lanni, E. L.; McNeil, A. J. *J. Am. Chem. Soc.* **2009**, *131*, 16573-16579.

(20) Lohwasser, R. H.; Thelakkat, M. *Macromolecules* **2011**, *44*, 3388-3397.

(21) The signals observed at m/z 7746 and 8575 were assigned to an H/I terminated polymer as adducts of Li and dihydroxybenzoic acid (DHB, the matrix material) according to the following formula: 414.3*n* (mass of *n* repeat units) + 1 (H) + 127 (I) + 7 (Li) + 154 (DHB). An H/I terminated polymer can arise from the generation of a small concentration of (2,5-bis(2-ethylhexyloxy)-4-(5-iodothiophen-2-yl)phenyl)magnesium chloride formed during the Grignard metathesis reaction, where the metalation of **1** occurs at the phenyl instead of at the thiophene moiety. This monomer can then initiate a polymerization reaction, thereby establishing an iodo group on one end of a polymer chain and, after catalyst transfer and quenching with HCl, a hydrogen group on the other.

(22) Yokoyama, A.; Kato, A.; Miyakoshi, R.; Yokozawa, T. *Macromolecules* **2008**, *41*, 7271-7273.

(23) Tkachov, R.; Senkovskyy, V.; Komber, H.; Sommer, J.-U.; Kiriy, A. *J. Am. Chem. Soc.* **2010**, *132*, 7803-7810.

(24) Bao, Z.; Chan, W.; Yu, L. *Chem. Mater.* **1993**, *5*, 2-3.

(25) Kim, Y. g.; Galand, E. M.; Thompson, B. C.; walker, J.; Fossey, S. A.; McCarley, T. D.; Abboud, K. A.; Reynolds, J. R. *J. Macromol. Sci., Part A: Pure Appl. Chem.* **2007**, *44*, 665-674.

(26) Lere-Porte, J.-P.; Moreau, J. J. E.; Serein-Spirau, F.; Torreilles, C.; Righi, A.; Sauvajol, J.-L.; Brunet, M. *J. Mater. Chem.* **2000**, *10*, 927-932.

(27) Tanese, M. C.; Farinola, G. M.; Pignataro, B.; Valli, L.; Giotta, L.; Conoci, S.; Lang, P.; Colangiuli, D.; Babudri, F.; Naso, F.; Sabbatini, L.; Zambonin, P. G.; Torsi, L. *Chem. Mater.* **2005**, *18*, 778-784.

(28) Xu, B.; Holdcroft, S. *Macromolecules* **1993**, *26*, 4457-4460.

(29) Kiriy, N.; Jähne, E.; Adler, H.-J.; Schneider, M.; Kiriy, A.; Gorodyska, G.; Minko, S.; Jehnichen, D.; Simon, P.; Fokin, A. A.; Stamm, M. *Nano Lett.* **2003**, *3*, 707-712.

(30) Liu, C.-Y.; Holman, Z. C.; Kortshagen, U. R. *Nano Lett.* **2008**, *9*, 449-452.

(31) Chen, Z.-K.; Lee, N. H. S.; Huang, W.; Xu, Y.-S.; Cao, Y. *Macromolecules* **2003**, *36*, 1009-1020.

Chapter 3: Controlled Catalyst Transfer Polycondensation and Surface-Initiated Polymerization of a p-Phenyleneethynylene-Based Monomer

3.1 Introduction

Poly(phenyleneethynylene)s (PPEs) are an important and versatile class of conjugated polymers that have found use in light emitting diodes,[1] explosives detection,[2] and molecular wires,[3] among other applications. The aforementioned polymers are most commonly prepared by condensing a 1,4-dihaloarene with a 1,4-diethynylbenzene using Sonogashira-type cross coupling chemistry[4] or by alkyne metathesis of a diyne,[5] although some variants of both methodologies are known. In all cases, however, the corresponding polymerizations proceed via a step-growth mechanism which precludes an ability to rigorously control the important properties exhibited by the polymer produced, including molecular weight, dispersity, and end-group fidelity when semi- or hetero-telechelic polymers are desired. Moreover, the lack of synthetic control often leads to ill-defined materials or batch-to-batch sample inconsistencies. A controlled, chain-growth polymerization of a phenyleneethynylene would not only alleviate the aforementioned drawbacks, but also enable the preparation of more complex PPE-containing macromolecular structures, such as block copolymers and surface-grafted polymer brushes, thereby facilitating the realization of applications long envisioned for PPEs.[4,5]

We postulated that a step-growth polymerization of phenyleneethynylene may be transformed into a chain-growth process by developing a suitable catalyst transfer polycondensation (CTP) method. Chain-growth CTP has been successfully utilized for the controlled synthesis of conjugated polymers including polythiophenes,[6] polyfluorenes,[7] and polyphenylenes,[8] as well as for the preparation of more complex donor–acceptor-type alternating copolymers.[9,10] Mechanistically, it is generally accepted

that CTPs undergo the same oxidative addition–reductive elimination cycles that are typical of transition metal-catalyzed cross-coupling reactions; however, their distinguishing feature is that the oxidative addition of the catalyst occurs in an intra-chain fashion that facilitates "living" chain-growth-like behavior of the corresponding polymerization. Herein the controlled chain-growth synthesis of PPE via a modified Stille-type CTP will be discussed.

3.2 Results and Discussion

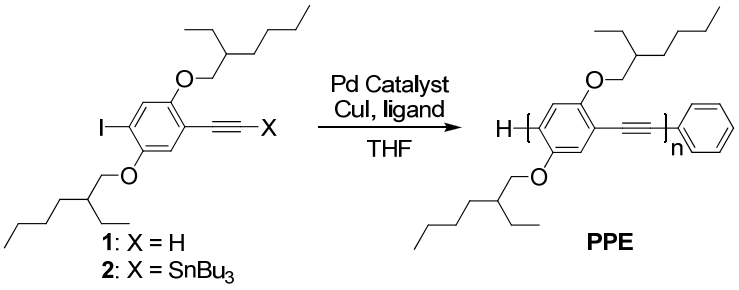

Scheme 3.1: Chain-growth synthesis of PPE. Pd Catalyst = PhPd(*t*-Bu_3P)Br; ligand: see Table 3.1.

As summarized in Scheme 3.1, initial efforts were directed toward the polymerization of 1,4-bis(2-ethylhexyloxy)-2-ethynyl-5-iodobenzene (**1**) using Sonogashira-coupling conditions. PhPd(*t*-Bu_3P)Br gave high molecular weight, monodisperse polymer in good yield. For example, treatment of **1** ($[\mathbf{1}]_0$ = 0.020 M) with copper iodide (20 mol%), PPh_3 (20 mol%), and PhPd(*t*-Bu_3P)Br[11] (2 mol%) in THF at 25 °C afforded a PPE in 58% yield (Table 3.1, entry 1). While the aforementioned reaction conditions did provide polymer of a desirable number-averaged molecular weight (M_n) and dispersity ($Đ$) (M_n = 10800, $Đ$ = 1.28), the low conversion of monomer **1** to polymer prompted the exploration of other conditions to optimize the polymerization reaction. Attention was directed toward using a stannylated monomer, ((2,5-bis(2-

ethylhexyloxy)-4-iodophenyl)ethynyl)tributylstannane (**2**), as alkynyltin reagents under Stille-type conditions have been shown to be more reactive than the corresponding terminal alkynes.[12,13] Indeed, under otherwise identical reaction conditions, the polymerization of **2** proceeded to high conversion (>99%) within 3 h, and a PPE was obtained by precipitation from methanol as a yellow solid in 94% yield (Table 3.1, entry 7). The isolated polymer exhibited a M_n of 14.4 kDa, a value close to the theoretically expected M_n of 17.8 kDa assuming quantitative initiation and complete consumption of monomer, and a low $Đ$ of 1.47.[14,15] Moreover, upon initiation, the catalyst afforded polymers with a phenyl group at a chain terminus,[8,16] as determined by ^{1}H NMR spectroscopy.

A key feature of the polymerization of **2** with PhPd(*t*-Bu_3P)Br is that both CuI[17] and additional phosphine ligand were necessary to achieve high molecular weight PPE (see Table 3.1, entries 5 and 6). Thus, to further optimize, the polymerization reaction, the effect of using different phosphine ligands as well as the ligand loadings was examined (Table 3.1). For example, the use of tri(2-furyl)phosphine (P(2-furyl)$_3$) afforded quantitative conversion of monomer to polymer, albeit with a higher $Đ$ (entry 3). Subsequent efforts focused on using PPh_3 since this ligand provided comparably high reaction conversions while still producing polymers that exhibited low dispersities. Although lowering the loading of PPh_3 and CuI as well as varying the ratio of PPh_3 to CuI did result in a narrowing of the $Đ$ (entries 8-10), the results were accompanied by decreases in both M_n and yield. These data were consistent with a controlled polymerization reaction that proceeded at a relatively reduced rate. Ultimately, the conditions summarized in Table 3.1, entry 7 were considered to be optimal and employed for subsequent polymerizations.

Entry [a]	CuI (mol%)	ligand (mol%)	M_n [b] (kDa)	$Đ$ [b] (M_w/M_n)	Yield (%) [c]
1	20	PPh_3 (20)	10.8	1.28	58
2	20	PCy_3 (20)	5.0	1.31	26
3	20	P(2-furyl)$_3$ (20)	17.2	1.69	99
4	20	P(*t*-Bu)$_3$ (20)	6.8	1.60	64
5	0	PPh_3 (20)	7.6	1.54	63
6	20	none	5.6	1.47	30
7	20	PPh_3 (20)	14.4	1.47	94
8	10	PPh_3 (10)	11.0	1.34	88
9	10	PPh_3 (15)	10.0	1.38	72
10	2	PPh_3 (2)	3.6	1.43	37

Table 3.1: Synthesis of PPE under various conditions. General polymerization conditions: $[\text{monomer}]_0 = 0.020$ M, Pd catalyst (2 mol%), THF, 25 °C, 2 to 3 h. [a] Entry 1: monomer **1** was used; entries 2-10: monomer **2** was used. [b] Determined by size exclusion chromatography (SEC) in THF against polystyrene standards. [c] Isolated yields.

The ability to synthesize a PPE with low dispersity and a molecular weight in agreement with the expected value was consistent with the polymerization proceeding in a chain-growth manner. To test, the molecular weight of the polymer formed as a function of monomer conversion was monitored over time. As shown in Figure 3.1A, the M_n of the polymer increased linearly with monomer conversion, while the $Đ$ remained relatively constant. Furthermore, when the polymerization of **2** was carried out at varying initial catalyst loadings, the M_n of the polymer (obtained at >99% monomer conversion) was proportional to the initial monomer to catalyst ratio (i.e., $[\mathbf{2}]_0/[\text{PhPd}(t\text{-Bu}_3\text{P})\text{Br}]_0$) while the dispersity remained constant (Figure 3.1B). Taken together, these results suggested to us that the polymerizations proceeded in a controlled, chain-growth manner.

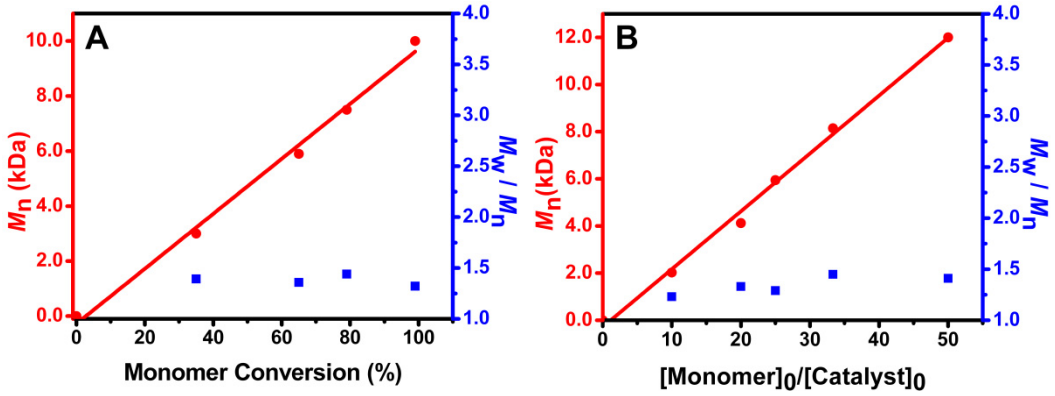

Figure 3.1: M_n (left Y-axis) and dispersity (right Y-axis) plotted (A) as a function of monomer conversion and (B) as a function of monomer/catalyst loading.

According to the CTP mechanism, all of the propagating polymer chains should contain the catalytically-active metal at the chain ends and therefore display living polymerization characteristics as long as chain termination is suppressed. Thus, dormant polymer chains synthesized by CTP should act as macroinitiators that provide access to chain extended polymers or well-defined block copolymers. To test this hypothesis, a chain extension experiment was carried out wherein a fresh batch of monomer **2** was added, upon the complete consumption of the initial bolus of monomer, to an unquenched solution of growing PPE. As shown in Figure 3.2A, the SEC curve of the polymer obtained at the end of the reaction shifted toward higher molecular weight than the PPE analyzed prior to the second monomer addition (isolated yield: 86%). Furthermore, the curve assigned to the chain extended polymer was monomodal and exhibited a $Đ$ similar to that displayed by the macroinitiator prior to the introduction of additional monomer. These results suggested to us that the macroinitiation efficiency was high and enabled the synthesis of well-defined block copolymers. Indeed, **2** was sequentially polymerized with 2-tributylstannylethynyl-7-iodo-9,9-dioctylfluorene, to afford a PPE-*b*-poly(fluorenylethynylene) copolymer in 92% yield (Figure 3.2B),[14,18] which is a rare

example of a fully conjugated poly(aryleneethynylene) block polymer expected to exhibit useful properties for light emitting diode applications.

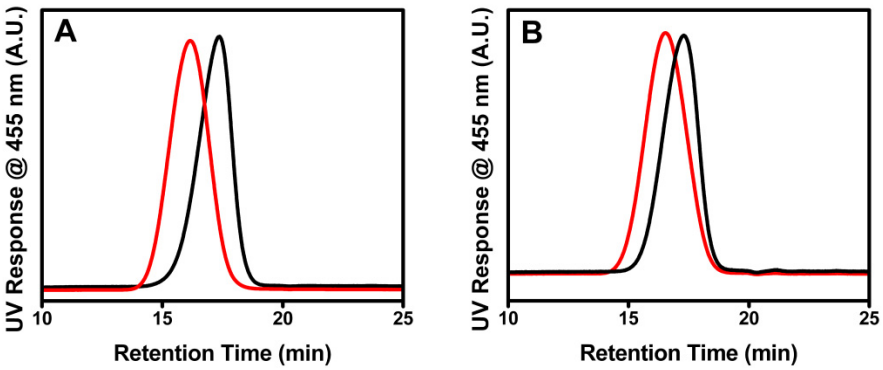

Figure 3.2: Size exclusion chromatograms of polymers obtained via chain extension. (A) PPE homopolymer before (black line; M_n = 10500 Da, $Đ$ = 1.40) and after (red line; M_n = 23700 Da, $Đ$ = 1.48) adding a second feed of **2**. (B) PPE homopolymer (black line; M_n = 10500 Da, $Đ$ = 1.39) and corresponding PPE-*b*-poly(fluorenylethynylene) block copolymer (red line; M_n = 16000 Da, $Đ$ = 1.55).

Having verified that the polymerization of **2** proceeded in a controlled, chain-growth fashion, we reasoned that this methodology would be an excellent candidate for the production of surface-bound PPE brushes via surface-initiated polymerization. The surface-initiated or "grafting-from" polymerization approach represents one of the most powerful methods for attaching polymers to surfaces because it offers a high degree of control over polymer grafting density, thickness, and composition.[19] To date, relatively few examples describe the surface-initiated polymerization of conjugated polymers from surfaces, all of which were accomplished through the use of Kumada or Suzuki-type CTP.[20]

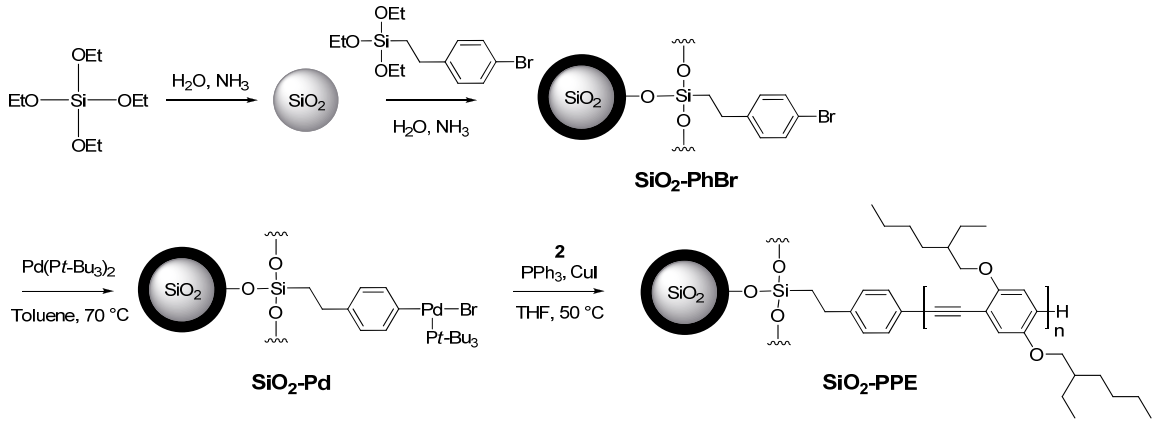

Scheme 3.2: Surface-initiated Polymerization of **2**.

We therefore turned our attention toward exploring the surface-initiated polymerization of **2**; our general approach is outlined in Scheme 2. Silica nanoparticles represented an ideal substrate for these studies due to their well-established surface chemistry and tendency to assemble into highly-ordered close-packed colloidal arrays,[21] a feature which may be exploited for optoelectronic applications[20d,22] and/or the generation of "smart" surfaces.[23] Furthermore, the use of silica nanoparticles offered a practical advantage because the immobilized polymers could be detached from the solid surface for further analysis by treating the silica-polymer composites with aqueous hydrofluoric acid (HF). Spherical silica particles with an average diameter of ~200 nm were prepared using the Stöber process.[23,24] In order to provide functional handles on the surface of the nanoparticles for catalyst immobilization, silanization was performed using [2-(4-bromophenyl)-ethyl]-triethoxysilane. Although scanning electron microscopy (SEM) images of the silica particles recorded before and after silanization showed that the size of the particles remained essentially unchanged (see Appendix A), thermogravimetric analysis (TGA) of the latter confirmed that organic residues were immobilized on the silica surface (see Figure 3.4) to afford **SiO_2-PhBr**. Using the weight retention values

obtained from the TGA data, a grafting density of 3.6 μmol/m^2 was calculated for the organosilane, which corresponded to a cross-sectional area of 0.46 nm^2/organosilane (see Appendix A). The aforementioned value was consistent with literature reports[23,25,26] and further verified by calculating the grafting density using elemental analysis, which gave a similar value of 4.19 μmol/m^2.

Having confirmed that surface coverage of the nanoparticles with the bromobenzene-containing organosilane was accomplished, subsequent efforts were directed toward the generation of a Pd(II)-containing polymerization initiator. Recently, Kiriy reported Pd-catalyzed Suzuki CTP of a poly(9,9-dialkylfluorene) from crosslinked poly(4-bromostyrene) films, having prepared the polymerization initiator by treating the poly(4-bromostyrene) film with a solution of $Pd(P\textit{t}\text{-}Bu_3)_2$.[20a] Building on this methodology, **SiO_2-PhBr** was reacted with an excess of $Pd(P\textit{t}\text{-}Bu_3)_2$ in toluene at 70 °C for 3 h. The particles were then subjected to numerous washings with THF to remove unbound Pd species. After drying under vacuum, the Pd-bound silica nanoparticles, **SiO_2-Pd**, were recovered as a pale yellow-brown powder, a distinct color change from the off-white hue of the **SiO_2-PhBr** particles. As shown in Figure 3.3, SEM coupled with energy dispersive X-ray spectroscopy (STEM-EDX) confirmed the presence of Br and Pd on **SiO_2-PhBr** and **SiO_2-Pd**, respectively.[27]

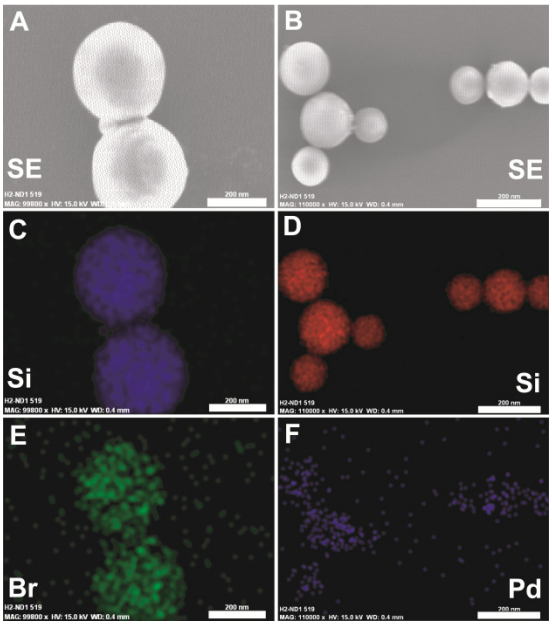

Figure 3.3: STEM-EDX analysis of **SiO_2-PhBr** (A, C, E) and **SiO_2-Pd** (B, D, F): Secondary electron (SE) image of (A) **SiO_2-PhBr** and (B) **SiO_2-Pd**. Elemental mapping analysis showing the presence of (C) Si on **SiO_2-PhBr**, (D) Si on **SiO_2-Pd**, (E) Br on **SiO_2-PhBr**, and (F) Pd on **SiO_2-Pd**. Scale bar = 200 nm.

The surface-initiated polymerization was accomplished by stirring **SiO_2-Pd** for 8 h in the presence of monomer **2**, copper iodide (20 mol%), and PPh_3 (20 mol%) in THF at 50 °C under an atmosphere of nitrogen. The resulting **SiO_2-PPE** particles were then purified by repeated centrifugation–redispersion cycles in THF until the supernatant became colorless and was isolated as a yellow powder in 62% yield. We attributed the modest percent recovery to material losses during the purification process;[28] however, the monomer was quantitatively consumed during the surface-initiated polymerization, as determined by ^{1}H NMR analysis against an internal standard. Thermal analysis of **SiO_2-PPE** revealed that the isolated material lost 14.1% of its weight between 100 and 800 °C, an increase of 5.4% and 7.8% when compared to the percent mass lost by **SiO_2-PhBr** and virgin SiO_2, respectively, over the same temperature range (Figure 3.4). To further

characterize the PPE produced in the reaction, the grafted polymers were detached from the silica surface by treating the nanoparticles with aq. HF, and analyzed in solution. The detached polymeric material exhibited a M_n of 24.5 kDa, as determined by SEC analysis, as well as ^{1}H NMR signals similar to those displayed by an analogous PPE synthesized under homogeneous conditions.

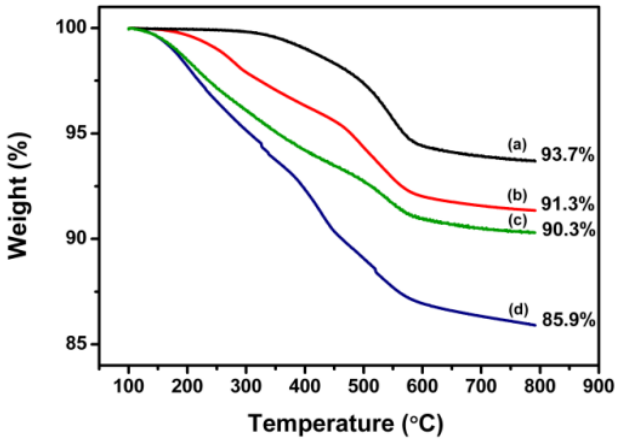

Figure 3.4: TGA curves of (a) bare SiO_2 particles, (b) **SiO_2-PhBr**, (c) **SiO_2-Pd**, and (d) **SiO_2-PPE**. The TGA experiments were performed under an atmosphere of nitrogen at a heating rate of 20 °C min^{-1}.

To gain further insight into the surface-initiated polymerization, a chain extension experiment similar to that previously performed for the homogeneous polymerization of **2** using PhPd(*t*-Bu_3P)Br was carried out as follows: A fresh feed of **2** was added to an unquenched solution of newly prepared **SiO_2-PPE**, allowed to react for 8 h, and then quenched with dilute aq. HCl. After purification by centrifugation, the resultant material, along with a sample isolated from an aliquot taken before the introduction of additional monomer, was treated with aq. HF to remove the silica core, and analyzed by SEC. The M_n of the liberated PPE was effectively doubled (11.3 kDa to 21.9 kDa) as measured from aliquots quenched before and after the second monomer addition, respectively (see Appendix A).[29] These results, coupled with a shift in the monomodal SEC trace toward

higher molecular weight, suggested to us that the controlled, chain-growth CTP mechanism was operative under heterogeneous conditions.

3.3 CONCLUSION

In conclusion, we report the first catalyst transfer polycondensation of a phenylacetylene-based monomer to afford PPE of controlled molecular weight and low dispersity. The polymerization methodology was determined to proceed in a chain-growth fashion, which facilitated the preparation of diblock copolymers by straightforward sequential monomer addition. We also demonstrated the first surface-initiated synthesis of surface-grafted PPE, using Pd-functionalized SiO_2 nanoparticles as the solid substrate and polymerization initiator, although we note that the presented methodology should be applicable to a variety of solid substrates, both curved and flat. We believe that the methodology described herein will create new opportunities in optoelectronic applications for an already well-established conjugated polymer in PPE. Of particular interest to us are the consequences of surface-immobilization on the optical properties of PPE and the self-assembly of composite nanoparticles such as **SiO_2-PPE**.[30] Findings along these lines will be presented in due course.

3.4 EXPERIMENTAL

3.4.1 General Considerations

Reagents. All solvents were purchased from Fisher and used without further purification unless otherwise noted. All other chemicals were purchased form Aldrich, Alfar Aesar, or Fisher and were used as received. 1,4-Bis(2-ethylhexyloxy)-2,5-diiodobenzene,[31] PdPh(*t*-Bu_3P)Br,[11] 2,7-diiodo-9*H*-fluorene,[32] and 1-(dodecyloxy)-4-methylbenzene[33] were prepared according to literature procedures. THF was distilled over Na/benzophenone under nitrogen.

Materials Characterization

NMR Spectroscopy. Proton NMR and ^{13}C NMR spectra were recorded on a Varian 300 or a Varian 400 spectrometer. ^{119}Sn NMR spectra were recorded on a Varian 600 spectrometer. Chemical shifts are reported in delta (δ) units and expressed in part per million (ppm) downfield from tetramethylsilane using the residual solvent as an internal standard. For ^{1}H NMR: $CDCl_3$, δ = 7.26 ppm. For ^{13}C NMR: $CDCl_3$, 77.16 ppm. For ^{119}Sn NMR: Me_4Sn, 0 ppm. Coupling constants (*J*) are expressed in Hertz.

Size Exclusion Chromatography. SEC was performed on a Viscotek GPCmax Solvent/Sample Module. Two fluorinated polystyrene columns (IMBHW-3078 and I-MBLMW-3078) were used in series and maintained at 24 °C. THF was used as the eluent at a flow rate of 1.0 mL/min. Detection was performed using a Viscotek VE 3580 Refractive Index Detector or a Viscotek 2600 Photodiode Array Detector (tuned at 455 nm). Molecular weight and dispersity data are reported relative to polystyrene standards.

Scanning Electron Microscopy: SEM was performed on a Hitachi S-5500 high resolution scanning transmission electron microscope (STEM) operating at 15 kV. Samples for analysis were prepared by dispersing the nanoparticles in THF by sonication and depositing the resulting dispersion onto carbon-coated copper TEM grids (Ted Pella) using a glass pipette.

Thermogravimetric Analysis. TGA was performed on a TA Instruments Q500 thermogravimetric analyzer. After drying under vacuum at 70 °C for at least 4 h, 5-10 mg of the sample was loaded onto a Pt crucible. Samples were first held at a constant temperature of 100 °C for 30 min, and then heated to 800 °C at a rate of 20 °C min^{-1} under an atmosphere of nitrogen.

Elemental Analysis. Elemental analyses were performed using a ThermoScientific Flash 2000 Organic Elemental Analyzer. Analyses were performed in triplicate and averaged.

Inductively-Coupled Mass Spectrometry: Quadrupole ICP-MS was performed on a Micromass Platform and Agilent 7500ce.

Surface Analysis. BET surface area analysis was performed on a Quantachrome NOVA 2000 surface analyzer. The samples were degassed at room temperature and measurements were determined using a 7-point BET method using molecular nitrogen as the adsorbate. The analyses were performed in triplicate and averaged. Using this method the specific surface area (S_{spec}) of the SiO_2 nanoparticles used in this work was determined to be 48.5 m^2/g. S_{spec} for **SiO_2-PhBr** and **SiO_2-PPE** were measured to be 19.4 m^2/g and 18.4 m^2/g, respectively.

3.4.2 Synthetic Procedures

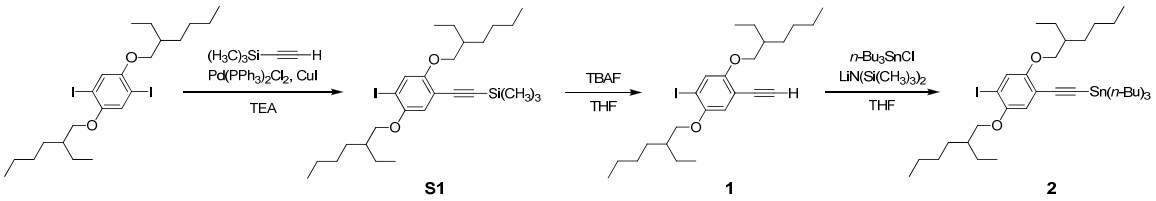

Scheme 3.3: Synthesis of **2**.

Synthesis of 1,4-bis(2-ethylhexyloxy)-2-iodo-5-trimethylsilylethynylbenzene (S1). To a 250 mL flame dried Schlenk flask was added 1,4-bis(2-ethylhexyloxy)-2,5-diiodobenzene (5.12 g, 8.73 mmol), trimethylsilyl acetylene (0.6 g, 6.11 mmol), CuI (16.6 mg, 0.0871 mmol), and triethylamine (100 mL). Upon dissolution, $Pd(PPh_3)_2Cl_2$ (0.30 g, 0.427 mmol) was added, and the reaction mixture was stirred for 6 h at room temperature under a nitrogen atmosphere. The reaction was then quenched with saturated

NH_4Cl (aq.) (50 mL). The organic layer was diluted with hexanes (50 mL), and then washed with water (2 × 50 mL). The combined water layers were extracted with hexanes (2 × 50 mL). The combined organic layers were dried over anhydrous Na_2SO_4, filtered and then concentrated under reduced pressure. Purification of the crude material by silica gel column chromatography (eluent: hexanes) afforded the desired product as a pale yellow oil (2.02 g, 41% yield). ^{1}H NMR (300 MHz, $CDCl_3$): δ 7.32 (s, 1H), 6.90 (s, 1H), 3.95-3.84 (m, 4H), 1.80-1.39 (m, 18H), 1.03-0.98 (m, 12H), 0.33 (s, 9H). ^{13}C NMR (75 MHz, $CDCl_3$): δ 155.14, 151.78, 123.43, 115.94, 113.32, 100.98, 99.31, 87.79, 72.18, 72.01, 39.75, 39.58, 30.66, 30.61, 29.24, 29.19, 24.09, 24.01, 23.21, 23.18, 14.26, 14.26, 11.43, 11.34, 0.08. HRMS (ESI): calcd for $[M+H]^+$ *m/z* 556.2234, found *m/z* 556.2238. Anal. calcd for $C_{27}H_{45}IO_2Si$: C, 58.26; H, 8.15; found: C, 58.40; H 7.81.

Synthesis of 1,4-bis(ethylhexyloxy)-2-iodo-5-ethynylbenzene (1). Compound **S1** (2.30 g, 4.13 mmol) was dissolved in THF (40 mL) in a 100 mL round bottom flask, and then tetrabutylammonium fluoride (1 M in THF, 6.2 mL, 6.20 mmol) was added. The resulting reaction mixture was stirred for 10 min at room temperature. After the addition of H_2O (20 mL) to quench the reaction, the water layer was extracted with diethyl ether (2 × 20 mL). The combined organic layers were dried over anhydrous Na_2SO_4, filtered and concentrated under reduced pressure. Purification of the crude material by silica gel column chromatography (eluent: 9:1 v/v hexanes/CH_2Cl_2) afforded the desired compound as a pale yellow oil (1.98 g, 99% yield). ^{1}H NMR (300 MHz, $CDCl_3$): δ 7.30 (s, 1H), 6.87 (s, 1H), 3.85-3.82 (m, 4H), 3.28 (s, 1H), 1.77-1.72 (m, 2H), 1.57-1.33 (m, 16H), 0.97-0.90 (m, 12H). ^{13}C NMR (75 MHz, $CDCl_3$): δ 155.17, 151.85, 123.75, 116.32, 112.34, 88.16, 81.81, 79.82, 72.37, 72.19, 34.54, 34.49, 30.64, 30.58, 29.17, 29.16, 23.99, 23.99, 23.16, 23.15, 14.24, 14.21, 11.33, 11.29. HRMS (ESI): calcd for $[M+H]^+$ *m/z* 484.1838,

found *m/z* 484.1832. Anal. calcd for $C_{24}H_{37}IO_2$: C, 59.50; H, 7.70; found: C, 59.78; H, 7.74.

Synthesis of 2. In a flame dried 100 mL Schlenk flask, **1** (2.36 g, 4.87 mmol) was dissolved in dry THF (40 mL) under a nitrogen atmosphere. The solution was cooled to -78 °C, and lithium bis(trimethylsilyl)amide (1 M in THF, 6.33 mL, 6.33 mmol) was added dropwise. After stirring for 1 h at -78 °C, *n*-Bu_3SnCl (2.06 g, 6.33 mmol) was added. The resulting reaction mixture was allowed to warm to room temperature, and stirred for another 90 min, at which point the reaction was quenched by adding saturated NH_4Cl (aq.) (40 mL). The aqueous phase was extracted with diethyl ether (2 × 40 mL). The combined organic layers were washed with water (100 mL) and brine (100 mL), and dried over anhydrous Na_2SO_4. After concentrating under reduced pressure, the resulting oil was dried overnight under vacuum to afford **2** (3.73 g, 99% yield) as a yellow oil (3.73 g, 99%). To avoid decomposition, the monomer was used directly without further purification. ^{1}H NMR (300 MHz, $CDCl_3$): δ 7.72 (s, 1H), 6.83 (s, 1H), 3.87-3.77 (m, 4H), 1.74-1.32 (m, 36H), 1.08-0.88 (m, 21H). ^{13}C NMR (75 MHz, $CDCl_3$): δ 154.95, 151.75, 123.41, 116.45, 114.30, 105.52, 98.71, 86.71, 72.16, 71.91, 39.63, 39.57, 30.66, 30.51, 29.19, 29.02, 27.98, 27.18, 24.09, 23.95, 23.21, 23.18, 16.13, 14.24, 13.79, 13.79, 11.32, 11.27. ^{119}Sn NMR (600 MHz, $CDCl_3$): δ -66.02. HRMS (ESI): calcd for $[M+H]^+$ *m/z* 774.2895, found *m/z* 774.2903. Anal. calcd for $C_{36}H_{63}IO_2Sn$: C, 55.9; H, 8.21; found: C, 55.80; H, 8.26.

General homopolymerization procedure. A flame dried 50 mL Schlenk flask was charged with CuI (2.46 mg, 12.9 μmol) and triphenylphosphine (3.4 mg, 12.9 μmol). A solution of **2** (0.10 g, 0.129 mmol) in dry THF (4 mL) was then added. After the solution was degassed using three freeze-pump-thaw cycles, the polymerization was initiated by adding via syringe a solution of PdPh(*t*-Bu_3P)Br (1.20 mg, 2.58 μmol) in

THF (0.2 mL). The resulting reaction mixture was stirred under nitrogen for 3 h at room temperature and quenched by precipitation into excess 4:1 v/v methanol/water. The precipitated solid was collected by filtration and washed with methanol (3 × 30 mL) and cold acetone (2 mL) to afford **PPE** homopolymer (41 mg, 88% yield) as a yellow solid. SEC: M_n = 11000 Da, $Đ$ (M_w/M_n) = 1.34. ^{1}H NMR (400 MHz, $CDCl_3$): δ 7.00 (s, 2H), 3.95-3.84 (m, 4H), 1.83-1.78 (m, 2H), 1.65-1.41 (m, 8H), 1.33-1.25 (m, 8H), 1.00-0.87 (m, 12H). ^{13}C NMR (100 MHz, $CDCl_3$): δ 153.83, 116.78, 114.35, 91.72, 72.03, 39.74, 30.77, 29.26, 24.22, 24.09, 23.25, 14.24, 11.47.

Chain extension polymerization procedure. To a flame dried 50 mL Schlenk flask was added CuI (4.92 mg, 25.8 μmol), triphenylphosphine (6.78 mg, 25.8 μmol), and 1-(dodecyloxy)-4-methylbenzene (20 mg, 72.3 μmol) as an internal standard. A solution of monomer **2** (0.10 g, 0.129 mmol) in dry THF (4 mL) was then added. After the solution was degassed by three freeze-pump-thaw cycles, the polymerization was initiated by adding via syringe a solution of PdPh(*t*-Bu_3P)Br (1.20 mg, 2.58 μmol) in THF (0.2 mL). The resulting reaction mixture was stirred for 3 h at room temperature, at which point an aliquot was removed for analysis. Proton NMR and SEC analysis of the aliquot confirmed the following characteristics: Conversion of monomer = >99%, M_n = 10500, $Đ$ = 1.40. The polymerization mixture was then transferred by syringe to a second reaction vessel containing a THF solution of **2** (0.10 g, 0.129 mmol in 4 mL THF) and CuI (4.92 mg, 25.8 μmol), and was degassed by three freeze-pump-thaw cycles. The resulting solution was stirred for another 3 h at room temperature, and then precipitated into excess 3:1 v/v methanol/water. The precipitated solid was collected by filtration and washed with methanol (3 × 30 mL) and cold acetone (5 mL) to afford the chain-extended polymer as a yellow solid (80.26 mg, 86%). Conversion of second batch of monomer: >99%; M_n = 23700, $Đ$ = 1.48.

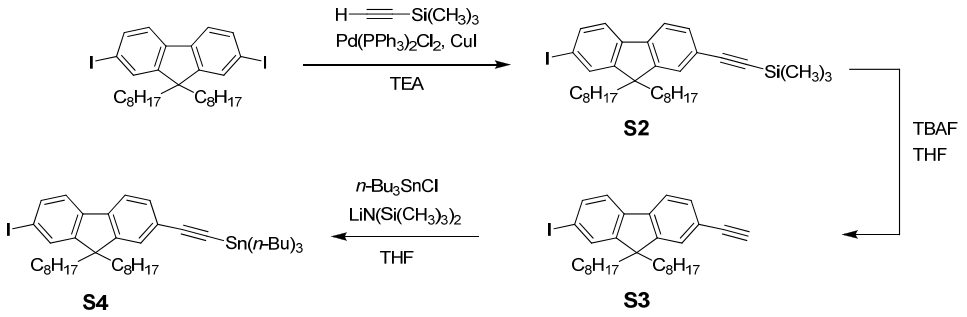

Scheme 3.4: Synthesis of fluorenyl ethynylene monomer **S4**.

Synthesis of ((7-iodo-9,9-dioctyl-9H-fluoren-2-yl)ethynyl)trimethylsilane (S2). To a flame dried 250 mL Schlenk flask was added 2,7-diiodo-9,9-dioctylfluorene (5.12 g, 7.97 mmol), trimethylsilyl acetylene (0.548 g, 5.58 mmol), CuI (15.2 mg, 79.7 μmol), and triethylamine (100 mL). Upon dissolution, $Pd(PPh_3)_2Cl_2$ (0.279 g, 0.397 mmol) was added, and the reaction mixture was stirred for 12 h at room temperature under a nitrogen atmosphere. The reaction was quenched with saturated NH_4Cl (aq.) (50 mL). The organic layer was diluted with hexanes (50 mL), and then washed with water (2 × 50 mL). The combined water layers were extracted with hexanes (2 × 50 mL). The combined organic layers were dried over anhydrous Na_2SO_4, filtered, and concentrated under reduced pressure. The crude compound was purified by silica gel column chromatography (eluent: hexanes) to afford the desired product as a pale yellow oil (3.13 g, 64% yield). ^{1}H NMR (400 MHz, $CDCl_3$): δ 7.66-7.64 (m, 2H), 7.58 (dd, J = 7.2, 0.8 Hz, 1H), 7.46 (dd, J = 6.4, 1.2 Hz, 1H), 7.42-7.40 (m, 2H), 1.94-1.90 (m, 4H), 1.25-1.03 (m, 20H), 0.84 (t, J = 8.0 Hz, 6H), 0.58-0.54 (m, 4H), 0.29 (s, 9H). ^{13}C NMR (100 MHz, $CDCl_3$): δ 153.51, 150.14, 140.68, 140.14, 136.09, 132.19, 131.38, 126.30, 122.07, 121.82, 119.74, 106.12, 94.41, 93.32, 55.52, 40.35, 31.92, 30.04, 29.34, 29.32, 23.73, 22.75, 14.25, 0.20. HRMS (ESI):

calcd for $[M+H]^+$ *m/z* 612.2640, found *m/z* 612.2648. Anal. calcd for $C_{34}H_{49}ISi$: C, 66.65; H, 8.06; found: C, 66.84; H, 8.07.

Synthesis of 2-ethynyl-7-iodo-9,9-dioctyl-9H-fluorene (S3). Compound S2 (3.10 g, 5.06 mmol) was dissolved in THF (30 mL) in a 100 mL round bottom flask, and then tetrabutylammonium fluoride (1 M in THF, 7.6 mL, 7.60 mmol) was added. The resulting reaction mixture was stirred for 20 min at room temperature. After the addition of H_2O (40 mL) to quench the reaction, the water layer was extracted with diethyl ether (2 × 40 mL). The combined organic layers were dried over anhydrous Na_2SO_4, filtered, and concentrated under reduced pressure. Purification by silica gel column chromatography (eluent: 9:1 v/v hexane/CH_2Cl_2) afforded the desired product as a pale yellow oil (2.72 g, 99% yield). 1H NMR (400 MHz, CDCl3): δ 7.67-7.65 (m, 2H), 7.61 (dd, J = 7.2, 0.4 Hz, 1H), 7.47 (dd, J = 6.8, 1.2 Hz, 1H), 7.44-7.41 (m, 2H), 3.15 (s, 1H), 1.93-1.89 (m, 4H), 1.27-0.96 (m, 20H), 0.83 (t, J = 7.2 Hz, 6H), 0.58-0.54 (m, 4H). 13C NMR (100 MHz, CDCl3): δ 157.37, 150.10, 140.81, 139.86, 135.98, 132.08, 131.24, 126.44, 121.72, 120.86, 119.69, 93.31, 84.48, 77.34, 55.36, 40.13, 31.76, 29.88, 29.19, 29.16, 23.62, 22.60, 14.10. HRMS (ESI): calcd for [M+H]+ m/z 540.2253, found m/z 540.2256. Anal. calcd for C31H41I: C, 68.88; H, 7.64; found: C, 68.93; H, 7.63.

Synthesis of 2-tributylstannylethynyl-7-iodo-9,9-dioctylfluorene (S4). To a 100 mL Schlenk flask was added compound **S3** (2.55 g, 4.71 mmol) and dry THF (30 mL) under a nitrogen atmosphere. The solution was cooled to -78 °C, and lithium bis(trimethylsilyl)amide (1 M in THF, 6.12 mL, 6.12 mmol) was added dropwise. After stirring for 1 h at -78 °C, *n*-Bu_3SnCl (1.98 g, 6.10 mmol) was added. The resulting reaction mixture was stirred for 90 min at room temperature. Saturated NH_4Cl (aq.) (30 mL) was added to quench the reaction, and the aqueous phase was extracted with diethyl ether (2 × 30 mL). The combined organic layers were washed with water (30 mL) and

brine (2 × 30 mL), dried over anhydrous Na_2SO_4, and concentrated under reduced pressure. Drying overnight under vacuum provided the desired compound as a yellow oil (3.82 g, 98% yield). ^{1}H NMR (400 MHz, $CDCl_3$): δ 7.65-7.62 (m, 2H), 7.56 (d, J = 7.6 Hz, 1H), 7.44-7.38 (m, 3H), 1.92-1.87 (m, 4H), 1.66-1.57 (m, 6H), 1.40-1.03 (m, 32H), 0.94-0.81 (m, 9H), 0.83 (t, J = 7.2 Hz, 6H), 0.57-0.55 (m, 4H). ^{13}C NMR (100 MHz, $CDCl_3$): δ 153.48, 150.44, 140.27, 140.00, 136.00, 132.12, 131.26, 126.25, 123.03, 121.67, 119.62, 111.09, 93.65, 93.03, 55.42, 40.35, 31.89, 30.06, 29.34, 29.31, 29.07, 27.16, 23.74, 22.73, 14.23, 13.85, 11.35. ^{119}Sn NMR (600 MHz, $CDCl_3$): δ -64.94; HRMS (ESI): calcd for $[M+H]^+$ *m/z* 830.3310, found *m/z* 830.3329. Anal. calcd for $C_{43}H_{67}ISn$: C, 62.25; H, 8.14; found: C, 62.31; H, 8.255.

Block copolymerization procedure. To a flame dried 50 mL Schlenk flask was added CuI (4.92 mg, 25.8 μmol), triphenylphosphine (6.78 mg, 25.8 μmol), and 1-(dodecyloxy)-4-methylbenzene (20 mg, 72.3 72.3 μmol) as an internal standard. A THF solution of **2** (0.10 g, 0.129 mmol) was then added. After the solution was degassed by 3 freeze-pump-thaw cycles, the polymerization was initiated by adding via syringe a solution of PdPh(*t*-Bu_3P)Br (1.2 mg, 2.58 μmol) in THF (0.2 mL). The resulting reaction mixture was stirred for 3 h at room temperature, at which point an aliquot was removed for analysis. Proton NMR and SEC analysis of the aliquot confirmed the following characteristics: conversion of monomer = 100%; M_n = 10500, $Đ$ = 1.39. A degassed THF (2 mL) solution of **S4** (54 mg, 0.0650 mmol) was then added into the polymerization mixture by syringe, and then stirred for another 3 h at room temperature. The reaction mixture was then precipitated into excess 3:1 v/v methanol/water. The precipitated solids were collected by filtration, and washed with methanol (3 × 30 mL) and cold acetone (5 mL) to afford the desired polymer as a yellow solid (67 mg, 92% yield). Conversion of

S4 = 99%; M_n = 16000, $Đ$ = 1.55. ^{1}H NMR (400 MHz, $CDCl_3$) δ 7.71-7.69 (m, 2H), 7.59-7.52 (m, 4H), 7.00 (s, 2H), 3.92-3.86 (m, 4H), 2.01-0.62 (m, 32H).

Synthesis of silica nanoparticles. Ammonium hydroxide (25% in water, 28.0 g) was dissolved in 380 mL of ethanol in a 1 L beaker and stirred for 10 minutes. Tetraethyl orthosilicate (TEOS) (14.16 g) dissolved in ethanol (10 mL) was then added to the beaker at once. The initial concentrations of ammonia, TEOS, and water in the reaction mixture were 0.45 M, 0.15 M, and 3.10 M, respectively. The mixture was stirred vigorously for 4 h. The nanoparticles were isolated by centrifugation (8000 rpm for 30 min), followed by redispersion by sonication in ethanol. This process was repeated four times with ethanol, then five times with water. Excess water was removed by drying the particles with a stream of air, and then placing in an oven to dry overnight at 160 °C, which afforded a white powder (3.84 g, 94% yield).

Synthesis of [2-(4-bromo-phenyl)-ethyl]-triethoxysilane.[34] A 50 mL round bottom flask was charged with triethoxysilane (5.0 g, 30.3 mmol) and 4-bromostyrene (5.05 g, 27.6), and cooled to 0 °C. To this mixture was added platinum(0)-1,3-divinyl-1,1,3,3-tetramethyldisiloxane (Karstedt's Catalyst, solution in xylene, Pt~2 wt%) (0.5 mL, ~0.17 wt% Pt). The reaction mixture was stirred for 2 h and allowed to warm to room temperature. Purification by vacuum distillation (110 °C, 50 mtorr) afforded the desired product as a clear oil (5.03 g, 50% yield). The isolated material was a 36/64 mixture of Markovnikov and anti-Markovnikov products, and was used without additional purification. ^{1}H NMR (400 MHz, $CDCl_3$) of the anti-Markovnikov product (major isomer): δ 7.38 (d, J = 8.4 Hz, 2H), 7.10 (d, J = 8.4 Hz, 2H), 3.85-3.79 (m, 6H), 2.71-2.66 (m, 2H), 1.23 (t, J = 7.2 Hz, 9H), 0.97-0.93 (m, 2H). ^{1}H NMR (400 MHz, $CDCl_3$) of Markovnikov product (minor isomer): δ 7.35 (d, J = 8.4 Hz, 2H), 7.08 (d, J = 8.4 Hz, 2H), 3.75-3.70 (m, 6H), 2.30-2.24 (m, 1H), 1.38 (d, J = 7.6 Hz, 3H), 1.16 (t, J =

6.8 Hz, 9H). ^{13}C NMR (100 MHz, $CDCl_3$) of anti-Markovnikov product (major isomer): δ 143.64, 131.43, 129.72, 119.37, 58.54, 28.51, 18.42, 12.55. ^{13}C NMR (100 MHz, $CDCl_3$) of Markovnikov product (minor isomer): δ 143.30, 131.11, 129.70, 118.48, 59.26, 25.84, 18.33, 15.49. HRMS (CI) calcd for [M+H]+: m/z 347.0678, found m/z 346.0676. Anal. calcd for $C_{14}H_{23}BrO_3Si$: C, 48.41; H, 6.67; found: C, 48.133; H, 6.738.

Synthesis of SiO_2-PhBr. To a 50 mL round bottom flask was added ammonium hydroxide (25% in water, 2.0 mL), deionized water (27 mL), and methanol (20 mL) and stirred for 10 min. [2-(4-bromo-phenyl)-ethyl]-triethoxysilane (0.1 g, 0.29 mmol) was then added to the stirring solution, at which point the reaction mixture became cloudy and white. After 20 min of stirring, silica nanoparticles (1.0 g) were added, and the suspension was stirred overnight. The nanoparticles were purified by repeated centrifugation and redispersion in ethanol (4 × 10 mL) and THF (2 × 10 mL). Removal of solvent by rotary evaporation, and drying under reduced pressure for 4 h at 120 °C afforded the desired material as an off-white powder (0.98 g).

Synthesis of SiO_2-Pd. In a nitrogen-filled glovebox, an 8 mL Teflon-capped glass vial was charged with a stirbar, **SiO_2-PhBr** (0.344 g), Pd(P*t*-Bu_3)$_2$ (0.035 g, ~10 wt%), and toluene (6 mL). The vial was sealed, removed from the glovebox, and sonicated for 30 minutes to disperse the nanoparticles. The reaction mixture was then heated to 70 °C in an oil bath and stirred for 2 h. After cooling to room temperature, the vial was taken back into the glovebox. The nanoparticles were purified via redispersion by stirring, followed by decantation of the supernatant. This redispersion/decantation cycle was repeated using toluene (2 × 10 mL), THF (5 × 10 mL), and pentane (3 × 10 mL) as the solvent, until the supernatant was colorless. Removal of the solvent under reduced pressure afforded the desired material as a light yellow-brown powder (0.285 g). **SiO_2-Pd** was stored in a freezer at -20 °C inside of the glovebox.

Synthesis of SiO_2-PPE by surface-initiated polymerization of 2. In a nitrogen-filled glovebox, an 8 mL Teflon-capped glass vial was charged with a stirbar, **SiO_2-Pd** (108 mg), PPh_3 (6.0 mg, 0.023 mmol), CuI (5.0 mg, 0.026 mmol), **2** (120 mg, 0.155 mmol), and THF (4 mL). The vial was sealed, removed from the glovebox, and sonicated for 30 min to disperse the nanoparticles. The reaction mixture was then heated to 50 °C in an oil bath and stirred for 8 h. The polymerization was quenched by opening the reaction vessel to air and injecting an aqueous solution of HCl (1 mL). Surface-bound polymers were isolated by repeated centrifugation/redispersion cycles in THF until the supernatant became colorless and non-fluorescent by UV irradiation (~8-10 cycles). Removal of the solvent under reduced pressure afforded **SiO_2-PPE** as a bright yellow powder (99 mg).

Cleavage of surface-grafted PPE from nanoparticles. SiO_2-PPE (51 mg) was added to a 20 mL plastic vial and dispersed in DI water (9 mL) by sonication. Hydrofluoric acid (HF, ~50% aq., 1 mL) was added, and the suspension was stirred at room temperature for 6 h. Organic materials were extracted with CH_2Cl_2 (3 × 10 mL) and the organic layer was separated. The organic extracts were combined, dried over Na_2SO_4, and concentrated to afford PPE as a yellow solid (7.3 mg). The isolated polymer was characterized by ^{1}H NMR spectroscopy and SEC.

Surface-initiated chain extension polymerization procedure. In a nitrogen-filled glovebox, an 8 mL Teflon-capped glass vial was charged with a stirbar, **SiO_2-Pd** (58 mg), PPh_3 (3.0 mg, 0.012 mmol), CuI (3 mg, 0.016 mmol), **2** (25 mg, 0.032 mmol), and THF (3 mL). The vial was sealed, removed from the glovebox, and sonicated for 30 minutes to disperse the nanoparticles. The reaction mixture was then heated to 50 °C in an oil bath and stirred for 8 h. The reaction vessel was then taken back into the glovebox. An aliquot (~ 1 mL) was removed for analysis, then a solution of PPh_3 (3.0 mg, 0.012 mmol), CuI (3 mg, 0.016 mmol), and **2** (25 mg, 0.032 mmol) in THF (2 mL) was added

to the polymerization mixture. The vial was resealed, taken out of the glovebox, and stirred for another 8 h at 50 °C. Both the aliquot removed prior to the second monomer addition and the polymerization mixture were quenched with HCl (aq.) and worked up in the same manner as described above. Treatment of the isolated materials with HF (aq.) afforded the liberated polymers, which were analyzed by SEC.

3.5 ACKNOWLEDGMENTS

Portions of this chapter were reprinted with permission from Kang, S.; Ono, R. J.; Bielawski, C. W. *J. Am. Chem. Soc.* **2013**, *135*, 4984-4987. Copyright 2012 American Chemical Society. Songsu Kang is gratefully acknowledged for his synthetic contributions. Prof. Christopher W. Bielawski is also gratefully acknowledged for helping to write the original manuscript.

3.6 REFERENCES

(1) (a) Grimsdale, A. C.; Leok Chan, K.; Martin, R. E.; Jokisz, P. G.; Holmes, A. B. *Chem. Rev*. **2009**, *109*, 897-1091. (b) Pschirer, N. G.; Miteva, T.; Evans, U.; Roberts, R. S.; Marshall, A. R.; Neher, D.; Myrick, M. L.; Bunz, U. H. F. *Chem. Mater*. **2001**, *13*, 2691-2696.

(2) (a) Thomas, S. W.; Joly, G. D.; Swager, T. M. *Chem. Rev.* **2007**, *107*, 1339-1386. (b) Yang, J.-S.; Swager, T. M. *J. Am. Chem. Soc.* **1998**, *120*, 11864-11873.

(3) Allara, D. L.; Arnold, J. J.; Bumm, L. A.; Burgin, T. P.; Cygan, M. T.; Dunbar, T. D.; Jones, L., II; Tour, J. M.; Weiss, P. S. *Science* **1996**, *271*, 1705-1707.

(4) Bunz, U. H. F. *Chem. Rev.* **2000**, *100*, 1605-1644.

(5) Bunz, U. H. F. *Acc. Chem. Res.* **2001**, *34*, 998-1010.

(6) (a) Osaka, I.; McCullough, R. D. *Acc. Chem. Res.* **2008**, *41*, 1202-1214. (b) Miyakoshi, R.; Yokoyama, A.; Yokozawa, T. *J. Am. Chem. Soc*. **2005**, *127*, 17542-17547.

(7) (a) Yokoyama, A.; Suzuki, H.; Kubota, Y.; Ohuchi, K.; Higashimura, H.; Yokozawa, T. *J. Am. Chem. Soc.* **2007**, *129*, 7236-7237. (b) Zhang, H.-H.; Xing, C.-H.; Hu, Q.-S. *J. Am. Chem. Soc.* **2012**, *134*, 13156-13159. (c) Elmalem, E.; Biedermann, F.; Johnson, K.; Friend, R. H.; Huck, W. T. S. *J. Am. Chem. Soc.* **2012**, *134*, 17769-17777.

(8) Yokozawa, T.; Kohno, H.; Ohta, Y.; Yokoyama, A. *Macromolecules* **2010**, *43*, 7095-7100.

(9) Elmalem, E.; Kiriy, A.; Huck, W. T. S. *Macromolecules* **2011**, *44*, 9057-9061.

(10) Ono, R. J.; Kang, S.; Bielawski, C. W. *Macromolecules* **2012**, *45*, 2321-2326.

(11) Stambuli, J. P.; Incarvito, C. D.; Bühl, M.; Hartwig, J. F. *J. Am. Chem. Soc.* **2004**, *126*, 1184-1194.

(12) Giardina, G.; Rosi, P.; Ricci, A.; Lo Sterzo, C. *J. Polym. Sci. Part A* **2000**, *38*, 2603-2621.

(13) Suraru, S.-L.; Würthner, F. *Synthesis* **2009**, *11*, 1841-1845.

(14) Using ICP-MS, less than 0.5 ppb of tin was detected in the isolated PPE homopolymer and less than 1.54 ppb of tin was detected in the PPE-b-poly(fluorenylethynylene) copolymer.

(15) The presence of diyne defects were not detected by ^{13}C NMR spectroscopy.

(16) Yokoyama, A.; Suzuki, H.; Kubota, Y.; Ohuchi, K.; Higashimura, H.; Yokozawa, T. *J. Am. Chem. Soc.* **2007**, *129*, 7236-7237.

(17) Farina, V.; Kapadia, S.; Krishnan, B.; Wang, C.; Liebeskind, L. S. *J. Org. Chem.* **1994**, *59*, 5905-5911.

(18) See Experimental section for polymerization conditions and further characterization details.

(19) Edmondson, S.; Osborne, V. L.; Huck, W. T. S. *Chem. Soc. Rev.* **2004**, *33*, 14-22.

(20) (a) Beryozkina, T.; Boyko, K.; Khanduyeva, N.; Senkovskyy, V.; Horecha, M.; Oertel, U.; Simon, F.; Stamm, M.; Kiriy, A. *Angew. Chem. Int. Ed.* **2009**, *48*, 2695-2698. (b) Tkachov, R.; Senkovskyy, V.; Horecha, M.; Oertel, U.; Stamm, M.; Kiriy, A. *Chem. Commun*. **2010**, *46*, 1425-1427. (c) Senkovskyy, V.; Khanduyeva, N.; Komber, H.; Oertel, U.; Stamm, M.; Kuckling, D.; Kiriy, A. *J. Am. Chem. Soc*. **2007**, *129*, 6626-6632. (d) Senkovskyy, V.; Tkachov, R.; Beryozkina, T.; Komber, H.; Oertel, U.; Horecha, M.; Bocharova, V.; Stamm, M.; Gevorgyan, S. A.; Krebs, F. C.; Kiriy, A. *J. Am. Chem. Soc*. **2009**, *131*, 16445-16453. (e) Doubina, N.; Jenkins, J. L.; Paniagua, S. A.; Mazzio, K. A.; MacDonald, G. A.; Jen, A. K. Y.; Armstrong, N. R.; Marder, S. R.; Luscombe, C. K. *Langmuir* **2012**, *28*, 1900-1908. (f) Sontag, S. K.; Sheppard, G. R.; Usselman, N. M.; Marshall, N.; Locklin, J. *Langmuir* **2011**, *27*, 12033-12041. (g) Marshall, N.; Sontag, S. K.; Locklin, J. *Macromolecules* **2010**, *43*, 2137-2144.

(21) Jiang, P.; Bertone, J. F.; Hwang, K. S.; Colvin, V. L. *Chem. Mater.* **1999**, *11*, 2132-2140.

(22) Labastide, J. A.; Baghgar, M.; Dujovne, I.; Yang, Y.; Dinsmore, A. D.; G. Sumpter, B.; Venkataraman, D.; Barnes, M. D. *J. Phys. Chem. Lett.* **2011**, *2*, 3085-3091.

(23) Li, D.; Sheng, X.; Zhao, B. *J. Am. Chem. Soc.* **2005**, *127*, 6248-6256.

(24) Stöber, W.; Fink, A.; Bohn, E. *J. Colloid Interface Sci.* **1968**, *26*, 62-69.

(25) Kim, J. W.; Kim, L. U.; Kim, C. K. *Biomacromolecules* **2006**, *8*, 215-222.

(26) Bartholome, C.; Beyou, E.; Bourgeat-Lami, E.; Chaumont, P.; Zydowicz, N. *Macromolecules* **2003**, *36*, 7946-7952.

(27) The presence of phosphine was also detected on **SiO_2-Pd** using STEM-EDX; see Appendix A.

(28) Some ungrafted PPE was also produced during the reaction and separated from the **SiO_2-PPE** composite particles by centrifugation. A control experiment ruled out nonspecific adsorption; see Appendix A for additional details.

(29) A $Đ$ of 2.5 and 3.8 was recorded for PPE samples isolated before and after the second monomer addition step, respectively. We surmise that slow initiation during the surface-initiated polymerization, when compared to the corresponding homogeneous polymerization, may contribute to broadening of the dispersity.

(30) For discussions regarding the ordering of PPE chains, see: (a) Bunz, U. H. F.; Imhof, J. M.; Bly, R. K.; Bangcuyo, C. G.; Rozanski, L.; Vanden Bout, D. A. *Macromolecules* **2005**, *38*, 5892-5896. (b) Bunz, U. H. F.; Enkelmann, V.; Kloppenburg, L.; Jones, D.; Shimizu, K. D.; Claridge, J. B.; zur Loye, H.-C.; Lieser, G. *Chem. Mater.* **1999**, *11*, 1416-1424. (c) Wilson, J. N.; Steffen, W.; McKenzie, T. G.; Lieser, G.; Oda, M.; Neher, D.; Bunz, U. H. F. *J. Am. Chem. Soc*. **2002**, *124*, 6830-6831.

(31) Swager, T. M.; Gil, C. J.; Wrighton, M. S. *J. Phys. Chem.* **1995**, *99*, 4886.

(32) Thivierge, C.; Loudet, A.; Burgess, K. *Macromolecules* **2011**, *44*, 4012.

(33) Liu, L.; Zang, Y.; Hadano, S.; Aoki, T.; Teraguchi, M.; Kaneko, T.; Namikoshi, T. *Macromolecules* **2010**, *43*, 9268.

(34) Senkovskyy, V.; Tkachov, R.; Beryozkina, T.; Komber, H.; Oertel, U.; Horecha, M.; Bocharova, V.; Stamm, M.; Gevorgyan, S. A.; Krebs, F. C.; Kiriy, A. *J. Am. Chem. Soc.* **2009**, *131*, 16445-16453.

Chapter 4: Synthesis and Self-Assembly of Poly(3-hexylthiophene)-*b*-Poly(acrylic acid) Copolymers

4.1 Introduction

Donor-acceptor block copolymers containing regioregular poly(3-hexylthiophene) (P3HT) have garnered considerable attention in recent years as promising materials for applications in optoelectronics.[1] Such copolymers are often prepared using a *grafting-from* approach, where an end-functionalized polythiophene is used as a macroinitiator for the chain extension polymerization of a second block.[2] A significant drawback to this strategy, however, is the need for multiple post-polymerization modifications as the requisite initiator must be installed onto the end of the P3HT chain. A convenient alternative is to use a *grafting-to* approach, whereby the constituent homopolymers are independently synthesized and then subsequently linked together.

Because the utility of the *grafting-to* method rests on the efficiency by which the chain-ends can react with each other, a reaction is needed that is both high-yielding and functional group tolerant. A transformation that fulfills these criteria is the Cu-catalyzed "click" azide–alkyne cycloaddition,[3] which has found remarkable utility in the field of polymer science,[4] including the synthesis of P3HT-containing block copolymers. For example, Urien synthesized a series of P3HT-containing di- and triblock copolymers from alkyne end-functionalized P3HT and azide end-functionalized polystyrenes.[5] More recently, Segalman reported a block copolymer where an ethynyl-terminated P3HT was "clicked" with a polyacrylate that was grown from an azido-functionalized initiator.[6]

While these seminal reports highlight the potential of using grafting methods to synthesize P3HT-based block copolymers, the materials obtained often contain inseparable homopolymer impurities that impede copolymer formation. A simple method

that effectively overcomes these issues and rapidly affords appreciable quantities of P3HT-containing block copolymers in high yield and free of homopolymer impurities remains an important challenge in synthetic polymer chemistry, especially within the context of optoelectronic applications, where materials of high purity are needed.

Here, we discuss a convenient synthesis of P3HT-containing rod–coil diblock copolymers *via* the "click" reaction of ethynyl-terminated P3HT[7] (P3HT–C≡CH) and azide-terminated poly(*t*-butyl acrylate)[8] (P*t*BA–N_3). Central to our results is the discovery that P3HT–C≡CH is unstable and engages in homocoupling over time. This limitation was effectively surmounted with the development of an improved isolation procedure which facilitated access to pure samples of P3HT–C≡CH and strongly influenced the outcome of its subsequent cycloaddition reactivity. The choice of P*t*BA as the coil block enabled access to the amphiphilic diblock copolymer, P3HT-*b*-poly(acrylic acid) (P3HT-*b*-PAA), which was recently been shown[9] by McCullough to exhibit solvatochromic behavior in a variety of polar and non-polar solvents. Prompted by this report and as part of a newly launched program aimed at studying donor–acceptor copolymers that adopt highly ordered structures, we also discuss the characterization of the self-assembly behavior of P3HT-*b*-PAA using dynamic light scattering (DLS) and transmission electron microscopy (TEM).

4.2 RESULTS AND DISCUSSION

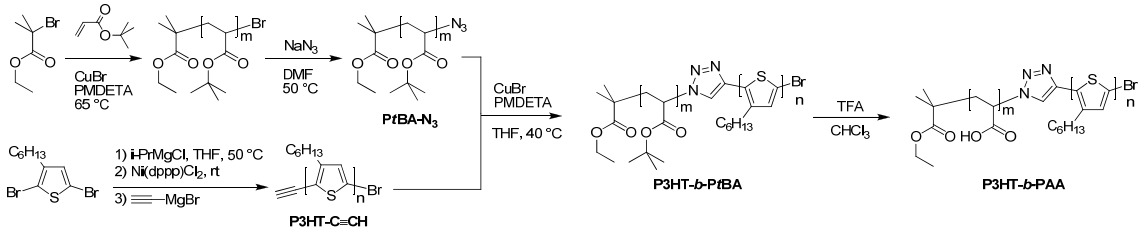

Scheme 4.1: Synthesis of P3HT-*b*-P*t*BA and P3HT-*b*-PAA block copolymers.

As summarized in Scheme 4.1, P*t*BA–Br with different chain lengths was synthesized *via* Cu-mediated atom transfer radical polymerization (65 °C, neat) by varying the initial *t*-butyl acrylate to initiator (ethyl 2-bromoisobutyrate; EBiB) ratios. After precipitation from a methanol/water mixture (1/1, v/v), the desired polymers were isolated *via* filtration and then characterized by gel permeation chromatography (GPC) as well as ^{1}H NMR spectroscopy (see Table 4.1; entries 1 – 3). Displacement of the bromide end-group was accomplished with NaN_3 in DMF (50 °C), which afforded the respective azide-functionalized P*t*BA (P*t*BA–N_3) in 85 – 90% isolated yields after washing the products with water.[8] Incorporation of the azide group was confirmed by ^{1}H NMR spectroscopy through the observation of an upfield shift in the signal attributed to the terminal methine from δ = 4.05 (C*H*–Br) to 3.78 ppm (C*H*–N_3) ($CDCl_3$), and by IR spectroscopy from the characteristic frequency observed at ν_{N3} = 2110 cm^{-1} (KBr).

Regioregular ethynyl-terminated P3HT (P3HT–C≡CH) was prepared from 2,5-dibromo-3-hexylthiophene and isopropylmagnesium chloride[10,11] *via* a Ni-catalyzed Grignard metathesis (GRIM) polymerization according to literature procedures.[5,7] After allowing the reaction to proceed for 10 min at room temperature, ethynylmagnesium bromide was added which simultaneously installed an ethynyl end-group and quenched the polymerization. Using this method, a variety of P3HT–C≡CH homopolymers were synthesized by adjusting the initial monomer to catalyst ratio. Following precipitation

from methanol, the materials were isolated in 50–60% yields by filtration (Table 4.1; entries 4–6). Analysis of the isolated polymers by GPC showed narrow molecular weight distributions characteristic of GRIM polymerizations, and the incorporation of the ethynyl end-group was confirmed by ^{1}H NMR spectroscopy where a signal was observed at δ = 3.52 ppm ($CDCl_3$), consistent with literature values.[12]

entry	Polymer[a]	$[M]_0/[I]_0$[b]	Isolated yield	M_n (Da)[c]	M_w/M_n [c]
1	P*t*BA$_{57}$N$_3$	80/1	87%	7,400	1.27
2	P*t*BA$_{112}$N$_3$	120/1	85%	14,650	1.32
3	P*t*BA$_{170}$N$_3$	300/1	85%	22,000	1.32
4	P3HT$_{29}$C≡CH	50/1	60%	4,900	1.24
5	P3HT$_{96}$C≡CH	100/1	50%	16,200	1.14
6	P3HT$_{138}$C≡CH	150/1	52%	23,300	1.23
7	P3HT$_{96}$-*b*-P*t*BA$_{57}$	–	77%	24,100	1.22
8	P3HT$_{96}$-*b*-P*t*BA$_{112}$	–	72%	32,000	1.24
9	P3HT$_{96}$-*b*-P*t*BA$_{170}$	–	66%	41,400	1.25
10	P3HT$_{29}$-*b*-P*t*BA$_{112}$	–	60%	24,900	1.40
11	P3HT$_{138}$-*b*-P*t*BA$_{112}$	–	69%	42,000	1.32

Table 4.1: Molecular weight and dispersity data for P*t*BA, P3HT, and resulting block copolymers. [a] The subscripted numbers denote the respective homopolymer's degree of polymerization, as determined by GPC. [b] Initial monomer (*t*BA or 2,5-dibromo-3-hexylthiophene) to initiator (EBiB or Ni(dppp)Cl_2) (dppp = 1,3-bis(diphenylphosphino)propane) ratio. [c] M_n and M_w/M_n were determined by GPC and are reported as their polystyrene equivalents.

Over the course of these syntheses, it was discovered that P3HT–C≡CH was highly sensitive to the isolation and purification conditions employed. For example,

subjecting the product to sequential Soxhlet extractions—a standard protocol[7] for the purification of P3HTs, including P3HT–C≡CH—we observed the gradual growth of a high molecular weight material that corresponded to nearly twice that of the bulk of the P3HT material, as determined by GPC (Figure 4.1A). Neat samples of P3HT–C≡CH left on the benchtop under ambient conditions for extended periods of time (>1 d) exhibited similar behavior. The origin of these high molecular weight polymers was attributed to alkyne–alkyne homocoupling reactions catalyzed by residual metal catalyst. In support of this hypothesis, a trimethylsilyl protected ethynyl P3HT was found to be stable to ambient conditions for indefinite periods of time (see Experimental section for details).

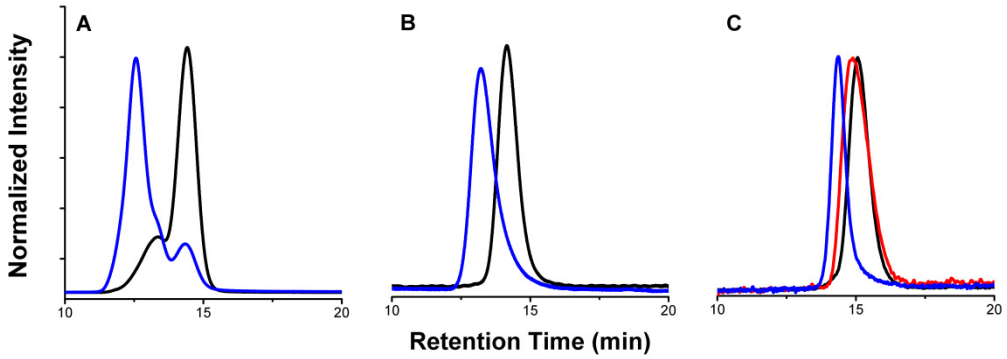

Figure 4.1: Representative GPC traces of A) P3HT–C≡CH purified using standard methodology (black) and its corresponding P3HT-b-PtBA copolymer (blue) obtained using UV-vis detection at 450 nm; B) $P3HT_{96}$–C≡CH purified using the methodology reported herein (black) and its corresponding $P3HT_{96}$-b-$PtBA_{170}$ copolymer (blue) obtained using UV-vis detection at 450 nm; and C) $P3HT_{96}$–C≡CH purified using the methodology reported herein (black), $PtBA_{170}$–N_3 homopolymer (red), and their corresponding $P3HT_{96}$-b-$PtBA_{170}$ copolymer (blue) obtained using refractive index detection. GPC conditions: 25 °C, THF as eluent.

Regardless, an improved purification procedure that eliminated the use of Soxhlet extractions altogether was developed: Upon conclusion of the aforementioned GRIM

polymerization reactions and addition of ethynylmagnesium bromide, the corresponding mixtures were poured into excess methanol and the precipitated polymers were collected via filtration, and then washed with excess methanol and hexanes. As shown in Figure 4.1B, this method afforded pure, monomodal samples of P3HT–C≡CH that were free of high molecular weight impurities.[13]

With the aforementioned homopolymers in hand, efforts shifted toward linking these materials. Under the optimized reaction conditions, equimolar amounts of P3HT–C≡CH and P*t*BA–N_3 were combined with two equiv. of N,N,N′,N″,N″-pentamethyldiethylenetriamine (PMDETA) / CuBr as the catalyst system,[4,5] and then stirred for 24 h at 40 °C in THF. After filtering the resulting reaction mixture through neutral alumina (eluent = THF) to remove the catalyst, the desired P3HT-*b*-P*t*BA block copolymers were obtained in 60 – 77% isolated yields by precipitating the reaction mixtures into methanol. Signals attributable to both coupling partners along with the disappearance of the signal assigned to the alkynyl moiety (δ = 3.52 ppm, $CDCl_3$) were observed by ^{1}H NMR spectroscopy and were accompanied by disappearance of the diagnostic ν_{N3} IR signal. Moreover, the GPC traces of the isolated copolymers were monomodal with narrow distributions and correlated well with their expected molecular weights (see Table 4.1, entries 7 – 11). It should be noted that Urien reported[5] that P3HT–C≡CH was deactivated and did not react at all with azide-terminated polystyrenes under analogous polymer–polymer coupling conditions. In light of the results presented herein, which also employ P3HT–C≡CH under nearly identical reaction conditions, we believe that the quality of this polymer is critical to determining the outcome of its cycloaddition with organic azides.

Building on the synthesis of pure P3HT-*b*-P*t*BA copolymers, we shifted our attention toward exploring amphiphilic derivatives. Acidolysis of the P3HT-*b*-P*t*BA

block copolymers was performed according to literature procedures,[9] using an excess of trifluoroacetic acid (TFA) in $CHCl_3$ and afforded P3HT-*b*-PAA in high yield (97%). The disappearance of the ^{1}H NMR signal attributed to the *t*-butyl group in P3HT-*b*-P*t*BA (δ = 1.40 ppm; THF-d_8) accompanied by the presence of the –OH stretch at ~3400 cm^{-1} in the IR spectrum indicated that the deprotection reaction was complete.

Slowly adding an equal volume of water (a good solvent for PAA and a poor solvent for P3HT) to a stirred THF solution of P3HT-*b*-PAA (initial conc. = 1.0 mg mL^{-1}) at room temperature afforded a purple solution that was accompanied by a bathochromic shift (433 $\rightarrow$ 507 nm) in the UV/vis absorption maxima. This behavior is consistent with the well-established solvatochromism of regioregular P3HT,[9,14] and is in agreement with the color change observed[15] during the formation of P3HT-encapsulated micelles. Following dialysis against de-ionized water to remove the residual THF, visually transparent aqueous solutions were obtained.

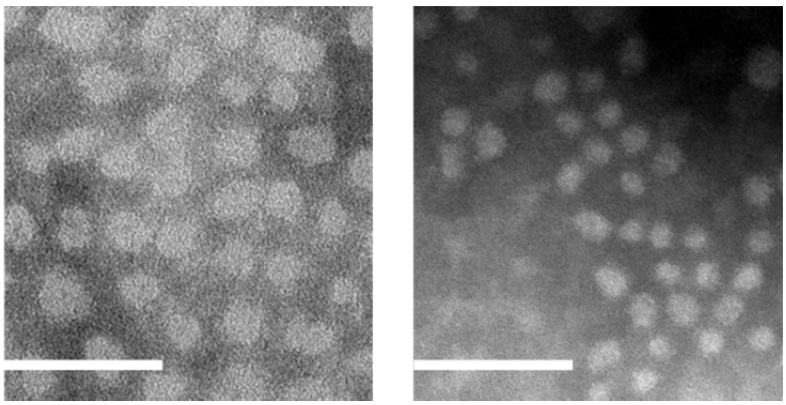

Figure 4.2: TEM images of micelles (stained with 1 wt% aqueous solution of phosphotungstic acid) formed from $P3HT_{96}$-*b*-PAA_{170} (left) and $P3HT_{29}$-*b*-PAA_{112} (right) (scale bar = 100 nm).

As shown in Figure 4.2, TEM revealed that spherical micellar nanostructures with narrow size distributions were formed for $P3HT_{96}$-*b*-PAA_{170} and $P3HT_{29}$-*b*-PAA_{112} (Table 1;

entries 9 and 10, respectively). The micelles assembled from the former exhibited larger average diameters (D_{av}) (25.6 ± 4.8 nm) than those prepared from the latter (D_{av} = 17.2 ± 5.3 nm), consistent with the difference in molecular weights of the constituent homopolymers. Intensity-averaged hydrodynamic diameters (D_h) of the nanoparticles, as determined by DLS, exhibited a similar trend, with $P3HT_{96}$-*b*-PAA_{170} having a D_h of 63.6 ± 2.2 nm and $P3HT_{29}$-*b*-PAA_{112} a D_h of 37.5 ± 2.4 nm.

3.3 CONCLUSION

In conclusion, we have prepared P3HT-*b*-P*t*BA copolymers *via* coupling of ethynyl-terminated P3HT with azide-terminated P*t*BA. Access to pristine P3HT–C≡CH was found to be critical for the success of the aforementioned reaction and a new, convenient method for cleanly isolating this polymer was developed. The amphiphilic block copolymer P3HT-*b*-PAA was obtained upon acidolysis of P3HT-*b*-P*t*BA and was found to self-assemble into micellar structures with sizes dependent on copolymer molecular weight and composition. We believe that the method discussed here will facilitate the creation and development of new block copolymers of high purity that are suitable for use and study in a broad range optoelectronic and semiconducting devices.

4.4 EXPERIMENTAL

4.4.1 General Considerations

All solvents were purchased from Fisher Scientific and used without additional further purification unless otherwise noted. Prior to use, t-butyl acrylate (tBA) was filtered through a short plug of alumina to remove the 4-methoxyphenol (MEHQ) stabilizer. All other chemicals were purchased from Aldrich, Alfa Aesar, or Fisher, and were used as received. 2,5-Dibromo-3-hexylthiophene was prepared according to literature procedures.[11] THF was dried over 3 Å molecular sieves and deoxygenated

using a Vacuum Atmospheres Company solvent purification system. The separation tubing used for dialysis (molecular weight cutoff or MWCO = 6–8 kDa) were purchased from Spectrum Medical Industries Inc. Proton NMR spectra were recorded using a Varian Gemini (300 MHz or 400 MHz) spectrometer. Chemical shifts are reported in delta (δ) units and expressed in parts per million (ppm) downfield from tetramethylsilane using the residual solvent as an internal standard ($CDCl_3$, 7.24 ppm; THF-d_8, 1.73 and 3.58 ppm). Gel permeation chromatography (GPC) was performed on a Viscotek system equipped with a VE 1122 pump, a VE 7510 degasser, two fluorinated polystyrene columns (IMBHW-3078 and I-MBLMW-3078) thermostated to 30 °C (using a ELDEX CH 150 column heater) and arranged in series or on a home-built system equipped with a Waters Model 510 HPLC pump, two fluorinated polystyrene columns (IMBHW-3078 and I-MBLMW-3078) arranged in series, and a Waters 486 Tunable Absorbance Detector. Molecular weight and polydispersity data are reported relative to polystyrene standards in tetrahydrofuran (THF). IR spectra were recorded using Perkin-Elmer Spectrum BX FT-IR system using KBr pellets. Differential scanning calorimetry analyses were performed on a Mettler Toledo DSC 823e. UV–vis spectra were recorded using a Perkin Elmer Instruments Lambda 35 spectrometer.

Transmission electron microscopy. TEM was performed in bright-field mode with a TECNAI Spirit Biotwin at 80 kV accelerating voltage. Samples for TEM measurements were diluted with equal volume of 1 wt% aqueous solution of phosphotungstic acid stain and cast onto carbon-coated copper mesh grids. Micrographs were collected at 100,000× magnification. The number average particle diameters (Davg) and standard deviations were generated from the analysis of a minimum of 150 particles from at least three different micrographs.

Dynamic Light Scattering. Hydrodynamic diameters (Dh) and size distributions were measured in aqueous media by DLS. The custom-built DLS instrument consisted of a Brookhaven Instruments Limited (Worcestershire, U.K.) system, a model BI-9000AT digital correlator, a model EMI-9865 photomultiplier, and a model 17 mW He-Ne laser (NSG America, SELFOC micro-lens, 1.8 mm diameter, 0.25 pitch) operated at 632.8 nm. Measurements were performed at 20 °C. Prior to analysis, solutions were filtered through a 0.45 μm Millex GV PVDF membrane filter (Millipore Corp., Medford, MA) to remove dust particles. Scattered light was collected at a fixed angle of 90°. The digital correlator was operated with 522 ratio spaced channels, an initial delay of 2 μs, a final delay of 100 ms, and a duration of 3 min. A photomultiplier aperture was used and the incident laser intensity was adjusted to obtain a photon counting of between 200 and 300 kcps. Only data in which the measured and calculated baselines of the intensity autocorrelation function agreed to within 0.1% were used to calculate particle sizes. The calculations of the particle size distributions and distribution averages were performed with the ISDA software package (Brookhaven Instruments), which employed single-exponential fitting, cumulants analysis, and non-negatively constrained least-squares (CONTIN) particle size distribution analysis routines. All determinations were made in triplicate.

4.4.2 Synthetic Procedures

Representative Procedure for the Synthesis of Poly(t-butyl acrylate) (PtBA). An oven-dried 100 mL flask was charged with copper(I) bromide (365 mg, 2.54 mmol), t-butyl acrylate (20.0 g, 156 mmol), N,N,N′,N″,N″-pentamethyldiethylenetriamine (PMDETA) (440 mg, 2.54 mmol), and a stir bar. After one freeze-pump-thaw cycle, ethyl 2-bromoisobutyrate (248 mg, 1.27 mmol) was added using nitrogen flushed syringes. After three additional freeze-pump-thaw cycles, the reaction mixture was warmed to

ambient temperature and placed in an oil bath at 65 °C. After stirring the mixture for 120 min, the reaction was quenched by immersion of the flask in liquid nitrogen. The reaction mixture was then taken up in THF and passed through a short column of neutral alumina (eluent = THF) to remove the residual catalyst. The polymer mixture was then concentrated, precipitated into cold methanol/water mixture (50/50 v/v) (3×), and collected via filtration (16.6 g, 80% yield). Data for P*t*BA$_{112}$: GPC: M_n = 14.6 kDa, M_w/ M_n = 1.32. ^{1}H NMR ($CDCl_3$, ppm): δ 4.05 (broad overlapping m, CH_3CH_2O and C*H*Br end groups), 2.30-2.10 (broad, C*H* of the polymer backbone), 1.88-1.68 (broad, *meso* CH_2 of the polymer backbone), 1.65-1.30 (broad, *meso* and *racemo* CH_2 of the polymer backbone and $(CH_3)_3C$). Using end-group analysis, the M_n = 14.5 kDa. FTIR (KBr): 3448, 2981, 2933, 1734, 1367, 1259, 1150, 846 cm^{-1}.

Representative Procedure for the Synthesis of PtBA-N$_3$. A 50 mL flask was charged with PtBA (M_n = 7.4 kDa, 410 mg, 55 μmol), NaN_3 (36 mg, 550 μmol), DMF (8 mL), and a stir bar. The resulting mixture was stirred at 50 °C for 12 h and then cooled to ambient temperature. After adding CH_2Cl_2 (50 mL) and water (50 mL), the organic phase was separated and extracted with water (4 × 50 mL), and then dried over Na_2SO_4. Removal of the residual solvent under reduced pressure afforded the desired product in 87% yield (350 mg). Data for P*t*BA$_{57}$-N_3: ^{1}H NMR ($CDCl_3$, ppm): δ 4.05 (broad m, CH_3CH_2O), 3.78 (broad, C*H*-N_3), 2.30-2.10 (broad, C*H* of the polymer backbone), 1.88-1.68 (broad, *meso* CH_2 of the polymer backbone), 1.70-1.30 (broad, *meso* and *racemo* CH_2 of the polymer backbone and $(CH_3)_3C$). FTIR (KBr): 3450, 2980, 2123, 1730, 1560, 1459, 1369, 1259, 1150, 846 cm^{-1}.

Representative Procedure for the Synthesis of Poly(3-hexylthiophene)-C≡CH (P3HT-C≡CH). A 50 mL oven-dried flask was charged with 2,5-dibromo-3-hexylthiophene (500 mg, 1.53 mmol), dry THF (12 mL), and a stir bar. After adding

isopropylmagnesium chloride (0.76 mL, 2.0 M solution in THF), the resulting mixture was placed in an oil bath at 50 °C for 2 h. Upon cooling to ambient temperature, Ni(dppp)Cl_2 (16.6 mg, 2 mol%; dppp = 1,3-bis(diphenylphosphino)propane) and, after 10 min, ethynylmagnesium bromide (0.4 mL, 0.5 M in THF) were added to the mixture. After an additional 5 min, 30 mL of methanol was poured into the reaction flask, which caused a dark-purple solid to precipitate. The solid was then isolated via filtration, and washed with excess methanol and hexanes to remove residual metal salts, unreacted monomer and oligomers. The purple solid was then dried under vacuum to afford 150 mg (60% yield) of the desired polymer. The microstructure of the polymer was determined by ^{1}H NMR spectroscopy to be 97% head-to-tail. GPC: M_n = 4.9 kDa, M_w/M_n = 1.24. ^{1}H NMR ($CDCl_3$, ppm): δ 6.98 (s, C*H* of the thiophene ring), 3.52 (s, terminal ethynyl C*H*), 2.80 (t, C*H*$_2$$CH_2CH_2CH_2CH_2CH_3$), 1.71 (m, CH_2C*H*$_2$$CH_2CH_2CH_2CH_3$), 1.50-1.30 (broad m, CH_2CH_2C*H*$_2$C*H*$_2$C*H*$_2$$CH_3$), 0.90 (t, $CH_2CH_2CH_2CH_2CH_2$C*H*$_3$).

Representative Procedure for the Synthesis of P3HT-b-PtBA. A 25 mL flask was charged with P3HT-C≡CH (26.4 mg, 5.38 μmol), P*t*BA-N_3 (80.5 mg, 5.55 μmol), CuBr (1.5 mg, 10 μmol), PMDETA (2.0 mg, 11 μmol) and dry THF (10 mL). The mixture was degassed by one freeze-pump-thaw cycle and was then immersed into an oil bath thermostatted to 40 °C. After stirring for 24 h, the reaction mixture was passed through a short column of neutral alumina (eluent = THF) to remove the residual catalyst. The crude product was then concentrated and precipitated into methanol to remove unreacted P*t*BA-N_3. The desired product was collected in 60% yield (67 mg) *via* filtration. ^{1}H NMR ($CDCl_3$, ppm): δ 6.98 (s, C*H* of the thiophene ring), 2.81 (t, C*H*$_2$$CH_2CH_2CH_2CH_2CH_3$), 2.30-2.10 (broad, C*H* of the polymer backbone), 1.90-1.75 (broad, *meso* C*H*$_2$ of the polymer backbone), 1.71 (m, CH_2C*H*$_2$$CH_2CH_2CH_2CH_3$), 1.50-

1.30 (broad m, $CH_2CH_2CH_2CH_2CH_2CH_3$, *meso* and *racemo* CH_2 of the P*t*BA backbone and $(CH_3)_3C$)), 0.90 (t, $CH_2CH_2CH_2CH_2CH_2CH_3$).

Representative Procedure for the Synthesis of P3HT-b-PAA. After dissolving P3HT$_{96}$-*b*-P*t*BA$_{170}$ (14.3 mg, 0.35 μmol) in chloroform (5 mL), trifluoacetic acid (0.20 mL, 33 mmol) was added. The reaction mixture was allowed to stir at room temperature for 24 h, after which the solvent was removed under reduced pressure. The resulting crude solid was then washed with cold hexanes and dried under reduced pressure to afford the desired product (9.5 mg, 97% yield). ^{1}H NMR (THF-d_8): δ 7.08 (s, C*H* on the thiophene ring), 2.85 (t, $CH_2CH_2CH_2CH_2CH_2CH_3$), 2.55-2.38 (broad, C*H* of the polymer backbone), 2.00-1.85 (broad, *meso* CH_2 of the polymer backbone), 1.75-1.30 (broad m, $CH_2CH_2CH_2CH_2CH_2CH_3$, *meso* and *racemo* CH_2 of the PAA backbone), 0.98 (t, $CH_2CH_2CH_2CH_2CH_2CH_3$).

Procedure for the Synthesis of Poly(3-hexylthiophene)-C≡C-TMS (P3HT-C≡C-TMS). The polymerization was conducted analogously to the synthesis of P3HT-C≡CH by quenching the polymerization with 2-(trimethylsilyl)ethynylmagnesium bromide.[16] Following precipitation into methanol and collection by filtration, the isolated solids were washed with excess methanol, and subjected to Soxhlet extraction with chloroform. The polymer was isolated from the chloroform solution upon evaporation of the residual solvent in 78% yield. GPC: M_n = 4.6 kDa, M_w/M_n = 1.33. ^{1}H NMR ($CDCl_3$, ppm): δ 6.96 (s, C*H* of the thiophene ring), 2.78 (t, $CH_2CH_2CH_2CH_2CH_2CH_3$), 1.69 (m, $CH_2CH_2CH_2CH_2CH_2CH_3$), 1.50-1.30 (broad m, $CH_2CH_2CH_2CH_2CH_2CH_3$), 0.90 (t, $CH_2CH_2CH_2CH_2CH_2CH_3$), 0.25 (s, $Si(CH_3)_3$).

Procedure Used for Micelle Assembly. To a round-bottom flask equipped with a magnetic stir bar was added P3HT-*b*-PAA followed by THF (8.0 mL). The mixture was stirred for 2 h at room temperature to ensure that a homogeneous solution (final polymer

concentration = *ca.* 1.0 mg/mL) had formed. To this solution, an equal volume of de-ionized water (8.0 mL) was added dropwise *via* a syringe pump over 3 h. The mixture was then stirred for 12 h at room temperature before being transferred to a pre-soaked dialysis tube and then dialyzed against de-ionized water for 4 d, which afforded a transparent purple micelle solution (*ca.* 16 mL) with the final polymer concentration in the range of 0.20 to 0.30 mg/mL.

4.5 ACKNOWLEDGMENTS

Portions of this chapter were reprinted with permission from Li, Z.; Ono, R. J.; Wu, Z.-Q.; Bielawski, C. W. *Chem. Commun.* **2011**, *47*, 197. Copyright 2011 The Royal Society of Chemistry. Zicheng Li and Zong-Quan Wu are gratefully acknowledged for their synthetic contributions. Prof. Christopher W. Bielawski is also gratefully acknowledged for helping to write the original manuscript.

4.6 REFERENCES

(1) (a) Sivula, K.; Ball, Z. T.; Watanabe, N.; Frechet, J. M. J. *Adv. Mater.* **2006**, *18*, 206-210. (b) Yang, C.; Lee, J. K.; Heeger, A. J.; Wudl, F. *J. Mater. Chem.* **2009**, *19*, 5416-5423. (c) Richard, F.; Brochon, C.; Leclerc, N.; Eckhardt, D.; Heiser, T.; Hadziioannou, G. *Macromol. Rapid Commun.* **2008**, *29*, 885-891. (d) Zhang, Q.; Cirpan, A.; Russell, T. P.; Emrick, T. *Macromolecules* **2009**, *42*, 1079-1082. (e) Lee, J. U.; Cirpan, A.; Emrick, T.; Russell, T. P.; Jo, W. H. *J. Mater. Chem.* **2009**, *19,* 1483. (f) Tsai, J.-H.; Lai, Y.-C.; Higashihara, T.; Lin, C.-J.; Ueda, M.; Chen, W.-C. *Macromolecules* **2010**, *43*, 6085.

(2) (a) Liu, J.; Sheina, E.; Kowalewski, T.; McCullough, R. D. *Angew. Chem. Int. Ed.* **2002**, *41*, 329-332. (b) Iovu, M. C.; Craley, C. R.; Jeffries-El, M.; Krankowski, A. B.; Zhang, R.; Kowalewski, T.; McCullough, R. D. *Macromolecules* **2007**, *40*, 4733-4735. (c) Iovu, M. C.; Jeffries-El, M.; Sheina, E. E.; Cooper, J. R.; McCullough, R. D. *Polymer* **2005**, *46*, 8582-8586. (d) Dai, C.-A.; Yen, W.-C.; Lee, Y.-H.; Ho, C.-C.; Su, W.-F. *J. Am. Chem. Soc.* **2007**, *129*, 11036-11038. (e) Boudouris, B. W.; Frisbie, C. D.; Hillmyer, M. A. *Macromolecules* **2010**, *43*, 3566-3569. (f) Botiz, I.; Darling, S. B. *Macromolecules* **2009**, *42*, 8211-8217. (g) Radano, C. P.; Scherman, O. A.; Stingelin-Stutzmann, N.; Muller, C.; Breiby, D. W.; Smith, P.; Janssen, R. A. J.; Meijer, E. W. *J. Am. Chem. Soc.* **2005**, *127*, 12502-12503.

(3) Hartmuth, C. K.; Finn, M. G.; Sharpless, K. B. *Angew. Chem. Int. Ed.* **2001**, *40*, 2004-2021.

(4) A peak attributable to a 1,2,3-triazole group was not observed by ^{1}H NMR spectroscopy.

(5) Urien, M.; Erothu, H.; Cloutet, E.; Hiorns, R. C.; Vignau, L.; Cramail, H. *Macromolecules* **2008**, *41*, 7033-7040.

(6) Tao, Y.; McCulloch, B.; Kim, S.; Segalman, R. A. *Soft Matter* **2009**, *5*, 4219-4230.

(7) Jeffries-El, M.; Sauve, G.; McCullough, R. D. *Macromolecules* **2005**, *38*, 10346-10352.

(8) Qingchun, L.; Yongming, C. *J. Polym. Sci. Part A: Polym. Chem.* **2006**, *44*, 6103-6113.

(9) Craley, C. R.; Zhang, R.; Kowalewski, T.; McCullough, R. D.; Stefan, M. C. *Macromol. Rapid Commun.* **2009**, *30*, 11-16.

(10) Miyakoshi, R.; Yokoyama, A.; Yokozawa, T. *J. Am. Chem. Soc.* **2005**, *127*, 17542-17547.

(11) Loewe, R. S.; Ewbank, P. C.; Liu, J.; Zhai, L.; McCullough, R. D. *Macromolecules* **2001**, *34*, 4324-4333.

(12) Benanti, T. L.; Kalaydjian, A.; Venkataraman, D. *Macromolecules* **2008**, *41*, 8312-8315.

(13) Storage of purified P3HT-C≡CH was found to form high molecular weight impurities over time. It is recommended that the material be used immediately upon preparation, or stored under inert atmosphere in a freezer (–20 °C).

(14) Scherf, U.; Gutacker, A.; Koenen, N. *Acc. Chem. Res.* **2008**, *41*, 1086-1097.

(15) Wang, M.; Kumar, S.; Lee, A.; Felorzabihi, N.; Shen, L.; Zhao, F.; Froimowicz, P.; Scholes, G. D.; Winnik, M. A. *J. Am. Chem. Soc.* **2008**, *130*, 9481-9491.

(16) Ohmiya, H.; Yorimitsu, H.; Oshima, K. *Org. Lett.* **2006**, *8*, 3093-3096.

Chapter 5: Mimicking Conjugated Polymer Thin Film Photophysics with a Well-Defined Triblock Copolymer in Solution

5.1 INTRODUCTION

Poly(3-hexylthiophene) (P3HT) and its derivatives are among the most studied π-conjugated polymers and widely utilized in organic photovoltaics (OPVs)[1] because of their high hole mobilities.[2] While the power conversion efficiencies for some OPVs derived from P3HT and related polymers are approaching the levels of interest for industrial exploitation, that is, 8.3%,[3] a fundamental understanding of the photophysics and morphologies of thin films of P3HT is crucial to optimize OPV performance.[4] However, the inherent heterogeneity of these polymer thin films makes them exceedingly difficult to probe on any submacroscopic level. To avoid the complexity of such systems, many groups have tried to mimic the thin-film photophysics in solution by adding a poor solvent to solutions of P3HT and P3HT derivatives.[5-11] Unfortunately, none of them were able to fully reproduce in a controllable way the spectroscopic properties of thin films of P3HT. Specifically, the kinetic stability and the number of chains involved in the resulting aggregates were uncontrolled and unknown.

Here, we report on the photophysics of a newly synthesized conjugated rod−coil−rod triblock copolymer composed of two regioregular P3HT chains covalently linked to both ends of a poly(*tert*-butyl acrylate) (P*t*BA) chain: P3HT-*b*-PtBA-*b*-P3HT (Figure 5.1). This new model system has rendered it possible to reproduce the electronic spectra—in solution—of P3HT in both the solvated and the condensed phases; the triblock copolymer in a good solvent behaves as P3HT in solution, whereas in a poor solvent, the two chains of P3HT interface as they would in a thin film. The collapsed triblock copolymer in solution is fully reversible, stable for long periods (> 1 year), and its formation is concentration-independent. As such, the triblock copolymer in a poor

solvent is a good model system to address open questions regarding film photophysics and if these phenomena are related to the interaction of two chains or the result of the larger three dimensional structure in the thin film. For example, thin films of P3HT exhibit a dramatic drop in the fluorescence quantum yield compared with solution. This fluorescence quenching in CP chains has been attributed to a number of causes: A high yield of nonemitting species, such as polarons, or charge-transfer excitons directly generated from the photoexcitation,[12,13] and/or by the lower oscillator strength for emission in H-aggregates in the interchain interactions.[14,15] The delocalization of polarons over a number of neighboring chains as a result of interchain interactions appears to be a key parameter in the generation of charge-transfer states as well as in the quenching of fluorescence.[16,17] With our model system, where only two chains of P3HT are interacting, a long-range energy transfer within a three-dimensional network is not possible given the small size of the system. However, the interchain electronic interactions are nearly identical to those of the film and are sufficient to explain the large fluorescence quenching present in thin films of P3HT. We also report on the presence of charge-transfer excitons involved in the fluorescence quenching mechanism.

5.2 Results and Discussion

Synthesis and Purification

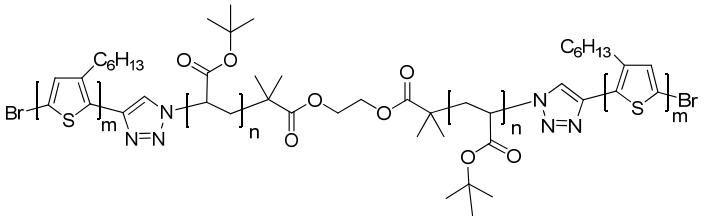

P3HT-*b*-P*t*BA-*b*-P3HT

Figure 5.1: The rod–coil–rod triblock copolymer shown consists of two poly(3-hexylthiophene) (P3HT) chains covalently linked to both ends of a poly(*tert*-butyl acrylate) (P*t*BA) chain.

The rod–coil–rod triblock copolymer, P3HT-*b*-P*t*BA-*b*-P3HT, was synthesized by "clicking" two low dispersity ($Đ$; M_w/M_n) P3HT chains with alkynyl termini to a P*t*BA core that featured complementary azide end groups (for more details on the synthesis, see the Experimental Section).[18] After purification via gel permeation chromatography (GPC), a triblock copolymer composed of two rodlike 10 kDa regioregular P3HT chains covalently linked to a 26 kDa PtBA coil polymer with an overall number-average molecular weight (M_n) of 46 kDa and $Đ$ = 1.2 was obtained (Figure A11, Appendix A).

Addition of a Poor Solvent

Previous studies have shown that, upon addition of a poor solvent to solutions of P3HT or P3HT derivatives, the absorption spectrum is red shifted[5-10] similarly to the shift observed upon concentration (i.e., from solution to the formation of a thin film).[12] As a poor solvent (methanol) is added to a solution of the aforementioned triblock copolymer in a good solvent (toluene),[10] the absorption peak is red shifted from 455 to 560 nm, as shown in Figure 5.2a. The red shift of the absorption spectrum in thin films of P3HT[19-21] and in P3HT aggregates in solution[5-10] was interpreted to arise from the increased coplanarity forced by interchain interactions. Similarly, the red shift observed for the triblock copolymer in a poor solvent can be attributed to the interchain interactions of P3HT chains generating more planar conformations. Despite the lowering of the solvent quality by the addition of a poor solvent, the solution of collapsed triblock copolymer is stable over time (at least a year, Figure A12, Appendix A), in contrast to previous reports which have described the precipitation of P3HT homopolymer aggregates formed in poor solvents.[7] The stability of the triblock copolymer is likely the result of it being a unimolecular aggregate composed of two intramolecularly interacting chains of P3HT, which does not generate larger aggregates, and the presence of the P*t*BA polymer, which has a higher solubility in methanol.[22]

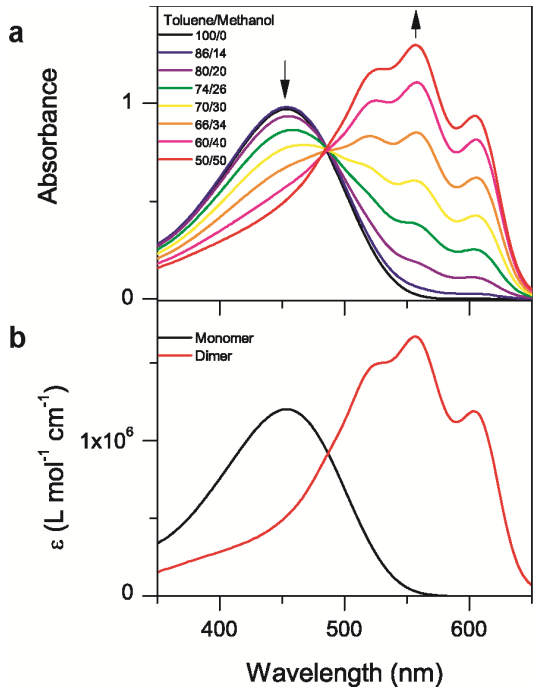

Figure 5.2: Addition of a poor solvent to the triblock copolymer. UV-vis absorption spectra of the P3HT-*b*-P*t*BA-*b*-P3HT triblock copolymer for various ratios of toluene and methanol solvents with respect to toluene (a). The arrows show the decay and increase of the bands centered at 455 nm and 560 nm, respectively. Molar extinction coefficient spectra of the triblock monomer (b, black) and the triblock dimer (b, red) extracted from the UV-vis absorption spectra represented in (a).

The spectral changes that occur upon lowering the solvent quality exhibit a clear isosbestic point at 487 nm, indicating an interconversion between only two absorbing species. The molar extinction coefficient spectra of these two species, which will be referred to as the extended triblock and the collapsed triblock, respectively, are represented in Figure 5.2b. These two spectra were extracted from the absorption spectra of the triblock copolymer in 100% toluene (good solvent) and 50/50% toluene/methanol (poor solvent) with respect to the overlaying of the two molar extinction coefficient spectra at 487 nm, per the definition of an isosbestic point. The extended triblock spectrum shows a broad π–π^* electronic transition band centered at 455 nm, which

closely resembles the photophysical characteristics of highly regioregular P3HT chains in a good solvent.[23] The collapsed triblock spectrum was red shifted, with a peak centered at 560 nm and two additional vibronic structures at 525 and 605 nm and were attributed to the C═C double bond stretching vibrational mode (energy of 0.18 eV)[24] coupled to the π–π* electronic transition. This result suggested to us that the ground state of the collapsed triblock contains a smaller distribution of torsional conformers and conjugation lengths compared with that of the extended triblock. The ratio of the 0–0 transition to the 0–1 transition increases with increasing methanol content, which we interpret to signify an increase of the collapsed triblock concentration in comparison to the extended triblock concentration. Moreover, the collapsed triblock appears to have features similar to those of a thin film of P3HT.

Spano et al. have developed a weakly coupled H-aggregates model to reproduce the experimental data obtained for thin films of P3HT.[14,24,25] This H-aggegrates model assumes that the spectra have a Franck–Condon vibronic progression. Following previous H-aggregates models for P3HT, we utilize a Huang–Rhys factor of 1 and assume that the 0.18 eV C═C stretching vibration predominantly couples the electronic transition.[24] The weak coupling assumes that the interchain interactions gives rise to an excitonic band with a bandwidth that is on par or smaller than the energy of this dominant vibronic mode coupled to the π–π* electronic transition. As the collapsed triblock appears to be a good model for the P3HT thin film, we applied the weakly coupled H-aggregates model to it to extract the exciton bandwidth. The collapsed triblock molar extinction coefficient spectrum was fit to the sum of three Gaussian functions sharing the same spectral width with a constant energy spacing, chosen to be 0.18 eV. The good quality of this fit (Figure A13) is consistent with previous theoretical results for P3HT films.[24] The peak ratio of the 0–0 transition and the 0–1 transition of the absorption spectrum can be used to

estimate the strength of the excitonic coupling. From this fit, we estimate an exciton bandwidth of 114 meV for the collapsed triblock. This value is in good agreement with the values reported for P3HT films under different processing methods.[14,26]

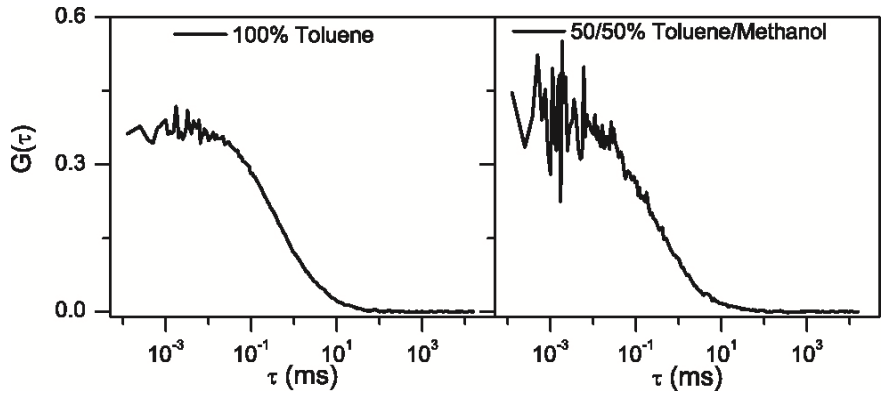

Figure 5.3: Fluorescence correlation spectroscopy (FCS). Fluorescence correlation spectroscopy (FCS) curves of the same initial concentration of P3HT-*b*-P*t*BA-*b*-P3HT triblock copolymer in 100% toluene (good solvent, left panel) and 50/50% toluene/methanol (poor solvent, right panel) under excitation at 488 nm.

An important remaining question was whether the collapsed triblock arises from the interaction of the two P3HT segments within a single triblock copolymer chain or if it results from aggregation of many different copolymers with one another. As noted above, the collapsed triblock is stable over time despite the low solvent quality, suggesting that only the two P3HT chains on either end of the P*t*BA linker are involved in the aggregation event. To characterize the number of chains involved in the formation of the collapsed triblock, fluorescence correlation spectroscopy (FCS) measurements were carried out on the same initial concentration of triblock copolymer in good and poor solvents, respectively (Figure 5.3). FCS allows us to evaluate the number of emitting molecules within the focused spot of a 488 nm laser in a confocal microscope by detecting correlations in the fluctuations of the fluorescence signal detected by two

avalanche photodiodes.[27] From the fluorescence correlation traces, the inverse of the average emitting molecule numbers in the focal volume is determined directly from the amplitude of the initial plateau in the autocorrelated signal. For the same initial concentration of the triblock copolymer, the average number of emitting molecules is 2.4 ± 0.6 and 2.8 ± 0.8 in good and poor solvents, respectively. Therefore, the number of emitting sites remains constant in both solutions. The above results demonstrate that the collapsed triblock is an aggregate involving just the two chains of P3HT within a single triblock copolymer molecule.

It is possible that the lower concentration used for FCS measurements (~1000 times more diluted than for absorption conditions) results in a sample free of large aggregates. However, we have shown that the triblock aggregation kinetics and spectra are independent of the initial concentration of the copolymer. As shown in Figure 5.4, the addition of methanol to the solution of triblock copolymer in 100% toluene was performed for three different initial concentrations of the triblock copolymer, ranging from 0.13 to 0.81 μmol L^{-1}. The evolution of the absorbances at 455 nm and 560 nm (absorbance peaks for the triblock monomer and triblock dimer, respectively) are identical for the three initial concentrations of triblock copolymer; thus, the formation of the triblock dimer is independent of the initial concentration of the triblock copolymer. This is the first report of an aggregate of P3HT chains in which the number of chains is rigorously known.

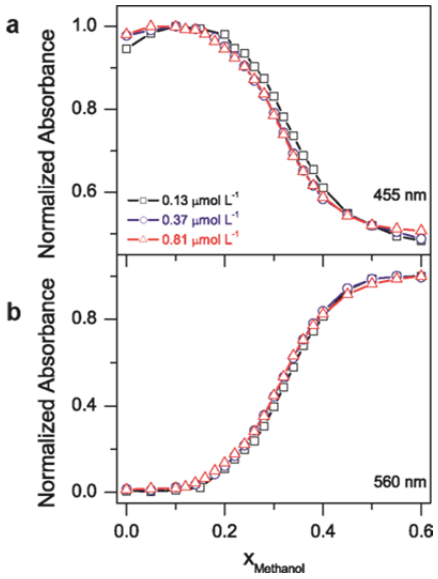

Figure 5.4: Initial concentration dependence. Normalized absorption evolution as a function of the volume fraction of methanol added to the triblock copolymer in 100% toluene at 455 nm (**a**) and 560 nm (**b**) for three different initial concentrations of triblock copolymer: 0.13 µmol L^{-1} (black squares), 0.37 µmol L^{-1} (blue circles), 0.81 µmol L^{-1} (red triangles).

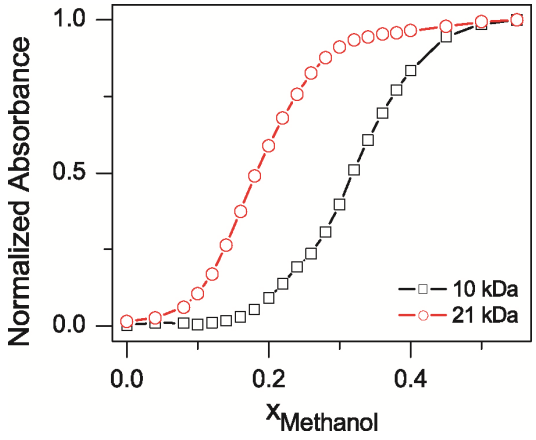

Figure 5.5: Normalized absorption evolution at 560 nm (absorption peak of the collapsed triblock) as a function of the volume fraction of methanol added to the triblock copolymers in 100% toluene for two different molecular weight triblock copolymers. M_n(P3HT) = 10 kDa (black squares) and M_n(P3HT) = 21 kDa (red circles); M_n(P*t*BA) = 21 kDa for both copolymers.

Molecular Weight Effect on the Interchain Interactions in Two Different Triblock Copolymers

A second triblock copolymer (M_n = 63 kDa, $Đ$ = 1.2) with larger P3HT chains (M_n = 21 kDa, $Đ$ = 1.1) and a P*t*BA chain of similar length (M_n = 21 kDa) was synthesized to probe whether the interchain interactions in the collapsed triblock are dependent on P3HT chain length. As shown in Figure 5.5, for the same amount of methanol added, the percentage of the collapsed triblock that is present in solution is larger for the longer triblock copolymer (63 kDa). A plateau, describing a mixture composed of 90% collapsed triblock and 10% extended triblock, is reached after the addition of 50% and 30% of methanol to the 46 and 63 kDa triblock copolymers, respectively. The absorption spectra of both copolymers in a 40/60% toluene/methanol mixture are similar after normalization (data not shown). Thus, the two P3HT chains within a triblock copolymer more readily interact with one another when their molecular weight is higher. However, the nature of the interchain interactions is nearly identical in both triblock copolymers, and it was not possible to obtain a solution containing more than 90% of the collapsed triblock.

Comparison to a Thin Film of P3HT

The triblock copolymer in a poor solvent generates a new species that is stable over time (> 1 year) at different initial concentrations, is fully reversible (Figure A15, Appendix A), and involves only the two chains of P3HT in one triblock copolymer molecule. We have shown that the collapsed triblock is well described by the weakly coupled H-aggregates model (Figure A13), initially developed for thin films of P3HT. To compare the triblock copolymer in a poor solvent with a thin film of P3HT directly, the absorption spectra of the triblock copolymer in 50/50% toluene/methanol solution and that of a spin-coated thin film of 10 kDa P3HT were overlaid, as shown in Figure 5.6a.

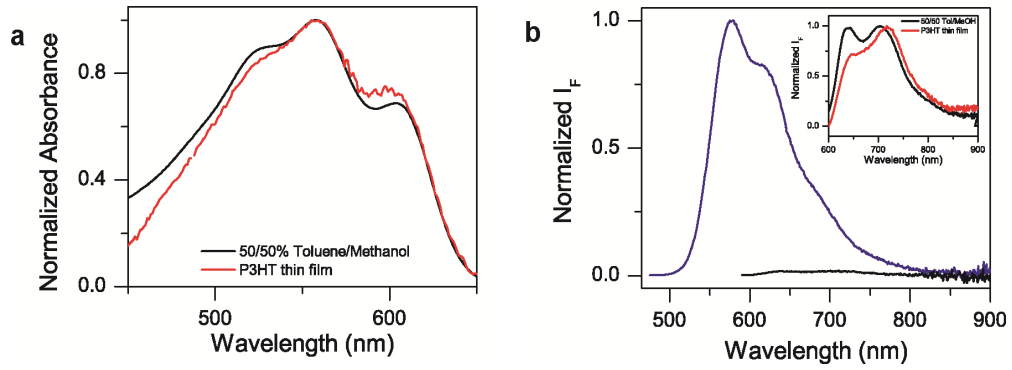

Figure 5.6: UV-vis absorption spectra of the triblock copolymer in 50/50% toluene/methanol (poor solvent, a, black) and a thin film of P3HT (10 kDa) spin-coated from toluene (a, red) after normalization at 560 nm, that is, the 0–1 transition. Emission spectra of the triblock copolymer in 100% toluene (b, blue, $\lambda_{exc} = 455$ nm) and 50/50% toluene/methanol (b, black, $\lambda_{exc} = 560$ nm) after normalization by the maximum of emission of the triblock copolymer in 100% toluene. Inset is the comparison of the emission spectra of the triblock copolymer in 50/50% toluene/methanol (black) and a thin film of P3HT (10 kDa) (red).

The peak positions are identical, although the 0–0 transition is slightly reduced in intensity for the triblock copolymer in a poor solvent after normalization at the 0–1 transition. The intensity of the 0–0 transition in comparison to that of the 0–1 transition is known to be correlated with the degree of crystallinity[28] as well as to the molecular weight of P3HT chains.[29] As the molecular weights of P3HT are identical for both systems, only the first hypothesis can be considered. Moreover, a direct comparison between the fluorescence spectra of the triblock copolymer in a poor solvent and of a thin film of P3HT reveals similar features (inset in Figure 5.6b). The two spectra are similar, although the 0–0 transition is more intense in the emission spectrum of the triblock copolymer in a poor solvent compared to a thin film of P3HT. The 0–0 transition is forbidden in H-aggregates, and the ratio of the 0–0 and 0–1 peak absorbance reflects the

disorder in the H-aggregates.[24,25] Thus, the triblock copolymer is a good model for thin films of P3HT, but involves significantly fewer chromophores than are typically used in the weakly coupled H-aggregates model. Therefore, it is not surprising that the H-aggregates are more disordered in the triblock copolymer in a poor solvent than for a thin film of P3HT cast from toluene.

A Model System to Probe the Effects of Interchain Interactions in Thin Films

Because the collapsed triblock copolymer mimicks P3HT thin-film photophysics, it can serve as a model for understanding the effects of interchain interactions found in thin films. Many properties of conjugated polymers change upon going from well-solvated chains in solution to densely packed chains in a film. This is due to primarily two effects, the first of which is interchain interactions or electronic states that arise from the close proximity of multiple polymer chains. Second, as a consequence of the chains being closer together, there is now a large three-dimensional network of interacting chains. This greatly amplifies the effects of any defects, as long-range energy transfer within this network allows excitation to migrate to these sites. Even if they are few in number, they can dominate the excited-state lifetime and emission spectroscopy. The collapsed triblock allows us to isolate only the effect of interchain interactions—in the absence of long-range, three dimentional energy transfer—as it is composed of only two interacting polymer chains. As such, it is easier to investigate the origin of issues that can be difficult to determine in thin films. For instance, upon going from solution to thin films, the fluorescence of P3HT is quenched ~20 times with the quantum yield falling from 33–42% to 1.6–2%.[9,12,30,31] The origins of this phenomenon remain unclear, although it has been hypothesized that it could result from the interchain excitation having a lower emission yield, or from a small number of interchain traps that quench the emission from a large number of chains. To examine this, the quantum yield of the

triblock copolymer fluorescence in both good and poor solvents was quantified. After adjusting for differences in the solvent refractive indices and the absorbances at the excitation wavelengths, the quantum yield of the triblock in a good solvent (100% toluene) was found to be 41%, and fell to a mere 2% in a poor solvent (50/50% toluene/methanol). The corresponding fluorescence spectra are represented in Figure 5.6b after normalization by its maximum of fluorescence intensity in 100% toluene. The triblock copolymer fluorescence is quenched by a factor of 20 in going from a good to a poor solvent just as P3HT fluorescence is quenched by 20 times in going from solution to thin film. This reduction in fluorescence intensity was also observed in the FCS experiment, evidenced by the reduced signal-to-noise for the triblock fluorescence in going from good to poor solvent (cf. Figures 5.3 and A14).

It was previously demonstrated that the fluorescence quenching of P3HT in going from solution to a film cannot be explained by a reduction of the exciton lifetime.[32,33] Three main explanations have been proposed for the fluorescence quenching in thin films of P3HT: (i) photogeneration of nonemitting species, such as delocalized polarons, that can be associated with a three-dimensional energy transfer;[16,17] (ii) the presence of H-aggregates with a lower oscillator strength for the emission of the Frenkel excitons;[14,15] and (iii) production of interchain charge-transfer excitons (noted CT excitons).[12,13] The hypothesis that involves polaron quenching is unlikely as the source of the reduced quantum yield for the triblock as it uniformly shows a reduced quantum yield. It is unlikely in the absence of energy transfer among a large number of chains that each triblock would produce a quenching site in equal yield. However, even with only two interacting chains, it is possible to generate delocalized excited states, such as CT excitons, that will have a lower emission yield. Moreover, the two chains in the triblock system could fold back on themselves to generate states that may involve more than just

two chromophores. This could lead to either a case of lower oscillator strength from H-aggregate-like states and/or delocalized charge-transfer states (or states that are a mixture of both).

To probe the hypothetical presence of excitons with CT character as the origin of the fluorescence quenching in the triblock copolymer in a poor solvent, we measured the absorption spectra of the triblock copolymer in two poor solvent systems, 50/50% toluene/methanol (polar solvent) and 15/85% toluene/hexanes (nonpolar solvent), as shown in Figure 5.7a. In both solvents, a mixture of the extended triblock and the collapsed triblock is observed; in both polar and nonpolar solvent systems, 90% of the collapsed triblock was formed. Thus, the polarity of solvent is not the driving force to generate the collapsed triblock.

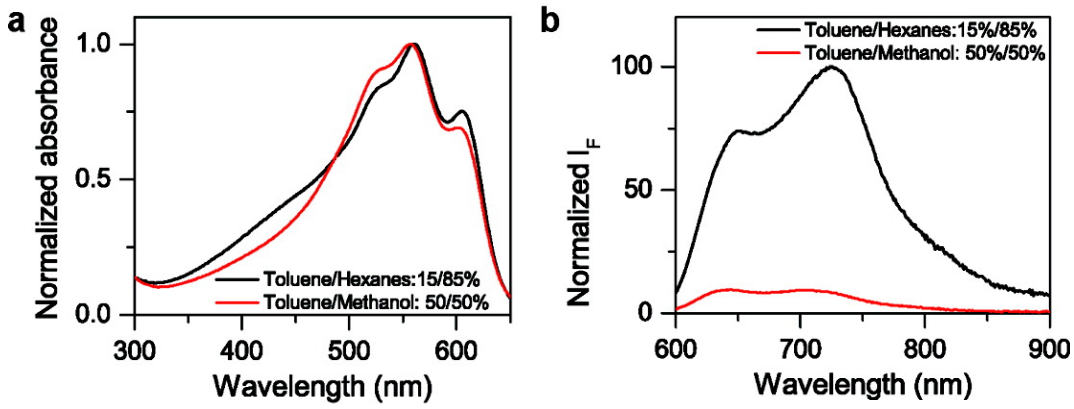

Figure 5.7: UV–vis absorption spectra of the triblock copolymer in 50/50% toluene/methanol (polar solvent, a, red) and in 15/85% toluene/hexanes (nonpolar solvent, a, black) after normalization at 560 nm, that is, the 0–1 transition. Emission spectra of the triblock copolymer in 50/50% toluene/methanol (b, red, λ_{exc} = 560 nm) and 15/85% toluene/hexanes (b, black, λ_{exc} = 560 nm) after normalization by the maximum of emission of the triblock copolymer in 15/85% toluene/methanol.

Subsequently, we determined the fluorescence quantum yield of the triblock copolymer in the two abovementioned solvent systems (Figure 5.7b). Methanol and hexanes are the poor polar and poor nonpolar solvents, respectively. As polar solvents are known to stabilize charge-transfer states, we expected the quantum yield of fluorescence to increase as the polarity of the solvent decreased. Indeed, the quantum yield of fluorescence of the triblock copolymer in the nonpolar solvent system (15/85% toluene/hexanes) was found to be 10 times higher than that measured in the polar solvent system (50/50% toluene/methanol) (20% compared with 2%, Figure 5.7b). Having established that the triblock copolymer as a suitable model for thin films of P3HT, we therefore concluded that the quenching of fluorescence observed in thin films of P3HT results primarily from interchain interactions that include contributions from excitons with CT character.

5.3 CONCLUSION

In conclusion, we have presented a new conjugated triblock copolymer composed of two chains of regioregular P3HT covalently attached to a flexible P*t*BA polymer. This triblock copolymer fully reproduces the spectroscopic characteristics of P3HT in solution and as thin films in good and poor solvents, respectively, evidenced by a red shifted ground-state absorption, the appearance of vibronic structures probing the ordering of the new species, and fluorescence quenching. The collapsed form of the triblock copolymer is stable over time, fully reversible, and concentration-independent. Interchain interactions of P3HT were found to be more efficient with larger P3HT chains. In the collapsed triblock obtained in a poor solvent, we have proven by FCS measurements that only two P3HT chains are interacting. Given their nearly identical spectral characteristics, this new, stable solution species makes an excellent model for thin films

of P3HT. Collectively, this new model system has allowed us to clarify the origin of the large fluorescence quenching of P3HT from solution to thin film, which we observed for the triblock copolymer in going from a good solvent to a poor solvent. The nature of this fluorescence quenching cannot be explained by a three-dimensional energy transfer, but only by interchain interactions that generate charge-transfer states and/or H-aggregates. As such, the triblock copolymer is a promising compound because the thin film properties of P3HT can be probed directly in solution, as we did for the quantum yield of fluorescence. Fluorescence quenching in going from solution to thin film has also been observed for several other CP systems.[30,31,34,35] That its origins arise solely from interchain interactions might be generalized to all CP chains and not only to P3HT.

5.4 EXPERIMENTAL

5.4.1 General Considerations

All chemicals were purchased from Aldrich, Alfa Aesar, or Fisher and were used as received. THF was dried over 3 Å molecular sieves and deoxygenated using a Vacuum Atmospheres Company solvent purification system. GPC was performed at 40 °C on a GPCmax VE-2001 (Viscotek) equipped with three fluorinated polystyrene columns (IMBHMW-3078, IMBMMW-3078, and IMBLMW-3078) arranged in series. The detector was a UV–vis photodiode array detector tuned at 450 nm. The eluent was tetrahydrofuran (THF) stabilized with butylated hydroxytoluene (BHT). The number-average molecular weight (M_n) and dispersity ($Đ$) are reported relative to polystyrene standards. Proton and $^{13}C[^1H]$ NMR spectra were recorded using a Varian 300, 400, or 500 MHz spectrometer. Chemical shifts are reported in delta (δ) units and expressed in parts per million (ppm) downfield from tetramethylsilane using the residual protio solvent as an internal standard. For ^1H NMR: $CDCl_3$, 7.24 ppm. For ^{13}C NMR: $CDCl_3$,

77.0 ppm. Coupling constants (*J*) are expressed in hertz. IR spectra were recorded on neat samples using a Thermo Scientific Nicolet iS5 spectrometer equipped with iD3 attenuated total reflectance (ATR) attachment (Ge crystal).

Steady-State Spectroscopy. UV–vis absorption spectra were recorded from 350 to 650 nm with a monobeam UV spectrophotometer (8453 UV–visible spectroscopy system, Agilent Technologies Inc.). Fluorescence spectra were measured with a fully corrected Fluorolog-3 (Jobin-Yvon) spectrofluorometer. Samples in solution were contained in a 1 cm fused-silica cuvette. Thin films of P3HT were spin-coated on a microscope cover glass and out of a highly concentrated solution of 10 kDa P3HT in toluene. The quantum yields of fluorescence were determined by using P3HT in toluene as a standard (Φ_F(P3HT) = 42%).[9] Fits were done using Origin software with the sum of three Gaussian functions sharing the same spectral width with a constant energy spacing, chosen to be 0.18 eV.

Molar Extinction Coefficient Spectrum. The molar extinction coefficient spectrum of the extended triblock was extracted from the absorption spectrum of the triblock copolymer in 100% toluene after normalization by the concentration of the triblock copolymer. This concentration was determined from Beer–Lambert law using the absorbance at 455 nm and the extinction molar coefficient of the triblock copolymer at 455 nm, that is, ε = 964 000 L mol^{-1} cm^{-1} (considering an extinction molar coefficient of 8000 L mol^{-1} cm^{-1} per monomer unit).[12] The molar extinction coefficient spectrum of the collapsed triblock was obtained by subtraction of the extended triblock spectrum to the concentration-normalized triblock copolymer absorption spectrum in 50/50% toluene/methanol. The subtraction was afforded until the two extinction molar coefficient spectra were overlaid at 487 nm, by definition of an isosbestic point.

Fluorescence Correlation Spectroscopy. Fluorescence correlation spectroscopy (FCS) measurements were performed on a confocal microscope described in ref. [36] with an extended beam of the collimated 488 nm line of an Ar^+ gas laser to a diameter of about 1 cm and coupled into the objective. The fluorescence signal was collected through the same objective, focused on two avalanche photodiodes (SPCM-AQR-16, PerkinElmer) for detection, and the signal was correlated by an ALV-5000 fast hardware correlation card.

5.4.2 Synthetic Procedures

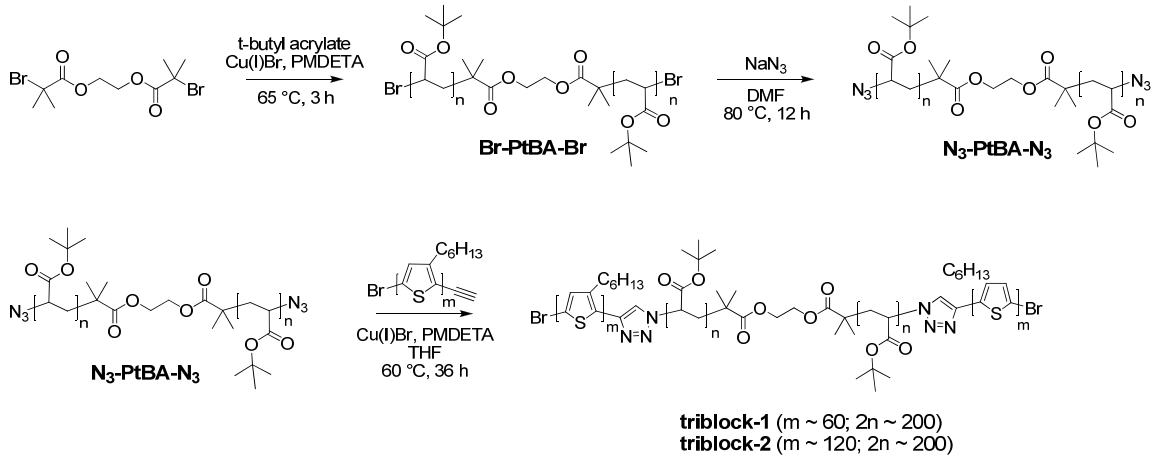

Scheme 5.1: Synthetic scheme for the preparation of P3HT-*b*-P*t*BA-*b*-P3HT**.**

Synthesis of Br-P*t*BA-Br. An oven-dried 25 mL flask was charged with copper(I) bromide (44 mg, 0.31 mmol), *t*-butyl acrylate (4.0 g, 31 mmol), N,N,N′,N″,N″-pentamethyldiethylenetriamine (PMDETA) (100.0 mg, 0.56 mmol), and a stir bar. After one freeze-pump-thaw cycle, 1,2-bis(bromoisobutyryloxy)ethane[37] (50.0 mg, 0.14 mmol) was added using a nitrogen flushed syringe. After three additional freeze-pump-thaw cycles, the reaction mixture was warmed to ambient temperature and placed in an oil bath at 65 °C. After stirring the mixture for 3 h, the reaction was quenched by immersion of

the flask in liquid nitrogen. The reaction mixture was then taken up in THF and passed through a short column of neutral alumina (eluent = THF) to remove the residual catalyst. The polymer mixture was then concentrated, precipitated into cold methanol/water mixture (50/50 v/v) (3×), and collected via filtration (2.64 g, 66% yield). $M_{n,\,GPC}$ = 21 kDa; M_w/M_n = 1.3. ^{1}H NMR ($CDCl_3$, ppm): δ 4.20 (broad s, OCH_2CH_2O), 4.05 (broad, C*H*-Br), 2.18 (broad, C*H* of the polymer backbone), 1.70-1.90 (broad, *meso* CH_2 of the polymer backbone), 1.20-1.60 (broad, *meso* and *racemo* CH_2 of the polymer backbone and $(CH_3)_3C$). FTIR (neat sample): $\nu_{C=O}$ = 1726 cm^{-1}. See Figures A16 and A17, Appendix A.

Synthesis of N_3-P*t*BA-N_3. A 50 mL flask was charged with **Br-P*t*BA-Br** (575 mg), NaN_3 (370 mg, 5.7 mmol), DMF (8 mL), and a stir bar. The resulting mixture was stirred at 50 °C for 12 h and then cooled to ambient temperature. After adding CH_2Cl_2 (50 mL) and water (50 mL), the organic phase was separated and extracted with water (4 × 50 mL), and then dried over Na_2SO_4. Removal of the residual solvent under reduced pressure afforded the desired product in 90% yield (526 mg). $M_{n,\,GPC}$ = 21 kDa; M_w/M_n = 1.3. ^{1}H NMR ($CDCl_3$, ppm): δ 4.21 (broad s, OCH_2CH_2O), 3.72 (broad, C*H*-N_3), 2.19 (broad, C*H* of the polymer backbone), 1.60-1.90 (broad, *meso* CH_2 of the polymer backbone), 1.20-1.60 (broad, *meso* and *racemo* CH_2 of the polymer backbone and $(CH_3)_3C$). FTIR (neat sample): $\nu_{C=O}$ = 1726 cm^{-1}; ν_{N3} = 2109 cm^{-1}. See Figures A16 and A17, Appendix A.

Synthesis of P3HT-*b*-P*t*BA-*b*-P3HT. Triblock copolymer P3HT-*b*-P*t*BA-*b*-P3HT was synthesized by the Cu-catalyzed coupling of ethynyl-terminated P3HT and α,ω-diazido-P*t*BA using a modified, previously reported procedure.[18] Briefly, a 25 mL Schlenk flask charged with a stir bar, THF (5 mL), ethynyl-terminated P3HT (25 mg, 0.0025 mmol),[38] α,ω-diazido-P*t*BA (25 mg, 0.0010 mmol), copper(I) bromide (10 mg,

0.070 mmol), and pentamethyldiethylenetriamine (24 mg, 0.140 mmol) was degassed using three consecutive freeze–pump–thaw cycles, refilled with N_2, and stirred at 60 °C for 36 h. After cooling to room temperature, the reaction mixture was filtered through neutral alumina and concentrated in vacuo to afford the crude product. Pure triblock copolymer was obtained from this mixture by preparative gel permeation chromatography (GPC).

Characterization data for P3HT$_{60}$-*b*-P*t*BA$_{200}$-*b*-P3HT$_{60}$ (triblock-1). $M_{n,\,GPC}$ = 46 kDa ; M_w/M_n = 1.2. ^{1}H NMR ($CDCl_3$, ppm): δ 6.96 (s, C*H* of the thiophene ring), 2.78 (t, C*H*$_2$CH$_2$CH$_2$CH$_2$CH$_2$CH$_3$), 2.20 (broad, C*H* of the polymer backbone), 1.81 (broad, *meso* C*H*$_2$ of the PtBA backbone), 1.69 (m, CH$_2$C*H*$_2$CH$_2$CH$_2$CH$_2$CH$_3$), 1.50-1.30 (broad m, CH$_2$CH$_2$C*H*$_2$C*H*$_2$C*H*$_2$CH$_3$, *meso* and *racemo* C*H*$_2$ of the P*t*BA backbone and (C*H*$_3$)$_3$C)), 0.89 (t, CH$_2$CH$_2$CH$_2$CH$_2$CH$_2$C*H*$_3$). See Figure A18, Appendix A.

Characterization data for P3HT$_{120}$-*b*-P*t*BA$_{200}$-*b*-P3HT$_{120}$ (triblock-2). $M_{n,\,GPC}$ = 63 kDa; M_w/M_n = 1.2. ^{1}H NMR ($CDCl_3$, ppm): δ 6.96 (s, C*H* of the thiophene ring), 2.78 (t, C*H*$_2$CH$_2$CH$_2$CH$_2$CH$_2$CH$_3$), 2.20 (broad, C*H* of the polymer backbone), 1.81 (broad, *meso* C*H*$_2$ of the PtBA backbone), 1.69 (m, CH$_2$C*H*$_2$CH$_2$CH$_2$CH$_2$CH$_3$), 1.50-1.30 (broad m, CH$_2$CH$_2$C*H*$_2$C*H*$_2$C*H*$_2$CH$_3$, *meso* and *racemo* C*H*$_2$ of the P*t*BA backbone and (C*H*$_3$)$_3$C)), 0.89 (t, CH$_2$CH$_2$CH$_2$CH$_2$CH$_2$C*H*$_3$). See Figure A19, Appendix A.

5.5 ACKNOWLEDGMENTS

Portions of this chapter were reprinted with permission from Brazard, J.; Ono, R. J.; Bielawski, C. W.; Barbara, P. F.; Vanden Bout, D. A. *J. Phys. Chem. B,* **2013**, *117*, 4170-4176. Copyright 2013 American Chemical Society. Johanna Brazard is gratefully acknowledged for performing the photophysical experiments. I also thank Johanna

Brazard, Prof. Christopher W. Bielawski, and Prof. David. A. Vanden Bout for their shared efforts in writing the original manuscript.

5.6 REFERENCES

(1) Peet, J.; Heeger, A. J.; Bazan, G. C. *Acc. Chem. Res.* **2009**, *42*, 1700-1708.

(2) McCulloch, I.; Heeney, M.; Bailey, C.; Genevicius, K.; MacDonald, I.; Shkunov, M.; Sparrowe, D.; Tierney, S.; Wagner, R.; Zhang, W.; Chabinyc, M. L.; Kline, R. J.; McGehee, M. D.; Toney, M. F. *Nat. Mater.* **2006**, *5*, 328-33.

(3) Green, M. A.; Emery, K.; Hishikawa, Y.; Warta, W. *Prog. Photovoltaics* **2011**, *19*, 84-92.

(4) Groves, C.; Reid, O. G.; Ginger, D. S. *Acc. Chem. Res.* **2010**, *43*, 612-620.

(5) Inganas, O.; Salaneck, W. R.; Osterholm, J. E.; Laakso, J. *Synth. Met.* **1988**, *22*, 395-406.

(6) Kiriy, N.; Jahne, E.; Adler, H.-J.; Schneider, M.; Kiriy, A.; Gorodyska, G.; Minko, S.; Jehnichen, D.; Simon, P.; Fokin, A. A.; Stamm, M. *Nano Lett.* **2003**, *3*, 707-712.

(7) Park, Y. D.; Lee, H. S.; Choi, Y. J.; Kwak, D.; Cho, J. H.; Lee, S.; Cho, K. *Adv. Funct. Mater.* **2009**, *19*, 1200-1206.

(8) Rumbles, G.; Samuel, I. D. W.; Magnani, L.; Murray, K. A.; DeMello, A. J.; Crystall, B.; Moratti, S. C.; Stone, B. M.; Holmes, A. B.; Friend, R. H. *Synth. Met.* **1996**, *76*, 47-51.

(9) Samuel, I. D. W.; Magnani, L.; Rumbles, G.; Murray, K.; Stone, B. M.; Moratti, S. C.; Holmes, A. B. *Proc. SPIE* **1997**, *3145*, 163-170.

(10) Yamamoto, T.; Komarudin, D.; Arai, M.; Lee, B.-L.; Suganuma, H.; Asakawa, N.; Inoue, Y.; Kubota, K.; Sasaki, S.; Fukuda, T.; Matsuda, H. *J. Am. Chem. Soc.* **1998**, *120*, 2047-2058.

(11) Lee, E.; Hammer, B.; Kim, J.-K.; Page, Z.; Emrick, T.; Hayward, R. C. *J. Am. Chem. Soc.* **2011**, *133*, 10390-10393.

(12) Cook, S.; Furube, A.; Katoh, R. *Energy Environ. Sci.* **2008**, *1*, 294-299.

(13) Sheng, C. X.; Tong, M.; Singh, S.; Vardeny, Z. V. *Phys. Rev. B* **2007**, *75*, 085206.

(14) Clark, J.; Silva, C.; Friend, R. H.; Spano, F. C. *Phys. Rev. Lett.* **2007**, *98*, 4.

(15) Jiang, X. M.; Osterbacka, R.; Korovyanko, O.; An, C. P.; Horovitz, B.; Janssen, R. A. J.; Vardeny, Z. V. *Adv. Funct. Mater.* **2002**, *12*, 587-597.

(16) Brown, P. J.; Sirringhaus, H.; Harrison, M.; Shkunov, M.; Friend, R. H. *Phys. Rev. B* **2001**, *63*, 125204.

(17) Sirringhaus, H.; Brown, P. J.; Friend, R. H.; Nielsen, M. M.; Bechgaard, K.; Langeveld-Voss, B. M. W.; Spiering, A. J. H.; Janssen, R. A. J.; Meijer, E. W.; Herwig, P. *Nature* **1999**, *401*, 685- 688.

(18) Li, Z.; Ono, R. J.; Wu, Z.-Q.; Bielawski, C. W. *Chem. Commun.* **2011**, *47*, 197-199.

(19) Park, Y. D.; Cho, J. H.; Kim, D. H.; Jang, Y.; Lee, H. S.; Ihm, K.; Kang, T.-H.; Cho, K. *Electrochem. Solid-State Lett.* **2006**, *9*, G317-G319.

(20) Reitzel, N.; Greve, D. R.; Kjaer, K.; Howes, P. B.; Jayaraman, M.; Savoy, S.; McCullough, R. D.; McDevitt, J. T.; Bjornholm, T. *J. Am. Chem. Soc.* **2000**, *122*, 5788-5800.

(21) Xu, B.; Holdcroft, S. *Macromolecules* **1993**, *26*, 4457-4460.

(22) Brandrup, J.; Immergut, E. H.; Grulke, E., Eds. *Polymer Handbook*, 4th ed.; Wiley: New York, **1999**.

(23) Mao, H.; Xu, B.; Holdcroft, S. *Macromolecules* **1993**, *26*, 1163-1169.

(24) Clark, J.; Chang, J. F.; Spano, F. C.; Friend, R. H.; Silva, C. *Appl. Phys. Lett.* **2009**, *94*, 3.

(25) Spano, F. C. *Acc. Chem. Res.* **2010**, *43*, 429-439.

(26) Paquin, F.; Latini, G.; Sakowicz, M.; Karsenti, P. L.; Wang, L. J.; Beljonne, D.; Stingelin, N.; Silva, C. *Phys. Rev. Lett.* **2011**, *106*, 4.

(27) Haustein, E.; Schwille, P. *Annu. Rev. Biophys. Biomol. Struct.* **2007**, *36*, 151-169.

(28) Brown, P. J.; Thomas, D. S.; Kohler, A.; Wilson, J. S.; Kim, J.-S.; Ramsdale, C. M.; Sirringhaus, H.; Friend, R. H. *Phys. Rev. B* **2003**, *67*, 064203.

(29) Chang, J.-F.; Clark, J.; Zhao, N.; Sirringhaus, H.; Breiby, D. W.; Andreasen, J. W.; Nielsen, M. M.; Giles, M.; Heeney, M.; McCulloch, I. *Phys. Rev. B* **2006**, *74*, 115318.

(30) Greenham, N. C.; Samuel, I. D. W.; Hayes, G. R.; Phillips, R. T.; Kessener, Y. A. R. R.; Moratti, S. C.; Holmes, A. B.; Friend, R. H. *Chem. Phys. Lett.* **1995**, *241*, 89-96.

(31) Li, Y.; Vamvounis, G.; Holdcroft, S. *Macromolecules* **2002**, *35*, 6900-6906.

(32) Beljonne, D.; Cornil, J.; Silbey, R.; Millie, P.; Bredas, J. L. *J. Chem. Phys.* **2000**, *112*, 4749-4758.

(33) Banerji, N.; Cowan, S.; Vauthey, E.; Heeger, A. J. *J. Phys. Chem. C* **2011**, *115*, 9726-9739.

(34) Burrows, H. D.; de Melo, J. S.; Serpa, C.; Arnaut, L. G.; Monkman, A. P.; Hamblett, I.; Navaratnam, S. *J. Chem. Phys.* **2001**, *115*, 9601-9606.

(35) Kim, J.; Swager, T. M. *Nature* **2001**, *411*, 1030-1034.

(36) Adachi, T.; Brazard, J.; Chokshi, P.; Bolinger, J. C.; Ganesan, V.; Barbara, P. F. *J. Phys. Chem. C* **2010**, *114*, 20896-20902.

(37) Karanam, S.; Goossens, H.; Klumperman, B.; Lemstra, P. *Macromolecules* **2003**, *36*, 3051-3060.

(38) Jeffries-El, M.; Sauve, G. v.; McCullough, R. D. *Macromolecules* **2005**, *38*, 10346-10352.

Chapter 6: Synthesis of Conjugated Diblock Copolymers via Two Mechanistically Distinct, Sequential Polymerizations Using a Single Catalyst

6.1 Introduction

The self-assembly of semiconducting block copolymers has recently emerged as a promising approach to achieving the hierarchical and morphological control needed for understanding and optimizing the charge separation and shuttling processes inherent to organic photovoltaic (OPV) devices.[1] Block copolymers containing regioregular poly(3-hexylthiophene) (P3HT) are widely studied for such applications due to P3HT's excellent electronic properties, synthetic accessibility[2] and the numerous methods available for modification.[3] The preparation of these block copolymers typically involve elaborating an end-functionalized polythiophene into an appropriate macroinitiator for the chain extension of a second block *via* a polymerization process that is mechanistically distinct from that of P3HT,[4] or coupling pre-formed homopolymers with complementary end-functionalities.[5] Such methodologies, however, can be complex and inefficient, frequently resulting in materials that contain inseparable homopolymer impurities. A convenient method that employs a single set of reaction conditions and/or a single catalyst system to grow two mechanistically distinct homopolymers in a sequential fashion[6] would overcome these issues and facilitate access to a broad range of P3HT-containing block copolymers.

Regioregular P3HT is most frequently prepared *via* a Ni-catalyzed Grignard metathesis (GRIM) polymerization of 2,5-dibromo-3-hexylthiophene.[2,7] In the generally accepted mechanism, the polymerization is initiated by the homocoupling of two organomagnesium monomer species, reducing the Ni(II) catalyst to Ni(0), which then oxidatively adds to the recently produced homo-coupled dimer. Transmetalation at Ni by

remaining monomer and subsequent re-addition of the Ni(0) catalyst to the new chain-end after reductive elimination ultimately affords a reactive Ni(II) species that resides at the chain terminus (poly-**1**, Scheme 6.1). While treatment of this species with various organomagnesium reagents effectively quenches the controlled polymerization reaction, often with concomitant installation of a functional group,[3] we reasoned that the resulting Ni(II) complex may possess sufficient reactivity to catalyze the polymerization of other monomers, such as isocyanides, which have been reported to undergo polymerization under similar conditions.[8] Moreover, poly(isocyanide)s have been prepared from a large pool of readily-available monomers, may adopt helical architectures,[7c,9] and recent reports have prompted their utility in OPV devices.[10] Hence, block copolymers containing P3HT and poly(isocyanide)s constitute valuable targets for study in such applications.

6.2 Results and Discussion

6.2.1 Synthesis of Poly(3-alkylthiophene)–Poly(arylisocyanide) Diblock Copolymers

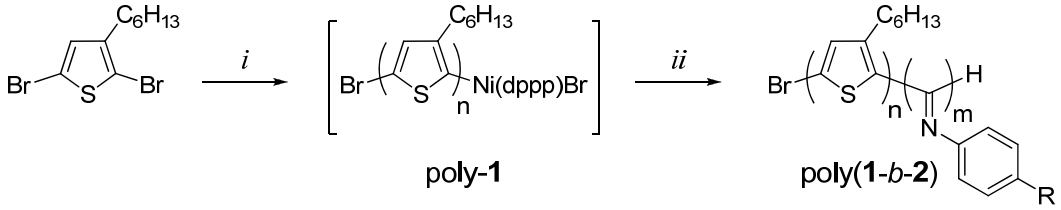

Scheme 6.1: Synthesis of poly(3-hexylthiophene)-*b*-poly(*n*-decyl 4-isocyanobenzoate) *via* sequential monomer addition. (*i*) 1) *i*PrMgCl, THF; 2) Ni(dppp)Cl_2. (*ii*) 1) CNPh-p-$CO_2C_{10}H_{21}$ (**2**), THF; 2) CH_3OH. R = $CO_2C_{10}H_{21}$

As summarized in Scheme 6.1, initial efforts focused on exploring the ability to grow a poly(phenylisocyanide) (PPI) from P3HT. Using standard methods,[2] 2-bromo-3-

hexyl-5-chloro-magnesiothiophene (generated *in situ* from 2,5-dibromo-3-hexyl-thiophene and *i*PrMgCl) was polymerized in THF using Ni(dppp)Cl_2 ($[monomer]_0/[Ni]_0$ = 30) to generate poly-**1**. When no further molecular weight increase was observed by size exclusion chromatography (SEC), an aliquot was removed for further analysis (see below) and *n*-decyl 4-isocyanobenzoate (**2**) ($[\mathbf{2}]_0/[Ni]_0$ = 30) was added to the reaction vessel. After 1 h, the mixture was poured into excess methanol and the precipitated solids were collected in 82% isolated yield (over the two polymerization steps) *via* filtration.

As shown in Figure 6.1A, GPC analysis revealed that the isolated material was of higher molecular weight (M_n = 7.28 kDa) than that contained within the aliquot removed after completion of the thiophene polymerization (M_n = 4.19 kDa), while retaining a monomodal distribution. These results were consistent with the chain extension of poly-**1** and, combined with ^{1}H NMR spectroscopy which revealed signals attributable to both P3HT and PPI, indicated that poly(**1**-*b*-**3**) was successfully formed.

The narrow molecular weight distributions exhibited by the copolymer prepared in our preliminary experiment suggested to us that the polymerization of **2** occurred *via* a controlled, chain-growth process. To test this hypothesis, a series of chain extension polymerizations was performed by equally dividing a THF solution of macroinitiator poly-**1** (M_n = 2.70 kDa; $Đ$ = 1.31) and adding different quantities of **2** to each fraction. As shown in Figure 6.1B, a linear correlation between the M_n of the crude reaction polymer products and the feed ratio of **2**:poly-**1** was observed, and each copolymer synthesized exhibited a narrow dispersity ($Đ$ < 1.35). These results support the established[2] quasi-living nature of GRIM polymerizations, and confirmed that the polymerization of **2**, as initiated by poly-**1**, also proceeded in a similar, controlled manner.[11]

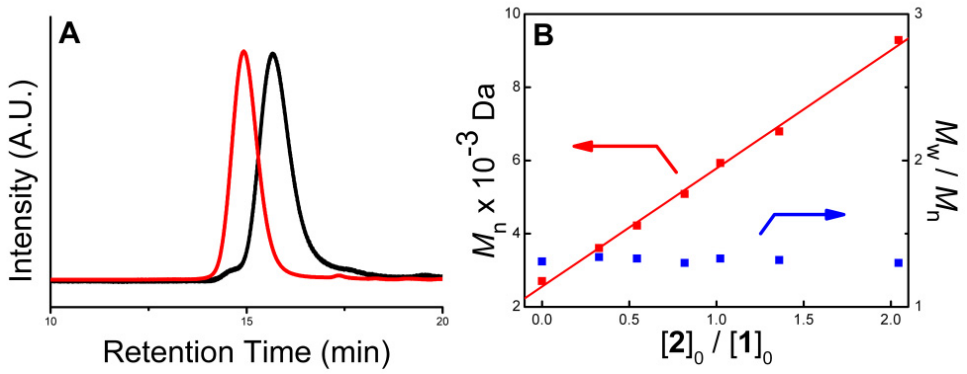

Figure 6.1: (A) Representative gel permeation chromatograms of homopolymer poly-**1** (black) and its respective diblock copolymer poly(**1**-*b*-**3**) (red); see Table 6.1 for M_n and dispersity data. (B) Plot of M_n and M_w/M_n values of **3** measured as a function of the feed ratio of **2** to poly-**1** (M_n = 2.70 kDa; $Đ$ = 1.31). M_n and M_w/M_n were determined by GPC (eluent = THF, 25 °C).

As summarized in Table 6.1, a variety of copolymers with different molecular weights and compositions were synthesized using the aforementioned method by simply varying the initial feed ratio of monomers. In addition, each of the copolymers poly(**1**-*b*-**3**) synthesized were isolated in high yields (81–90%) and exhibited narrow, monomodal distributions with no detectable amounts of homopolymeric impurities by GPC. Collectively, these results support the successful union of two mechanistically distinct polymerization reactions within a single reaction vessel to obtain well-defined block copolymers containing P3HT.

Entry	$[\mathbf{2}]_0/[\mathbf{1}]_0$[b]	$M_{n,\,GPC}$[c] (kDa)	M_w/M_n[c]	P3HT[d] (wt%)	Yield[e] (%)
1	34/1 (2.70)	9.29	1.30	29	90
2	16/1 (4.19)	7.28	1.15	57	82
3	25/1 (7.58)	11.6	1.13	65	85
4	12/1 (5.47)	7.72	1.17	71	85
5	10/1 (11.6)	13.7	1.17	85	81

Table 6.1: Selected molecular weight and dispersity data. Various P3HT-*b*-PPI poly(**1**-*b*-**3**) were synthesized as shown in Scheme 6.1 by first preparing macroinitiator poly-**1** of different M_ns followed by addition of **2**. [b] The M_n of poly-**1** (indicated in parenthesis; in kDa) were determined by removing and analyzing by GPC aliquots from the respective reaction mixtures prior to the addition of **2**. [c] M_n and M_w/M_n were determined by GPC and are reported as their polystyrene equivalents. [d] Determined by ^{1}H NMR spectroscopy. [e] Isolated yields over the two steps are indicated.

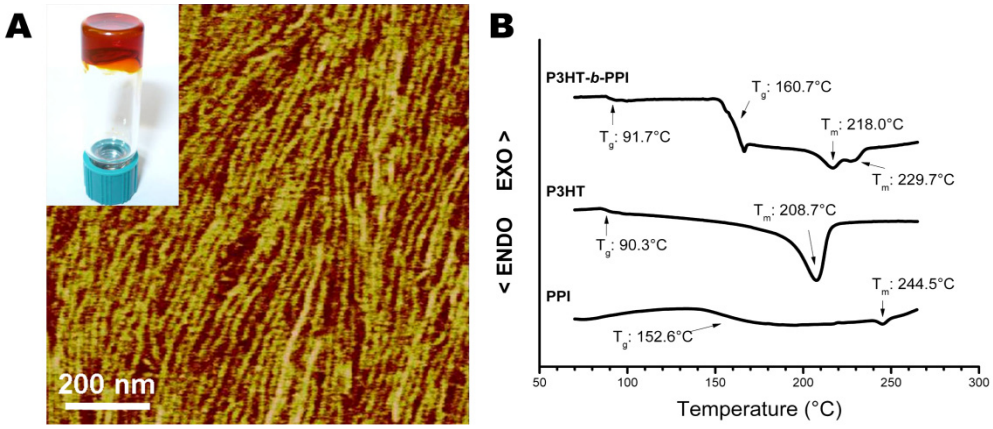

Figure 6.2: (a) AFM phase image of poly(**1**-*b*-**3**) drop cast from $CHCl_3$ ([poly(**1**-*b*-**3**)] = 10 mg mL^{-1}) onto a Si wafer (film thickness = 80 nm). Inset: Photograph showing gelation behavior of poly(**1**-*b*-**3**) in $CHCl_3$ ([poly(**1**-*b*-**3**)] = 30 mg mL^{-1}; the critical gelator concentration was determined to be 15 mg mL^{-1} at 25 °C). (b) Differential scanning calorimetry thermograms of (top) P3HT-*b*-PPI (poly(**1**-*b*-**3**)), (middle) a P3HT homopolymer (M_N = 8.17 kDa), and (bottom) a homopolymer of **2** (M_N = 17 kDa) (heating rate = 10 °C min^{-1}; atmosphere = N_2).

During the course of our synthesis and characterization studies, poly(**1**-*b*-**3**) was observed to undergo gelation upon dissolution in $CHCl_3$, THF, and chlorobenzene, suggesting the formation of an entangled network of polymer chains in these solvents (Figure 6.2A, inset). To determine if P3HT-*b*-PPI copolymers were capable of assembling into higher order structures in the solid state, a film of poly(**1**-*b*-**3**) drop casted from $CHCl_3$ was investigated by tapping mode atomic force microscopy (AFM). As shown in Figure 6.2A, the film exhibited a nanofibrillar morphology consistent with other films of P3HT-containing block copolymers.[4,6] The nanofibrils were unidirectionally aligned and exhibited long-range order with persistent lengths of up to 1 μm. Differential scanning calorimetry of poly(**1**-*b*-**3**) provided further evidence that these diblock copolymers were capable of undergoing phase separation as glass transition (T_g) and melting (T_m) temperatures assignable to both P3HT and PPI phases were observed (Figure 6.2B).

6.2.2 Synthesis and Self-Assembly of Amphiphilic P3HT-*b*-poly(arylisocyanide)

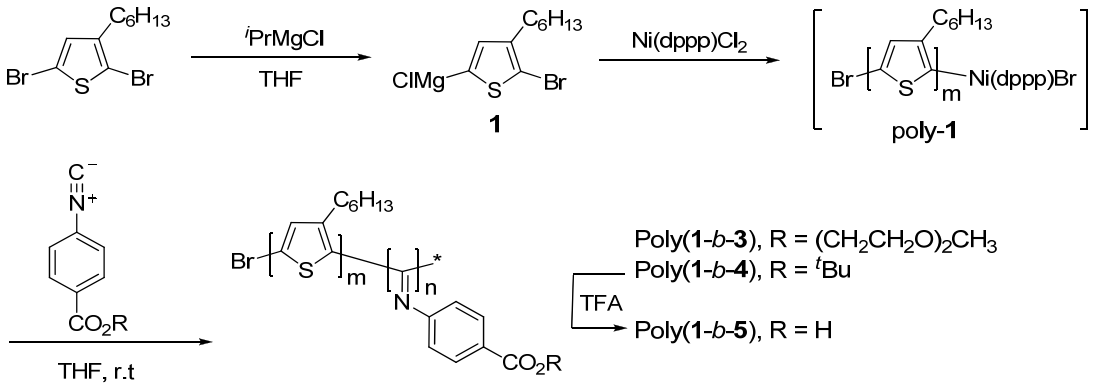

Scheme 6.2: Synthesis of poly-**1** and amphiphilic block copolymers poly(**1**-*b*-**3**), poly(**1**-*b*-**4**) and poly(**1**-*b*-**5**).

It has been previously demonstrated that P3HT-containing amphiphilic block copolymers can adopt micellar or vesicular aggregates in solution.[12,13] Inspired in part by these results, we sought to determine if our copolymerization method was tolerant to different arylisocyanide functionalities. In particular, we were interested in monomers which contained hydrophilic functional groups that could generate a range of amphiphilic block copolymers capable of forming higher order structures when copolymerized with P3HT. As summarized in Scheme 6.2, the macroinitiator poly-**1** was prepared according to the standard GRIM polymerization method described above.[7,14] Briefly, Ni(dppp)Cl_2 was added to a solution of 2-bromo-3-hexyl-5-chloromagnesiothiophene (generated in situ from 2,5-dibromo-3-hexylthiophene and *i*PrMgCl at 50 °C for 2 h) in THF at room temperature using an initial monomer to initiator ratio of 60. Aliquots were then taken from the reaction mixture at timed intervals and analyzed by GPC. After 1 h, the M_n of poly-**1** ceased to increase which resulted in the formation of poly-**1** that exhibited a M_n of 10.2 kDa and a molecular weight distribution ($Đ$, M_w/M_n) of 1.20. Monomer **3** was then added to the reaction vessel and, after 1 h, excess methanol was added to the mixture. The precipitated solids were collected via filtration in high isolated yield (88%) and analysed by GPC. As shown in Figure 6.3A, the isolated polymer (poly(**1**-*b*-**3**)) was of higher M_n and narrower molecular weight distribution (M_n = 12.3 kDa, M_w/M_n = 1.15) than its macroinitiator precursor (poly-**1**; M_n = 10.2 kDa, M_w/M_n = 1.20) which was not observed as an impurity. As summarized in Table 6.2, two poly(**1**-*b*-**3**)s with different molecular weights and narrow molecular weight distribution were synthesized by varying the initial feed ratio of monomers. GPC analysis along with ^{1}H NMR spectroscopy, which revealed signals attributable to both P3HT and poly-**3**, provided additional evidence for the formation of the diblock copolymers.

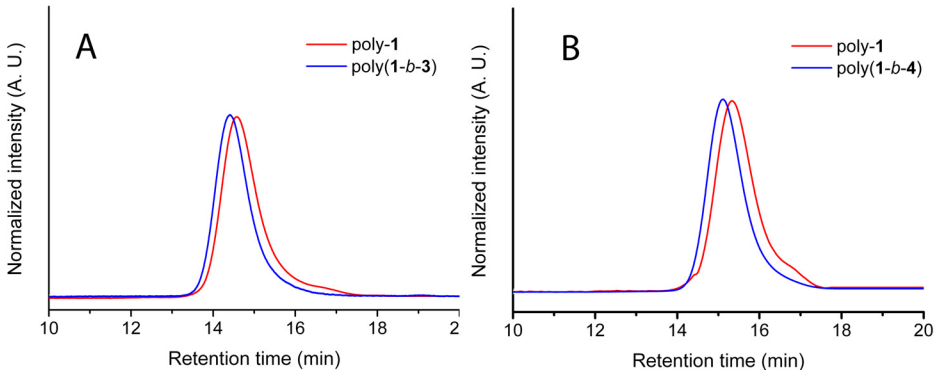

Figure 6.3: (A) Representative gel permeation chromatograms of macroinitiator poly-**1** (red) and its respective block copolymer poly(**1**-*b*-**3**) (blue). (B) Gel permeation chromatograms of macroinitiator poly-**1** (red) and its respective block copolymer poly(**1**-*b*-**4**) (blue).

Using similar methods, we also prepared an amphiphilic block copolymer bearing pendant carboxylic acid groups. As summarized in Scheme 6.2 and Table 6.2, a series of *tert*-butyl protected poly(**1**-*b*-**4**)s of varying M_ns and narrow $Đ$s were prepared in high yield (82-86%) over two steps. The GPC trace of poly(**1**-*b*-**4**) (Table 6.2, entry 4), shown in Figure 6.3B, indicated that the isolated material was of higher M_n and narrower molecular weight distribution (M_n = 6.10 kDa M_w/M_n = 1.20) than its macroinitiator precursor (poly-**1**; M_n = 4.96 kDa M_w/M_n = 1.27). Hydrolysis of the poly(**1**-*b*-**4**)s using an excess of trifluoroacetic acid (TFA) in THF afforded the deprotected poly(**1**-*b*-**5**)s in high isolated yield (97%). The disappearance of the ^{1}H NMR signal attributed to the *tert*-butyl group in poly(**1**-*b*-**4**) (δ = 1.40 ppm; THF-d_8), accompanied by the appearance of a υOH stretch at ~3400 cm^{-1} in the solution state IR spectrum ($CHCl_3$) were consistent with complete deprotection (Figure A25).

Entry	Polymers[a]	Macroinitiators			Block copolymers			Yield (%)[e]	% P3HT[f]
		[**1**$_a$]/[Ni][b]	M_n[c] (Da)	M_w/M_n[c]	[M_o]/[Ni][d]	M_n[c] (Da)	M_w/M_n[c]		
1	Poly(**1**-*b*-**2**)	20	3572	1.28	20	7395	1.25	76	59
2	Poly(**1**-*b*-**3**)	60	10209	1.20	15	12279	1.15	88	20
3	Poly(**1**-*b*-**3**)	35	5802	1.24	20	8802	1.19	78	36
4	Poly(**1**-*b*-**4**)	30	4964	1.27	10	6104	1.20	82	25
5	Poly(**1**-*b*-**4**)	70	11176	1.32	20	13245	1.17	86	22

Table 6.2: Selected molecular weight and dispersity data of poly-**1** and its respective block copolymers. [a] As shown in Scheme 6.2, the block copolymers were synthesized by first preparing macroinitiator poly-**1** of different M_ns, followed by the addition of either **3** or **4** (M_o). [b] The concentration of **1** was determined by ^{1}H NMR spectroscopy ($CDCl_3$). [c] The M_n and M_w/M_n values were determined by GPC and are reported as their polystyrene equivalents. [d] The M_n of poly-**1** (in Da) was determined via GPC anslysis of aliquots removed from the respective reaction mixtures prior to the addition of **3** or **4**. [e] Isolated yields over two steps are indicated. [f] Determined by ^{1}H NMR spectroscopy ($CDCl_3$).

Having successfully synthesized the aforementioned amphiphilic block copolymers, we next explored how the changes in arylisocyanide functionality would influence their self-assembly properties. To enable self-assembly in solution, our initial efforts involved the slow addition of methanol to a THF solution of poly(**1**-*b*-**3**) (initial conc. = 0.13 mg mL^{-1}, M_n = 8.8 kDa, M_n/M_w = 1.19) at room temperature, resulting in a color change from orange to transparent purple that was accompanied by a bathochromic shift (439 nm → 512 nm) in the UV/vis absorption maxima (Figure A23). These spectroscopic data were consistent with the well-established solvatochromism of regioregular P3HT and in agreement with the color change observed during the formation of P3HT-encapsulated micelles.[15,16] As shown in Figure 6.4A, transmission electron microscopy (TEM) images of the aggregates revealed that spherical micellar

nanostructures with narrow size distributions were formed from poly(**1**-*b*-**3**). Moreover, dynamic light scattering (DLS) measurements of a poly(**1**-*b*-**3**) dispersion in 50:50 THF/MeOH revealed a monomodal size distribution (Figure A21) with an average particle diameter of 41 ± 4 nm.

To determine if poly(**1**-*b*-**3**) assembled into higher order structures in the solid state, a film of the block copolymer (Table 6.2, entry 2) was spin-coated from a $CHCl_3$ solution and investigated by tapping-mode atomic force microscopy (AFM). As shown in Figure 6.5A, the film exhibited a nanofibrillar surface morphology, consistent with other films of P3HT-containing block copolymers.[17-19] The nanofibrils exhibited long-range order with persistent lengths of up to 0.5 μm (Figure A30). Differential scanning calorimetry (DSC) of poly(**1**-*b*-**3**) provided further evidence that these block copolymers were capable of undergoing phase separation, as two distinct glass transition temperatures (T_gs) were observed: one corresponding to that of the P3HT segment (T_g = 79.5 ^{o}C) and the other to the segment of poly(**3**) (T_g = 126.0 ^{o}C) (Figure A26).

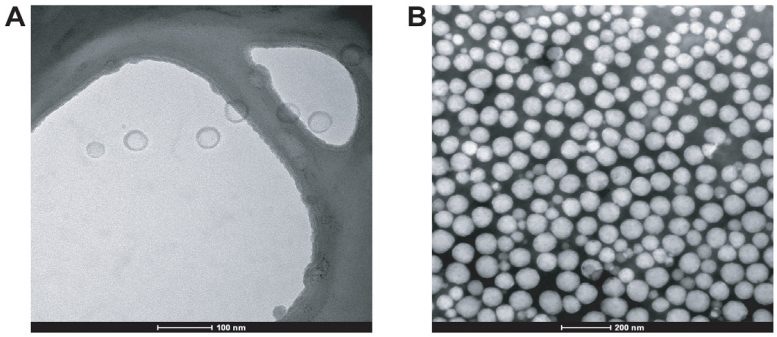

Figure 6.4: (A) TEM image of micelles formed from poly(**1**-*b*-**3**) (M_n = 8.8 kDa, M_w/M_n = 1.19; entry 3 in Table 6.2) in THF/methanol (1/1, v/v), observed after solvent evaporation on a graphene oxide (GO) sheet suspended on a lacy carbon support. (B) TEM image of micelles (stained with 1 wt% aqueous solution of phosphotungstic acid) formed from poly(**1**-*b*-**5**) (M_n = 13.2 kDa, M_w/M_n = 1.17; entry 5 in Table 6.2) in water.

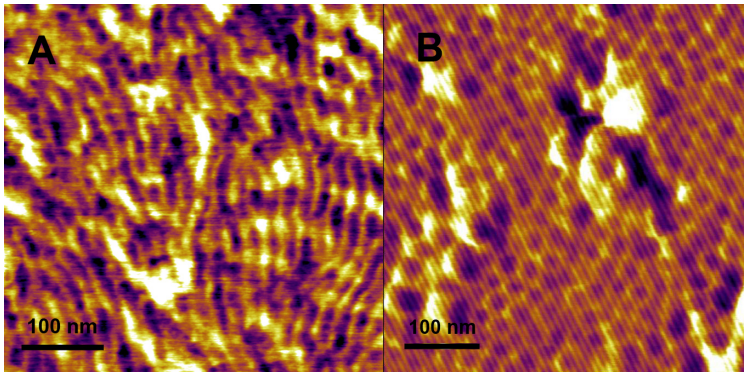

Figure 6.5: (A) AFM phase image of poly(**1**-*b*-**3**) (M_n = 12.3 kDa, $Đ$ = 1.15) (entry 2, Table 6.2) spin-coated from $CHCl_3$ ([poly(**1**-*b*-**3**)]$_0$ = 1.4 mg mL^{-1}) onto a Si wafer. (B) AFM phase image of poly(**9**-*b*-**2**) (M_n = 11.2 kDa, $Đ$ = 1.25), spin-coated from $CHCl_3$ ([poly(**9**-*b*-**2**)]$_0$ = 5 mg mL^{-1}) onto a Si wafer.

The solution self-assembly behaviour of poly(**1**-b-**5**) was also investigated. Slow addition of water to a stirring THF solution of poly(**1**-*b*-**5**) induced a colour change from bright orange to purple that was accompanied by a bathochromic shift (414 nm → 510 nm) in the UV-vis absorption maxima (Figure A24), consistent with the aggregation of P3HT chains. After the removal of THF by dialysis, the dispersion of poly(**1**-*b*-**5**) in water was characterized by light scattering and microscopy techniques. DLS measurements of the poly(**1**-*b*-**5**) showed a single relaxation mode (Figure A22), and that the average diameter of the particles was 89 ± 6 nm. Following evaporation of the solvent, analysis of the resulting dried aggregates by TEM revealed the formation of spherical particles (Figure 6.4B) consistent with the DLS results.

Although the respective poly(arylisocyanide) blocks of poly(**1**-*b*-**3**) and poly(**1**-*b*-**5**) differ, comparison of the particle sizes with the molecular weights of the respective polymers qualitatively showed that particle size increases with the molecular weight of the constituent block copolymer. Furthermore, the measured particle sizes were larger than the respective approximated polymer chain lengths in contrast to that observed for

analogous rod–coil amphiphilic block copolymers.[15] The disparity may be a consequence of the rigidity of both the P3HT and the poly(arylisocyanide) blocks. Regardless, the data collected for poly(**1**-*b*-**3**) and poly(**1**-*b*-**5**), along with those previously reported,[18] suggested to us that block copolymers of P3HT and poly(arylisocyanide)s exhibit are capable of displaying higher order structures in solution and in the solid state. In addition, the methodology described herein effectively enabled the self-assembly character of the block copolymer to be tailored by varying the functionality of the poly(arylisocyanide) block.

6.2.3 Synthesis and Self-assembly of P3HT-*b*- poly(alkylisocyanide)

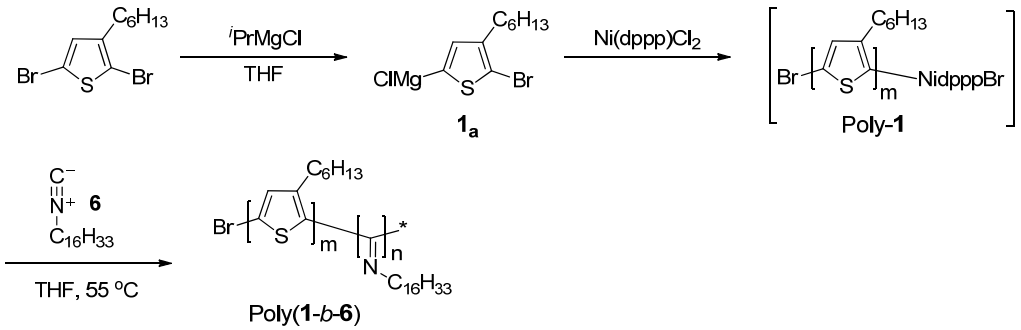

Scheme 6.3: Synthesis of the macroinitiator poly-**1** and the respective block copolymer poly(**1**-*b*-**6**).

To investigate further the scope of the aforementioned copolymerization methodology, we attempted the block copolymerization of P3HT with an alkylisocyanide. As illustrated in Scheme 6, copolymerization of 1-isocyanohexadecane (**6**), chosen for its anticipated solubilizing character, from poly-1 required a slightly elevated temperature (50 °C) compared to analogous examples which employed arylisocyanides. Regardless, chain extension was observed and the formation of the targeted block copolymer, poly(**1**-*b*-**6**), was confirmed by GPC (Figure 6.3). As

summarized in Table 6.3, a variety of poly(**1**-*b*-**6**) with different molecular weights and compositions were synthesized by varying the initial feed ratio of **6** to poly-**1**. Although longer reaction times and higher temperatures were required than for any of the P3HT-*b*-poly(arylisocyanide) syntheses, the obtained products had narrow polydispersities and were recovered in good yields.

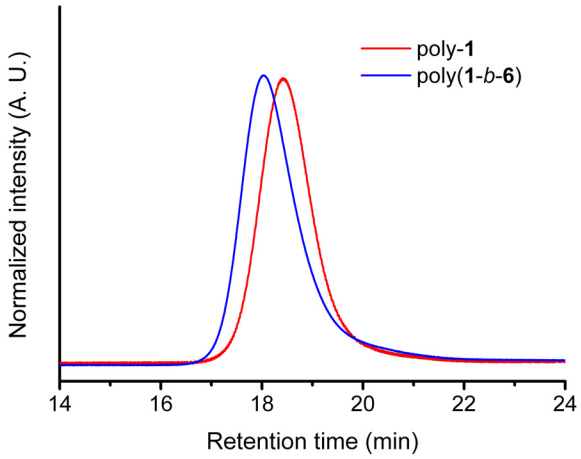

Figure 6.6: Representative gel permeation chromatograms of homopolymer poly-**1** (red) and its respective block copolymer poly(**1**-*b*-**6**) (blue) (Table 6.3, entry 1).

To determine if poly(**1**-*b*-**6**)assembled into higher order structures in the solid state, a thin film of the polymer (Table 6.3, entry 2) was prepared by spin-coating from a $CHCl_3$ solution, which was then imaged by tapping-mode AFM. Although the film exhibited microphase separation, no distinct morphology could be discerned (Figure A31). As further evidence that these block copolymers were capable of undergoing phase separation, DSC analysis of poly(**1**-*b*-**6**) revealed a distinct melting temperature corresponding to P3HT (197.7 °C) and a distinct Tg that was assigned to poly-**6** (172.0 °C) (Figure A27). Although a higher order stucture was not observed in the poly(**1**-*b*-**6**) samples prepared, our results do demonstrate that the block copolymerization

methodology presented may be extended beyond the use of arylisocyanides, thereby extending the scope of monomers amendable to the methodology described herein.

Entry	Poly-**1** (P3HT)			Poly(**1**-*b*-**6**)[a]			Yield (%)[e]	% P3HT[f]
	$[\mathbf{1_a}]_0/[Ni]_0$[b]	M_n[c]	M_w/M_n[c]	$[\mathbf{6}]_0/[Ni]_0$[d]	M_n[c]	M_w/M_n[c]		
1	15	2427	1.19	10	3014	1.22	70	60
2	50	8329	1.33	30	10130	1.22	65	63
3	35	5852	1.16	40	8385	1.38	72	47
4	25	3879	1.25	20	4259	1.20	67	55

Table 6.3: Selected Molecular Weight and Dispersity Data of poly-**1** and Its Respective Block Copolymers, Poly(**1**-*b*-**6**). As shown in Scheme 6.3, the copolymers were synthesized by first preparing macroinitiator poly-**1** of different M_ns, followed by the addition of **6**. [b] The concentration of **1** was determined by ^{1}H NMR spectroscopy ($CDCl_3$). [c] M_n (in Da) and M_w/M_n were determined by GPC and are reported relative to polystyrene equivalents. [d] The M_n of poly-**1** in Da was determined via GPC of aliquots removed from the respective reaction mixtures prior to the addition of **6**. [e] Isolated yields over two steps are indicated. [f] Determined by ^{1}H NMR spectroscopy ($CDCl_3$).

6.2.4 Block Copolymer Synthesis and Self-assembly of GRIM Compatible Monomers and Poly(arylisocyanide)

The GRIM method has commonly been used for the preparation of regioregular P3HT; however, this chain-growth method has been applied to the polymerization of additional monomers, including 2,5-bis(hexyloxy)phenylene, 9,9-dioctylfluorene, 2,3-dihexylthienopyrazine, *N*-octylcarbazole, *N*-dodecylpyrrole, and 3-alkoxythiophene.[20,21] Since each of these polymerizations afford a polymer chain with an active Ni endgroup, we envisioned that other π-conjugated polymers prepared by the GRIM method could also be utilized as macroinitiators to grow chains of arylisocyanides.

Synthesis and self-assembly of poly(pyrrole)-b-poly(arylisocyanide)

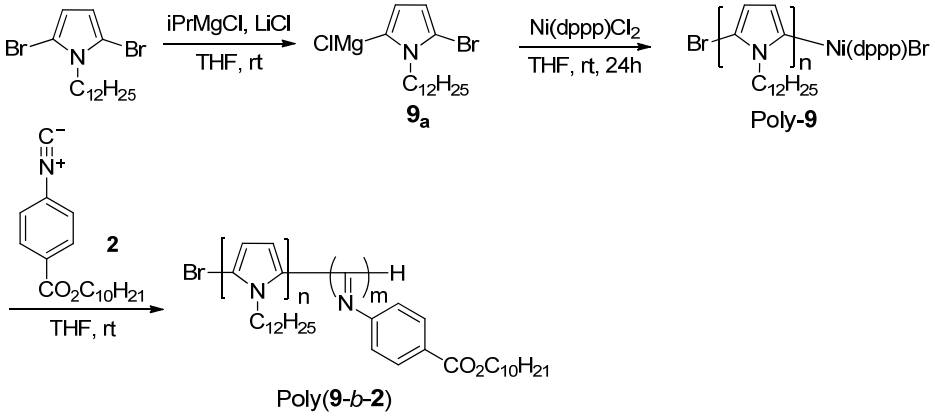

Scheme 6.4: Synthesis of the macroinitiator poly-**9** and the respective block copolymer poly(**9**-*b*-**2**).

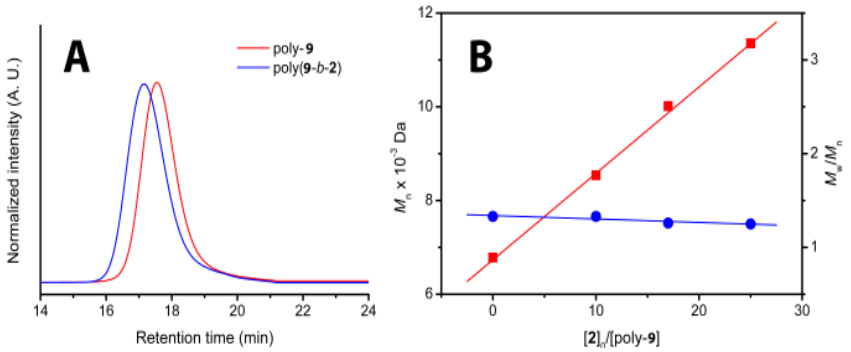

Figure 6.7: (A) Representative gel permeation chromatograms of homopolymer poly-**9** (red) and its respective block copolymer poly(**9**-*b*-**2**) (blue). (B) Plot of M_n and M_w/M_n values of block copolymer poly(**9**-*b*-**2**) measured as a function of the feed ratio of **2** to poly-**9** (M_n = 6.78 kDa; M_w/M_n = 1.33). M_n and M_w/M_n were determined by GPC (eluent = THF, 25 °C).

Entry	Poly-**9** (PPR)			Poly(**9**-*b*-**2**)[a]			Yield (%)[e]	% PPR[f]
	$[\mathbf{9_a}]_0/[Ni]_0$[b]	M_n[c]	M_w/M_n[c]	[**2**]/[Ni][d]	M_n[c]	M_w/M_n[c]		
1	50	7329	1.27	20	11152	1.25	82	71
2	35	4644	1.23	10	6341	1.22	75	78
3	8	1050	1.16	16	4050	1.21	80	33
4	8	1050	1.16	25	6019	1.23	79	24
5	47	6782	1.33	10	8540	1.33	80	82
6	47	6782	1.33	17	10016	1.26	81	73
7	47	6782	1.33	25	11354	1.25	85	65

Table 6.4: Selected molecular weight and dispersity data for poly(**9**-*b*-**2**). [a] As shown in Scheme 6.3, the block copolymers were synthesized by first preparing macroinitiator poly-**9** of different M_ns, followed by the addition of **2**. [b] The concentration of $\mathbf{9}_a$ was determined by ^{1}H NMR spectroscopy ($CDCl_3$). [c] The M_n (in Da) and M_w/M_n values were determined by GPC and are reported as their polystyrene equivalents. [d] The M_n of poly-**9** (in Da) was determined via GPC analysis of aliquots removed from the respective reaction mixtures prior to the addition of **2**. [e] Isolated yields over two steps are indicated. [f] Determined by ^{1}H NMR spectroscopy ($CDCl_3$).

Initial efforts focused on exploring the ability to grow a poly(arylisocyanide) from poly(1-dodecylpyrrole) (PPR). As summarized in Scheme 6.4, 2-bromo-3-chloromagnesio-N-dodecylpyrrole (**9**) was generated from 2,5-dibromo-N-docecylpyrrole and 1 equiv. of *i*PrMgCl / LiCl in THF at room temperature. Ni(dppp)Cl_2 was then added at room temperature under N_2 protection to generate poly-**9**. Once the M_n of poly-**9** ceased to increase as determined by GPC, monomer **2** was added to the reaction vessel under N_2 protection. After 1 h, the mixture was poured into excess methanol and the precipitated solid was collect by filtration (80% yield). As shown in Figure 6.7A, GPC analysis revealed that the isolated material, poly(**9**-*b*-**2**), was of higher molecular weight (M_n = 11.2 kDa) and displayed a narrower molecular weight distribution (M_w/M_n = 1.25) than its macroinitiator precursor, poly-**9** (M_n = 7.33 kDa, M_w/M_n = 1.27), indicating that residual homopolymer was not present. Moreover, a linear correlation between the M_n of poly(**9**-*b*-**2**) and the feed ratio of **2** to poly-**9** was also observed (Figure 6.7B), and each block copolymer analyzed exhibited a narrow dispersity ($Đ$ < 1.35). Collectively, these results support the established quasi-living nature of GRIM polymerizations and that the polymerization of **2**, as initiated by poly-**9**, also proceeded in a similarly controlled manner. As summarized in Table 6.4, a variety of poly(**9**-*b*-**2**) with different molecular weights and compositions were synthesized by varying the initial feed ratio of monomers in high yields and narrow $Đ$s.

To determine if poly(**9**-*b*-**2**) assembled into higher order structures in the solid state, a film of the block copolymer (Table 6.4, entry 1) was spin coated from a $CHCl_3$ solution and investigated by tapping-mode atomic force microscopy. As shown in Figure 6.5B, the film exhibited a surface morphology that was consistent with either spherical or hexagonal structures. These features were approximately 20 nm in diameter and were persistent across the thin film surface.

Synthesis and self-assembly of poly(phenylene)-*b*-poly(arylisocyanide)

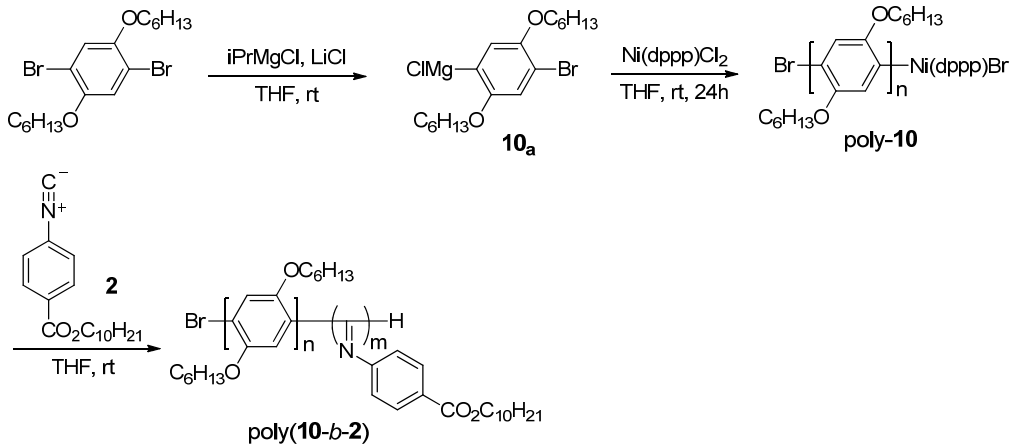

Scheme 6.5: Synthesis of the macroinitiator poly-**10** and the respective block copolymer poly(**10**-*b*-**2**).

Using reaction conditions similar to those described for the preparation of poly(**9**-*b*-**2**), we attempted to grow poly(arylisocyanide) from poly(2,5-bis(hexyloxy)phenylene) (PPH) as illustrated in Scheme 6.5. GPC analysis revealed the isolated material poly(**10**-*b*-**2**) was of higher M_n (M_n = 8.36 kDa) and narrower molecular weight distribution (M_w/M_n = 1.16) than its macroinitiator poly-**10** (M_n = 3.11 kDa, M_w/M_n = 1.25), a result that was consistent with the successful formation of a block copolymer (see Figure 6.8A). A linear correlation between the M_n of poly(**10**-*b*-**2**) and the feed ratio of **2** to poly-**10** was observed, and each copolymer analysed exhibited a narrow dispersity index ($Đ$ < 1.4) (see Figure 6.8B). These results provide support for the established quasi-living nature of GRIM polymerizations and that the polymerization of **2**, as initiated by poly-**10**, also proceeded in a controlled manner. As summarized in Table 6.5, a variety of poly(**10**-*b*-**2**) with different molecular weights and compositions were synthesized according to

Scheme 6.5 by varying the initial feed ratio of monomers in high yields and narrow *Đ*s as determined by GPC.

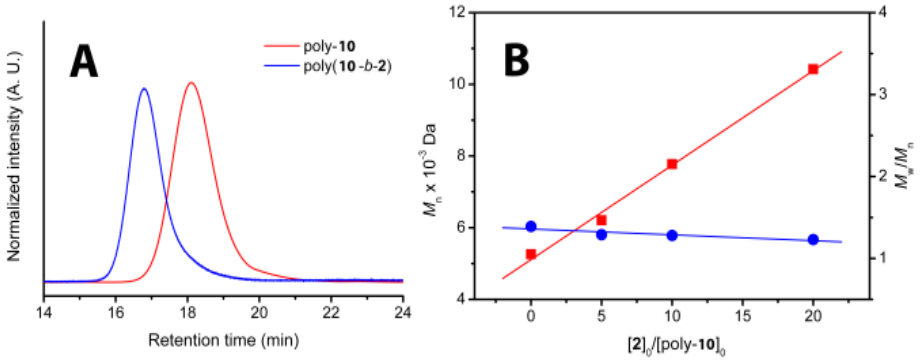

Figure 6.8: (A) Representative gel permeation chromatograms of macroinitiator poly-**10** (red) and its respective block copolymer poly(**10**-*b*-**2**) (blue). (B) Plot of M_n and M_w/M_n values of block copolymer poly(**10**-*b*-**2**) measured as a function of the feed ratio of **2** to poly-**10** (M_n = 5.26 kDa; M_w/M_n = 1.39). M_n and M_w/M_n were determined by GPC (eluent = THF, 25 °C).

To determine if poly(**10**-*b*-**2**) assembled into higher order structures in the solid state, a film of poly(**10**-*b*-**2**) was spin-coated from $CHCl_3$ and then imaged by tapping-mode AFM. Although the film exhibited microphase separation, no distinct morphology could be discerned (Figure A32). DSC of poly(**10**-*b*-**2**) provided further evidence that these block copolymers were capable of undergoing phase separation, as two distinct glass transition temperatures, corresponding to that of a segment of PPH (T_g = 62.5 °C) and a segment of poly(**2**) (T_g = 152.3 °C), were observed (Figure A29).

Entry	Poly-**10**			Poly(**10**-*b*-**2**)[a]			Yield (%)[e]	% PPH[f]
	$[\mathbf{10_a}]_0/[Ni]_0$[b]	M_n[c]	M_w/M_n[c]	[**2**]/[Ni][d]	M_n[c]	M_w/M_n[c]		
1	21	3107	1.25	18	8360	1.16	72	54
2	45	5712	1.36	25	12156	1.36	75	64
3	30	4504	1.35	40	15343	1.16	83	43
4	25	4043	1.35	6	5510	1.27	78	80
5	35	5262	1.39	5	6208	1.29	77	88
6	35	5262	1.39	10	7775	1.28	80	78
7	35	5262	1.39	20	10422	1.32	82	64

Table 6.5: Selected molecular weight and dispersity data of poly-**10**, and its respective block copolymers, poly(**10**-*b*-**2**). As shown in Scheme 6.5, the block copolymers were synthesized by first preparing macroinitiator poly-**10** of different M_ns, followed by the addition of **2**. [b] The concentration of $\mathbf{10_a}$ was determined by ^{1}H NMR spectroscopy ($CDCl_3$). [c] M_n (in Da) and M_w/M_n were determined by GPC and are reported as their polystyrene equivalents. [d] The M_n of poly-**10** in Da was determined via GPC of aliquots removed from the respective reaction mixtures prior to the addition of **2**. [e] Isolated yields over two steps are indicated. [f] Determined by ^{1}H NMR spectroscopy ($CDCl_3$).

6.3 CONCLUSION

In sum, the synthesis of a broad range of conjugated block copolymers was accomplished using a grafting-from polymerization method. The key to this process was the use of a single Ni(II) catalyst that facilitated two mechanistically distinct polymerizations of two different monomers. Both polymerization reactions proceeded a controlled manner and afforded well-defined copolymers with low polydispersities. Amphiphilic block copolymers containing P3HT and poly(arylisocyanide)s with pendant polar functional groups were found to aggregate in solution as determined by UV-Vis spectroscopy, TEM and DLS and/or exhibit microphase separation in the solid state, as determined by DSC and AFM. The block copolymers containing P3HT and an poly(alkylisocyanide) were found to exhibit microphase separation in the solid state, as

determined by DSC and AFM. Furthermore, the copolymerization was found to be general for other conjugated polymers synthesized via the GRIM method, such as PPR and PPH. Given these results, and that the method described herein also tolerates changes in isocyanide functionality, whilst retaining control over the polymerization, it is uniquely poised for preparing materials suitable for examining the role of nano-scale morphology in organic electronic materials. Looking ahead, we envision the method will facilitate the syntheses of block copolymers containing complementary electronic functionalities (e.g., p-type and n-type) that can self-assemble into ordered bulk heterojunctions.[1,22] Such efforts, as well as investigation of the structure–property relationships of self-assembled nano-structures therein, are currently underway.

6.4 EXPERIMENTAL

6.4.1 General Considerations

All solvents were purchased from Fisher Scientific and used without further purification unless otherwise noted. All other chemicals were purchased from Aldrich, Alfa Aesar, or Fisher, and were used as received. 2,5-Dibromo-3-hexylthiophene,[7] *t*-butyl 4-isocyanobenzoate (**4**),[23] 1-isocyanohexadecane (**6**),[24] *N*-Dodecyl-2,5-dibromopyrrole (**9**),[25] 2,5-bis(hexyloxy)phenylene (**10**),[26] 2-(2-methoxyethoxy)ethyl 4-aminobenzoate (**14**)[27] A regioregular poly(3-hexylthiophene) homopolymer (M_N = 8.17 kDa, PDI = 1.30) was synthesized according to literature procedure.[7] THF was dried over 3 Å molecular sieves and deoxygenated using a Vacuum Atmospheres Company solvent purification system. ^{1}H and ^{13}C[^{1}H] NMR spectra were recorded using a Varian 300, 400, or 500 MHz spectrometer. Chemical shifts are reported in delta (δ) units and expressed in parts per million (ppm) downfield from tetramethylsilane using the residual protio solvent as an internal standard. For ^{1}H NMR: $CDCl_3$, 7.26 ppm. For ^{13}C NMR: $CDCl_3$, 77.0 ppm.

Coupling constants (*J*) are expressed in hertz. Gel permeation chromatography (GPC) was performed at ambient temperature on a home-built system equipped with a Waters Model 510 HPLC pump, two fluorinated polystyrene columns (IMBHW-3078 and I-MBLMW-3078) arranged in series, and a Waters 486 Tunable Absorbance Detector (λ = 450 nm). Molecular weight and polydispersity data are reported relative to polystyrene standards in tetrahydrofuran (THF). IR spectra were recorded using Perkin-Elmer Spectrum BX FT-IR system using KBr pellets. UV/vis spectra were recorded using a Perkin Elmer Instruments Lambda 35 spectrometer. Microanalyses were performed by Midwest Microlabs, LLC (Indianapolis, IN). Melting points were obtained with a Mel-Temp apparatus and are uncorrected. High resolution mass spectra (HRMS) were obtained with a VG analytical ZAB2-E instrument (ESI or CI).

Microscopy. Samples for atomic force microscopy (AFM) measurements were prepared by drop casting $CHCl_3$ solutions (10 mg mL^{-1}) of the polymer onto pre-cleaned silicon wafers, placed in covered Petri dishes to slow the evaporation process. AFM images were acquired in tapping mode with a Digital Instruments Dimension 3100 Scanning Probe Microscope, performed at room temperature under an atmosphere of air using standard silicon cantilevers with a nominal spring constant of 50 N/m and resonance frequency of ~300 kHz. The images were acquired at a scan frequency of 1 Hz over 1 × 1 μm^2 scan areas. Differential scanning calorimetry (DSC) was performed using a Mettler-Toledo DSC823e under an atmosphere of nitrogen at a heating/cooling rate of 10 °C min^{-1}. Transmission electron microscopy (TEM) was performed in bright-field mode with a TECNAI Spirit Biotwin at 80 kV accelerating voltage. Samples were prepared by one of two methods: (1) Samples for TEM measurements were diluted with equal volume of 1 wt% aqueous solution of phosphotungstic acid stain and cast onto copper mesh grids; or (2) Samples for TEM measurements were cast onto lacey carbon

grids that were pretreated with a 0.25 mg mL^{-1} aqueous dispersion of graphene oxide (GO).[8] Micrographs were collected at 100,000× magnification. The number average particle diameters (*Davg*) and standard deviations were generated from the analysis of a minimum of 150 particles from at least three different micrographs.

Dynamic Light Scattering. Samples for DLS were measured in aqueous media. The custom-built DLS instrument consisted of a Brookhaven Instruments Limited (Worcestershire, U.K.) system, a model BI-9000AT digital correlator, a model EMI-9865 photomultiplier, and a model 17 mW He-Ne laser (NSG America, SELFOC micro-lens, 1.8 mm diameter, 0.25 pitch) operated at 632.8 nm. Measurements were performed at 20 °C. Prior to analysis, solutions were filtered through a 0.45 μm Millex GV PVDF membrane filter (Millipore Corp., Medford, MA) to remove dust particles. Scattered light was collected at a fixed angle of 90°. The digital correlator was operated with 522 ratio spaced channels, an initial delay of 2 μs, a final delay of 100 ms, and a duration of 3 min. A photomultiplier aperture was used and the incident laser intensity was adjusted to obtain a photon counting of between 200 and 300 kcps. Only data in which the measured and calculated baselines of the intensity autocorrelation function agreed to within 0.1% were used to calculate particle sizes. The calculations of the particle size distributions and distribution averages were performed with the ISDA software package (Brookhaven Instruments), which employed single exponential fitting, cumulants analysis, and non-negatively constrained least-squares (CONTIN) particle size distribution analysis routines. All measurements were made in triplicate.

6.4.2 Synthetic Procedures

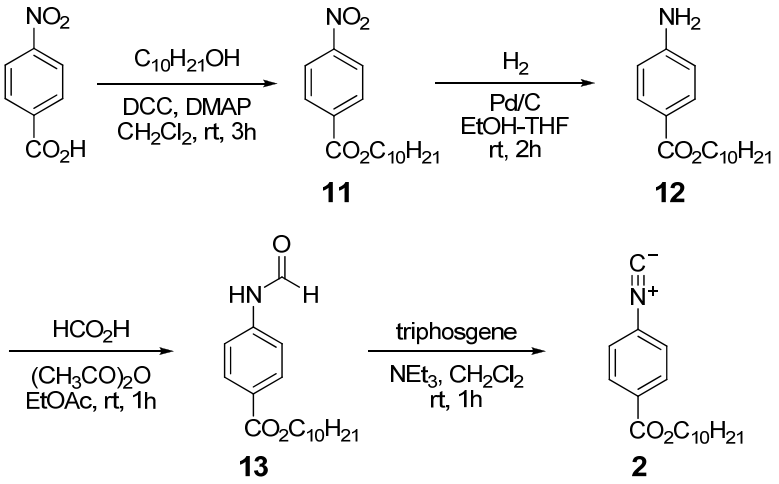

Scheme 6.6: Synthesis of **2**.

Decyl 4-nitrobenzoate (11). 4-Dimethylaminopyridine (DMAP) (0.122 g, 1.00 mmol) and *N*,*N*′-dicyclohexylcarbodiimide (DCC) (6.17 g, 29.9 mmol) were added to a solution of 4-nitrobenzoic acid (5.00 g, 29.9 mmol) in dry CH_2Cl_2 (100 mL). After the reaction mixture was stirred at 0 °C for 30 min under an atmosphere of argon, decyl alcohol (4.73 g, 29.9 mmol) was added to the mixture. The dispersion was stirred at room temperature for 5 h. After filtering the resulting reaction mixture, the residual solvent was removed by evaporation. The crude product was purified by column chromatography (silica gel; 5:1 v/v hexanes:ethyl acetate) to afford the desired product as a yellow liquid (5.52 g, 60% yield). IR (KBr, cm^{-1}): 1728 ($\nu_{C=O}$ ester). ^1H NMR ($CDCl_3$, 300 MHz): δ 0.88 (t, J = 6.8 Hz, CH_3, 3H), 1.21–1.48 (m, CH_2, 14H), 1.75–1.84 (m, $OCH_2C\underline{H_2}$, 2H), 4.37 (t, J = 6.6 Hz, OCH_2, 2H), 8.21 (d, J = 8.5 Hz, aromatic, 2H), 8.29 (d, J = 8.5 Hz, aromatic, 2H). ^{13}C NMR ($CDCl_3$, 75 MHz): δ 14.24, 22.81, 26.11, 28.73, 29.38, 29.42, 29.64, 32.01, 66.26, 123.64, 130.78, 136.02, 150.59, 164.87. HRMS m/z calcd for

C17H25NO4 $[M+H]^+$: 308.1862; Found: 308.1862. Anal. Calcd (%) for $C_{17}H_{25}NO_4$ (307.18): C, 66.43; H, 8.20; N, 4.56; Found (%): C, 66.72; H, 8.20; N, 4.50.

Decyl 4-aminobenzoate (12). A solution of **11** (5.00 g, 16.3 mmol) in ethanol (30 mL) and THF (30 mL) was charged with 10% Pd/C (0.30 g). The resulting mixture was stirred at room temperature for 9 h under an atmosphere of H_2. Following filtration through Celite, the filtrate was concentrated by evaporation. The crude product was then purified by recrystallization with hexanes:ethyl acetate (10:1 v/v) to afford the desired product as a white crystalline solid (4.16 g, 91% yield). m.p. 61–63 °C. IR (KBr, cm^{-1}): 3332 (ν_{N-H}), 1682 ($\nu_{C=O}$ ester). ^1H NMR ($CDCl_3$, 300 MHz): δ 0.88 (t, J = 6.4 Hz, CH_3, 3H), 1.27–1.44 (m, CH_2, 14H), 1.68–1.77 (m, $OCH_2C\underline{H}_2$, 2H), 4.04 (br, NH_2, 2H), 4.25 (t, J = 6.7 Hz, OCH_2, 2H), 6.64 (d, J = 8.7 Hz, aromatic, 2H), 7.85 (d, J = 8.7 Hz, aromatic, 2H). ^{13}C NMR ($CDCl_3$, 75 MHz): δ 14.27, 22.83, 26.23, 28.97, 29.46, 29.69, 32.04, 64.68, 113.91, 120.32, 131.68, 150.80, 166.88. HRMS m/z calcd for C17H27NO2 $[M+H]^+$: 278.2120; Found: 278.2118. Anal. Calcd (%) for $C_{17}H_{27}NO_2$ (277.20): C, 73.61; H, 9.81; N, 5.05; Found (%): C, 73.48; H, 9.69; N, 5.24.

Decyl 4-formamidobenzoate (13). After a mixture of formic acid (1.08 mL, 28.7 mmol) and acetic anhydride (0.543 mL, 5.74 mmol) was stirred at room temperature for 1 h under an atmosphere of argon, a solution of **12** (1.30 g, 5.74 mmol) in dry ethyl acetate (50 mL) was added to the aforementioned mixture at 0 °C. The resulting mixture was stirred at 0 °C for 30 min, and then at room temperature for 30 min. Ethyl acetate (50 mL) was then added to the solution and the resulting mixture was filtered. The filtrate was washed with H_2O (100 mL) and brine (100 mL), and then dried over anhydrous $MgSO_4$. After the residual solvent was removed by evaporation, the crude product was purified by column chromatography (silica gel; 2 : 1 hexanes : ethyl acetate, v/v) then recrystallized with hexanes : ethyl acetate (5 : 1 v/v) to afford the desired product as a

white crystalline solid (1.40 g, 80% yield). m.p. 68–70 °C. IR (KBr, cm^{-1}): 3303 (ν_{N-H}), 1714 ($\nu_{C=O}$ ester), 1614 (amide). ^1H NMR ($CDCl_3$, 300 MHz): δ 0.87 (t, J = 6.6 Hz, CH_3, 3H), 1.21–1.36 (m, CH_2, 14H), 1.57–1.66 (m, CH_2, 2H), 4.14–4.20 (m, CH_2, 2H), 7.10–7.12 (m, 0.6H), 7.24–7.25 (m, 0.8H), 7.61–7.64 (m, 1.6H), 8.00–8.04 (m, 2H), 8.44 (s, 0.6H), 8.81–8.85 (m, 0.4H). ^{13}C NMR ($CDCl_3$, 75 MHz): δ 15.25, 23.68, 29.61, 30.19, 30.41, 32.73, 65.52, 65.64, 116.66, 118.52, 125.85, 126.34, 139.91, 140.02, 157.89, 160.74, 164.60, 164.81. HRMS m/z calcd for $C_{18}H_{28}NO_3$ $[M+H]^+$: 306.2069; Found: 306.2072. Anal. Calcd (%) for $C_{18}H_{27}NO_3$ (305.20): C, 70.79; H, 8.91; N, 4.59; Found (%): C, 70.84; H, 9.01; N, 4.64.

Decyl 4-isocyanobenzoate (2). Triethylamine (0.493 mL, 3.53 mmol) was added to a solution of **13** (540 mg, 1.77 mmol) in dry CH_2Cl_2 (20 mL). After the reaction mixture was stirred at 0 °C for 10 min under an atmosphere of argon, a solution of triphosgene (290 mg, 0.973 mmol) in CH_2Cl_2 (33 mL) was added dropwise to the mixture *via* syringe. The resulting mixture was stirred at room temperature for 1 h and then additional CH_2Cl_2 (150 mL) was added. After filtration, the resulting solution was washed with aqueous $NaHCO_3$ (150 mL; 10 wt% $NaHCO_3$) and then dried over anhydrous $MgSO_4$. After the residual solvent was removed by evaporation, the crude product was purified by column chromatography (silica gel; 5 : 1 hexane : ethyl acetate, v/v) then recrystallized with hexanes : ethyl acetate (10 : 1 v/v) to afford the desired product as a white crystalline solid (406 mg, 80% yield). m.p. 38–40 °C. IR (KBr, cm^{-1}): 2122 ($\nu_{C\equiv N}$), 1724 ($\nu_{C=O}$ ester). ^1H NMR ($CDCl_3$, 300 MHz): δ 0.88 (t, J = 6.8 Hz, CH_3, 3H), 1.27–1.46 (m, CH_2, 14H), 1.72–1.81 (m, CH_2, 2H), 4.33 (t, J = 6.7 Hz, OCH_2, 2H), 7.45 (d, J = 8.4 Hz, aromatic, 2H), 8.08 (d, J = 8.4 Hz, aromatic, 2H). ^{13}C NMR ($CDCl_3$, 75 MHz): δ 14.23, 22.79, 26.10, 28.74, 29.37, 29.41, 29.63, 32.00, 65.89, 126.53, 130.91, 131.43, 165.18, 167.04. HRMS m/z calcd for C18H26NO2 $[M+H]^+$: 288.1964; Found:

288.1964. Anal. Calcd (%) for $C_{18}H_{25}NO_2$ (287.2): C, 75.22; H, 8.77; N, 4.87; Found (%): C, 75.17; H, 8.85; N, 4.91.

Procedure Used to Grow Poly(isocyanide)s of Various Molecular Weights from a Common Macroinitiator. Under an atmosphere of nitrogen, various quantities (0.4, 0.6, 0.8, 1.0, 1.5, 2.5 mL) of freshly prepared 1 (M_n = 2703 Da, PDI = 1.31) in THF ($[1]_0$ = 0.086 mM) were added *via* syringe to a series of degassed solutions of **2** in THF (20 mg, 0.070 mmol; $[2]_0$ = 0.028 mM). Each of the reaction mixtures were then stirred for 1 h at room temperature and quenched by the addition of methanol (5 mL). The resulting block copolymers were then collected *via* filtration, washed with methanol, hexane, and dried under vacuum to afford poly(**1**-*b*-**2**) (> 98% yield). The polymers were characterized by NMR spectroscopy and GPC.

Representative Copolymerization Procedure (Synthesis of poly(1-*b*-2)). A 25 mL oven-dried flask was charged with 2,5-dibromo-3-hexylthiophene (0.26 g, 0.81 mmol), dry THF (8.7 mL), and a stir bar. After adding isopropylmagnesium chloride (0.41 mL, 2.0 M solution in THF), the resulting mixture was stirred at ambient temperature for 2 h. Ni(dppp)Cl_2 (23 mg, 0.042 mmol) (dppp = 1,3-bis(diphenylphosphino)propane) was then added to the reaction mixture, and the polymerization progress was monitored by GPC until the molecular weight of poly-**1** ceased to increase. GPC analysis of an aliquot removed from the reaction mixture showed that the polymer prepared *in situ* exhibited the following characteristics: M_n = 4186 Da, M_w/M_n = 1.35. Under an atmosphere of nitrogen, **2** (233 mg, 0.81 mmol) was then added to the reaction solution. After the reaction mixture was stirred at room temperature for 1 h, 30 mL of methanol was poured into the reaction flask, which caused a dark-purple solid to precipitate. The solid was then isolated *via* filtration, and washed with excess methanol and hexanes to remove residual metal salts, unreacted monomer and oligomers.

The resulting purple solid was then dried under vacuum to afford 298 mg (82% yield, two steps) of the desired block copolymer 3b. GPC: M_n = 7277 Da, M_w/M_n = 1.15. ^{1}H NMR ($CDCl_3$, 400 MHz): δ 0.84–1.71 (m, CH_2 and CH_3), 2.80–2.81 (t, thiophene CH_2) 3.56–4.49 (br, OCH_2), 5.34–6.31 (br, Ph), 6.97–7.01 (s, thiophene ArH), 7.15–7.40 (br, Ph).

Synthesis of a Homopolymer of 2. Decyl 4-isocyanobenzoate (**2**) (30 mg, 0.10 mmol) was placed in an oven dried two-neck flask, which was then evacuated on a vacuum line and refilled with dry N_2. After this vacuum–refill procedure was repeated three times, dry CH_2Cl_2 (2.0 mL) was added with a syringe. After complete dissolution of the monomer, a solution of $NiCl_2 \cdot 6H_2O$ in dry methanol (0.05 M, 0.12 mL) was then added, and the mixture stirred under a dry N_2 atmosphere at room temperature for 6 h. The polymer was isolated by precipitation from excess methanol, collected by centrifugation, and then dried under reduced pressure at room temperature to afford poly(**2**) as a yellow solid (15 mg, 50% yield). GPC: M_n = 17 kDa, PDI = 1.7. ^{1}H NMR ($CDCl_3$, 400 MHz): δ 0.43–1.97 (br, CH_2 and CH_3), 3.21–4.71 (br, OCH_2), 5.06–6.30 (br, Ph), 6.06–7.89 (br, Ph).

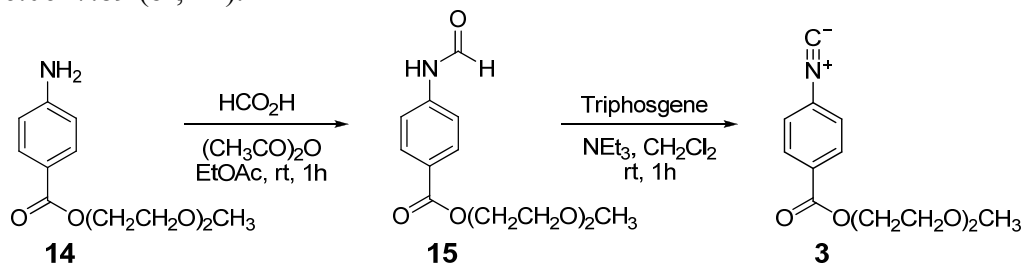

Scheme 6.7: Synthesis of 2-(2-methoxyethoxy)ethyl 4-isocyanobenzoate.

2-(2-methoxyethoxy)ethyl 4-formamidobenzoate (15). After a mixture of formic acid (1.08 mL, 28.7 mmol) and acetic anhydride (0.543 mL, 5.74 mmol) was stirred at room temperature for 1 h under argon, a solution of **14** (1.37 g, 5.74 mmol) in dry ethyl acetate (50 mL) was added to the aforementioned mixture at 0 °C. The resulting

mixture was stirred at 0 °C for 30 min, and then at room temperature for 30 min. Ethyl acetate (50 mL) was then added to the solution and the resulting mixture was filtered. The filtrate was washed with H_2O (100 mL) and brine (100 mL), and then dried over anhydrous $MgSO_4$. After the residual solvent was removed by evaporation, the crude product was purified by column chromatography (silica gel; 1:1 hexanes: ethyl acetate, v/v) to afford the desired product as a clear oil (1.15 g, 75% yield). IR (KBr, cm^{-1}): 3274 (ν_{N-H}), 1704 ($\nu_{C=O}$ ester), 1603 ($\nu_{C=O}$ amide). ^1H NMR ($CDCl_3$, 300 MHz): δ 3.38 (s, OCH_3, 3H), 3.56–3.59 (m, OCH_2, 2H), 3.38–3.72 (m, OCH_2, 2H), 3.82–3.85 (m, OCH_2, 2H), 3.45–4.45 (m, OCH_2, 2H), 7.11 (d, J = 8.7 Hz, 0.6 H, NH), 7.55–7.62 (m, 1.2H, NH and Ar), 7.75–7.92 (m, 0.4 H, Ar), 7.95–8.12 (m, 2.4 H, Ar), 8.25–8.50 (m, 1.0 H, Ar and CHO), 8.84 (d. J = 11.4 Hz, 0.4 H, CHO). ^{13}C NMR ($CDCl_3$, 75 MHz): δ 59.16, 64.17, 69.41, 70.66, 72.01, 117.22, 119.13, 126.05, 126.60, 131.11, 131.79, 141.11, 141.29, 159.25, 161.87, 165.86, 166.06. HRMS m/z calcd for $C_{13}H_{18}NO_5$ $[M+H]^+$: 268.1185; Found: 268.1186. Anal. Calcd (%) for $C_{13}H_{17}NO_5$ (268.12): C, 58.42; H, 6.41; N, 5.24; Found (%): C, 58.21; H, 6.45; N, 5.22.

2-(2-methoxyethoxy)ethyl 4-isocyanobenzoate (3). Triethylamine (1.05 mL, 7.48 mmol) was added to a solution of **12** (1.0 g, 3.75 mmol) in dry CH_2Cl_2 (50 mL). After the reaction mixture was stirred at 0 °C for 10 min under argon, a solution of triphosgene (677 mg, 2.27 mmol) in CH_2Cl_2 (50 mL) was added dropwise to the mixture *via* syringe. The resulting mixture was stirred at room temperature for 1 h and then additional CH_2Cl_2 (150 mL) was added. After filtration, the resulting solution was washed with aqueous $NaHCO_3$ (100 mL; 10 wt% $NaHCO_3$) and then dried over anhydrous $MgSO_4$. After the residual solvent was removed by evaporation, the crude product was purified by column chromatography (silica gel; 2 : 1 hexane : ethyl acetate, v/v) to afford the desired product as a clear liquid (654 mg, 70% yield). IR (KBr, cm^{-1}):

2124 (ν_{CN}), 1724 ($\nu_{C=O}$ ester). ^{1}H NMR ($CDCl_3$, 300 MHz): δ 3.38 (s, CH_3, 3H), 3.55-3.58 (m, CH_2, 2H), 3.68-3.70 (m, CH_2, 2H), 3.82-3.85 (m, CH2, 2H), 4.48-4.51 (m, CH_2, 2H), 7.44 (d, J = 6.6 Hz, Ar, 2H), 8.10 (d. J = 6.6 Hz, Ar, 2H). ^{13}C NMR ($CDCl_3$, 75 MHz): δ 59.26, 64.76, 69.25, 70.74, 72.05, 126.57, 131.06, 131.12, 165.13, 167.12. HRMS m/z calcd for C13H16NO4 $[M+H]^+$: 250.1079; Found: 250.1078. Anal. Calcd (%) for $C_{13}H_{15}NO_4$ (249.10): C, 62.64; H, 6.07; N, 5.62; Found (%): C, 62.56; H, 6.21; N, 5.58.

Representative Copolymerization Procedure: Poly(1-*b*-3) and Poly(1-*b*-4). Following the procedure reported for the synthesis of poly(**1**-*b*-**2**), a 25 mL oven-dried flask was charged with 2,5-dibromo-3-hexylthiophene (0.15 g, 0.47 mmol), dry THF (4.5 mL), and a stir bar. After adding isopropylmagnesium chloride (0.48 mL, 1.0 M solution in THF), the resulting mixture was placed in an oil bath thermostatted to 50 °C for 2 h. Upon cooling to ambient temperature, Ni(dppp)Cl_2 (7.3 mg, 0.013 mmol) (dppp = 1,3-bis(diphenylphosphino)propane) was added to the reaction mixture, and the polymerization progress was monitored by SEC until the molecular weight of poly-**1** ceased to increase. SEC analysis of an aliquot removed from the reaction mixture showed that the polymer prepared in situ exhibited the following characteristics: M_n = 5802 Da, M_w/M_n = 1.24. Under nitrogen, **3** (70 mg, 0.28 mmol) was then added to the reaction solution. After the reaction mixture was stirred at room temperature for 1 h, 30 mL of methanol was poured into the reaction flask, which caused a dark-purple solid to precipitate. The solid was then isolated *via* filtration, and washed with excess methanol and hexanes to remove residual metal salts, unreacted monomer and oligomers. The resulting purple solid was then dried under vacuum to afford 113 mg (78% yield, two steps) of the desired block copolymer poly(**1**-*b*-**3**). ^{1}H NMR ($CDCl_3$, 400 MHz): δ 0.83–0.97 (br, CH_3), 1.19–1.49 (br, CH_2), 1.58–1.76 (br, CH_2), 2.66–2.88 (br, CH_2), 3.13–3.99

(br, OCH_2), 4.11–4.64 (br, CO_2CH_2), 5.08–6.44 (br, aromatic), 6.86–7.10 (br, thiophene), 7.36–8.36 (br, aromatic).

Poly(**1**-*b*-**4**) was prepared in a similar manner to poly(**1**-*b*-**3**): 233 mg (86% yield) ^{1}H NMR ($CDCl_3$, 400 MHz): δ 0.79–0.98 (br, CH_3), 1.13–1.83 (br, CH_2), 2.69–2.87 (br, CH_2), 4.86–6.29 (br, aromatic), 6.74–8.14 (br, aromatic).

Representative Procedure for the Synthesis of Poly(1-*b*-5). After dissolving poly(**1**-*b*-**4**) (15 mg, 2.46 μmol) in THF (10 mL), trifluoacetic acid (0.20 mL, 33 mmol) was added. The reaction mixture was allowed to stir at room temperature for 24 h, after which the solvent was removed under reduced pressure. The resulting crude solid was then washed with cold hexanes and dried under reduced pressure to afford the desired product (12 mg, 80% yield). ^{1}H NMR ($CDCl_3$, 400 MHz): δ 0.84–0.98 (br, CH_3), 1.13–1.83 (br, CH_2), 2.69–2.87 (br, CH_2), 4.86–6.29 (br, aromatic), 6.74–8.14 (br, aromatic).

Representative Copolymerization Procedure: Poly(1-*b*-6). A 25 mL oven-dried flask was charged with 2,5-dibromo-3-hexylthiophene (0.14 g, 0.43 mmol), dry THF (4.5 mL), and a stir bar. After adding isopropylmagnesium chloride (0.45 mL, 1.0 M solution in THF), the resulting mixture was placed in an oil bath thermostatted to 50 °C for 2 h. Upon cooling to ambient temperature, Ni(dppp)Cl_2 (4.8 mg, 0.0089 mmol) (dppp = 1,3-bis(diphenylphosphino)propane) was added to the reaction mixture, and the polymerization progress was monitored by SEC until the molecular weight of poly-**1** ceased to increase. SEC analysis of an aliquot removed from the reaction mixture showed that the polymer prepared in situ exhibited the following characteristics: M_n = 8329 Da, M_w/M_n = 1.33. Under nitrogen, **6** (68 mg, 0.27 mmol) was then added to the reaction mixture. After heating to 50 °C and stirring overnight, 30 mL of methanol was poured into the reaction flask, which caused a dark-purple solid to precipitate. The solid was then isolated *via* filtration, and washed with excess methanol and hexanes to remove residual

metal salts, unreacted monomer and oligomers. The resulting purple solid was then dried under vacuum to afford 90 mg (65% yield, two steps) of the desired block copolymer poly(**1**-*b*-**6**).. ^{1}H NMR ($CDCl_3$, 400 MHz): δ 0.82–0.95 (br, CH_3), 1.09–1.48 (br, CH_2), 1.64–1.76 (br, CH_2), 2.60–2.95 (br, CH_2), 3.04–3.67 (br, C=NCH_2), 6.94–7.01 (br, aromatic).

Representative Polymerization Procedure of Poly(9-*b*-2) and Poly(10-*b*-2). A 10 mL oven-dried flask containing anhydrous lithium chloride (32.1 mg, 0.76 mmol) was heated under reduced pressure, and then cooled to room temperature under a nitrogen atmosphere. Monomer **9** (0.300 g, 0.76 mmol) was then added to the flask, and the atmosphere in the flask was replaced with nitrogen. THF (5.0 mL) was added via syringe, and the mixture was stirred at room temperature. Isopropylmagnesium chloride (1.0 M solution in THF, 0.76 mL, 0.76 mmol) was then added via syringe, and the mixture was stirred at room temperature for 24 h. To this mixture was added Ni(dppp)Cl_2 (7.8 mg, 0.015 mmol), and the polymerization progress was monitored by SEC until the molecular weight of poly-**9** ceased to increase. SEC analysis of an aliquot removed from the reaction mixture showed that the polymer prepared in situ exhibited the following characteristics: M_n = 7329 Da, M_w/M_n = 1.27. Under nitrogen, **2** (85 mg, 0.30 mmol) was then added to the reaction solution. After the reaction mixture was stirred at room temperature for 1 h, 30 mL of methanol was poured into the reaction flask, which caused a dark-purple solid to precipitate. The solid was then isolated *via* filtration, and washed with excess methanol and hexanes to remove residual metal salts, unreacted monomer and oligomers. The resulting purple solid was then dried under vacuum to afford 222 mg (85% yield, two steps) of the desired block copolymer poly(**9**-*b*-**2**). ^{1}H NMR ($CDCl_3$, 400 MHz): δ 0.73–1.66 (br, CH_2, CH_3), 3.36–3.92 (br, CH_2N), 4.00–4.65 (br, OCH_2), 5.59–6.95 (br, aromatic), 7.34–8.32 (br, aromatic). Poly(**10**-*b*-**2**) was prepared in a similar

manner to that of poly(**9**-*b*-**2**). 236 mg (72% yield) ^{1}H NMR ($CDCl_3$, 400 MHz): δ 0.62–2.13 (br, CH_2, and CH_3), 3.50–4.64 (br, OCH_2, and CO_2CH_2), 5.24–6.22 (br, aromatic), 6.75–7.12 (br, aromatic), 7.34–8.06 (br, aromatic).

Synthesis of the Poly-4 and Poly-6 Homopolymers. *t*-Butyl 4-isocyanobenzoate (**4**), (30 mg, 0.15 mmol) was placed in an oven dried two-neck flask, which was then evacuated on a vacuum line and refilled with dry N_2. After this vacuum–refill procedure was repeated three times, dry CH_2Cl_2 (3.0 mL) was added with a syringe. After complete dissolution of the monomer, a solution of $NiCl_2 \cdot 6H_2O$ in dry methanol (0.05 M, 0.30 mL, 0.015 mmol) was added, and the mixture stirred under N_2 atmosphere at room temperature for 6 h. The polymer was isolated by precipitation from excess methanol, collected by centrifugation, and then dried under reduced pressure at room temperature to afford poly-**6** as a yellow solid (20 mg, 67% yield). SEC: M_n = 19.0 kDa, PDI = 1.30. ^{1}H NMR (CDCl3, 400 MHz): δ 1.04–2.01 (br, CH3), 4.95–6.34 (br, aromatic), 6.51–7.95 (br, aromatic).

Poly-**6** was prepared in a similar manner as poly-**4**. Yield: 70%. SEC: M_n = 4.4 kDa, PDI = 1.60. ^{1}H NMR (CDCl3, 400 MHz): δ 0.74–0.85 (br, CH_3), 1.00–1.72 (br, CH_2), 2.86–3.83 (br, NCH_2).

6.5 ACKNOWLEDGMENTS

Portions of this chapter were reprinted with permission from Wu, Z.-Q.; Ono, R. J.; Chen, Z.; Bielawski, C. W. *J. Am. Chem. Soc.* **2010**, *132*, 14000-14001, Copyright 2010 American Chemical Society and Wu, Z.-Q.; Radcliffe, J. R.; Ono, R. J.; Chen, Z.; Li, Z.; Bielawski, C. W. *Polym. Chem.* **2012**, *3*, 874-881, Copyright 2012 The Royal Society of Chemistry. Zong-Quan Wu and Jonathan D. Radcliffe are gratefully acknowledged for their synthetic contributions. I also thank Jonathan D. Radcliffe and

Prof. Christopher W. Bielawski for their shared efforts in writing the original manuscripts.

6.6 REFERENCES

(1) Segalman, R. A.; McCulloch, B.; Kirmayer, S.; Urban, J. J. *Macromolecules* **2009**, *42*, 9205-9216.

(2) Miyakoshi, R.; Yokoyama, A.; Yokozawa, T. *J. Am. Chem. Soc.* **2005**, *127*, 17542-17547.

(3) Jeffries-El, M.; Sauve, G.; McCullough, R. D. *Macromolecules* **2005**, *38*, 10346-10352.

(4) (a) Park, S.-J.; Kang, S.-G.; Fryd, M.; Saven, J. G.; Park, S.-J. *J. Am. Chem. Soc.* **2010**, *132*, 9931. (b) Higashihara, T.; Ueda, M. *React. Funct. Polym.* **2009**, *69*, 457. (c) Alemseghed, M. G.; Gowrisanker, S.; Servello, J.; Stefan, M. C. *Macromol. Chem. Phys*. **2009**, *210*, 2007. (d) Botiz, I.; Darling, S. B. *Macromolecules* **2009**, *42*, 8211. (e) Iovu, M. C.; Craley, C. R.; Jeffries-El, M.; Krankowski, A. B.; Zhang, R.; Kowalewski, T.; McCullough, R. D. *Macromolecules* **2007**, *40*, 4733. (f) Dai, C.-A.; Yen, W.-C.; Lee, Y.-H.; Ho, C.-C.; Su, W.-F. *J. Am. Chem. Soc.* **2007**, *129*, 11036. (g) Iovu, M. C.; Jeffries-El, M.; Sheina, E. E.; Cooper, J. R.; McCullough, R. D. *Polymer* **2005**, *46*, 8582.

(5) (a) Tao, Y.; McCulloch, B.; Kim, S.; Segalman, R. A. *Soft Matter* **2009**, *5*, 4219. (b) Urien, M.; Erothu, H.; Cloutet, E.; Hiorns, R. C.; Vignau, L.; Cramail, H. *Macromolecules* **2008**, *41*, 7033.

(6) Copolymers containing P3HT and other mechanistically similar homopolymers have been synthesized via sequential monomer additon. For examples, see: (a) Yokoyama, A.; Kato, A.; Miyakoshi, R.; Yokozawa, T. *Macromolecules* **2008**, *41*, 7271. (b) Javier, A. E.; Varshney, S. R.; McCullough, R. D. *Macromolecules* **2010**, *43*, 3233. (c) Hollinger, J.; Jahnke, A. A.; Coombs, N.; Seferos, D. S. *J. Am. Chem. Soc.* **2010**, *132*, 8546. (d) Zhang, Y.; Tajima, K.; Hirota, K.; Hashimoto, K. *J. Am. Chem. Soc.* **2008**, *130*, 7812.

(7) Loewe, R. S.; Ewbank, P. C.; Liu, J.; Zhai, L.; McCullough, R. D. *Macromolecules* **2001**, *34*, 4324-4333.

(8) (a) Deming, T. J.; Novak, B. M.; Ziller, J. W. *J. Am. Chem. Soc.* **1994**, *116*, 2366. (b) Kamer, P. C. J.; Nolte, R. J. M.; Drenth, W. *J. Am. Chem. Soc.* **1988**, *110*, 6818. (c) Yamada, T.; Suginome, M. *Macromolecules* **2010**, *43*, 3999. (e) Kajitani, T.; Okoshi, K.; Sakurai, S.-i.; Kumaki, J.; Yashima, E. *J. Am. Chem. Soc.* **2005**, *128*, 708.

(9) (a) Wu, Z.-Q.; Nagai, K.; Banno, M.; Okoshi, K.; Onitsuka, K.; Yashima, E. *J. Am. Chem. Soc.* **2009**, *131*, 6708.(b) Onouchi, H.; Okoshi, K.; Kajitani, T.;

Sakurai, S.-i.; Nagai, K.; Kumaki, J.; Onitsuka, K.; Yashima, E. *J. Am. Chem. Soc.* **2007**, *130*, 229.

(10) Foster, S.; Finlayson, C. E.; Keivanidis, P. E.; Huang, Y.-S.; Hwang, I.; Friend, R. H.; Otten, M. B. J.; Lu, L.-P.; Schwartz, E.; Nolte, R. J. M.; Rowan, A. E. *Macromolecules* **2009**, *42*, 2023.

(11) No polymerization of **2** was observed in the presence of purified, isolated P3HT that was free of Ni.

(12) Park, S.-J.; Kang, S.-G.; Fryd, M.; Saven, J. G.; Park, S.-J. *J. Am. Chem. Soc.* **2010**, *132*, 9931-9933.

(13) Patra, S. K.; Ahmed, R.; Whittell, G. R.; Lunn, D. J.; Dunphy, E. L.; Winnik, M. A.; Manners, I. *J. Am. Chem. Soc.* **2011**, *133*, 8842-8845.

(14) Miyakoshi, R.; Yokoyama, A.; Yokozawa, T. *J. Am. Chem. Soc.* **2005**, *127*, 17542-17547.

(15) Li, Z.; Ono, R. J.; Wu, Z.-Q.; Bielawski, C. W. *Chem. Commun.* **2011**, *47*, 197-199.

(16) Scherf, U.; Gutacker, A.; Koenen, N. *Acc. Chem. Res* **2008**, *41*, 1086-1097.

(17) Higashihara, T.; Ueda, M. *React. Funct. Polym.* **2009**, *69*, 457-462.

(18) Wu, Z.-Q.; Ono, R. J.; Chen, Z.; Bielawski, C. W. *J. Am. Chem. Soc.* **2010**, *132*, 14000-14001.

(19) Zhang, Q.; Cirpan, A.; Russell, T. P.; Emrick, T. *Macromolecules* **2009**, *42*, 1079-1082.

(20) Yokoyama, A.; Kato, A.; Miyakoshi, R.; Yokozawa, T. *Macromolecules* **2008**, *41*, 7271-7273.

(21) Stefan, M. C.; Javier, A. E.; Osaka, I.; McCullough, R. D. *Macromolecules* **2009**, *42*, 30-32.

(22) Sommer, M.; Huettner, S.; Thelakkat, M. *J. Mater. Chem.* **2010**, *20*, 10788-10797.

(23) Yamada, T.; Suginome, M. *Macromolecules* **2010**, *43*, 3999.

(24) Hoertz, P. G.; Niskala, J. R.; Dai, P.; Black, H. T.; You, W. *J. Am. Chem. Soc.* **2008**, *130*, 9763.

(25) Brockmann, T. W.; Tour, J. M. *J. Am. Chem. Soc.* **1995**, *117*, 4437.

(26) Miyakoshi, R.; Shimono, K.; Yokoyama, A.; Yokozawa, T. *J. Am. Chem. Soc.* **2006**, *128*, 16012.

(27) Chang, K.-J.; Kang, B.-N.; Lee, M.-H.; K.-S., J. *J. Am. Chem. Soc.* **2005**, *127*, 12214.

Chapter 7: Synthesis of a Donor–Acceptor Diblock Copolymer via Two Mechanistically Distinct, Sequential Polymerizations Using a Single Catalyst

7.1 Introduction

Interest in the field of solution-processable, organic solar cells has intensified in recent years as their power conversion efficiencies (PCEs) have continued to improve. Considering that the exciton diffusion lengths in organic materials are on the order of ~10 nm,[1,2] the donor and acceptor components of the aforementioned devices must be in close proximity to one another in order to maximize the likelihood of charge separation and transfer. A second consideration is the need for bicontinuous pathways to allow the separated charges to reach their corresponding electrodes. Currently, the highest performing organic photovoltaic (OPV) devices consist of heterogeneous, solution-processed blends of a conjugated polymer and a fullerene derivative as the donor and acceptor components, respectively, which yield PCEs approaching 10%.[3] Many methods exist for the optimization of such blend morphologies, including the incorporation of small-molecule processing additives;[4] however, due to their inherent non-equilibrium nature, these types of active layers lack well-defined, reproducible structures, and are susceptible to 'ripening' or coarsening of phase separated domains, factors which can severely degrade device stability. A higher degree of morphological control and the realization of a stable, well-defined nanoscale morphology is therefore desirable. Toward this end, the use of so-called donor–acceptor block copolymers, in which both donor and acceptor semiconducting materials are integrated into a single block copolymer, has emerged as a promising approach for overcoming many of the aforementioned drawbacks associated with bulk heterojunction blend devices. Indeed, donor–acceptor block

copolymers offer a means for realizing an ordered nanoscale morphology that is suitable for efficient charge separation and transfer in OPVs via self-assembly.[5,6]

The self-assembly of block copolymers containing conjugated segments is influenced by the interplay between the rod–rod Maier–Saupe interaction parameter (μ), the rod–coil Flory–Huggins interaction parameter (χ), and the volume fraction of the constituent blocks. In order for phase separation to occur, the blocks comprising the copolymer must be sufficiently chemically distinct from one another (i.e., high χ). The volume fraction of the blocks, along with the relative contributions of χ and μ, then determine the resulting morphology of the copolymer in the solid state.[6,7] For example, in cases where the contribution from μ is much greater than the Flory–Huggins interaction—a common scenario for many block copolymers containing conjugated segments that are rigid and tend to form crystalline or liquid crystalline phases—the dominant rod-rod interactions typically give rise to fibrillar or lamellar morphologies. One must therefore carefully select which types of homopolymers to incorporate into the block copolymer, while bearing in mind that the polymeric blocks must also contain chromophoric units with appropriately aligned HOMO and LUMO energy levels to ensure that photoinduced electron transfer can take place from the donor block to the acceptor block. Toward this end, several examples of donor–acceptor block copolymers comprising poly(3-hexylthiophene) (P3HT) donor blocks and perylene diimide (PDI) acceptor blocks have been reported.[8-11,12] P3HT is a semi-crystalline conjugated polymer that is widely used as a donor material in OPVs; PDI is an electron deficient aromatic compound that exhibits high electron mobilities (up to 2.1 $cm^2/(V\ s)$[13]) upon aggregation and also displays a favorable energy level offset with respect to that of P3HT, making it possible to elicit a photovoltaic response when the two materials are combined.[14]

From a synthetic standpoint, the majority of previously reported block copolymers containing P3HT and PDI have involved combinations of Grignard metathesis polymerization (GRIM) (to prepare the P3HT block) and controlled radical polymerization of acrylate-functionalized PDI monomers. For instance, Segalman and coworkers reported[10] a grafting-to synthesis of a diblock copolymer by coupling an alkyne-terminated P3HT with an azide-terminated polyacrylate using click chemistry. The polyacrylate block was then decorated with pendant PDI groups in a second step. In contrast, Emrick and coworkers utilized a grafting-from strategy by growing a PDI-functionalized polyacrylate from a P3HT macroinitiator via nitroxide-mediated radical polymerization.[9] Regardless, whilst suitable donor–acceptor block copolymers were obtained, all examples of P3HT–PDI donor–acceptor block copolymers reported thus far have required extensive and tedious post-polymerization manipulations of polymer end-groups to either facilitate polymer–polymer coupling (i.e., grafting-to) or to install an appropriate initiator to accommodate a change of polymerization mechanism (i.e., grafting-from).

To address the aforementioned limitations associated with the synthesis of mechanistically distinct block copolymers containing conjugated segments, we recently reported[15] a one pot synthesis of poly(3-hexylthiophene)-*b*-poly(arylisocyanide) using a single catalyst. The Ni-catalyzed GRIM polymerization of 5-chloromagnesio-2-bromo-3-hexylthiophene (**1**) was employed to grow a Ni(II)-terminated P3HT macroinitiator which, upon subsequent addition of an arylisocyanide monomer, afforded a controlled chain extension process to give the aforementioned diblock copolymer. Moreover, we found that the copolymerization process was amenable to a variety of aryl-Grignard as well as aryl- and alkyl-isocyanide monomers,[16] indicating that the method was general for many combinations of conjugated polymers (i.e., a range poly(N-alkylpyrrole)s and

poly(*p*-phenylene)s) were chain extended with various poly(isocyanide)s). We therefore reasoned that this copolymerization methodology would be useful for the preparation of donor–acceptor block copolymers, wherein the conjugated polymer would comprise the donor component (e.g., P3HT), and the poly(isocyanide) featured pendant acceptor units (e.g., PDI). Furthermore, because poly(isocyanide)s are known to adopt rigid helical conformations,[17] pendant chromophores such as PDI should be arranged into ordered, periodic helical arrays around the polymer backbone. Such an ordered arrangement of perylene units has been proven to be advantageous for attenuating the negative effects of uncontrolled perylene aggregation within photovoltaic blends, such as the macrophase separation of donor and acceptor components and increased trapped charges.[18] Herein, we present the synthesis and photophysical characterization of a novel P3HT-*b*-poly(isocyanide), the latter of which featured pendant perylene diimides, as the donor and acceptor blocks, respectively. The copolymerization was found to proceed in a single reaction vessel via mechanistically-distinct, sequential polymerizations involving an activated thiophene as well as a PDI-functionalized arylisocyanide and was facilitated with a single Ni catalyst.

7.2 RESULTS AND DISCUSSION

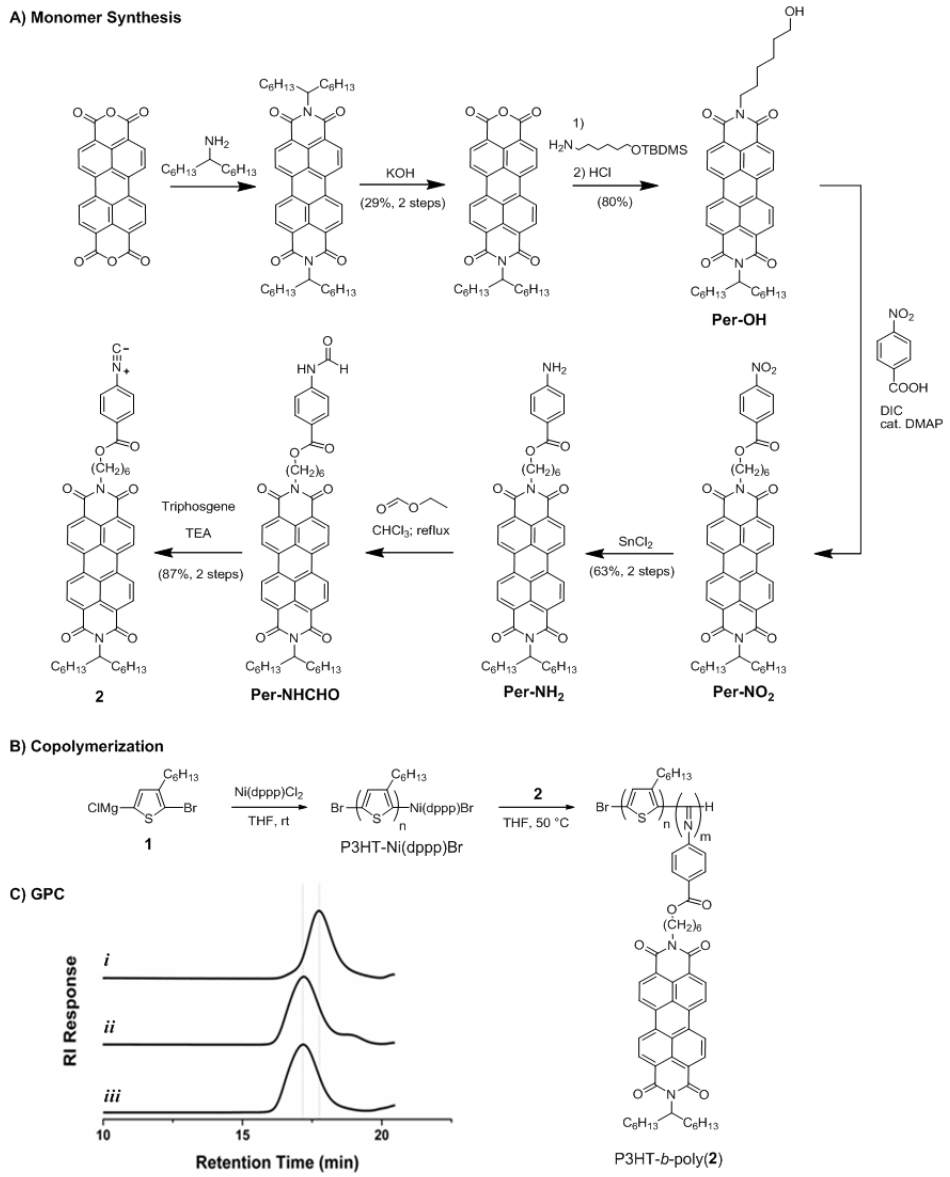

Figure 7.1: (A) Synthesis of PDI-functionalized arylisocyanide monomer **2**. (B) Synthesis of P3HT-*b*-poly(**2**) via sequential monomer addition. (C) GPC traces of (*i*) P3HT; (*ii*) crude P3HT-*b*-poly(**2**); and (*iii*) P3HT-*b*-poly(**2**) after purification *via* preparative size exclusion chromatography.

The synthesis of the PDI functionalized arylisocyanide monomer **2** and its copolymerization with **1** is summarized in Figure 1A. Building on our previous work,[15,16] we elected to design the perylene-containing monomer around a polymerizable 4-isocyanobenzoate derivative. Steglich esterification of the known hydroxy-functionalized intermediate **Per-OH**[9] with 4-nitrobenzoic acid and N,N'-diisopropylcarbodiimide (DIC) gave the corresponding ester **Per-NO_2** which, upon reduction with stannous chloride, afforded the 4-aminobenzoate **Per-NH_2** in 63% yield over the two steps. Subsequent formylation with ethyl formate, followed by dehydration with triphosgene (87% yield, two steps) furnished the desired 4-isocyanobenzoate monomer **2**. The synthesis was found to be scalable, and gram-scale quantities of **2** were successfully prepared. It should also be noted that **2** is stable, as decomposition was not detected by ^{1}H NMR spectroscopy after several months of storage in a freezer at -20 °C, and readily soluble in organic solvents, including: methylene chloride, chloroform, and THF.

With **2** in hand, we shifted our attention toward its copolymerization with 5-chloromagnesio-2-bromo-3-hexylthiophene (**1**) (Figure 1B). Using standard Kumada catalyst transfer polycondensation methods, **1** was polymerized using Ni(dppp)Cl_2 (dppp = 1,3-bis(diphenylphosphino)propane) in THF to generate a regioregular P3HT containing a reactive Ni terminus (P3HT-Ni(dppp)Br). Aliquots were removed from the reaction vessel and analyzed by gel permeation chromatography (GPC). When the polymerization was deemed complete, a THF solution of **2** ([**2**] = 0.01 M) was added to the unquenched reaction mixture. After 3 h, the mixture was poured into excess methanol, and the precipitated solids were collected in 48–66% yield via filtration. GPC analysis of the isolated material revealed a higher number-averaged molecular weight (M_n) and lower dispersity (M_w/M_n; $Đ$) (9.5 kDa; $Đ$ = 1.2) than that of the macroinitiator contained in the aliquot removed after polymerization of **1** (M_n = 5.0 kDa; $Đ$ = 1.3),

indicative of a successful chain extension to form P3HT-*b*-poly(**2**) (cf., Figure 1C). The small shoulder in the GPC trace of the isolated material (Figure 1C, curve *ii*) corresponds to small quantities of unreacted **2** which were not removed during precipitation due to its insolubility in methanol. Residual **2** was, however, removed via either preparative size exclusion chromatography or Soxhlet extraction with acetone, which is a selective solvent for **2**. The GPC trace of the purified block copolymer confirmed complete removal of **2** (Figure 1C, curve *iii*).

Entry	$[\mathbf{1}]_0$:$[\mathbf{2}]_0$:$[Ni]_0$	M_n of P3HT [kDa][a)]	M_n of copolymer [kDa][b)]	$Đ$ of copolymer [M_w/M_n][b)]	f_{P3HT} [wt %][c)]	Yield [%]
1	25:20:1	3.1	12.7	1.3	24	53
2	30:6:1	5.0	9.5	1.2	53	66
3	66:6:1	11.0	14.3	1.2	77	48

Table 7.1: Selected Molecular Weight and Polydispersity Data for P3HT-*b*-poly(**2**). The M_n of P3HT was determined by GPC analysis of aliquots removed from the reaction mixture prior to addition of **2**. $[Ni]_0 = [Ni(dppp)Cl_2]_0$; [b)] The M_n and $Đ$ were determined by GPC and are reported as their polystyrene equivalents; [c)] Calculated using the M_ns of P3HT from aliquots removed prior to addition of **2** and P3HT-*b*-poly(**2**), respectively.

The chain growth nature of the polymerizations of **1** and **2** permitted excellent control over both the molecular weight and the volume fraction of the respective blocks by varying the initial monomer to catalyst feed ratios. Indeed, as summarized in Table 1, P3HT-*b*-poly(**2**) having P3HT volume fractions ranging from 24–77% were synthesized. Increased reaction temperatures were required to achieve higher degrees of polymerization of **2** in the chain extension polymerization, likely due to increased solubility of the growing polymer chains in THF at elevated temperatures. Regardless,

under the optimized conditions, all block copolymers synthesized exhibited narrow, monomodal distributions by GPC, suggesting to us that a single catalyst mediated two mechanistically distinct polymerization reactions in a sequential manner.

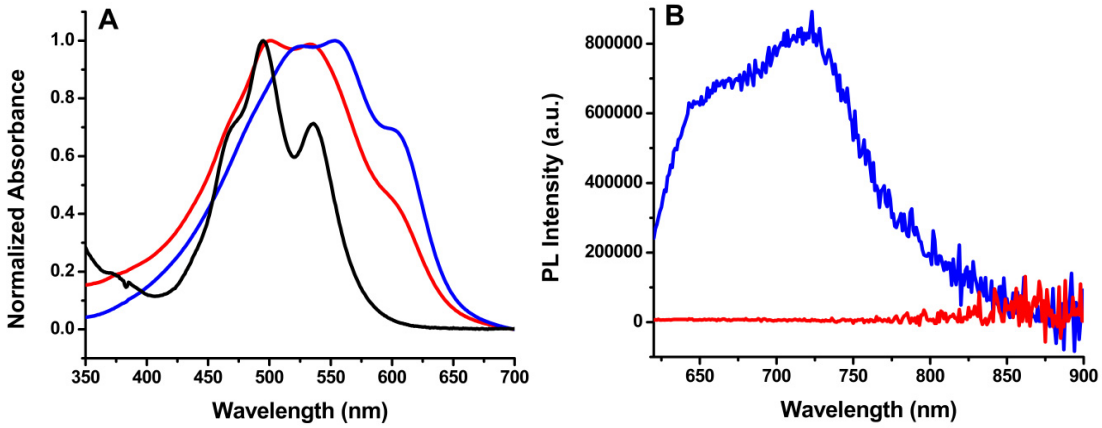

Figure 7.2: (A) Solid state absorption spectra of poly(**2**) (black curve), P3HT-*b*-poly(**2**) (red curve), and P3HT (blue curve). (B) Solid state photoluminescence spectra of P3HT (blue curve) and P3HT-*b*-poly(**2**) (red curve). λ_{ex} = 600 nm.

The optical properties of P3HT-*b*-poly(**2**) were next examined. In the solid state, the diblock copolymer exhibited an absorption profile with a maximum centered around 500 nm, along with two prominent shoulders at 534 nm and 600 nm (Figure 2). The solid state absorption spectra of a P3HT homopolymer and a poly(**2**) homopolymer were also recorded for comparison. When overlaid, the absorption spectrum of P3HT-*b*-poly(**2**) appeared to be the linear summation of the absorption profiles of its individual components (i.e., P3HT and poly(**2**)), and consistent with similar results observed for other P3HT- and PDI-containing block copolymers.[8,9,19] Figure 2B shows the solid state fluorescence spectra of P3HT and P3HT-*b*-poly(**2**). As opposed to the intense photoluminescence exhibited by P3HT, the emission of P3HT-*b*-poly(**2**) was quenched in the solid state, an expected result of efficient photoinduced electron transfer from P3HT

to poly(**2**). Similar behavior was observed in solution, wherein the fluorescence of P3HT-*b*-poly(**2**) was attenuated by 87% relative to that of P3HT (Figure A33, Appendix A). Collectively, these results suggested to us that, on a qualitative basis, the P3HT-*b*-poly(**2**) is poised to function as donor–acceptor active material in organic solar cells.[20] Moreover, the strong fluorescence quenching observed (especially in the solid state) for the block copolymer suggests that donor–acceptor interfaces were formed on length scales commensurate with the exciton diffusion length (i.e., ca. 10 nm).[21]

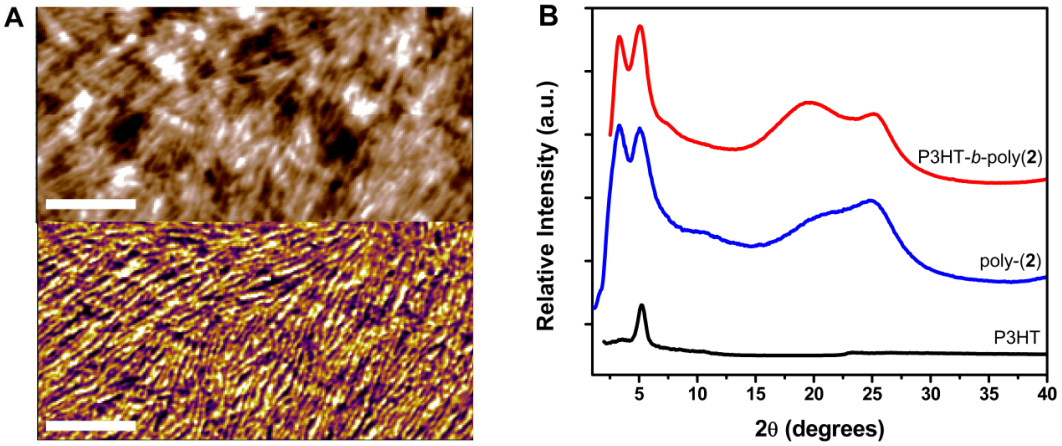

Figure 7.3: (A) Tapping mode AFM (top) height and (bottom) phase images of P3HT-*b*-poly(**2**) drop cast from chloroform onto a Si wafer, after annealing in saturated chloroform vapor for 24 h. Scale bar = 400 nm; scan size = 2 μm. (B) X-ray diffraction patterns for P3HT, poly(**2**), and P3HT-*b*-poly(**2**). Curves are offset along the y-axis.

Thus, to probe the surface morphology adopted by the P3HT-*b*-poly(**2**) copolymer, tapping mode atomic force microscopy (AFM) was conducted on thin films drop casted from chloroform solutions. As shown in Figure 7.3A, a fibrillar morphology was observed and found to become more pronounced upon solvent vapor annealing (see Figure A34, Appendix A) for the AFM image acquired prior to annealing). Fibrillar

nanoscale morphologies are characteristic of most P3HT-containing block copolymers,[14,22] including donor–acceptor block copolymers containing P3HT and PDI.[9,10] Further evidence for microphase separation was obtained by powder X-ray diffraction (XRD) of the diblock copolymer. As shown in Figure 3B, the diffraction pattern exhibited by P3HT-*b*-poly(**2**) contained reflections that were attributable to those belonging to P3HT and poly(**2**) (i.e., as their homopolymers), indicating a retention of the crystalline nature intrinsic to both blocks. For example, the broad reflection centered at $2\theta = 25.0°$ recorded for poly(**2**), which corresponded to a π–π stacking distance of 3.5 Å between two PDI units, was also visible in the diffraction pattern of the block copolymer. Considering that related PDI-functionalized helical poly(isocyanopeptide)s make one complete turn for every four repeat units, the abovementioned π–π stacking distance may correspond to an intermolecular interaction of PDI units between every n and n+4 monomers along the polymer backbone.[23,24] The intense signals recorded at the 2θ values of 3.3° and 5.1° recorded for poly(**2**), which are indicative of a lamellar structure of pendant PDI units on the polyisocyanide, also appeared in the XRD pattern recorded for P3HT-*b*-poly(**2**), and were consistent with reported values for related, side-chain PDI-functionalized polymers.[25,26] Note that the relative ratio of intensities of the reflections recorded at the 2θ values of 3.3° and 5.1° differ between poly(**2**) and P3HT-*b*-poly(**2**), with the latter signal being the more intense for the diblock copolymer. Presumably, the reflection at 5.1° is overlapping with the known[27] (001) reflection of lamellar stacks of P3HT ($2\theta = 5.2°$) in the XRD spectrum of the block copolymer, leading to the increased intensity in the signal at that value. Overall, the results suggested to us that both donor and acceptor components (i.e., P3HT and poly(**2**), respectively) of the block copolymer self-stacked into lamellar structures in the solid state and in a similar manner as the

individual homopolymers, and further confirmed the nanofibrillar surface morphology visualized via AFM.

7.3 Conclusion

In conclusion, we have developed a facile, one-pot synthesis of a donor–acceptor block copolymer comprised of P3HT and a perylene diimide functionalized polyisocyanide. The copolymerization proceeded via sequential addition of the corresponding monomers using a single Ni catalyst. Moreover, each mechanistically distinct polymerization proceeded in a controlled fashion to give molecular weights that were proportional to the monomer-to-catalyst feed ratios, a useful feature that may be used to tune the volume fractions of the resulting blocks (i.e., to gain morphological control) or to balance charge carrier mobilities within an active layer of a device (i.e., to maximize the collection of charges by reducing the space charge limited photocurrent). Our preliminary structural characterization revealed that the block copolymer underwent microphase separation in the solid state to form stacked structures of electron donors and acceptors, a desirable feature for the generation and transport of separated charges for photovoltaic applications. Indeed, the photoluminescence quenching observed in thin films of the donor–acceptor block copolymer is indicative of efficient photoinduced charge transfer between the P3HT and perylene diimide components, leading us to believe that these diblock copolymer materials are excellent candidates for use in OPV devices.

7.4 Experimental

7.4.1 General Considerations

All solvents were purchased from Fisher scientific and used without additional purification unless otherwise noted. All other chemicals were purchased from Aldrich,

Alfar Aesar, or Fisher and were used as received. 2-Bromo-5-chloromagnesio-3-hexylthiophene was prepared using a literature procedure.[28] **Per-OH** was synthesized following a modified literature procedure.[9] THF and methylene chloride were dried and degassed using a Vacuum atmospheres company solvent purification system.

^{1}H NMR and ^{13}C NMR spectra were recorded on a Varian 400 spectrometer. Chemical shifts are reported in delta (δ) units and expressed in parts per million (ppm) downfield from tetramethylsilane using the residual solvent as an internal standard. For ^{1}H NMR: $CDCl_3$, δ = 7.24 ppm. For ^{13}C NMR: $CDCl_3$, 77.00 ppm. Coupling constants (J) are expressed in Hertz. Gel permeation chromatography (GPC) was performed on a Viscotek GPCmax Solvent/Sample Module. Two fluorinated polystyrene columns (IMBHW-3078 and I-MBLMW-3078) were used in series and maintained at 24 °C. THF was used as the mobile phase at a flow rate of 1.0 mL/min. Detection was performed using a Viscotek VE 3580 Refractive Index Detector or a Viscotek 2600 Photodiode Array Detector (tuned at 450 nm). Molecular weight and dispersity data are reported relative to polystyrene standards in THF. Elemental analysis was performed using a ThermoScientific Flash 2000 Organic Elemental Analyzer. Analyses were performed in triplicate and averaged. Samples for atomic force microscopy (AFM) measurements were prepared by drop casting chloroform solutions (1 mg/mL) of the polymer onto precleaned silicon wafers, then placed in covered Petri dishes saturated with chloroform vapor for 24 h. AFM images were acquired in tapping mode with an Asylum MFP-3D AFM, performed at room temperature under an atmosphere of air using standard silicon cantilevers with a nominal spring constant of 50 N/m and resonance frequency of ~300 kHz. The images were acquired at a scan frequency of 1 Hz over 2 × 2 μm^2 scan areas. Powder X-Ray diffraction (XRD) measurements were recorded on an R-Axis Spider diffractometer using CuKα radiation and an exposure time of 10 min per sample. UV/vis

spectra were recorded using a Perkin Elmer Instruments Lambda 35 spectrometer. Emission spectra were recorded using a Horiba Jobin Yvon Fluorolog3 fluorimeter. Differential scanning calorimetry (DSC) was performed using a Mettler-Toledo DSC823e under an atmosphere of nitrogen at a heating/cooling rate of 5 °C min^{-1}. Thermogravimetric analysis (TGA) was performed on a TA Instruments Q500 thermogravimetric analyzer. Samples were first held at a constant temperature of 80 °C for 30 min, and then heated to 800 °C at a rate of 20 °C min^{-1} under an atmosphere of nitrogen. Melting points were determined using a Stanford Research Systems OptiMelt Automated Melting Point System. Elemental analyses were performed using a ThermoScientific Flash 2000 Organic Elemental Analyzer.

7.4.2 Synthetic Procedures

Per-NO_2. To a 100 mL round bottom flask was added **Per-OH** (1.88 g, 2.79 mmol), 4-nitrobenzoic acid (0.47 g, 2,79 mmol), N,N'-diisopropylcarbodiimide (DIC; 0.35 g, 2.79 mmol), 4-dimethylaminopyridine (DMAP; 0.017 g, 0.14 mmol), and CH_2Cl_2 (75 mL). The reaction mixture was stirred for 18 h at room temperature, concentrated to a volume of ~5-10 mL under reduced pressure, and purified by column chromatography (silica gel, eluent: $CHCl_3$) to afford the desired product as a red solid (2.15 g, 94% yield). ^{1}H NMR (400 MHz, $CDCl_3$): δ 8.65-8.57 (m, 8H), 8.25 (d, 2H, *J* = 8.0 Hz), 8.18 (d, 2H, *J* = 8.0 Hz), 5.17 (p, 1H), 4.36 (t, 2H), 4.21 (t, 2H), 2.23 (m, 2H), 1.87-1.82 (br, 6H), 1.55 (br,4H), 1.31-1.20 (br, 16H), 0.82 (t, 6H); ^{13}C NMR (75 MHz, $CDCl_3$): δ 164.69, 163.35, 163.11, 150.41, 135.78, 134.37, 133.93, 131.60, 131.08, 130.65, 129.35, 129.06, 126.09, 126.02, 123.48, 122.91, 122.76, 65.97, 54.83, 40.36, 32.35, 31.76, 29.23, 28.46, 27.89, 26.95, 26.70, 25.78, 22.58, 14.04. HRMS (MALDI) calcd for $C_{50}H_{51}N_3O_8$ $[M+H]^+$

m/z 821.3676, found *m/z* 821.3621. mp: 165-166 °C. Anal. calcd for $C_{50}H_{51}N_3O_8$: C, 73.06; H, 6.25; N, 5.11; found: C, 72.80; H, 6.30; N, 4.96.

Per-NH$_2$. To a 100 mL round bottom flask was added **Per-NO$_2$** (1.8 g, 2.2 mmol), stannous chloride (2.08 g, 10.9 mmol), $CHCl_3$ (40 mL) and ethanol (10 mL). The mixture was stirred for 18 h at 50 °C, concentrated under reduced pressure, and purified by column chromatography (silica gel, eluent: $CHCl_3$) to afford the desired compound as a red solid (1.17 g, 67% yield). ^{1}H NMR (400 MHz, $CDCl_3$): δ 8.59-8.41 (m, 8H), 7.81 (d, 2H, *J* = 4.0 Hz), 6.60 (d, 2H, *J* = 4.0 Hz), 5.16 (p, 1H), 4.79 (br, 2H), 4.23 (t, 2H), 2.23 (m, 2H), 1.89-1.82 (br, 2H), 1.76 (br, 4H), 1.51 (br, 4H), 1.32-1.21 (br, 16H), 0.81 (t, 6H); ^{13}C NMR (75 MHz, $CDCl_3$): δ 166.67, 163.20, 150.65, 134.44, 134.15, 131.53, 131.20, 130.95, 129.42, 129.17, 126.23, 126.14, 123.03, 122.94, 122.85, 120.07, 113.75, 64.37, 54.81, 40.45, 32.36, 31.75, 29.23, 28.72, 27.99, 26.94, 26.81, 25.89, 22.58, 14.04. HRMS (CI) calcd for $C_{50}H_{53}N_3O_6$ $[M+H]^+$ *m/z* 791.3934, found *m/z* 791.3935. mp: 229-231 °C. Anal. calcd for $C_{50}H_{53}N_3O_6$: C, 75.83; H, 6.75; N, 5.31; found: C, 74.91; H, 6.72; N, 4.98.

Per-NHCHO. To a 100 mL round bottom flask was added **Per-NH$_2$** (1.06 g, 1.34 mmol), ethyl formate (20 mL, 248 mmol), and $CHCl_3$ (40 mL). The flask was fitted with a condenser, and the reaction mixture was stirred under reflux for 18h. After cooling to room temperature, the reaction mixture was concentrated under reduced pressure, and purified by column chromatography (silica gel; first eluting with 0.2% v/v methanol in CH_2Cl_2, then 10% v/v methanol in CH_2Cl_2) to afford the desired compound as a red solid (1.05 g, 96% yield). ^{1}H NMR (400 MHz, $CDCl_3$): δ 8.81 (d, 0.4H, *J* = 12 Hz), 8.61-8.46 (br, 8H), 8.41 (s, 0.6H), 8.0 (overlapping d, 2H), 7.71 (d, 0.4H, *J* = 12 Hz), 7.6 (d, 1.2H, *J* = 8 Hz), 7.34 (s, 0.6H), 7.08 (d, 0.8H, *J* = 8 Hz), 5.16 (p, 1H), 4.29 (t, 2H), 4.18 (t, 2H), 2.23 (m, 2H), 1.88-1.78 (br, 6H), 1.53 (br, 4H), 1.35-1.20 (br, 16H), 0.80 (t, 6H); ^{13}C

NMR (75 MHz, $CDCl_3$): δ 165.98, 165.77, 164.43, 163.38, 163.08, 161.54, 158.91, 140.87, 140.72, 134.34, 134.25, 133.95, 131.52, 131.05, 130.86, 129.31, 129.00, 126.94, 126.45, 126.02, 123.20, 122.87, 122.76, 119.00, 117.13, 65.13, 65.02, 54.84, 40.39, 32.34, 31.75, 29.23, 28.56, 27.93, 26.96, 26.73, 25.45, 22.58, 14.04. HRMS (CI) calcd for $C_{51}H_{53}N_3O_7$ $[M+H]^+$ *m/z* 819.3884, found *m/z* 819.3892. mp: 200-201 °C. Anal. calcd for $C_{51}H_{53}N_3O_7$: C, 74.70; H, 6.51; N, 5.13; found: C, 74.73; H, 6.63; N, 4.83.

2. In an oven dried 100 mL Schlenk flask, triethylamine (0.33 mL, 2.4 mmol) was added to a solution of **Per-NHCHO** (0.976 g, 1.2 mmol) in dry CH_2Cl_2 (40 mL). The resulting solution was cooled to 0 °C and stirred for 10 min under an atmosphere of nitrogen. A solution of triphosgene (0.20 g, 0.67 mmol) in CH_2Cl_2 (10 mL) was then added dropwise to the reaction mixture via syringe. The resulting mixture was allowed to warm to room temperature, and stirred for another 3h. The reaction mixture was then washed with aq. $NaHCO_3$ (2 × 30 mL) and brine (1 × 30 mL), dried over Na_2SO_4, and concentrated under reduced pressure. Purification of the crude material by column chromatography (silica gel; eluent: $CHCl_3$) afforded the desired compound as a red solid (0.87 g, 91% yield). ^1H NMR (400 MHz, $CDCl_3$): δ 8.61-8.43 (br, 8H), 8.05 (d, 2H, J = 8 Hz), 8.41 (d, 2H, J = 8 Hz), 5.16 (p, 1H), 4.32 (t, 2H), 4.17 (t, 2H), 2.23 (m, 2H), 1.88-1.78 (br, 6H), 1.52 (br, 4H), 1.36-1.20 (br, 16H), 0.81 (t, 6H); ^{13}C NMR (75 MHz, $CDCl_3$): δ 166.84, 164.99, 164.34, 162.94, 134.13, 133.73, 131.19, 130.88, 130.76, 129.23, 128.87, 126.37, 125.87, 125.83, 122.74, 122.63, 65.60, 54.83, 52.56, 45.40, 40.33, 37.43, 32.33, 31.74, 29.2328.48, 27.87, 26.96, 26.71, 25.76, 22.58, 14.04. HRMS (CI) calcd for $C_{51}H_{51}N_3O_6$ $[M+H]^+$ *m/z* 801.3778, found *m/z* 801.3778. mp: 120-121 °C. Anal. calcd for $C_{51}H_{51}N_3O_6$: C, 76.38; H, 6.41; N, 5.24; found: C, 76.78; H, 6.72; N, 4.97.

Representative block copolymerization procedure (synthesis of P3HT-*b*-poly(2)). To an oven dried 10 mL Schlenk flask containing Ni(dppp)Cl_2 (3.4 mg, 0.006 mmol) was added a THF solution of 2-bromo-5-chloromagnesio-3-hexylthiophene (0.1M, 1.6 mL). The resulting orange mixture was stirred at room temperature under an atmosphere of nitrogen, and the polymerization progress was monitored by GPC until the molecular weight increase ceased (~1 h). GPC analysis of the aliquot removed from the reaction mixture showed that the *in situ* prepared P3HT exhibited the following characteristics: M_n = 3100, $Đ$ = 1.35. At this point, the reaction mixture was warmed to 50 °C, and a THF solution of **2** (0.04M, 3.13 mL) was added via syringe. The reaction mixture was then stirred for 3 h under nitrogen, cooled to ambient temperature and aq. HCl (6M, 2 mL) was added to quench the polymerization. The mixture was then poured into 50 mL of methanol, causing a dark solid to precipitate. The solids were collected via filtration, washed with methanol (3 × 30 mL), and dried under vacuum. Removal of residual monomer **2** via preperative size exclusion chromatography (Bio-Rad Bio-Beads^{TM} S-X1 Support; eluent: THF) afforded the desired block copolymer as a dark red-brown solid (67 mg, 53% yield). GPC: M_n = 12700, $Đ$ = 1.30.

Synthesis of a homopolymer of 2 (poly(2)). Monomer **2** (44 mg, 0.055 mmol) was added to an oven dried 10 mL Schlenk flask, which was sealed with a rubber septum. After replacing the atmosphere inside the flask with nitrogen, dry CH_2Cl_2 (5 mL) was added via syringe. After dissolution of the monomer, a solution of $NiCl_2 \cdot 6H_2O$ in dry methanol (0.017 M, 0.2 mL) was added, and the mixture stirred for 6 h at room temperature under a nitrogen atmosphere. The reaction mixture was poured into methanol, and the precipitated solids were collected via filtration. The solids were washed with methanol (3 × 30 mL) and dried under reduced pressure to afford poly(**2**) as a red solid (23 mg, 52% yield). GPC: M_n = 12500, $Đ$ = 1.41.

7.5 ACKNOWLEDGMENTS

Portions of this chapter were reprinted with permission from Ono, R. J.; Todd, A. D.; Hu. Z.; Vanden Bout, D. A.; Bielawski, C. W. *Macromol. Rapid Commun.* **2013**, *Vol. 34*, In Press (DOI: 10.1002/marc.201300440). Copyright 2013 John Wiley and Sons. Alex D. Todd and Zhongjian Hu are gratefully acknowledged for acquiring the XRD and photophysical data, respectively. I also thank Prof. Christopher W. Bielawski, who helped to write the original manuscript.

7.6 REFERENCES

(1) Coakley, K. M.; McGehee, M. D. *Chem. Mater.* **2004**, *16*, 4533-4542.

(2) Hoppe, H.; Sariciftci, N. S. *J. Mater. Res.* **2004**, *19*, 1924-1945.

(3) Green, M. A.; Emery, K.; Hishikawa, Y.; Warta, W.; Dunlop, E. D. *Prog. Photovoltaics* **2012**, *20*, 606-614.

(4) Lee, J. K.; Ma, W. L.; Brabec, C. J.; Yuen, J.; Moon, J. S.; Kim, J. Y.; Lee, K.; Bazan, G. C.; Heeger, A. J. *J. Am. Chem. Soc.* **2008**, *130*, 3619-3623.

(5) Sommer, M.; Huettner, S.; Thelakkat, M. *J. Mater. Chem.* **2010**, *20*, 10788-10797.

(6) Segalman, R. A.; McCulloch, B.; Kirmayer, S.; Urban, J. J. *Macromolecules* **2009**, *42*, 9205-9216.

(7) Olsen, B. D.; Segalman, R. A. *Mater. Sci. Eng., R* **2008**, *62*, 37-66.

(8) Rajaram, S.; Armstrong, P. B.; Kim, B. J.; Fréchet, J. M. J. *Chem. Mater.* **2009**, *21*, 1775-1777.

(9) Zhang, Q.; Cirpan, A.; Russell, T. P.; Emrick, T. *Macromolecules* **2009**, *42*, 1079-1082.

(10) Tao, Y.; McCulloch, B.; Kim, S.; Segalman, R. A. *Soft Matter* **2009**, *5*, 4219-4230.

(11) Sommer, M.; Lang, A. S.; Thelakkat, M. *Angew. Chem. Int. Ed.* **2008**, *47*, 7901-7904.

(12) For donor–acceptor block copolymers comprising P3HT and other n-type acceptor materials, see: Miyanishi, S.; Zhang, Y.; Tajima, K.; Hashimoto, K. *Chem. Commun.* **2010**, *46*, 6723-6725; Lee, J. U.; Cirpan, A.; Emrick, T.; Russell, T. P.; Jo, W. H. *J. Mater. Chem.* **2009**, *19*, 1483-1489; Yang, C.; Lee, J. K.; Heeger, A. J.; Wudl, F. *J. Mater. Chem.* **2009**, *19*, 5416-5423; Guo, C.; Lin, Y.-

H.; Witman, M. D.; Smith, K. A.; Wang, C.; Hexemer, A.; Strzalka, J.; Gomez, E. D.; Verduzco, R. *Nano Lett.* **2013**, *13*, 2957-2963; Mulherin, R. C.; Jung, S.; Huettner, S.; Johnson, K.; Kohn, P.; Sommer, M.; Allard, S.; Scherf, U.; Greenham, N. C. *Nano Lett.* **2011**, *11*, 4846-4851.

(13) Chesterfield, R. J.; McKeen, J. C.; Newman, C. R.; Ewbank, P. C.; da Silva Filho, D. t. A.; Brédas, J.-L.; Miller, L. L.; Mann, K. R.; Frisbie, C. D. *J. Phys. Chem. B* **2004**, *108*, 19281-19292.

(14) Dittmer, J. J.; Marseglia, E. A.; Friend, R. H. *Adv. Mater.* **2000**, *12*, 1270-1274.

(15) Wu, Z.-Q.; Ono, R. J.; Chen, Z.; Bielawski, C. W. *J. Am. Chem. Soc.* **2010**, *132*, 14000-14001.

(16) Wu, Z.-Q.; Radcliffe, J. D.; Ono, R. J.; Chen, Z.; Li, Z.; Bielawski, C. W. *Polym. Chem.* **2012**, *3*, 874-881.

(17) Schwartz, E.; Koepf, M.; Kitto, H. J.; Nolte, R. J. M.; Rowan, A. E. *Polym. Chem.* **2011**, *2*, 33-47.

(18) Foster, S.; Finlayson, C. E.; Keivanidis, P. E.; Huang, Y.-S.; Hwang, I.; Friend, R. H.; Otten, M. B. J.; Lu, L.-P.; Schwartz, E.; Nolte, R. J. M.; Rowan, A. E. *Macromolecules* **2009**, *42*, 2023-2030.

(19) Huettner, S.; Hodgkiss, J. M.; Sommer, M.; Friend, R. H.; Steiner, U.; Thelakkat, M. *J. Phys. Chem. B* **2012**, *116*, 10070-10078.

(20) The thermal properties of P3HT-*b*-poly(**2**) were examined by thermogravimetric analysis and differential scanning calorimetry. See Appendix A for details.

(21) To test whether the fluorescence quenching observed was due to microphase separation of the block copolymer on length scales on the order of the exciton diffusion length, fluorescence measurements were performed on a solution and thin film of a physical blend of P3HT and poly(**2**) homopolymers. See Appendix A for details.

(22) Stefan, M. C.; Bhatt, M. P.; Sista, P.; Magurudeniya, H. D. *Polym. Chem.* **2012**, *3*, 1693-1701.

(23) Schwartz, E.; Palermo, V.; Finlayson, C. E.; Huang, Y.-S.; Otten, M. B. J.; Liscio, A.; Trapani, S.; González-Valls, I.; Brocorens, P.; Cornelissen, J. J. L. M.; Peneva, K.; Müllen, K.; Spano, F. C.; Yartsev, A.; Westenhoff, S.; Friend, R. H.; Beljonne, D.; Nolte, R. J. M.; Samorì, P.; Rowan, A. E. *Chem. Eur. J.* **2009**, *15*, 2536-2547.

(24) De Witte, P. A. J.; Hernando, J.; Neuteboom, E. E.; van Dijk, E. M. H. P.; Meskers, S. C. J.; Janssen, R. A. J.; van Hulst, N. F.; Nolte, R. J. M.; García-Parajó, M. F.; Rowan, A. E. *J. Phys. Chem. B* **2006**, *110*, 7803-7812.

(25) Lang, A. S.; Neubig, A.; Sommer, M.; Thelakkat, M. *Macromolecules* **2010**, *43*, 7001-7010.

(26) Sommer, M.; Huttner, S.; Steiner, U.; Thelakkat, M. *Appl. Phys. Lett.* **2009**, *95*, 183308-1–183308-3.

(27) Prosa, T. J.; Winokur, M. J.; Moulton, J.; Smith, P.; Heeger, A. J. *Macromolecules* **1992**, *25*, 4364-4372.

(28) Loewe, R. S.; Ewbank, P. C.; Liu, J.; Zhai, L.; McCullough, R. D. *Macromolecules* **2001**, *34*, 4324-4333.

Appendix A: Supporting Information

A-2. SUPPORTING INFORMATION FOR CHAPTER 2

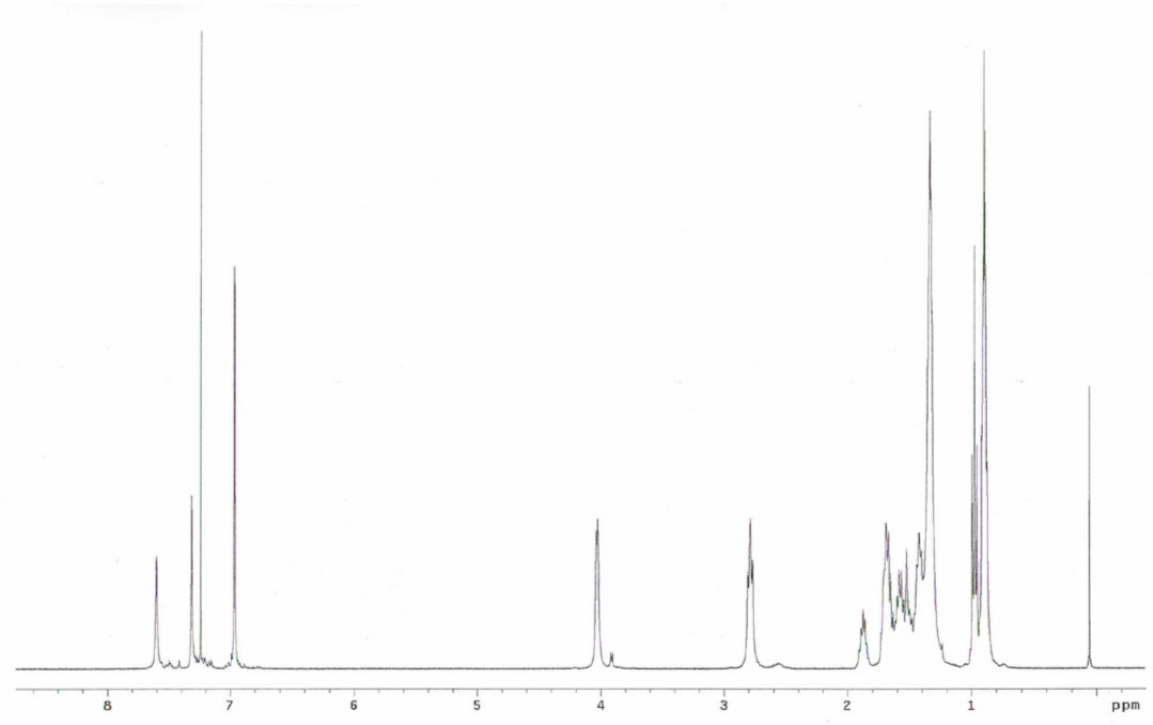

Figure A1: ^{1}H NMR spectrum of PTPP-*b*-P3HT(400 MHz, $CDCl_3$).

A-3. SUPPORTING INFORMATION FOR CHAPTER 3

Grafting Density Calculations: To determine the grafting density of [2-(4-bromophenyl)-ethyl]-triethoxysilane on the silica surface from the TGA data, eq 1 was used:

$$\text{Graft density } (\mu\text{mol/m}^2) = \frac{\left(\frac{W_{100\text{-}800}}{100 - W_{100\text{-}800}}\right) \times 100 - W_{SiO2}}{MW \times S_{spec} \times 100} \times 10^6 \qquad (1)$$

where $W_{100\text{-}800}$ is the percent weight loss between 100 and 800 °C for SiO_2-PhBr (8.7%, Figure 4); W_{SiO2} is the percent weight loss of the bare silica particles prior to the grafting over the same temperature range (6.3%); *MW* is the molecular weight of the grafted organosilane (184 g/mol); and S_{spec} is the specific surface area of the bare silica nanoparticles (48.5 m^2/g as determined by BET analysis).

The grafting density was also determined by carbon elemental analysis and calculated using eq 2:

$$\text{Graft density } (\mu\text{mol/m}^2) = \frac{10^6 \times \Delta C}{[(1200 N_c - \Delta C(MW - 1)] \times S_{spec}} \qquad (2)$$

where ΔC is the difference in carbon content of the nanoparticles after and before grafting as determined by elemental analysis (1.88); N_c is the number of carbon atoms in the grafted organosilane (8); *MW* is the molecular weight of the grafted organosilane (184 g/mol); and S_{spec} is the specific surface area of the bare silica nanoparticles (48.5 m^2/g).

Control experiment to rule out nonspecific adsorption of PPE on the SiO_2 nanoparticles.

Some ungrafted PPE was produced during the surface-initiated polymerization reaction. The ungrafted polymers were separated from the **SiO_2-PPE** composite particles by centrifugation. We presume that the ungrafted polymers arose from either residual unbound Pd species that were not removed during purification following the Pd-immobilization step or from surface-bound Pd catalysts that deviated from the expected intramolecular oxidative addition step and diffused into the solution over the course of the CTP reaction. Regardless, surface initiation was essential for achieving a high grafting content of PPE on the particle surface and the presence of surface-bound polymers strongly indicated that the catalyst proceeded mainly via a catalyst transfer (intrachain) type fashion. For example, a control experiment was conducted wherein **2** was polymerized in the presence of virgin **SiO_2** particles using PhPd(*t*-Bu_3P)Br as the initiator/catalyst. Thermal analysis of the isolated particles exhibited significantly lower weight loss when compared to **SiO_2-PPE**, thus ruling out nonspecific adsorption as a possible explanation for the high content of surface-bound polymers observed by TGA for **SiO_2-PPE** (see Figure A2).

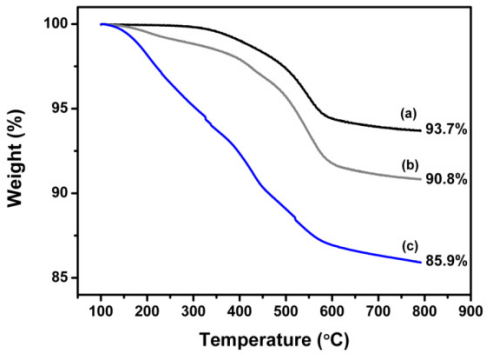

Figure A2: TGA curves of (a) bare SiO_2 particles; (b) bare SiO_2 particles isolated after stirring in the presence of a homogeneous polymerization wherein **2** was polymerized using PhPd(*t*-Bu_3P)Br as the initiator/catalyst. (c) **SiO_2-PPE**.

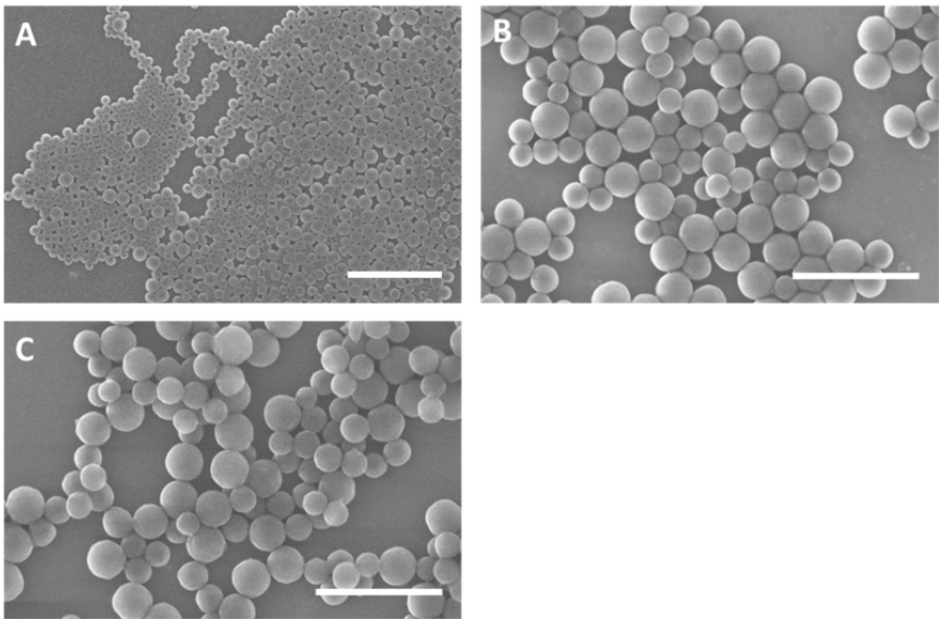

Figure A3. SEM images of (A) bare SiO_2 particles (scale bar = 2 um); (B) **SiO_2-PhBr** (scale bar = 1 um); (C) **SiO_2-PPE** (scale bar = 1 um).

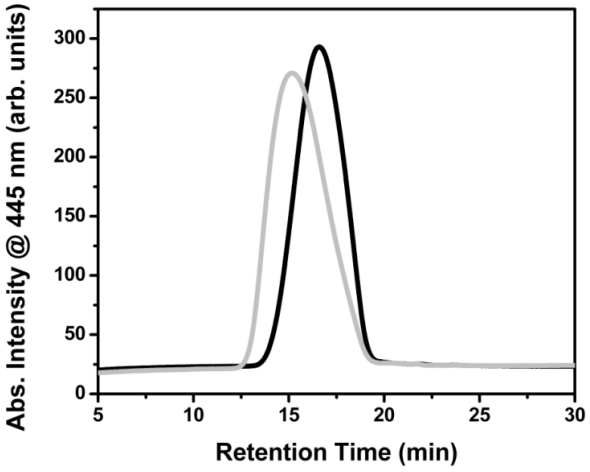

Figure A4: GPC traces of polymers obtained from a surface-initiated polymerization chain-extension experiment. Black line: polymer recovered from an aliquot taken from the polymerization prior to the second monomer addition (M_n = 11.3 kDa, $Đ$ = 2.5). Gray line: chain-extended polymer recovered after the second monomer addition (M_n = 21.9 kDa, $Đ$ = 3.8).

A-4: SUPPORTING INFORMATION FOR CHAPTER 4

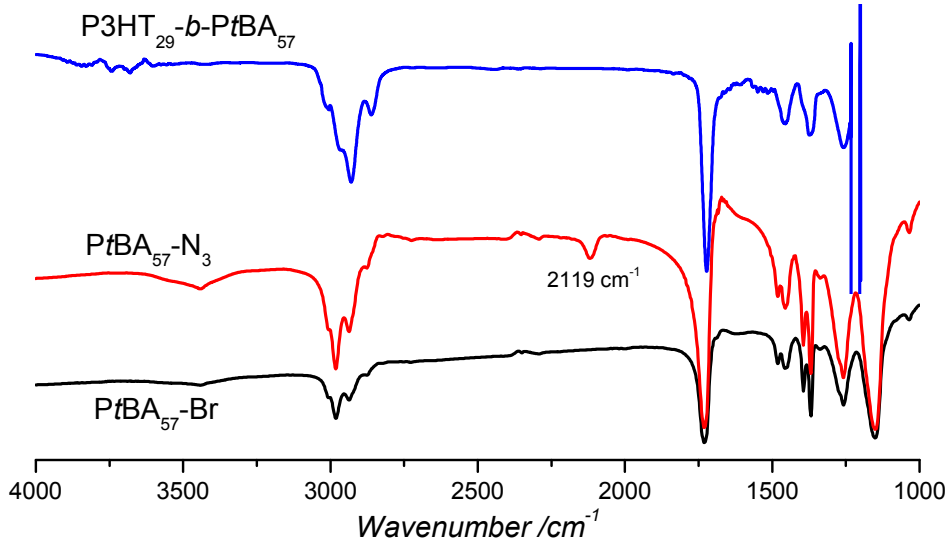

Figure A5: Representative IR spectra (KBr) of bromide-terminated P*t*BA (black), azide-terminated P*t*BA (red) and P3HT-*block*-P*t*BA (blue). The signal at 2119cm^{-1} was assigned to the azide stretching frequency.

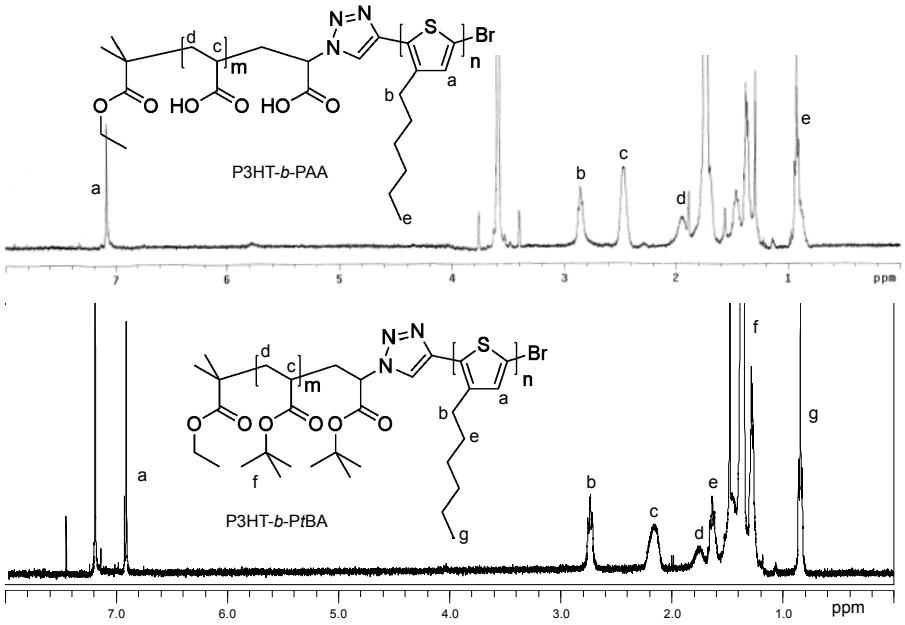

Figure A6: Representative ^{1}H NMR spectra of (bottom) P3HT$_{96}$-*b*-P*t*BA$_{170}$ ($CDCl_3$) and (top) P3HT$_{96}$-*b*-PAA$_{170}$ (THF-d_8).

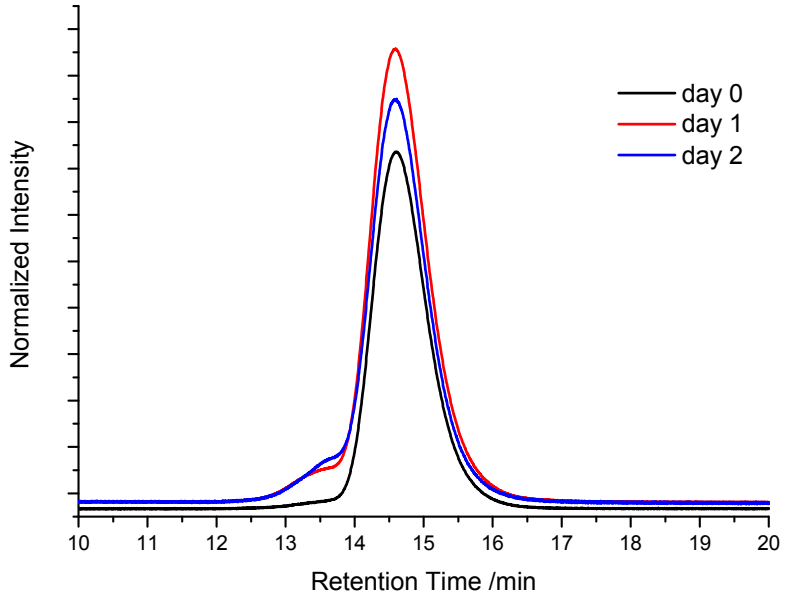

Figure A7: Gel permeation chromatograms (UV-vis detection at 450 nm) of $P3HT_{50}$-C≡CH (— immediately after reaction mixture was isolated using the improved procedure reported in the main text; — after being stored at ambient conditions for 24 in the solid state; — after being stored at ambient conditions for 48 h in the solid state).

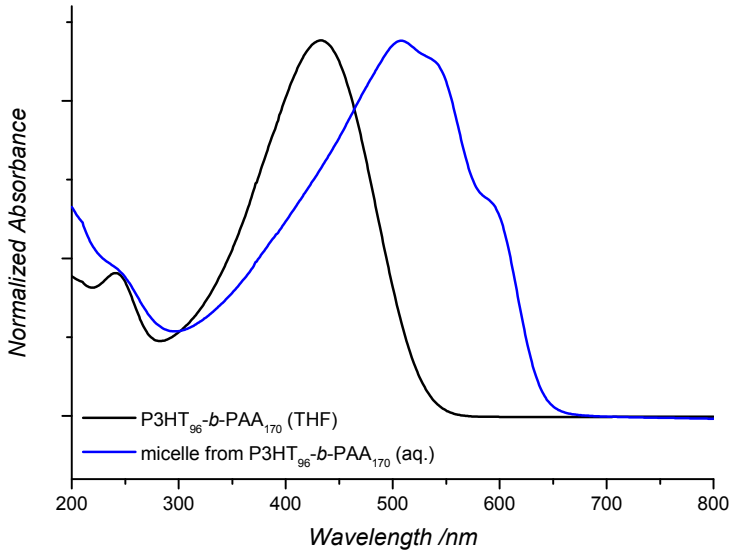

Figure A8: UV-vis spectra of the THF solution of P3HT-b-PAA (black) and the aqueous micelle solution assembled from P3HT-b-PAA (blue).

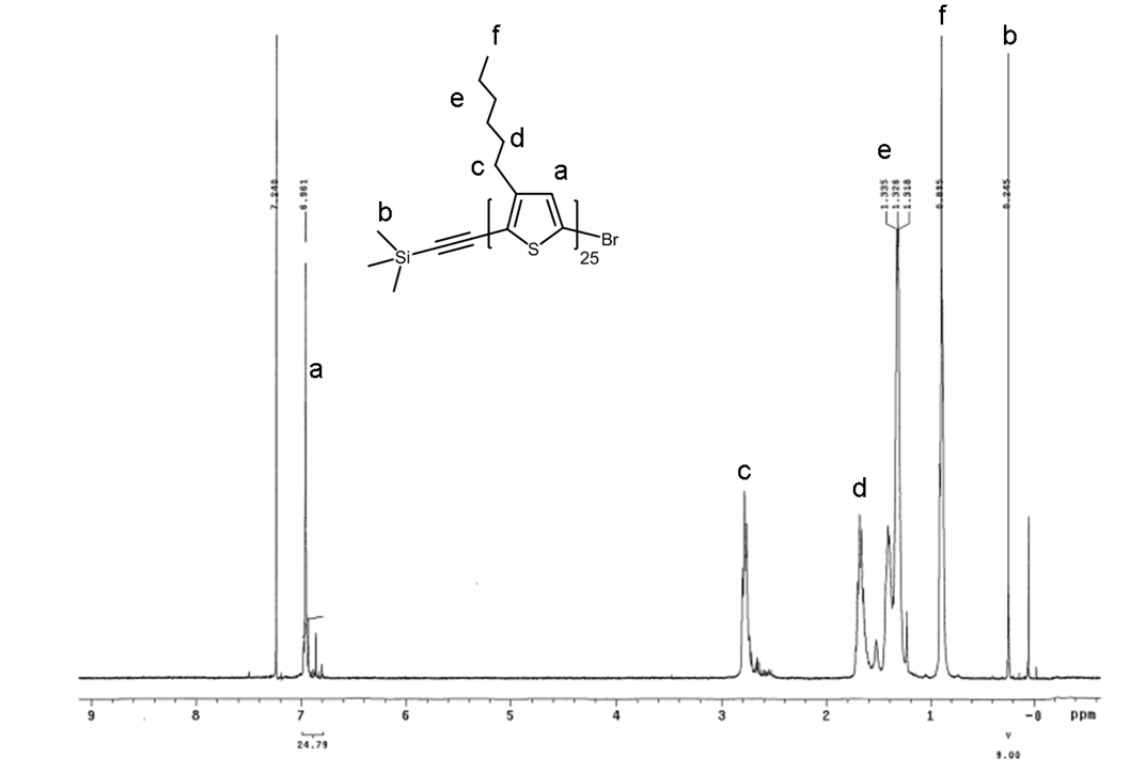

Figure A9: ^{1}H NMR spectrum of P3HT-C≡C-TMS ($CDCl_3$).

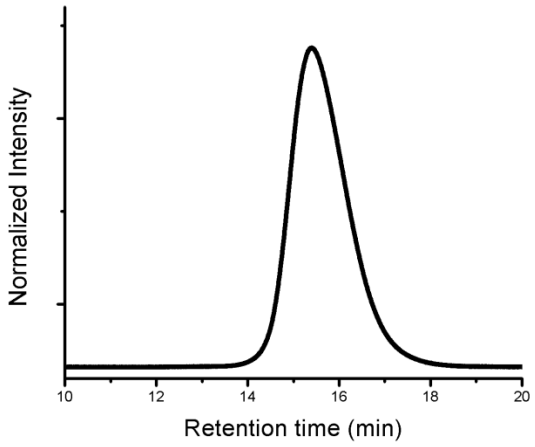

Figure A10: Gel permeation chromatogram (UV-vis detection at 450 nm) of TMS protected ethynyl-P3HT (P3HT25-C≡C-TMS), taken after Soxhlet treatments and storage in the solid state under ambient conditions for four days.

A-5: SUPPORTING INFORMATION FOR CHAPTER 5

Triblock copolymer characterization

Representative gel permeation chromatograms (GPC) of the crude product (Figure A11) shows a bimodal distribution with a high and low number average molecular weight (M_n) attributed to the triblock copolymer and the P3HT homopolymer, respectively. After purification by preparative GPC, two monomodal peaks were obtained and assigned to the triblock copolymer and P3HT homopolymer, respectively (Figure A11b).

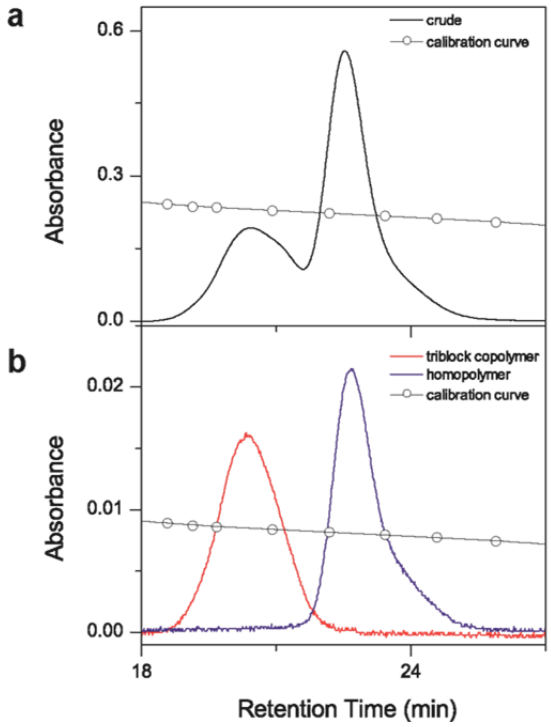

Figure A11: Purification of the triblock copolymer by GPC. Representative GPC traces of the crude product (a) and the purified triblock copolymer (b, red) and P3HT homopolymer (b, blue) obtained after GPC fractionation in tetrahydrofuran solvent and by using UV-vis detection at 450 nm. The calibration curve from polystyrene standards is represented in the line with circles.

Temporal stability

The triblock copolymer was dissolved in 100% toluene and 50/50% toluene/methanol. The absorption spectra of both solutions were recorded over nine hours. The evolution over nine hours of the absorbance at 455 nm (absorbance peak of the triblock monomer) and 560 nm (absorbance peak of the triblock dimer) are plotted in Figure A12. No significant changes were noticed. After *ca.* ten months, both solutions remained unchanged.

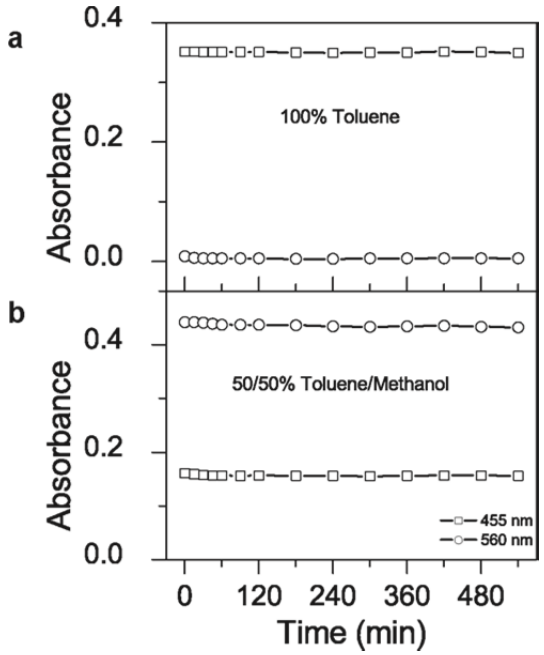

Figure A12: Temporal stability. Time evolution of the triblock copolymer in 100% toluene (a) and 50/50% toluene/methanol solvents (b) at 455 nm (line with squares) and 560 nm (line with circles).

Weakly coupled H-aggregates model

Spano *et al.* have developed a weakly coupled H-aggregates model to reproduce the experimental data obtained for P3HT thin film[1-3]. This H-aggegrates model assumes the spectra have a Franck-Condon vibronic progression. Following previous H-aggregate models for P3HT, we utilize a Huang-Rhys factor of 1 and assume that the 0.18 eV C=C stretching vibration predominantly couples the electronic transition[1]. The weak coupling assumes that the interchain interactions give rise to an excitonic band with a bandwidth that is on par or smaller than the energy of this dominant vibronic mode coupled to the π–π* electronic transition. As the triblock dimer looks to be a good model for the P3HT thin film, we applied the weakly coupled H-aggregates model to it to extract the exciton bandwidth. The triblock dimer molar extinction coefficient spectrum was fit to the sum of three Gaussian functions sharing the same spectral width with a constant energy spacing, chosen to be 0.18 eV. The good quality of this fit (Figure A13) is consistent with previous theoretical results for P3HT films[1]. The peak ratio of the 0-0 transition and the 0-1 transition of the absorption spectrum can be used to estimate the strength of the excitonic coupling. From this fit, we estimate an exciton bandwidth of the dimer triblock of 114 meV. This value is in good agreement with the values reported for P3HT films under different processing methods[3,4].

Fits were done using Origin with the sum of three Gaussian functions sharing the same spectral width with a constant energy spacing, chosen to be 0.18 eV.

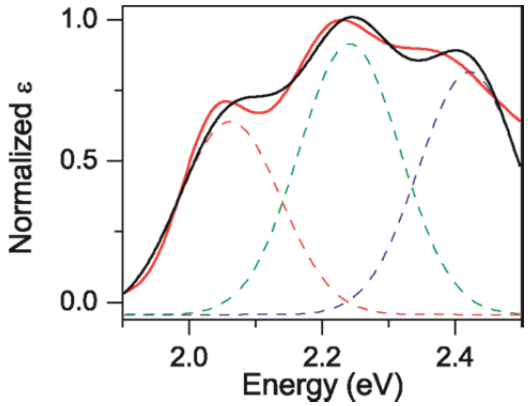

Figure A13: Weakly coupled H-aggregates model. Absorption spectrum of the triblock dimer (black) and its fit to the sum of three Gaussian functions (red) and the three Gaussians functions (green, blue and red dashed lines).

Fluorescence correlation spectroscopy

Additional fluorescence correlation curves are presented in Figure A14 for the same initial concentration of the triblock copolymer in a good solvent, *i.e.* 100% toluene, and in a poor solvent, *i.e.* 50/50% toluene/methanol. As discussed in the main text, the number of chains remains constant in both solvent systems, and the signal gets noisier in 50/50% toluene/methanol.

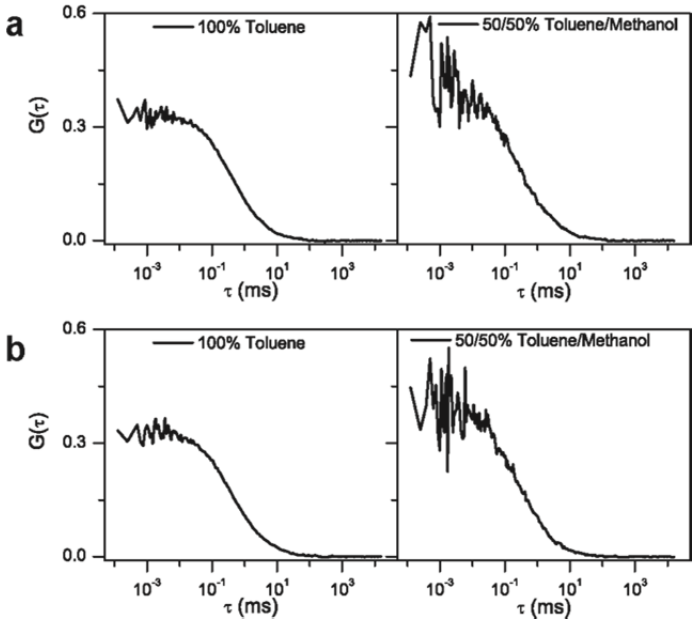

Figure A14: Fluorescence correlation spectroscopy (FCS) of the P3HT-b-PtBA-b-P3HT triblock copolymer in 100% toluene (left) and 50/50% toluene/methanol solvents (right) under excitation at 488 nm for two different measurements (a, b).

Fully reversible system

The addition of methanol to the triblock copolymer in 100% toluene was monitored at two wavelengths, 455 and 560 nm, which are the absorbance peaks of the triblock monomer and the triblock dimer, respectively. In 40/60% toluene/methanol the triblock copolymer is mainly a dimer. The addition of toluene to this solution was carried out to determine if the triblock monomer can be regenerated from the triblock dimer. Some hysteresis was observed, as shown in Figure A15, but the interchain interactions in the triblock dimer were broken to give rise to the triblock monomer. The triblock copolymer is a fully reversible system from the triblock dimer to the triblock monomer.

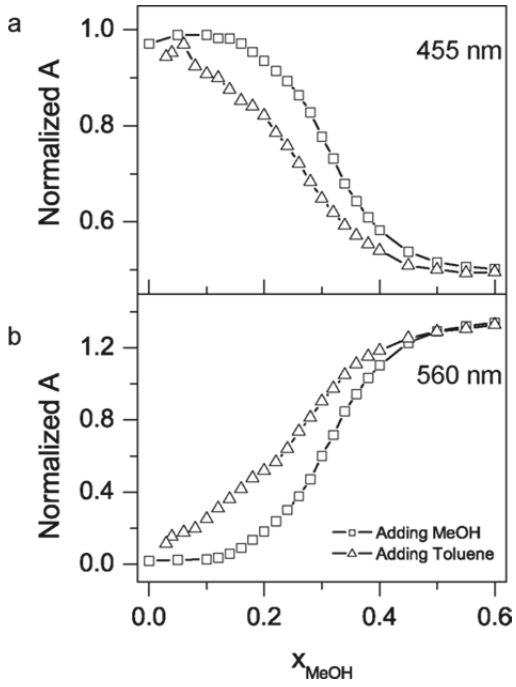

Figure A15: Reversible system. Normalized absorption evolution as a function of the volume fraction of methanol added to the triblock copolymer in 100% toluene (line with squares), and then as a function of the volume fraction of methanol as toluene is added to the triblock copolymer in 40/60% toluene/methanol (line with triangles) at 455 nm (a) and 560 nm (b).

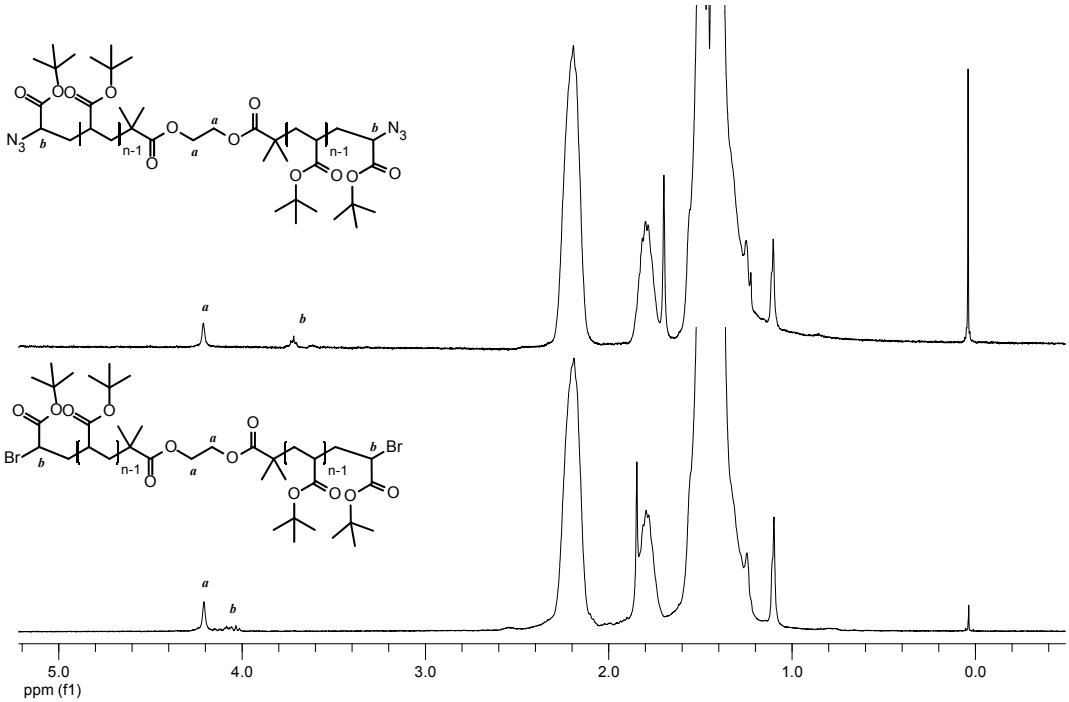

Figure A16: ^{1}H NMR spectra of Br-P*t*BA-Br (bottom) and N_3-P*t*BA-N_3 (top) ($CDCl_3$).

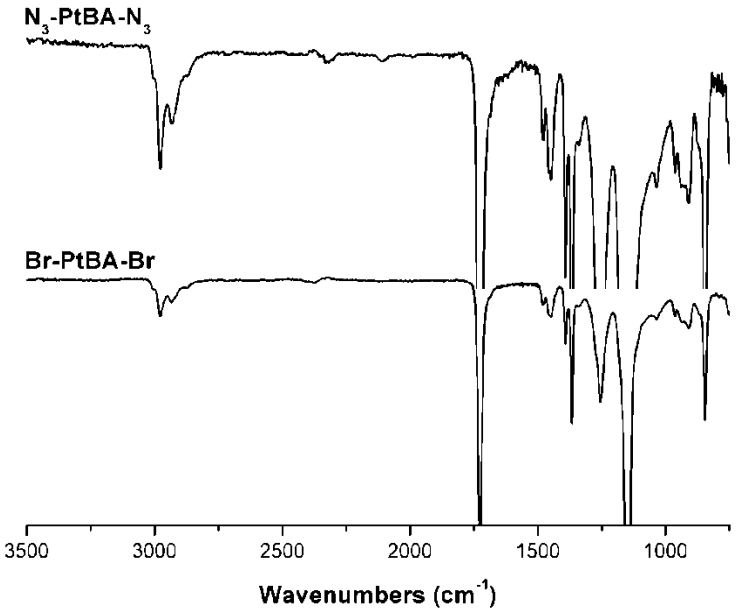

Figure A17: FT-IR spectra of Br-P*t*BA-Br (bottom) and N_3-P*t*BA-N_3 (top).

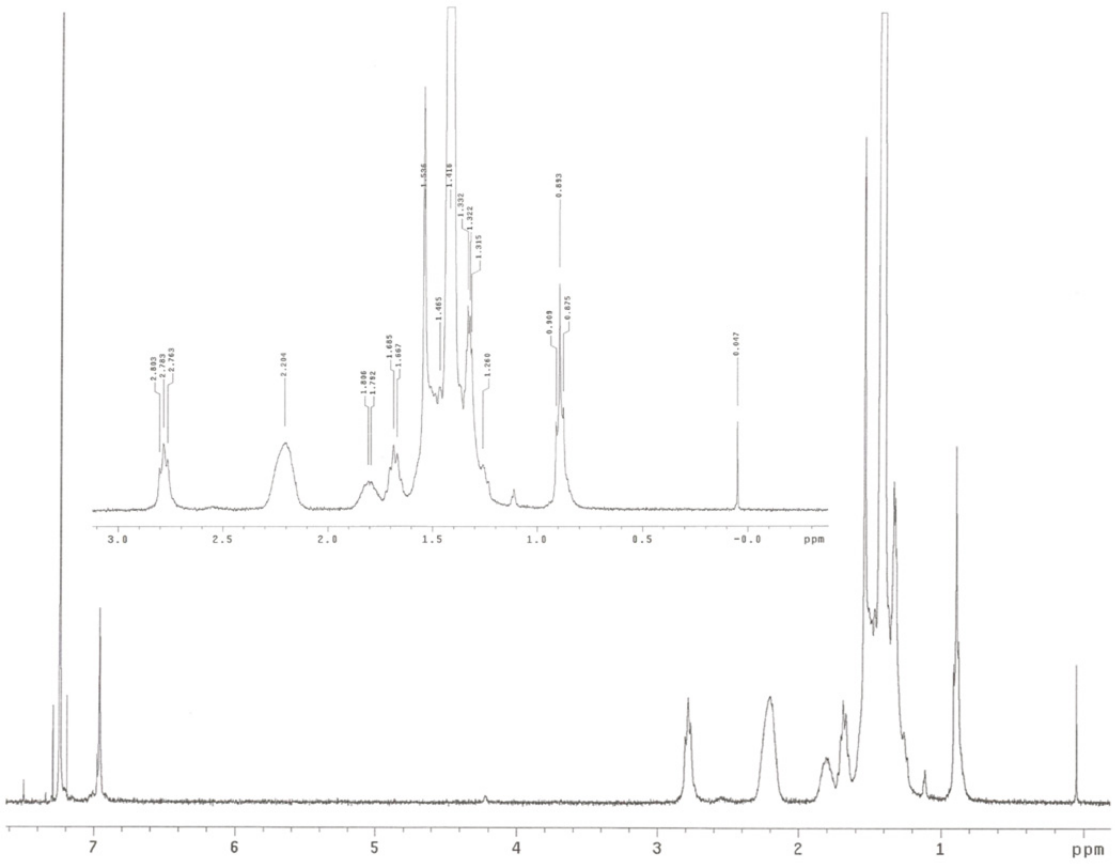

Figure A18: ^{1}H NMR spectrum of the triblock copolymer with 10 kDa P3HT chains (P3HT$_{60}$-*b*-P*t*BA$_{200}$-*b*-P3HT$_{60}$) ($CDCl_3$). The inset is an expanded view of the alkyl region.

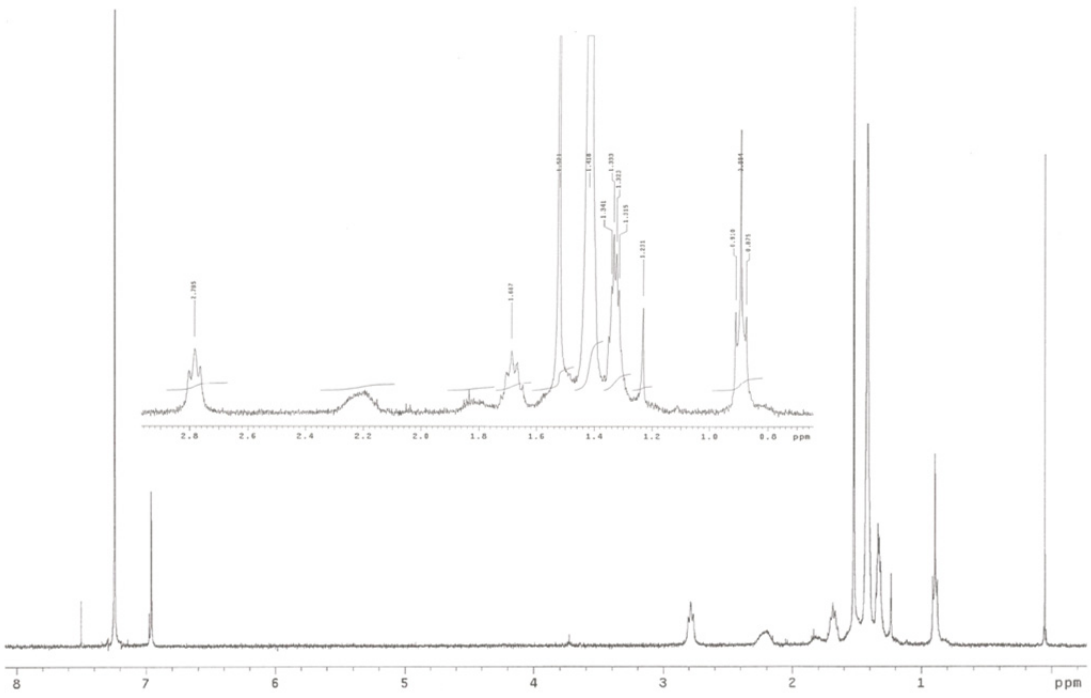

Figure A19: ^{1}H NMR spectrum of the triblock copolymer with 21 kDa P3HT chains ($P3HT_{120}$-*b*-P*t*BA_{200}-*b*-$P3HT_{120}$) ($CDCl_3$). The inset is an expanded view of the alkyl region.

A-6. SUPPORTING INFORMATION FOR CHAPTER 6

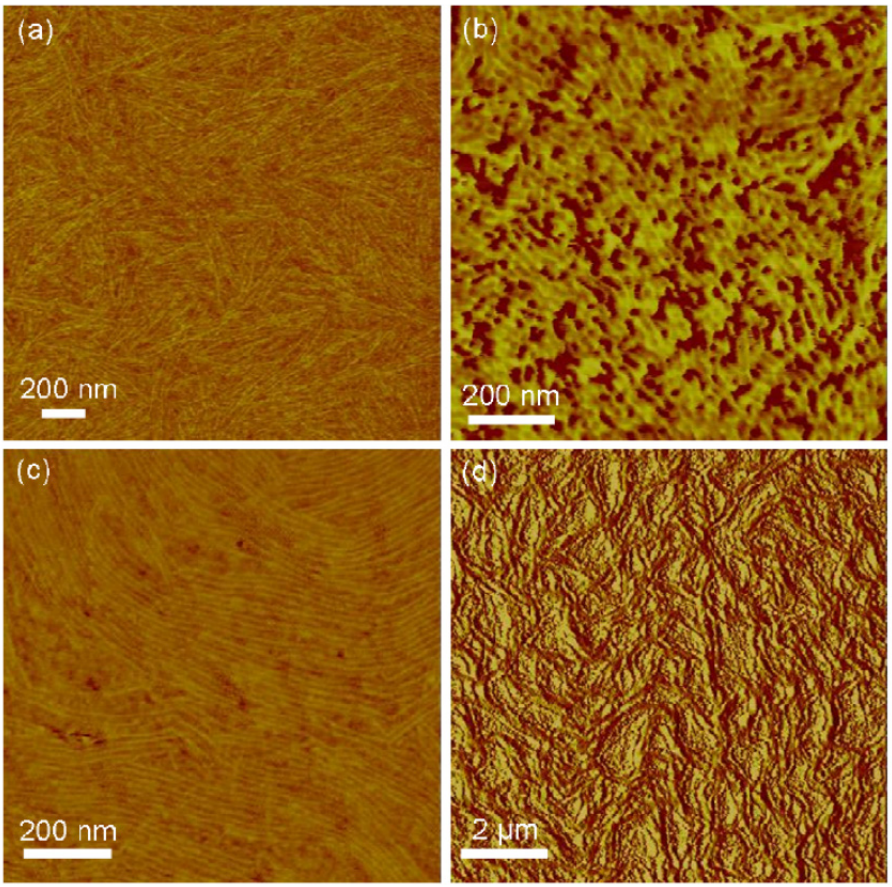

Figure A20: Tapping mode AFM phase images of thin films of (a) poly(**1**-*b*-**3**) (entry 1, Table 6.1) spin coated from $CHCl_3$ (film thickness = 200 nm). (b) poly(**1**-*b*-**3**) (entry 3, Table 6.1) spin coated from $CHCl_3$ (film thickness = 15 nm). (c) poly(**1**-*b*-**3**) (entry 4, Table 6.1) spin coated from $CHCl_3$ (film thickness = 60 nm). (d) poly(**1**-*b*-**3**) (entry 5, Table 6.1) spin coated from $CHCl_3$ (film thickness = 60 nm).

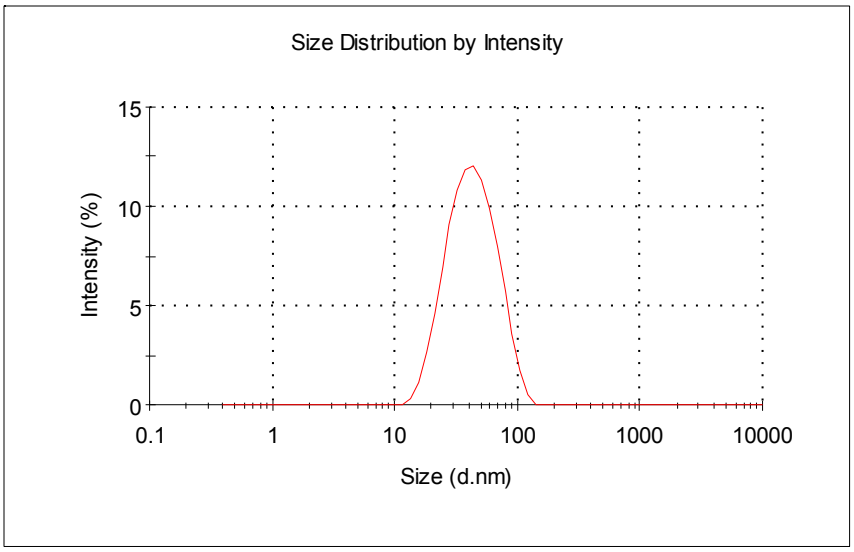

Figure A21: DLS data of nanoparticles formed from block copolymer poly(**1**-*b*-**3**) in THF and methanol (1/1, v/v) at 25 °C. The hydrodynamic diameter was determined to be 41 +/- 4 nm.

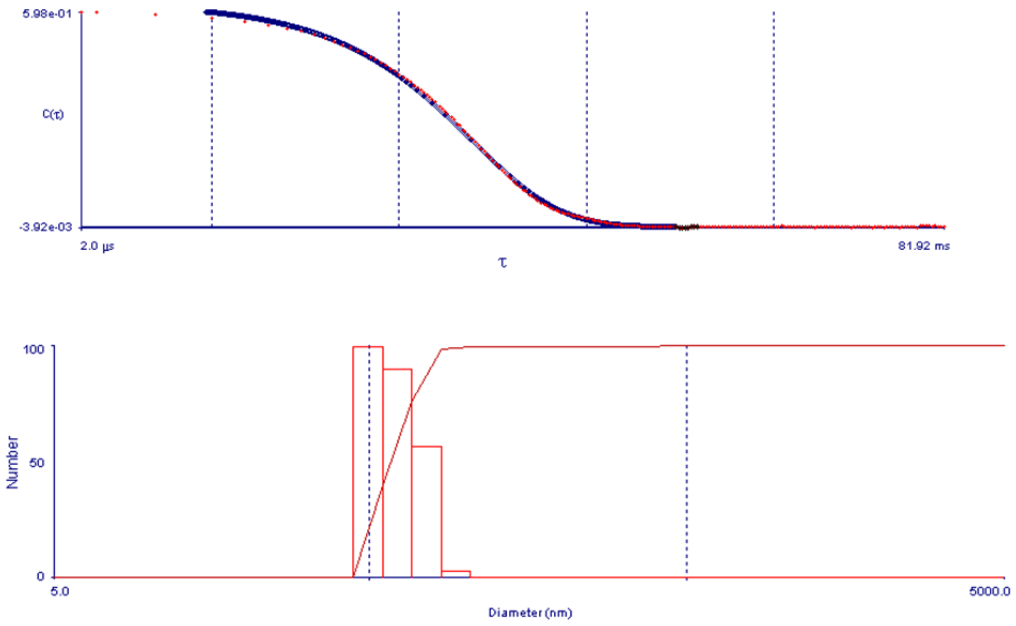

Figure A22: DLS data of nanoparticles formed from block copolymer poly(**1**-*b*-**5**) in water. The hydrodynamic diameter was determined to be 89 +/- 6 nm.

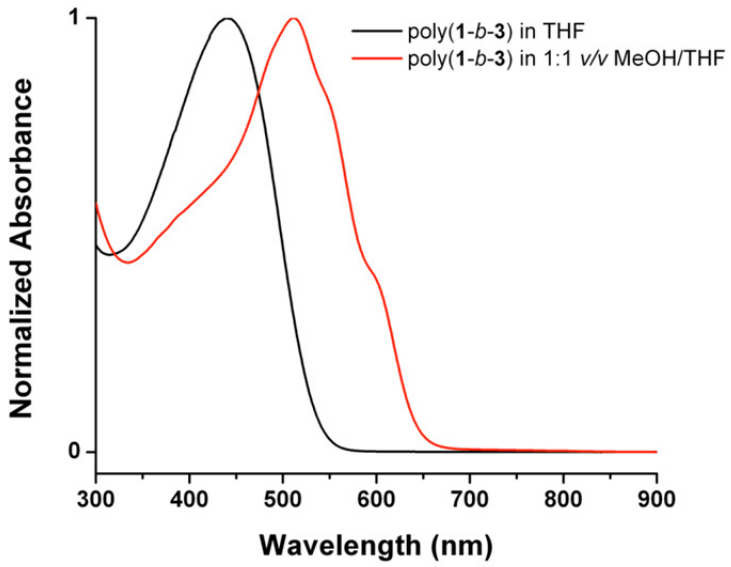

Figure A23: UV-vis spectra of poly(**1**-*b*-**3)** in THF before (black) and after (red) the addition of an equal volume of methanol at 25 °C.

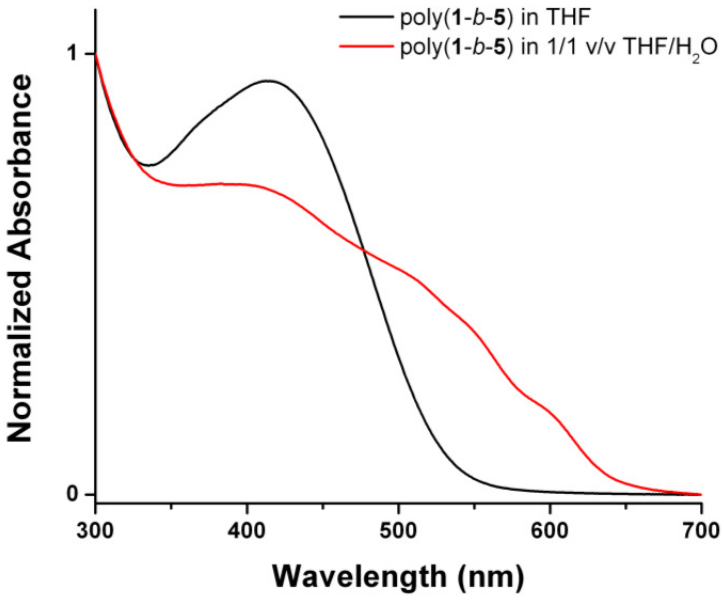

Figure A24: UV-vis spectra of poly(**1**-*b*-**5)** in THF before (black) and after (red) the addition of an equal volume of water at 25 °C.

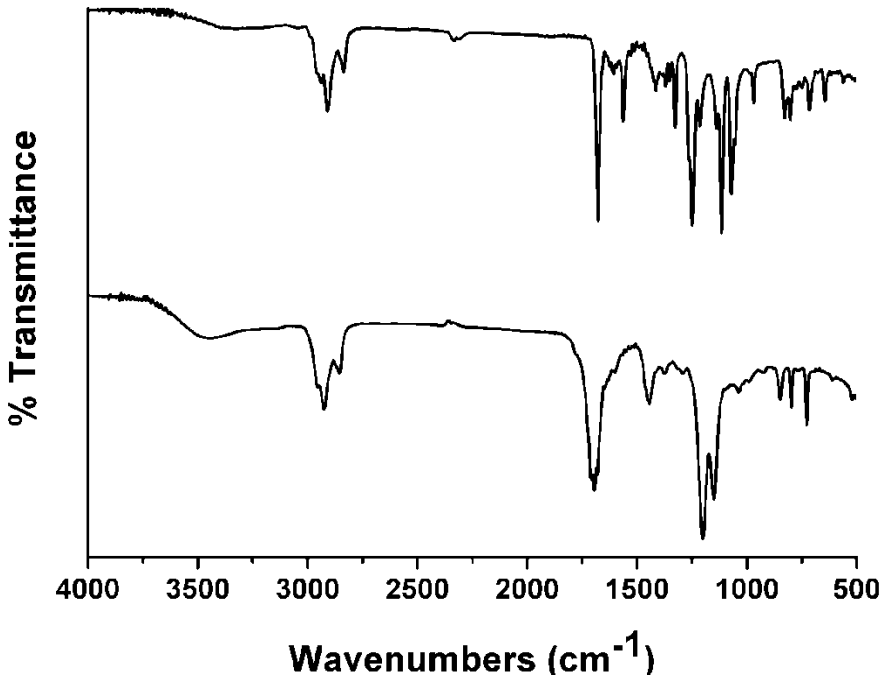

Figure A25: IR spectra of poly(**1**-*b*-**4**) (top spectrum) and the resulting poly(**1**-*b*-**5**) (bottom spectrum) after deprotection.

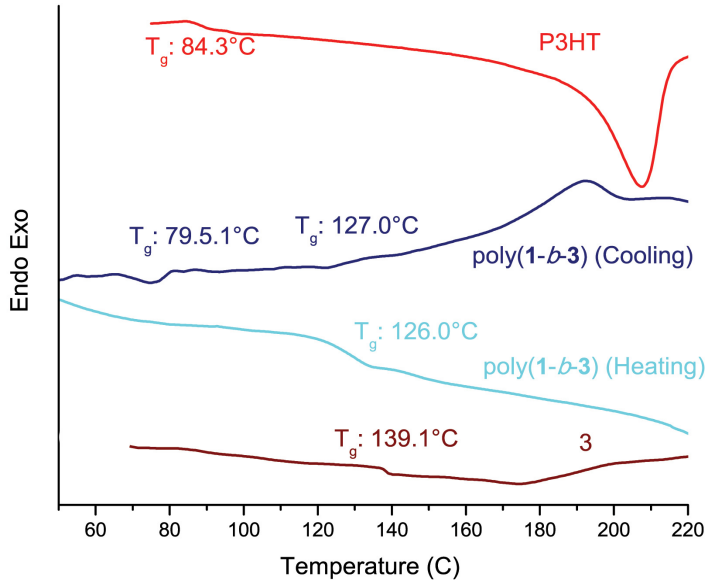

Figure A26: DSC thermograms of (top) P3HT (M_n = 8.2 kDa), (middle) poly(**1**-*b*-**3**) (M_n = 15.9 kDa) and (bottom) a homopolymer of **3** (M_n = 32 kDa) (rate = 20 °C min^{-1}).

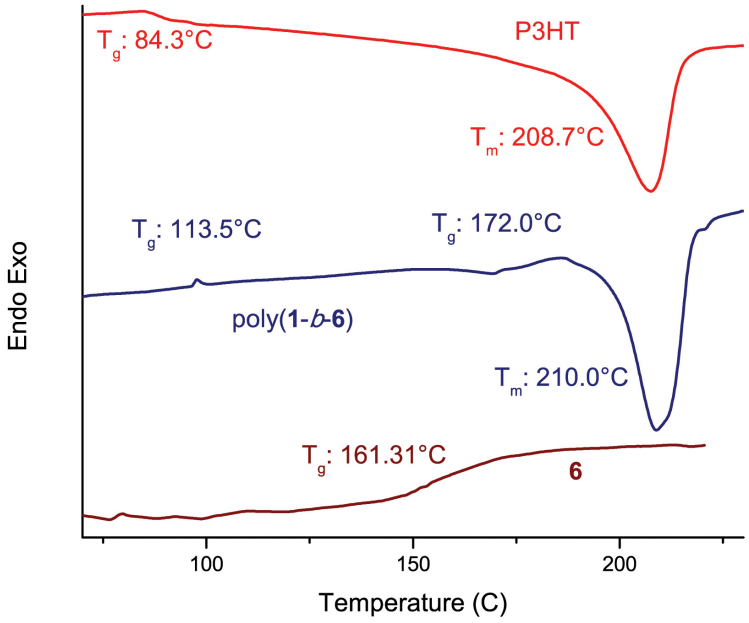

Figure A27: DSC thermograms of (top) P3HT (M_n = 8.2 kDa), (middle) poly(**1**-*b*-**6**) (M_n = 11.3 kDa) and (bottom) a homopolymer of **6** (M_n = 2.9 kDa) (rate = 20 °C min^{-1}).

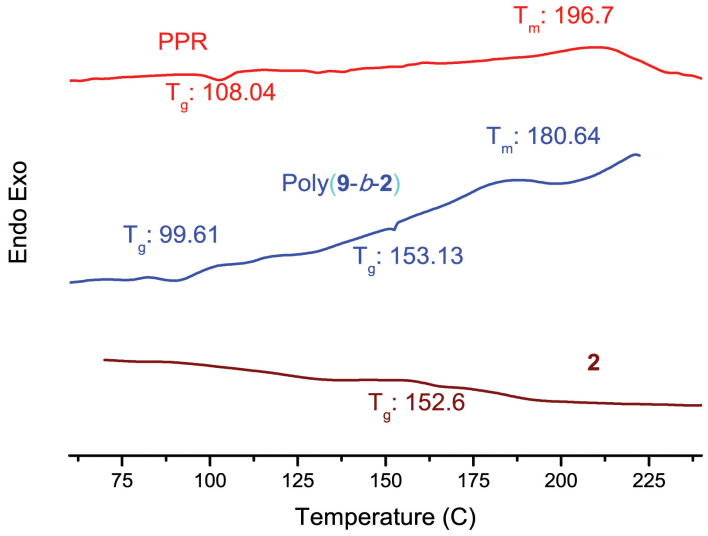

Figure A28: DSC thermograms of (top) poly-9 (M_n = 7.7 kDa), (middle) poly(**9**-*b*-**2**) (M_n = 11.2 kDa) and (bottom) a homopolymer of **2** (M_n = 17.0 kDa) (rate = 20 °C min^{-1}).

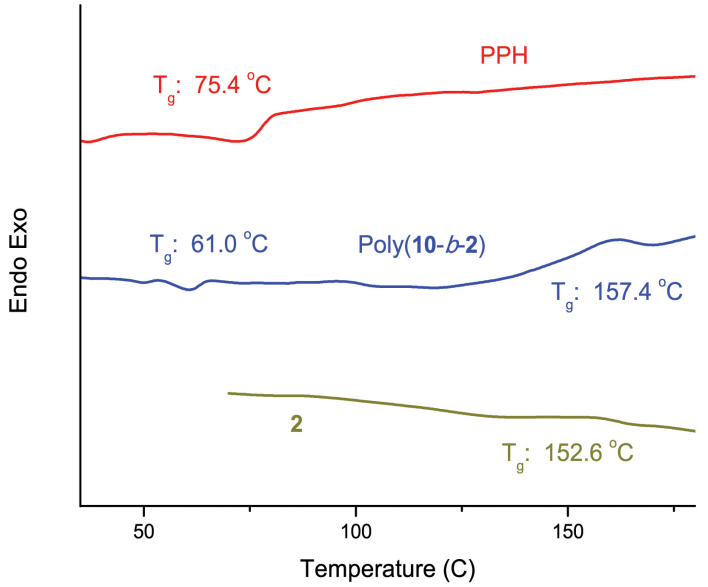

Figure A29: DSC thermograms of (top) poly-**10** (M_n = 6.2 kDa), (middle) poly(**10**-*b*-**2**) (M_n = 10.0 kDa) and (bottom) a homopolymer of **2** (M_n = 17.0 kDa) (rate = 20 °C min^{-1}).

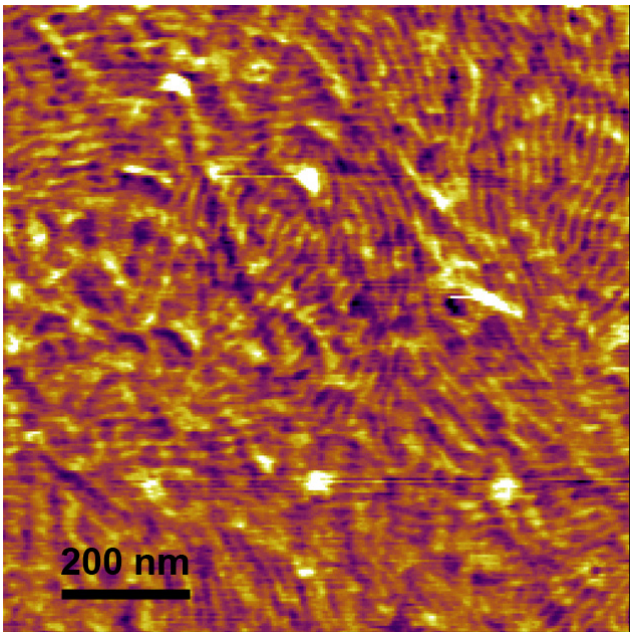

Figure A30: AFM phase image of poly(**1**-*b*-**3**) (M_n = 12.3 kDa) spin-coated from $CHCl_3$ (1.4 mg mL^{-1}) onto a Si wafer.

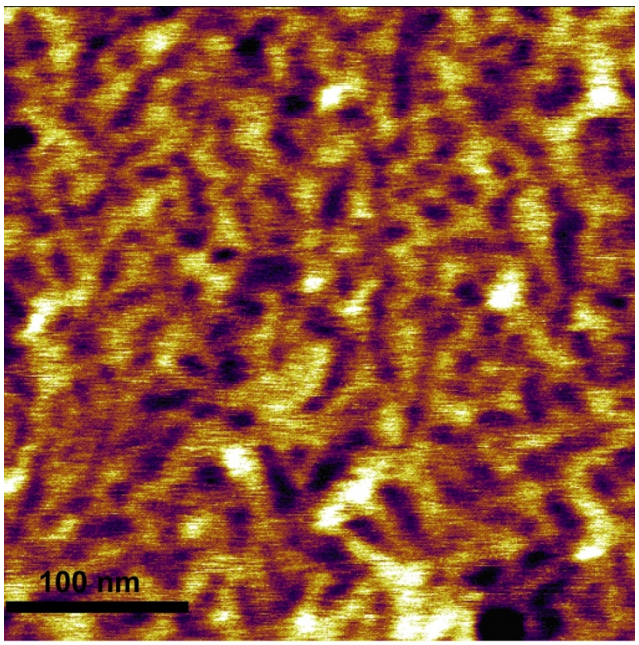

Figure A31: AFM phase image of poly(**1**-*b*-**6**) (M_n = 11.3 kDa) spin-coated from $CHCl_3$ (2.5 mg mL^{-1}) onto a Si wafer.

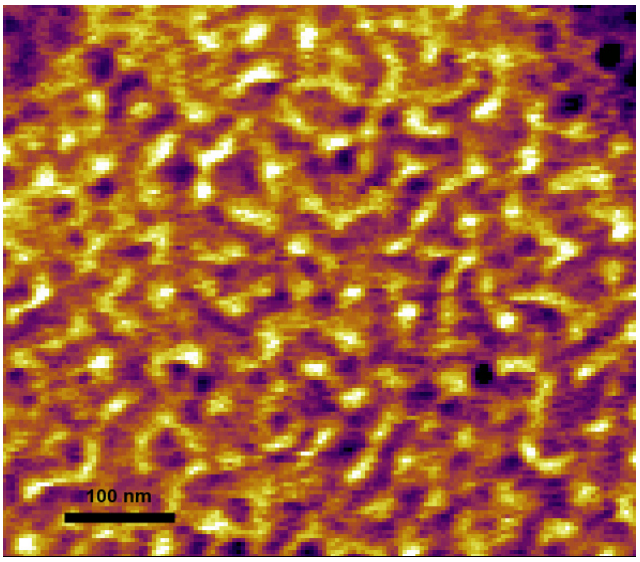

Figure A32: AFM phase image of poly(**10**-*b*-**2**) (M_n = 10 kDa) spin-coated from $CHCl_3$ (10 mg mL^{-1}) onto a Si wafer.

A-7. SUPPORTING INFORMATION FOR CHAPTER 7

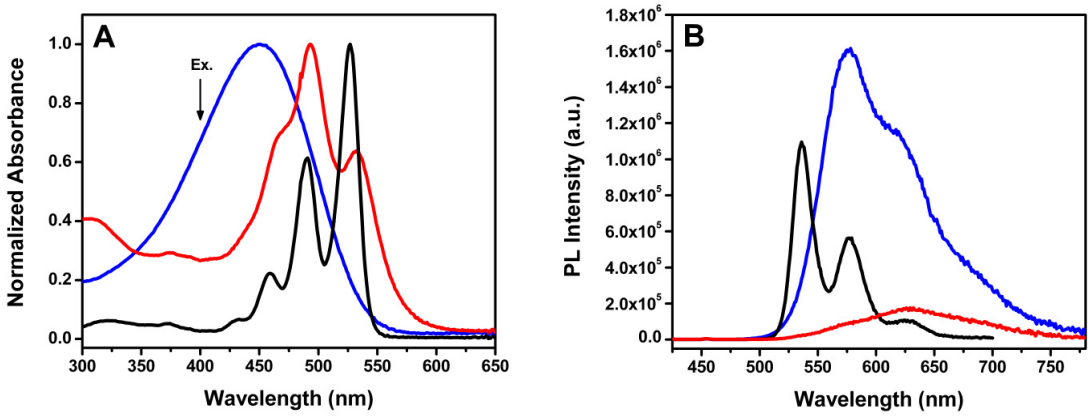

Figure A33: Normalized absorption spectra (A) and (non-normalized) emission spectra (B) of toluene solutions of PDI (black curves), P3HT-b-poly(**2**) (red curves), and P3HT (blue curves). For the emission spectra, λex = 400 nm (marked by the arrow). The concentrations of the P3HT and P3HT-b-poly(**2**) solutions were adjusted so that the P3HT contents were approx. equal.

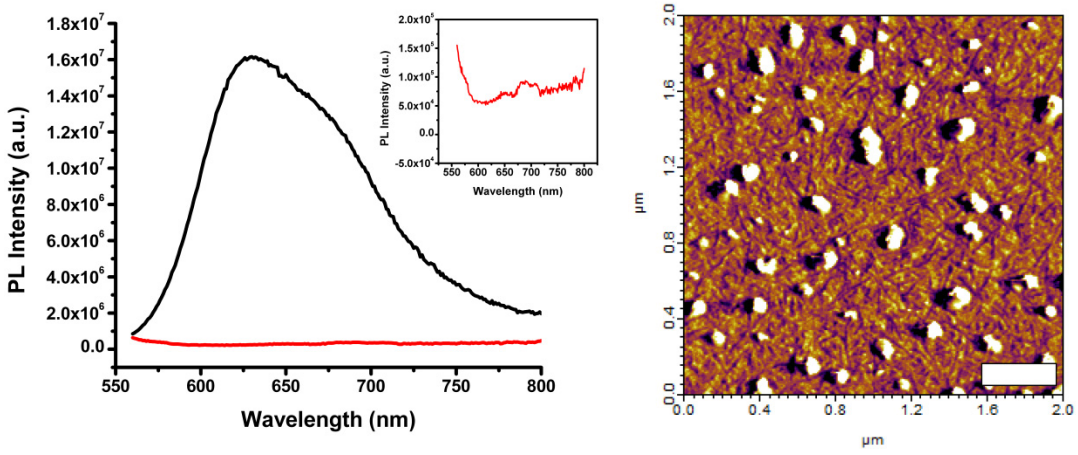

Figure A34: (left) Solid state photoluminescence spectra of PDI (black curve) and P3HT-*b*-poly(**2**) (red curve). Inset: expanded view of PL spectrum of P3HT-*b*-poly(**2**). (right) AFM phase image of P3HT-*b*-poly(**2**) drop cast from chloroform onto a Si wafer, taken "as-cast", prior to solvent vapor annealing. Scale bar = 400 nm; scan size = 2 μm.

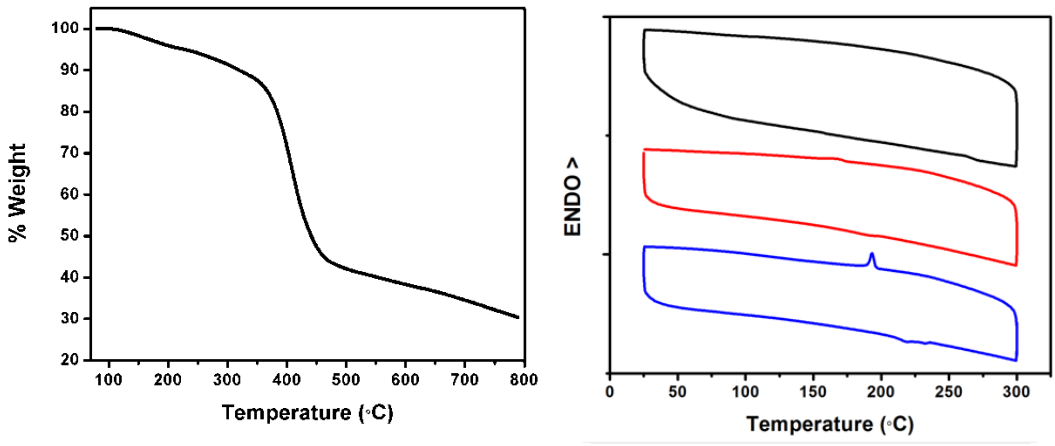

Figure A35: (left) TGA curve of P3HT-*b*-poly(**2**). The experiment was performed under an atmosphere of nitrogen at a heating rate of 20 °C min^{-1}. (right) DSC curves of poly(**2**) (black), P3HT-*b*-poly(**2**) (red), and P3HT (blue). Experiments were performed at a heating/cooling rate of 5 °C min^{-1}.

*Absorption and emission spectra of a physical blend of P3HT and poly(**2**) homopolymers*

To test whether the fluorescence quenching observed for P3HT-*b*-poly(**2**) was due to microphase separation on length scales on the order of the exciton diffusion length, fluorescence measurements were performed on a solution and thin film of a physical blend of P3HT and poly(**2**) homopolymers. Because the donor and acceptor components are not covalently bound in a physical blend, we expected that macrophase separation of the homopolymers would occur, forming donor-acceptor interfaces that are larger than the exiton diffusion length, and hence result in a higher photoluminescence quantum efficiency.

Considering that the absorption spectrum of P3HT-*b*-poly(**2**) was a linear combination of its individual homopolymer components, we prepared blends of P3HT and poly(**2**) homopolymers in varying weight fractions such that the resulting absorption spectrum would resemble that of the block copolymer as closely as possible. As shown in

Figures A36 and A37 (left panels), it was determined that a 1:7 w/w blend of P3HT:poly(**2**) gave an absorption profile that most closely matched that of P3HT-*b*-poly(**2**) in both the solution and solid states, respectively.

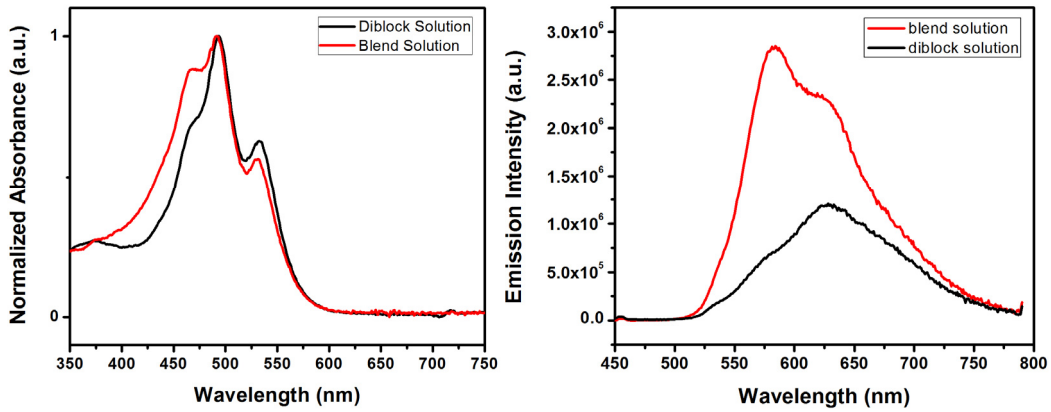

Figure A36: Absorption (left) and emission (right) spectra of a physical blend of P3HT and poly(**2**) homopolymers, measured in chlorobenzene solutions. Red lines = spectrum of the blend solution; black lines = spectrum of the P3HT-*b*-poly(**2**) solution. λ_{ex} = 400 nm.

The abovementioned P3HT:poly(**2**) blend was then examined by fluorescence. As shown in Figure A36 (right panel), a roughly threefold increase in fluorescence intensity was observed for a chlorobenzene solution of the P3HT:poly(**2**) blend in comparison to a corresponding solution of the block copolymer. This result suggests that, even in solution, the close proximity of the donor to the acceptor in the case of the block copolymer facilitates efficient photoinduced electron transfer. In contrast, the difference in emission intensity exhibited by thin films of the P3HT:poly(**2**) blend and the block copolymer was negligible (Figure A37, right panel), with only a slight attenuation in intensity observed for P3HT-*b*-poly(**2**) relative to the blend film. When different excitation wavelengths were explored, the difference in emission intensity between the two samples became more pronounced, especially with 450 nm excitation, and the expected attenuation of the

block copolymer emission was observed. It should be noted that the thin film samples used for this experiment were not annealed prior to measurement; it is therefore reasonable to expect that more distinct differences in the emission spectra of the blend and block copolymer would be observed after the polymer chains are given a chance to rearrange themselves upon annealing. Regardless, the presented fluorescence data is consistent with the ability of P3HT-*b*-poly(**2**) to form nanoscale donor-acceptor interfaces, a feature that should prove advantageous for efficiently generating a photovoltaic response upon irradiation.

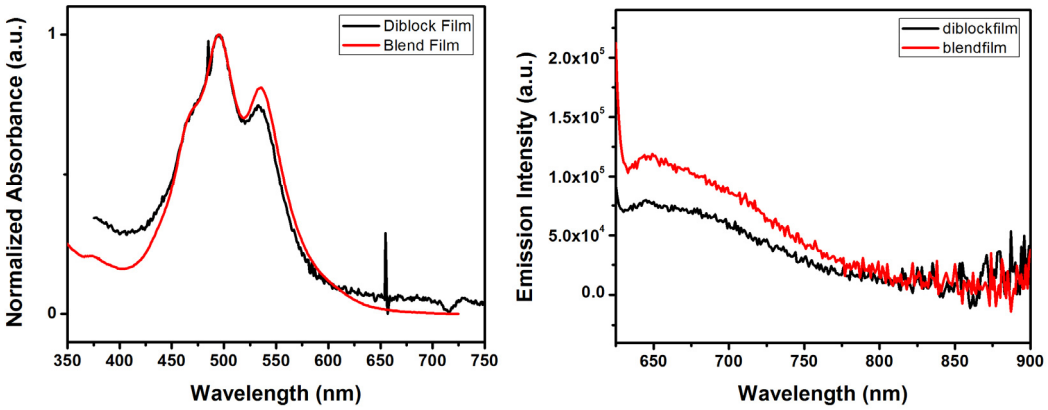

Figure A37: Solid-state absorption (left) and emission (right) spectra of a thin film of a physical blend of P3HT and poly(**2**) homopolymers, spin cast from chlorobenzene. Red lines = spectrum of the blend film; black lines = spectrum of the P3HT-*b*-poly(**2**) film. λ_{ex} = 600 nm.

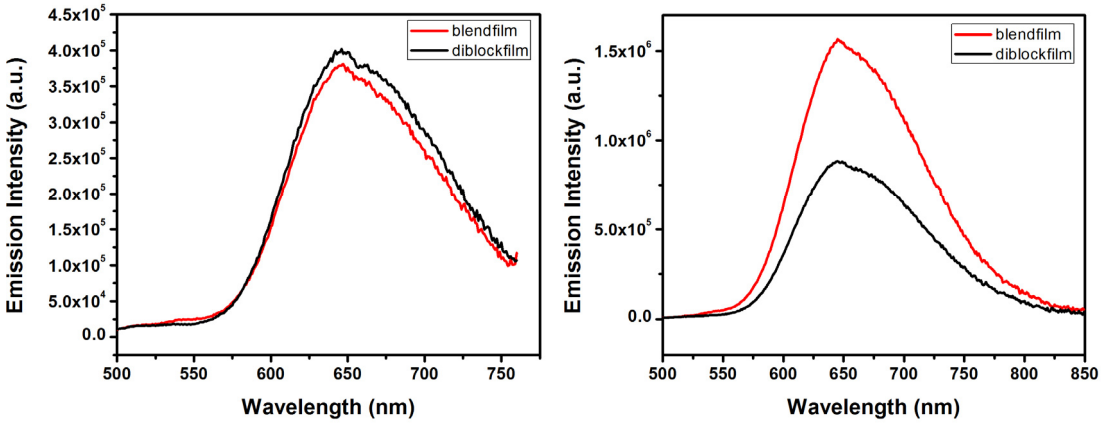

Figure A38: Solid-state emission spectra of a thin film of a physical blend of P3HT and poly(**2**) homopolymers, spin cast from chlorobenzene. (left) λ_{ex} = 400 nm; (right) λ_{ex} = 450 nm. Red lines = spectrum of the blend film; black lines = spectrum of the P3HT-*b*-poly(**2**) film.

References

Adachi, T.; Brazard, J.; Chokshi, P.; Bolinger, J. C.; Ganesan, V.; Barbara, P. F. *J. Phys. Chem. C* **2010**, *114*, 20896-20902.

Adachi, T.; Brazard, J.; Ono, R. J.; Hanson, B.; Traub, M. C.; Wu, Z.-Q.; Li, Z.; Bolinger, J. C.; Ganesan, V.; Bielawski, C. W.; Vanden Bout, D. A.; Barbara, P. F. *J. of Phys. Chem. Lett.* **2011**, *2*, 1400-1404.

Alemseghed, M. G.; Gowrisanker, S.; Servello, J.; Stefan, M. C. *Macromol. Chem. Phys*. **2009**, *210*, 2007.

Allara, D. L.; Arnold, J. J.; Bumm, L. A.; Burgin, T. P.; Cygan, M. T.; Dunbar, T. D.; Jones, L., II; Tour, J. M.; Weiss, P. S. *Science* **1996**, *271*, 1705-1707.

Banerji, N.; Cowan, S.; Vauthey, E.; Heeger, A. J. *J. Phys. Chem. C* **2011**, *115*, 9726-9739.

Bao, Z.; Chan, W.; Yu, L. *Chem. Mater.* **1993**, *5*, 2-3.

Bartholome, C.; Beyou, E.; Bourgeat-Lami, E.; Chaumont, P.; Zydowicz, N. *Macromolecules* **2003**, *36*, 7946-7952.

Beljonne, D.; Cornil, J.; Silbey, R.; Millie, P.; Bredas, J. L. *J. Chem. Phys.* **2000**, *112*, 4749-4758.

Benanti, T. L.; Kalaydjian, A.; Venkataraman, D. *Macromolecules* **2008**, *41*, 8312-8315.

Beryozkina, T.; Boyko, K.; Khanduyeva, N.; Senkovskyy, V.; Horecha, M.; Oertel, U.; Simon, F.; Stamm, M.; Kiriy, A. *Angew. Chem. Int. Ed.* **2009**, *48*, 2695-2698.

Beryozkina, T.; Senkovskyy, V.; Kaul, E.; Kiriy, A. *Macromolecules* **2008**, *41*, 7817-7823.

Botiz, I.; Darling, S. B. *Macromolecules* **2009**, *42*, 8211-8217.

Boudouris, B. W.; Frisbie, C. D.; Hillmyer, M. A. *Macromolecules* **2010**, *43*, 3566-3569.

Brandrup, J.; Immergut, E. H.; Grulke, E., Eds. *Polymer Handbook*, 4th ed.; Wiley: New York, **1999**.

Brockmann, T. W.; Tour, J. M. *J. Am. Chem. Soc.* **1995**, *117*, 4437.

Bronstein, H. A.; Luscombe, C. K. *J. Am. Chem. Soc.* **2009**, *131*, 12894-12895.

Brown, P. J.; Sirringhaus, H.; Harrison, M.; Shkunov, M.; Friend, R. H. *Phys. Rev. B* **2001**, *63*, 125204.

Brown, P. J.; Thomas, D. S.; Kohler, A.; Wilson, J. S.; Kim, J.-S.; Ramsdale, C. M.; Sirringhaus, H.; Friend, R. H. *Phys. Rev. B* **2003**, *67*, 064203.

Bunz, U. H. F. *Acc. Chem. Res.* **2001**, *34*, 998-1010.

Bunz, U. H. F. *Chem. Rev.* **2000**, *100*, 1605-1644.

Bunz, U. H. F.; Enkelmann, V.; Kloppenburg, L.; Jones, D.; Shimizu, K. D.; Claridge, J. B.; zur Loye, H.-C.; Lieser, G. *Chem. Mater.* **1999**, *11*, 1416-1424.

Bunz, U. H. F.; Imhof, J. M.; Bly, R. K.; Bangcuyo, C. G.; Rozanski, L.; Vanden Bout, D. A. *Macromolecules* **2005**, *38*, 5892-5896.

Burrows, H. D.; de Melo, J. S.; Serpa, C.; Arnaut, L. G.; Monkman, A. P.; Hamblett, I.; Navaratnam, S. *J. Chem. Phys.* **2001**, *115*, 9601-9606.

Chang, J.-F.; Clark, J.; Zhao, N.; Sirringhaus, H.; Breiby, D. W.; Andreasen, J. W.; Nielsen, M. M.; Giles, M.; Heeney, M.; McCulloch, I. *Phys. Rev. B* **2006**, *74*, 115318.

Chang, K.-J.; Kang, B.-N.; Lee, M.-H.; K.-S., J. *J. Am. Chem. Soc.* **2005**, *127*, 12214.

Chen, Z.-K.; Lee, N. H. S.; Huang, W.; Xu, Y.-S.; Cao, Y. *Macromolecules* **2003**, *36*, 1009-1020.

Cheng, Y.-J.; Yang, S.-H.; Hsu, C.-S. *Chem. Rev.* **2009**, *109*, 5868-5923.

Chesterfield, R. J.; McKeen, J. C.; Newman, C. R.; Ewbank, P. C.; da Silva Filho, D. t. A.; Brédas, J.-L.; Miller, L. L.; Mann, K. R.; Frisbie, C. D. *J. Phys. Chem. B* **2004**, *108*, 19281-19292.

Clark, J.; Chang, J. F.; Spano, F. C.; Friend, R. H.; Silva, C. *Appl. Phys. Lett.* **2009**, *94*, 3.

Clark, J.; Silva, C.; Friend, R. H.; Spano, F. C. *Phys. Rev. Lett.* **2007**, *98*, 4.

Coakley, K. M.; McGehee, M. D. *Chem. Mater.* **2004**, *16*, 4533-4542.

Cook, S.; Furube, A.; Katoh, R. *Energy Environ. Sci.* **2008**, *1*, 294-299.

Craley, C. R.; Zhang, R.; Kowalewski, T.; McCullough, R. D.; Stefan, M. C. *Macromol. Rapid Commun.* **2009**, *30*, 11-16.

Dai, C.-A.; Yen, W.-C.; Lee, Y.-H.; Ho, C.-C.; Su, W.-F. *J. Am. Chem. Soc.* **2007**, *129*, 11036-11038.

De Witte, P. A. J.; Hernando, J.; Neuteboom, E. E.; van Dijk, E. M. H. P.; Meskers, S. C. J.; Janssen, R. A. J.; van Hulst, N. F.; Nolte, R. J. M.; García-Parajó, M. F.; Rowan, A. E. *J. Phys. Chem. B* **2006**, *110*, 7803-7812.

Deming, T. J.; Novak, B. M.; Ziller, J. W. *J. Am. Chem. Soc.* **1994**, *116*, 2366.

Dittmer, J. J.; Marseglia, E. A.; Friend, R. H. *Adv. Mater.* **2000**, *12*, 1270-1274.

Dong, C.-G.; Hu, Q.-S. *J. Am. Chem. Soc.* **2005**, *127*, 10006-10007.

Doubina, N.; Jenkins, J. L.; Paniagua, S. A.; Mazzio, K. A.; MacDonald, G. A.; Jen, A. K. Y.; Armstrong, N. R.; Marder, S. R.; Luscombe, C. K. *Langmuir* **2012**, *28*, 1900-1908.

Edmondson, S.; Osborne, V. L.; Huck, W. T. S. *Chem. Soc. Rev.* **2004**, *33*, 14-22.

Elmalem, E.; Biedermann, F.; Johnson, K.; Friend, R. H.; Huck, W. T. S. *J. Am. Chem. Soc.* **2012**, *134*, 17769-17777.

Elmalem, E.; Kiriy, A.; Huck, W. T. S. *Macromolecules* **2011**, *44*, 9057-9061.

Farina, V.; Kapadia, S.; Krishnan, B.; Wang, C.; Liebeskind, L. S. *J. Org. Chem.* **1994**, *59*, 5905-5911.

Foster, S.; Finlayson, C. E.; Keivanidis, P. E.; Huang, Y.-S.; Hwang, I.; Friend, R. H.; Otten, M. B. J.; Lu, L.-P.; Schwartz, E.; Nolte, R. J. M.; Rowan, A. E. *Macromolecules* **2009**, *42*, 2023-2030.

Giardina, G.; Rosi, P.; Ricci, A.; Lo Sterzo, C. *J. Polym. Sci. Part A* **2000**, *38*, 2603-2621.

Green, M. A.; Emery, K.; Hishikawa, Y.; Warta, W. *Prog. Photovoltaics* **2011**, *19*, 84-92.

Green, M. A.; Emery, K.; Hishikawa, Y.; Warta, W.; Dunlop, E. D. *Prog. Photovoltaics* **2012**, *20*, 606-614.

Greenham, N. C.; Samuel, I. D. W.; Hayes, G. R.; Phillips, R. T.; Kessener, Y. A. R. R.; Moratti, S. C.; Holmes, A. B.; Friend, R. H. *Chem. Phys. Lett.* **1995**, *241*, 89-96.

Grimsdale, A. C.; Leok Chan, K.; Martin, R. E.; Jokisz, P. G.; Holmes, A. B. *Chem. Rev.* **2009**, *109*, 897-1091.

Groves, C.; Reid, O. G.; Ginger, D. S. *Acc. Chem. Res.* **2010**, *43*, 612-620.

Guo, C.; Lin, Y.-H.; Witman, M. D.; Smith, K. A.; Wang, C.; Hexemer, A.; Strzalka, J.; Gomez, E. D.; Verduzco, R. *Nano Lett.* **2013**, *13*, 2957-2963.

Hartmuth, C. K.; Finn, M. G.; Sharpless, K. B. *Angew. Chem. Int. Ed.* **2001**, *40*, 2004-2021.

Haustein, E.; Schwille, P. *Annu. Rev. Biophys. Biomol. Struct.* **2007**, *36*, 151-169.

Higashihara, T.; Ueda, M. *React. Funct. Polym.* **2009**, *69*, 457-462.

Hoertz, P. G.; Niskala, J. R.; Dai, P.; Black, H. T.; You, W. *J. Am. Chem. Soc.* **2008**, *130*, 9763.

Hollinger, J.; Jahnke, A. A.; Coombs, N.; Seferos, D. S. *J. Am. Chem. Soc.* **2010**, *132*, 8546-8547.

Hoppe, H.; Sariciftci, N. S. *J. Mater. Res.* **2004**, *19*, 1924-1945.

Huang, L.; Wu, S.; Qu, Y.; Geng, Y.; Wang, F. *Macromolecules* **2008**, *41*, 8944-8947.

Huettner, S.; Hodgkiss, J. M.; Sommer, M.; Friend, R. H.; Steiner, U.; Thelakkat, M. *J. Phys. Chem. B* **2012**, *116*, 10070-10078.

Inganas, O.; Salaneck, W. R.; Osterholm, J. E.; Laakso, J. *Synth. Met.* **1988**, *22*, 395-406.

Iovu, M. C.; Craley, C. R.; Jeffries-El, M.; Krankowski, A. B.; Zhang, R.; Kowalewski, T.; McCullough, R. D. *Macromolecules* **2007**, *40*, 4733-4735.

Iovu, M. C.; Jeffries-El, M.; Sheina, E. E.; Cooper, J. R.; McCullough, R. D. *Polymer* **2005**, *46*, 8582-8586.

Javier, A. E.; Varshney, S. R.; McCullough, R. D. *Macromolecules* **2010**, *43*, 3233-3237.

Jeffries-El, M.; Sauve, G.; McCullough, R. D. *Macromolecules* **2005**, *38*, 10346-10352.

Jiang, P.; Bertone, J. F.; Hwang, K. S.; Colvin, V. L. *Chem. Mater.* **1999**, *11*, 2132-2140.

Jiang, X. M.; Osterbacka, R.; Korovyanko, O.; An, C. P.; Horovitz, B.; Janssen, R. A. J.; Vardeny, Z. V. *Adv. Funct. Mater.* **2002**, *12*, 587-597.

Kajitani, T.; Okoshi, K.; Sakurai, S.-i.; Kumaki, J.; Yashima, E. *J. Am. Chem. Soc.* **2005**, *128*, 708.

Kamer, P. C. J.; Nolte, R. J. M.; Drenth, W. *J. Am. Chem. Soc.* **1988**, *110*, 6818.

Karanam, S.; Goossens, H.; Klumperman, B.; Lemstra, P. *Macromolecules* **2003**, *36*, 3051-3060.

Kim, J. W.; Kim, L. U.; Kim, C. K. *Biomacromolecules* **2006**, *8*, 215-222.

Kim, J.; Swager, T. M. *Nature* **2001**, *411*, 1030-1034.

Kim, Y. g.; Galand, E. M.; Thompson, B. C.; walker, J.; Fossey, S. A.; McCarley, T. D.; Abboud, K. A.; Reynolds, J. R. *J. Macromol. Sci., Part A: Pure Appl. Chem.* **2007**, *44*, 665-674.

Kiriy, N.; Jahne, E.; Adler, H.-J.; Schneider, M.; Kiriy, A.; Gorodyska, G.; Minko, S.; Jehnichen, D.; Simon, P.; Fokin, A. A.; Stamm, M. *Nano Lett.* **2003**, *3*, 707-712.

Labastide, J. A.; Baghgar, M.; Dujovne, I.; Yang, Y.; Dinsmore, A. D.; G. Sumpter, B.; Venkataraman, D.; Barnes, M. D. *J. Phys. Chem. Lett.* **2011**, *2*, 3085-3091.

Lang, A. S.; Neubig, A.; Sommer, M.; Thelakkat, M. *Macromolecules* **2010**, *43*, 7001-7010.

Lanni, E. L.; McNeil, A. J. *J. Am. Chem. Soc.* **2009**, *131*, 16573-16579.

Lanni, E. L.; McNeil, A. J. *Macromolecules* **2010**, *43*, 8039-8044.

Lee, E.; Hammer, B.; Kim, J.-K.; Page, Z.; Emrick, T.; Hayward, R. C. *J. Am. Chem. Soc.* **2011**, *133*, 10390-10393.

Lee, J. K.; Ma, W. L.; Brabec, C. J.; Yuen, J.; Moon, J. S.; Kim, J. Y.; Lee, K.; Bazan, G. C.; Heeger, A. J. *J. Am. Chem. Soc.* **2008**, *130*, 3619-3623.

Lee, J. U.; Cirpan, A.; Emrick, T.; Russell, T. P.; Jo, W. H. *J. Mater. Chem.* **2009**, *19,* 1483.

Lere-Porte, J.-P.; Moreau, J. J. E.; Serein-Spirau, F.; Torreilles, C.; Righi, A.; Sauvajol, J.-L.; Brunet, M. *J. Mater. Chem.* **2000**, *10*, 927-932.

Li, D.; Sheng, X.; Zhao, B. *J. Am. Chem. Soc.* **2005**, *127*, 6248-6256.

Li, Y.; Vamvounis, G.; Holdcroft, S. *Macromolecules* **2002**, *35*, 6900-6906.

Li, Z.; Ono, R. J.; Wu, Z.-Q.; Bielawski, C. W. *Chem. Commun.* **2011**, *47*, 197-199.

Liang, Y.; Feng, D.; Wu, Y.; Tsai, S.-T.; Li, G.; Ray, C.; Yu, L. *J. Am. Chem. Soc.* **2009**, *131*, 7792-7799.

Liao, L.; Pang, Y.; Ding, L.; Karasz, F. E. *Macromolecules* **2001**, *34*, 6756-6760.

Liu, C.-Y.; Holman, Z. C.; Kortshagen, U. R. *Nano Lett.* **2008**, *9*, 449-452.

Liu, J.; Lam, J. W. Y.; Tang, B. Z. *Chem. Rev.* **2009**, *109*, 5799-5867.

Liu, J.; Sheina, E.; Kowalewski, T.; McCullough, R. D. *Angew. Chem. Int. Ed.* **2002**, *41*, 329-332.

Liu, L.; Zang, Y.; Hadano, S.; Aoki, T.; Teraguchi, M.; Kaneko, T.; Namikoshi, T. *Macromolecules* **2010**, *43*, 9268.

Loewe, R. S.; Ewbank, P. C.; Liu, J.; Zhai, L.; McCullough, R. D. *Macromolecules* **2001**, *34*, 4324-4333.

Loewe, R. S.; Khersonsky, S. M.; McCullough, R. D. *Adv. Mater.* **1999**, *11*, 250-253.

Lohwasser, R. H.; Thelakkat, M. *Macromolecules* **2011**, *44*, 3388-3397.

Mao, H.; Xu, B.; Holdcroft, S. *Macromolecules* **1993**, *26*, 1163-1169.

Marshall, N.; Sontag, S. K.; Locklin, J. *Macromolecules* **2010**, *43*, 2137-2144.

McCulloch, I.; Heeney, M.; Bailey, C.; Genevicius, K.; MacDonald, I.; Shkunov, M.; Sparrowe, D.; Tierney, S.; Wagner, R.; Zhang, W.; Chabinyc, M. L.; Kline, R. J.; McGehee, M. D.; Toney, M. F. *Nat. Mater.* **2006**, *5*, 328-33.

Miyakoshi, R.; Shimono, K.; Yokoyama, A.; Yokozawa, T. *J. Am. Chem. Soc.* **2006**, *128*, 16012-16013.

Miyakoshi, R.; Yokoyama, A.; Yokozawa, T. *Chem. Lett.* **2008**, *37*, 1022-1023.

Miyakoshi, R.; Yokoyama, A.; Yokozawa, T. *J. Am. Chem. Soc.* **2005**, *127*, 17542-17547.

Miyanishi, S.; Zhang, Y.; Tajima, K.; Hashimoto, K. *Chem. Commun.* **2010**, *46*, 6723-6725.

Moratti, S. C.; Cervini, R.; Holmes, A. B.; Baigent, D. R.; Friend, R. H.; Greenham, N. C.; Grüner, J.; Hamer, P. J. *Synth. Met.* **1995**, *71*, 2117-2120.

Mulherin, R. C.; Jung, S.; Huettner, S.; Johnson, K.; Kohn, P.; Sommer, M.; Allard, S.; Scherf, U.; Greenham, N. C. *Nano Lett.* **2011**, *11*, 4846-4851.

Ohmiya, H.; Yorimitsu, H.; Oshima, K. *Org. Lett.* **2006**, *8*, 3093-3096.

Olsen, B. D.; Segalman, R. A. *Mater. Sci. Eng., R* **2008**, *62*, 37-66.

Ono, R. J.; Kang, S.; Bielawski, C. W. *Macromolecules* **2012**, *45*, 2321-2326.

Onouchi, H.; Okoshi, K.; Kajitani, T.; Sakurai, S.-i.; Nagai, K.; Kumaki, J.; Onitsuka, K.; Yashima, E. *J. Am. Chem. Soc.* **2007**, *130*, 229.

Osaka, I.; McCullough, R. D. *Acc. Chem. Res.* **2008**, *41*, 1202-1214.

Paquin, F.; Latini, G.; Sakowicz, M.; Karsenti, P. L.; Wang, L. J.; Beljonne, D.; Stingelin, N.; Silva, C. *Phys. Rev. Lett.* **2011**, *106*, 4.

Park, S.-J.; Kang, S.-G.; Fryd, M.; Saven, J. G.; Park, S.-J. *J. Am. Chem. Soc.* **2010**, *132*, 9931-9933.

Park, Y. D.; Cho, J. H.; Kim, D. H.; Jang, Y.; Lee, H. S.; Ihm, K.; Kang, T.-H.; Cho, K. *Electrochem. Solid-State Lett.* **2006**, *9*, G317-G319.

Park, Y. D.; Lee, H. S.; Choi, Y. J.; Kwak, D.; Cho, J. H.; Lee, S.; Cho, K. *Adv. Funct. Mater.* **2009**, *19*, 1200-1206.

Patra, S. K.; Ahmed, R.; Whittell, G. R.; Lunn, D. J.; Dunphy, E. L.; Winnik, M. A.; Manners, I. *J. Am. Chem. Soc.* **2011**, *133*, 8842-8845.

Peet, J.; Heeger, A. J.; Bazan, G. C. *Acc. Chem. Res.* **2009**, *42*, 1700-1708.

Peet, J.; Kim, J. Y.; Coates, N. E.; Ma, W. L.; Moses, D.; Heeger, A. J.; Bazan, G. C. *Nat. Mater.* **2007**, *6*, 497-500.

Prosa, T. J.; Winokur, M. J.; Moulton, J.; Smith, P.; Heeger, A. J. *Macromolecules* **1992**, *25*, 4364-4372.

Pschirer, N. G.; Miteva, T.; Evans, U.; Roberts, R. S.; Marshall, A. R.; Neher, D.; Myrick, M. L.; Bunz, U. H. F. *Chem. Mater*. **2001**, *13*, 2691-2696.

Qingchun, L.; Yongming, C. *J. Polym. Sci. Part A: Polym. Chem.* **2006**, *44*, 6103-6113.

Radano, C. P.; Scherman, O. A.; Stingelin-Stutzmann, N.; Muller, C.; Breiby, D. W.; Smith, P.; Janssen, R. A. J.; Meijer, E. W. *J. Am. Chem. Soc.* **2005**, *127*, 12502-12503.

Rajaram, S.; Armstrong, P. B.; Kim, B. J.; Fréchet, J. M. J. *Chem. Mater.* **2009**, *21*, 1775-1777.

Reitzel, N.; Greve, D. R.; Kjaer, K.; Howes, P. B.; Jayaraman, M.; Savoy, S.; McCullough, R. D.; McDevitt, J. T.; Bjornholm, T. *J. Am. Chem. Soc.* **2000**, *122*, 5788-5800.

Richard, F.; Brochon, C.; Leclerc, N.; Eckhardt, D.; Heiser, T.; Hadziioannou, G. *Macromol. Rapid Commun.* **2008**, *29*, 885-891.

Rumbles, G.; Samuel, I. D. W.; Magnani, L.; Murray, K. A.; DeMello, A. J.; Crystall, B.; Moratti, S. C.; Stone, B. M.; Holmes, A. B.; Friend, R. H. *Synth. Met.* **1996**, *76*, 47-51.

Samuel, I. D. W.; Magnani, L.; Rumbles, G.; Murray, K.; Stone, B. M.; Moratti, S. C.; Holmes, A. B. *Proc. SPIE* **1997**, *3145*, 163-170.

Scherf, U.; Gutacker, A.; Koenen, N. *Acc. Chem. Res.* **2008**, *41*, 1086-1097.

Schwartz, E.; Koepf, M.; Kitto, H. J.; Nolte, R. J. M.; Rowan, A. E. *Polym. Chem.* **2011**, *2*, 33-47.

Schwartz, E.; Palermo, V.; Finlayson, C. E.; Huang, Y.-S.; Otten, M. B. J.; Liscio, A.; Trapani, S.; González-Valls, I.; Brocorens, P.; Cornelissen, J. J. L. M.; Peneva, K.; Müllen, K.; Spano, F. C.; Yartsev, A.; Westenhoff, S.; Friend, R. H.; Beljonne, D.; Nolte, R. J. M.; Samorì, P.; Rowan, A. E. *Chem. Eur. J.* **2009**, *15*, 2536-2547.

Segalman, R. A.; McCulloch, B.; Kirmayer, S.; Urban, J. J. *Macromolecules* **2009**, *42*, 9205-9216.

Senkovskyy, V.; Khanduyeva, N.; Komber, H.; Oertel, U.; Stamm, M.; Kuckling, D.; Kiriy, A. *J. Am. Chem. Soc*. **2007**, *129*, 6626-6632.

Senkovskyy, V.; Tkachov, R.; Beryozkina, T.; Komber, H.; Oertel, U.; Horecha, M.; Bocharova, V.; Stamm, M.; Gevorgyan, S. A.; Krebs, F. C.; Kiriy, A. *J. Am. Chem. Soc*. **2009**, *131*, 16445-16453.

Senkovskyy, V.; Tkachov, R.; Komber, H.; Sommer, M.; Heuken, M.; Voit, B.; Huck, W. T. S.; Kataev, V.; Petr, A.; Kiriy, A. *J. Am. Chem. Soc.* **2011**, *133*, 19966-19970.

Sheina, E. E.; Liu, J.; Iovu, M. C.; Laird, D. W.; McCullough, R. D. *Macromolecules* **2004**, *37*, 3526-3528.

Sheng, C. X.; Tong, M.; Singh, S.; Vardeny, Z. V. *Phys. Rev. B* **2007**, *75*, 085206.

Sirringhaus, H.; Brown, P. J.; Friend, R. H.; Nielsen, M. M.; Bechgaard, K.; Langeveld-Voss, B. M. W.; Spiering, A. J. H.; Janssen, R. A. J.; Meijer, E. W.; Herwig, P. *Nature* **1999**, *401*, 685- 688.

Sivula, K.; Ball, Z. T.; Watanabe, N.; Frechet, J. M. J. *Adv. Mater.* **2006**, *18*, 206-210.

Sommer, M.; Huettner, S.; Thelakkat, M. *J. Mater. Chem.* **2010**, *20*, 10788-10797.

Sommer, M.; Huttner, S.; Steiner, U.; Thelakkat, M. *Appl. Phys. Lett.* **2009**, *95*, 183308-1–183308-3.

Sommer, M.; Lang, A. S.; Thelakkat, M. *Angew. Chem. Int. Ed.* **2008**, *47*, 7901-7904.

Sontag, S. K.; Sheppard, G. R.; Usselman, N. M.; Marshall, N.; Locklin, J. *Langmuir* **2011**, *27*, 12033-12041.

Spano, F. C. *Acc. Chem. Res.* **2010**, *43*, 429-439.

Stambuli, J. P.; Incarvito, C. D.; Bühl, M.; Hartwig, J. F. *J. Am. Chem. Soc.* **2004**, *126*, 1184-1194.

Stefan, M. C.; Bhatt, M. P.; Sista, P.; Magurudeniya, H. D. *Polym. Chem.* **2012**, *3*, 1693-1701.

Stefan, M. C.; Javier, A. E.; Osaka, I.; McCullough, R. D. *Macromolecules* **2008**, *42*, 30-32.

Stöber, W.; Fink, A.; Bohn, E. *J. Colloid Interface Sci.* **1968**, *26*, 62-69.

Suraru, S.-L.; Würthner, F. *Synthesis* **2009**, *11*, 1841-1845.

Swager, T. M.; Gil, C. J.; Wrighton, M. S. *J. Phys. Chem.* **1995**, *99*, 4886.

Tanese, M. C.; Farinola, G. M.; Pignataro, B.; Valli, L.; Giotta, L.; Conoci, S.; Lang, P.; Colangiuli, D.; Babudri, F.; Naso, F.; Sabbatini, L.; Zambonin, P. G.; Torsi, L. *Chem. Mater.* **2005**, *18*, 778-784.

Tao, Y.; McCulloch, B.; Kim, S.; Segalman, R. A. *Soft Matter* **2009**, *5*, 4219-4230.

Thivierge, C.; Loudet, A.; Burgess, K. *Macromolecules* **2011**, *44*, 4012.

Thomas, S. W.; Joly, G. D.; Swager, T. M. *Chem. Rev.* **2007**, *107*, 1339-1386.

Tkachov, R.; Senkovskyy, V.; Horecha, M.; Oertel, U.; Stamm, M.; Kiriy, A. *Chem. Commun*. **2010**, *46*, 1425-1427.

Tkachov, R.; Senkovskyy, V.; Komber, H.; Sommer, J.-U.; Kiriy, A. *J. Am. Chem. Soc.* **2010**, *132*, 7803-7810.

Tsai, J.-H.; Lai, Y.-C.; Higashihara, T.; Lin, C.-J.; Ueda, M.; Chen, W.-C. *Macromolecules* **2010**, *43*, 6085.

Urien, M.; Erothu, H.; Cloutet, E.; Hiorns, R. C.; Vignau, L.; Cramail, H. *Macromolecules* **2008**, *41*, 7033-7040.

Wang, F.; Wilson, M. S.; Rauh, R. D.; Schottland, P.; Thompson, B. C.; Reynolds, J. R. *Macromolecules* **2000**, *33*, 2083-2091.

Wang, M.; Kumar, S.; Lee, A.; Felorzabihi, N.; Shen, L.; Zhao, F.; Froimowicz, P.; Scholes, G. D.; Winnik, M. A. *J. Am. Chem. Soc.* **2008**, *130*, 9481-9491.

Weber, S. K.; Galbrecht, F.; Scherf, U. *Org. Lett.* **2006**, *8*, 4039-4041.

Wilson, J. N.; Steffen, W.; McKenzie, T. G.; Lieser, G.; Oda, M.; Neher, D.; Bunz, U. H. F. *J. Am. Chem. Soc*. **2002**, *124*, 6830-6831.

Wu, S.; Bu, L.; Huang, L.; Yu, X.; Han, Y.; Geng, Y.; Wang, F. *Polymer* **2009**, *50*, 6245-6251.

Wu, S.; Sun, Y.; Huang, L.; Wang, J.; Zhou, Y.; Geng, Y.; Wang, F. *Macromolecules* **2010**, *43*, 4438-4440.

Wu, Z.-Q.; Nagai, K.; Banno, M.; Okoshi, K.; Onitsuka, K.; Yashima, E. *J. Am. Chem. Soc.* **2009**, *131*, 6708.

Wu, Z.-Q.; Ono, R. J.; Chen, Z.; Bielawski, C. W. *J. Am. Chem. Soc.* **2010**, *132*, 14000-14001.

Wu, Z.-Q.; Radcliffe, J. D.; Ono, R. J.; Chen, Z.; Li, Z.; Bielawski, C. W. *Polym. Chem.* **2012**, *3*, 874-881.

Xu, B.; Holdcroft, S. *Macromolecules* **1993**, *26*, 4457-4460.

Yamada, T.; Suginome, M. *Macromolecules* **2010**, *43*, 3999.

Yamamoto, T.; Komarudin, D.; Arai, M.; Lee, B.-L.; Suganuma, H.; Asakawa, N.; Inoue, Y.; Kubota, K.; Sasaki, S.; Fukuda, T.; Matsuda, H. *J. Am. Chem. Soc.* **1998**, *120*, 2047-2058.

Yamamoto, T.; Morita, A.; Miyazaki, Y.; Maruyama, T.; Wakayama, H.; Zhou, Z. H.; Nakamura, Y.; Kanbara, T.; Sasaki, S.; Kubota, K. *Macromolecules* **1992**, *25*, 1214-1223.

Yang, C.; Lee, J. K.; Heeger, A. J.; Wudl, F. *J. Mater. Chem.* **2009**, *19*, 5416-5423.

Yang, J.-S.; Swager, T. M. *J. Am. Chem. Soc.* **1998**, *120*, 11864-11873.

Yokoyama, A.; Kato, A.; Miyakoshi, R.; Yokozawa, T. *Macromolecules* **2008**, *41*, 7271-7273.

Yokoyama, A.; Miyakoshi, R.; Yokozawa, T. *Macromolecules* **2004**, *37*, 1169-1171.

Yokoyama, A.; Suzuki, H.; Kubota, Y.; Ohuchi, K.; Higashimura, H.; Yokozawa, T. *J. Am. Chem. Soc.* **2007**, *129*, 7236-7237.

Yokozawa, T.; Kohno, H.; Ohta, Y.; Yokoyama, A. *Macromolecules* **2010**, *43*, 7095-7100.

Yokozawa, T.; Nanashima, Y.; Ohta, Y. *ACS Macro Lett.* **2012**, *1*, 862-866.

Yokozawa, T.; Yokoyama, A. *Chem. Rev.* **2009**, *109*, 5595-5619.

Yoshikai, N.; Matsuda, H.; Nakamura, E. *J. Am. Chem. Soc.* **2008**, *130*, 15258-15259.

Zenkina, O. V.; Karton, A.; Freeman, D.; Shimon, L. J. W.; Martin, J. M. L.; van der Boom, M. E. *Inorg. Chem.* **2008**, *47*, 5114-5121.

Zhang, H.-H.; Xing, C.-H.; Hu, Q.-S. *J. Am. Chem. Soc.* **2012**, *134*, 13156-13159.

Zhang, Q.; Cirpan, A.; Russell, T. P.; Emrick, T. *Macromolecules* **2009**, *42*, 1079-1082.

Zhang, Y.; Tajima, K.; Hirota, K.; Hashimoto, K. *J. Am. Chem. Soc.* **2008**, *130*, 7812.

Vita

Robert Ono was born in Saitama, Japan to parents Kenichi and Kimberly Ono. In 2001, at the age of 15, he and his family moved to New Jersey, where he attended Bridgewater-Raritan High School. Robert went on to earn a B.A. in Chemistry from Rutgers University in the spring of 2008, and subsequently matriculated into the Chemistry PhD program at The University of Texas, Austin in the fall of the same year. There, he joined the research group of Prof. Christopher Bielawski where, while also being co-advised by Prof. Jonathan Sessler, he conducted research on chain-growth syntheses of conjugated polymers and block copolymers for optoelectronic applications.

Permanent email: ono@utexas.edu

This dissertation was typed by Robert J. Ono.